Environment of the Mid-Atlantic Ridge area under the contract for polymetallic sulphide exploration between the International Seabed Authority and the Ministry of Environment of the Republic of Poland

Literature Review, edited by Teresa Radziejewska, Jan Marcin Węsławski and Michał Tomczak

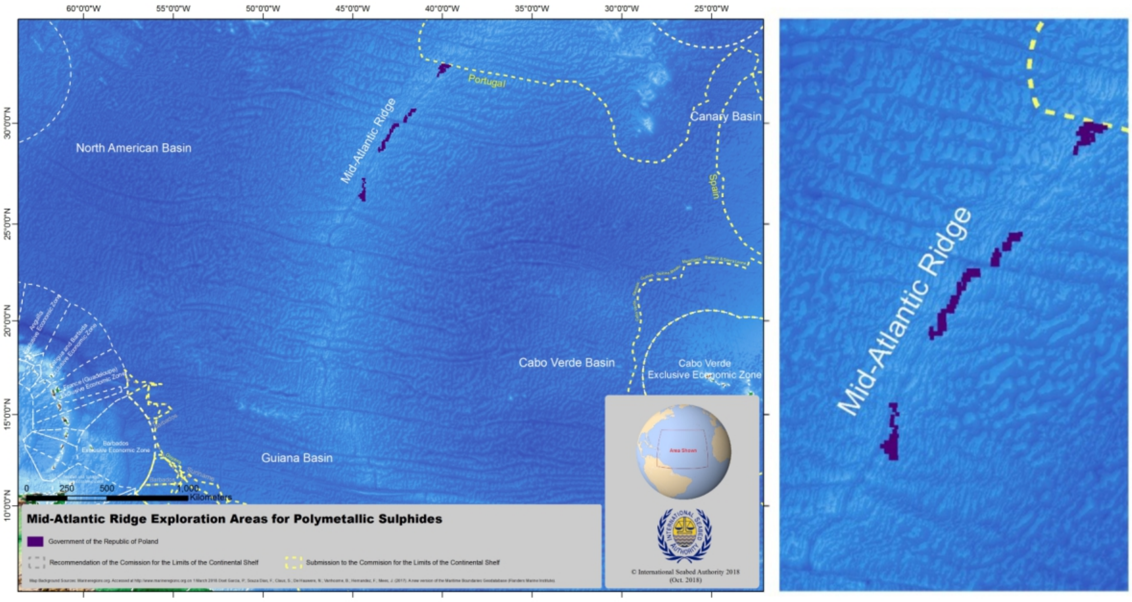

Gdańsk – Łódź – Poznań – Sopot – Szczecin – Warszawa 2020

Executive summary - Teresa Radziejewska and Jan Marcin Węsławski

The Atlantic seabed area under the contract (Fig. 1.1) is situated near the central part of the Mid-Atlantic Ridge (MAR), one of the major geological formations on Earth (Fig. 1.2.), featuring – like other mid-oceanic ridges – active and inactive hydrothermal vent fields with their unusual and unique ecosystems. The commercial interest in MAR exploration is due to the deposits of massive polymetallic sulphides, formed as a result of hydrothermal fluid precipitation.

Activities associated with exploration of any area should be underpinned by knowledge on what is known about the area and its inhabitants, what gaps in knowledge still exist, what the 'rules of the game' (in the form of legal framework and regulations) are, and what methods should and need to be used to fill the gaps. Therefore, before exploration begins, the existing information on the area, including both its abiotic and biotic components, should be collected, processed and summarized. The present report is an attempt at such a summary. The Google Scholar lists over 0.5 million scientific papers, notes and books that mention the MAR, the relevant peer-reviewed papers counting over 60 thousand documents. For the present review, we have selected mostly recent publications focused on the central part of the MAR

With regard to the climate conditions, the contract area is situated in the subtropics, between the easterly and westerly mid-latitude atmospheric circulation (Fig. 2.1). It is also the area on the edge of the tropical storms and hurricane tracks (Fig. 2.5).

The depth of the ocean in the contract area varies between 800 and 4900 m; the area – situated within the North Atlantic Gyre - is affected by the Gulf Stream and Canary Currents. The complex seabed topography results in a number of local deep currents of smaller magnitude.

The deep water layers are formed by the North Atlantic Deep Water with temperatures between 1.5°C and 4°C and the full marine salinity of 34-35.

The water transparency in the area is high, with visibility reaching down to the 50m depth, as in other mid-ocean gyres, hence the chlorophyll concentration and primary production are low.

The geological age of the seabed in the contract area is younger than 3.3 million years. The contract area features two distinct vent fields: the Broken Spur and the Lost City (Fig. 3.8). The sedimentary cover is from few to 20m thick, and is composed mainly of carbonate ooze.

The pelagic environment over the contract area supports typical oceanic microplankton assemblages, with coccolitophora and prominent contribution of diatoms and radiolarians, while the zooplankton is dominated by minute copepods, and is often concentrated in the sub-surface layers of 300-100m depth. Dense concentrations of macroplankton and small fish are recorded in the mesopelagic zone. The pelagic fishery is moderately developed and targets large species such as tuna and swordfish; the commercial bottom fishing is not feasible in the area.

The pelagic vertebrate fauna of the area counts at least 60 seabird species, 28 species of whales and four sea turtles; all those species are of conservation value, eight species being listed in the IUCN Red Book as vulnerable to critically endangered.

The organisms inhabiting the seabed in the contract area are, to large extent, adapted to the particular conditions of the hydrothermal vent environment. These organisms include chemoautotrophic and methane-consuming microorganisms (bacteria and archaea), the meiobenthos – an important component of the local fauna because of its diversity and potential utility as an indicators of local conditions. The benthic macrofauna forms dense aggregations; particularly important are deep-sea shrimps and other macrofaunal crustaceans, with a record-breaking biomass exceeding 1 kg/m^2. The endemism (uniqueness) of the deep-sea vent fauna is associated with the whole system of Mid-Atlantic Ridge rather than with individual sites. This is related to a high degree of temporal stability of the benthic communities, on the scale of decades.

The conservation status of deep-sea fauna is regulated by the UN Convention on the Law of the Sea, which recognizes the deep sea as the common heritage of mankind and expects any activity to observe the precautionary principle, as described in the Convention on Biological Diversity. Specific recommendations for contract-holders are issued by the International Seabed Authority, and – on the next level – by the national/governmental regulations. All activities in the area shall be subject to an Environmental Impact Assessment and long term monitoring of the biota. Methods for studying the extremely difficult deep-sea environment of the MAR involve the use of technologically advanced equipment, a strong emphasis being placed on non-invasive techniques, mainly optical and acoustic remote sensing as well as the use of robots.

Cover image: Location of the Polish contract area on the Mid-Atlantic Ridge (source: *isa.org.jm*)

Authors with their affiliations and specialisation (in alphabetical order):

Katarzyna Błachowiak-Samołyk, professor at the IO PAN; zooplankton ecology and oceanic Ostracoda taxonomy
Magdalena Błażewicz, professor at the Univeristy of Łódź; deep sea crustacean taxonomy
Mateusz Damrat, director of the Polish Geological Institute – National Research Institute; marine geology, sedimentology
Katarzyna Jankowska, professor at the Technical University of Gdańsk; marine microbiology
Piotr Jóźwiak, assistant professor at the University of Łodź; macrobenthos
Bartosz Kotrys, main specialist at the Polish Geological Institute – National Research Institute; marine micropalaeontology, palaeoreconstructions
Agata Kozłowska-Roman, senior specialist at the Polish Geological Institute – National Research Institute; geology, legal and regulatory framework
Tomasz B. Linkowski, professor emeritus at the National Marine Fisheries Institute; ichthyology, Myctophidae, oceanic mesopelagic fish
Elżbieta Maszloch, specialist at the Polish Geological Institute – National Research Institute; marine geology
Krzysztof Pabis, professor at the University of Łódź; marine benthos, Polychaeta
Jacek Piskozub, professor at the IO PAN; atmospheric physics, climatology
Teresa Radziejewska, professor at the University of Szczecin; meiobenthos ecology, deep sea fauna and conservation
Sławomir Sagan, professor at the IO PAN; marine physics, optics, satelite imagery
Łukasz Smajdor, senior specialist at the Polish Geological Institute – National Research Institute; geophysic
Lech Stempniewicz, professor emeritus at the University of Gdańsk; marine vertebrate ecology, ornithology
Paweł Sydor, senior specialist at the Polish Geological Institute – National Research Institute; marine geology, sedimentology, geological cartography
Witold Szczuciński, professor at the Adam Mickiewicz University in Poznań; marine geology, sedimentology, geohazards
Agata Szyduk, specialist at the Polish Geological Institute – National Research Institute; biology, legal and regulatory framework
Michał Tomczak, senior specialis at the Polish Geological Institute – National Research Institute; marine geology, sedimentology
Waldemar Walczowski, professor at the IO PAN; physical oceanography
Jan Marcin Węsławski, professor at the IO PAN; marine ecology, environmental protection
Maria Włodarska-Kowalczuk, professor at the IO PAN; marine benthic ecology, deep sea fauna
Tomasz Żuk, senior specialis at the Polish Geological Institute – National Research Institute; geology, geophysical modeling

TABLE OF CONTENTS

1. Introduction

Teresa Radziejewska, Jan Marcin Węsławski and Mateusz Damrat

The Polish intrest in the study area is reflected by the contract for polymetallic sulphide exploration between the International Seabed Authority and the Ministry of Environment of the Republic of Poland signed in 2018. The Polish exploration contract area is located in the central part of the Atlantic Ocean (Fig. 1.1.) between 26°09'N-32°50'N and 39°38'W-44°43'W near the central part of the Mid-Atlantic Ridge (MAR), one of the major geological formations on Earth (Fig. 1.2.), featuring – like other mid-oceanic ridges – active and inactive hydrothermal vent fields with their unusual and unique ecosystems. The water depth varies from 700 m above the MAR to more than 4,900 m in fracture zones and basins. The Polish exploration blocks are located to the south-west of the Portuguese submission to the Commission on the Limits of the Continental Shelf and to the north-east of the French exploration contract area. It covers a total area of 10,000 km2 and consists of 100 exploration blocks, 10x10km each. The blocks are grouped in 5 clusters (Fig. 1.1.).

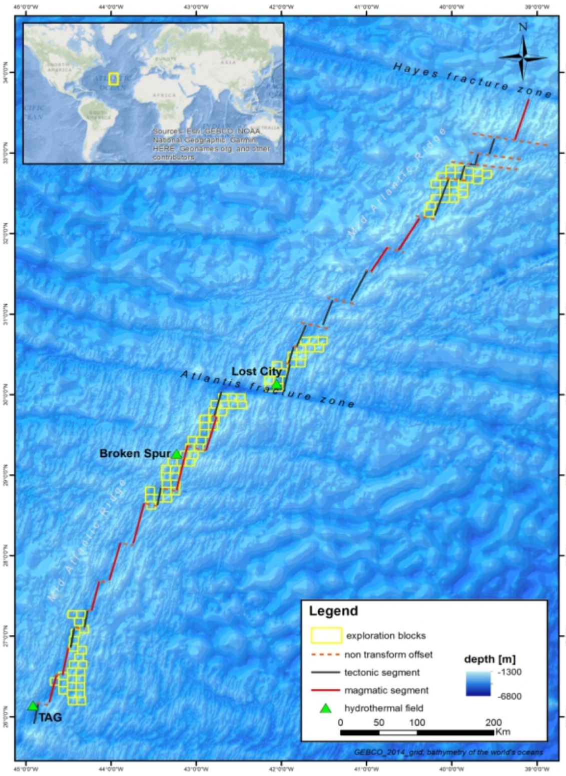

Fig. 1.1. The Polish contract area on the Mid-Atlantic Ridge (MAR) divided into 5 clusters (Kozłowska-Roman et al., 2019).

In recent decades, the MAR has received extreme attention both for its scientific value and potential commercial interest. The commercial interest in MAR exploration is due to the deposits of polymetallic massive sulphides (PMS), formed as a result of hydrothermal fluid precipitation. Those deposits are considered a strategic mineral resource of the future. As such, and because most of the MAR lies beyond borders of national jurisdiction, the MAR seafloor and its resources – as part of the common heritage of mankind – are managed by the

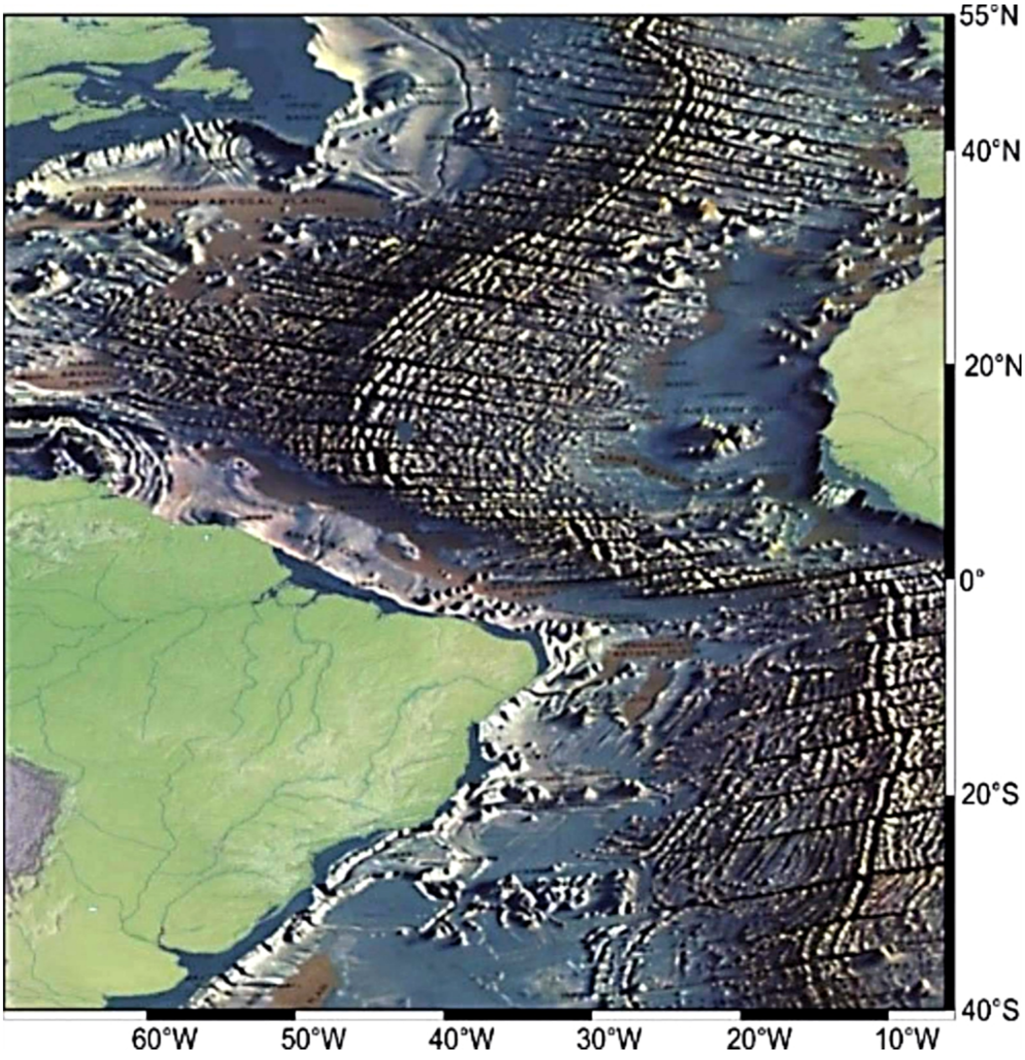

Fig. 1.2. The Mid-Atlantic Ridge with its seabed relief: a fragment of the National Geographic seabed map of 1998.

International Seabed Authority (ISA), an international entity entitled to conclude contracts for exploration of those resources with suitably qualified parties (contractors). In 2018, Poland concluded such a contract and should commence exploration.

The main objective of the contract is the identification of hydrothermally-based polymetallic massive sulphides and their economic evaluation. Hydrothermal sulfides mainly contain Cu, Zn, Fe and smaller concentrations of Au, Ag, Co, Ni, Cd, In, REE and other elements. As the seabed spreads, the active hydrothermal areas are gradually cut off from the energy source and become inactive (extinct or dormant), which in contrast to hydrothermally active zones, are barely known. The identification of hydrothermally inactive sites is more difficult and based on the imaging of the seabed with high-resolution multibeam echoesounders, cameras and the identification of negative self (electrical) potential anomalies. Despite these limitations, the total mass of polymetallic sulphide deposits in hydrothermally inactive areas is estimated to 600 Mt, which is 20 times higher than land-based recognized deposits, thus form areas of potential massive sulphide exploitations. An integral part of exploration are comprehensive environmental baseline studies, which should serve for the assessment of the potential impact of future exploitation.

Currently, most evidence on depositional conditions, environmental parameters and biodiversity of the areas is provided by research conducted under research (exploration) concessions, issued under agreements with the International Seabed Authority (ISA), established in 1982 under the United Nations Convention on the Law of the Sea (the so-called Jamaican Convention). These concessions provide a stable platform for comprehensive oceanographic, biological and geological research carried out according to strictly defined rules and under the control of the ISA and in cooperation at national and international level. Thanks to the possibility of exploring a unique environment of the mid-Atlantic ridge, Polish scientists will provide their contribution to the international community in terms of new data and research results.

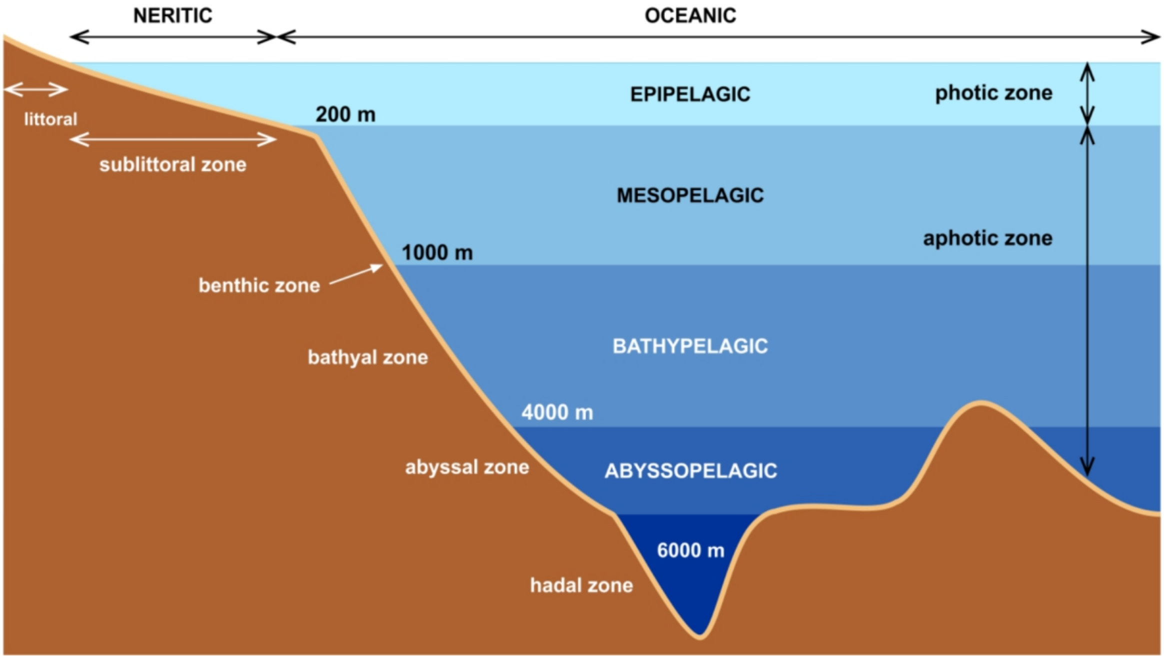

Fig. 1.3. Division of the oceanic domain into major ecological zones (compilation from various sources)

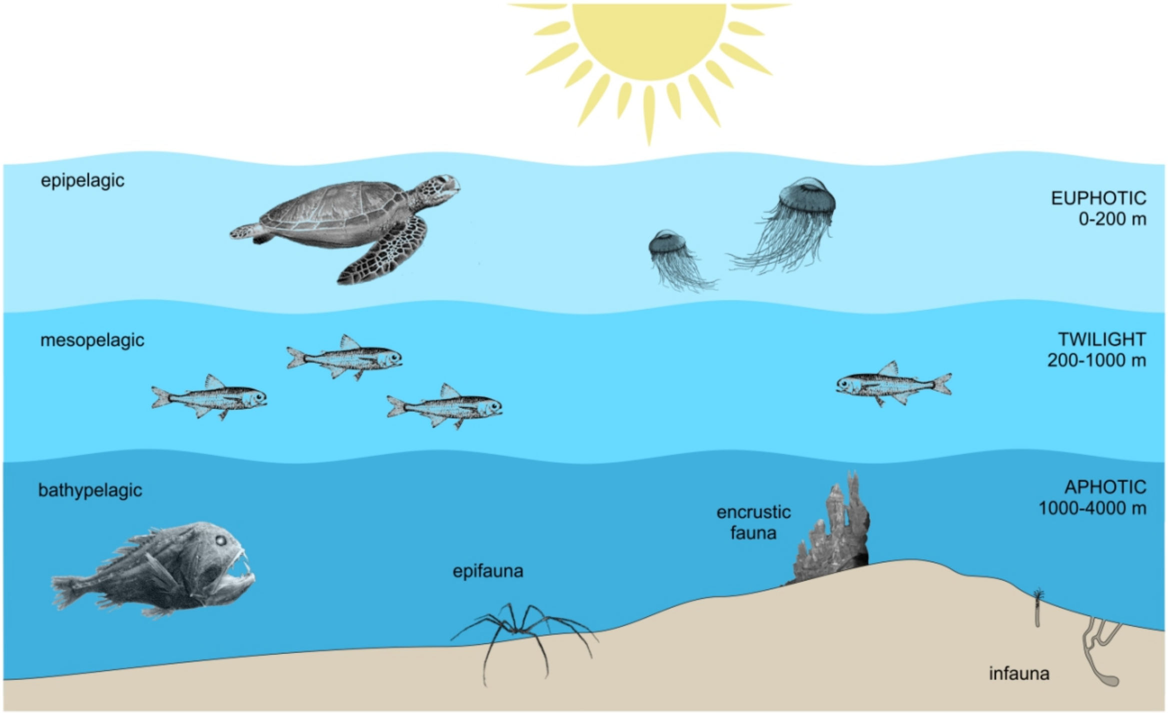

Fig. 1.4. Division of the oceanic system into ecological zones and the representative organisms (compilation from various sources)m various sources)

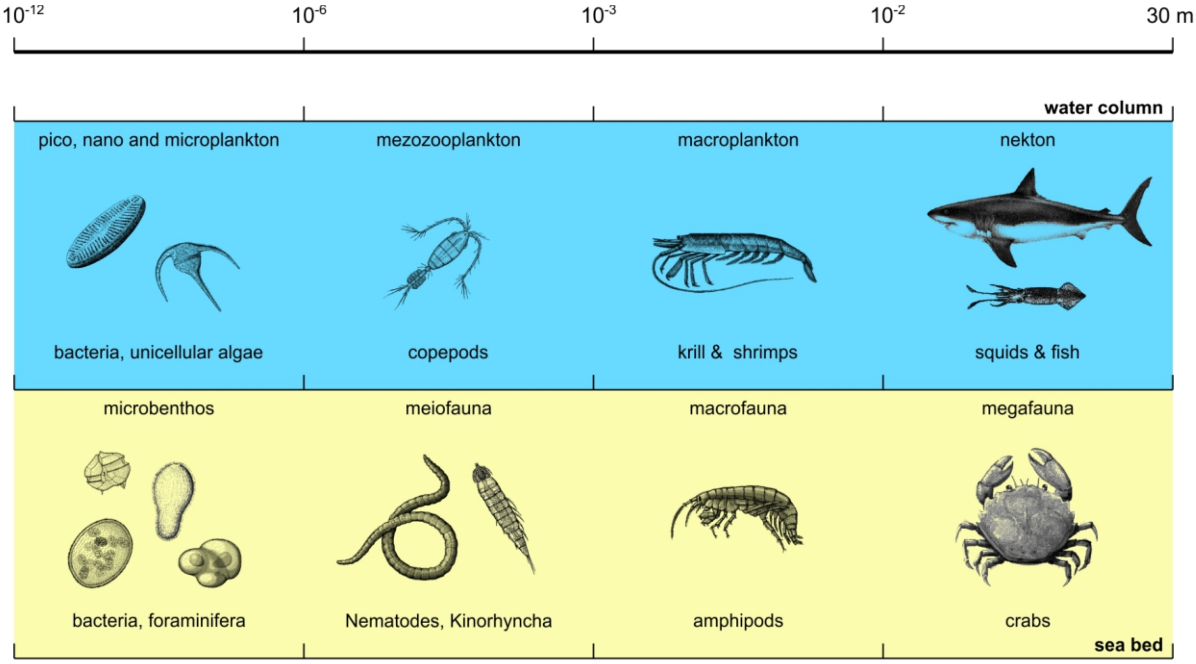

Fig. 1.5. Main size-based ecological categories of oceanic organisms in the water column and on the seabed, with dominant taxa indicated (compilation from various sources)

References

Kozłowska-Roman, A., Tomczak, M., Skowronek, A. Characteristic of the Polish reserved exploration area in the Mid-Atlantic Ridge. 48th Underwater Mining Conference, Sanya, China, September 22-27, 2019. Abstract book, p.112-118.

2. Hydrological and meteorological conditions in the contract area

Jacek Piskozub, Waldemar Walczowski and Sławomir Sagan

2.1. Meteorology and air-sea interaction (Jacek Piskozub)

2.1.1. General atmospheric circulation

The Polish contract area on the Mid Atlantic Ridge (MAR) between 26° 09 '- 32° 50' N; 39° 38' - 44° 43' W is technically placed in the subtropics defined usually as having the northern boundary at the 35° N latitude (AMS 2020). However, in practice the area is situated on the border between the easterly subtropical circulation (trade winds) of the subtropics and the westerly circulation of the middle latitudes (Fig. 2.1.). The actual position of the border changes seasonally, moving northward during the (boreal) warm seasons and southward during cold ones (Holton and Hakim, 2012).

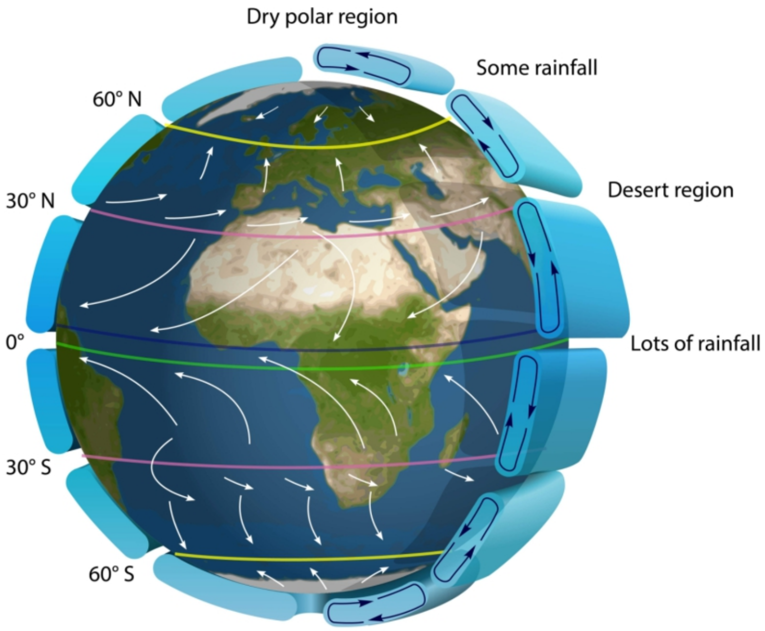

Fig. 2.1. Global atmospheric circulation showing the border between easterly (trade winds) and westerly circulation close to 30°N (source: Wikipedia)

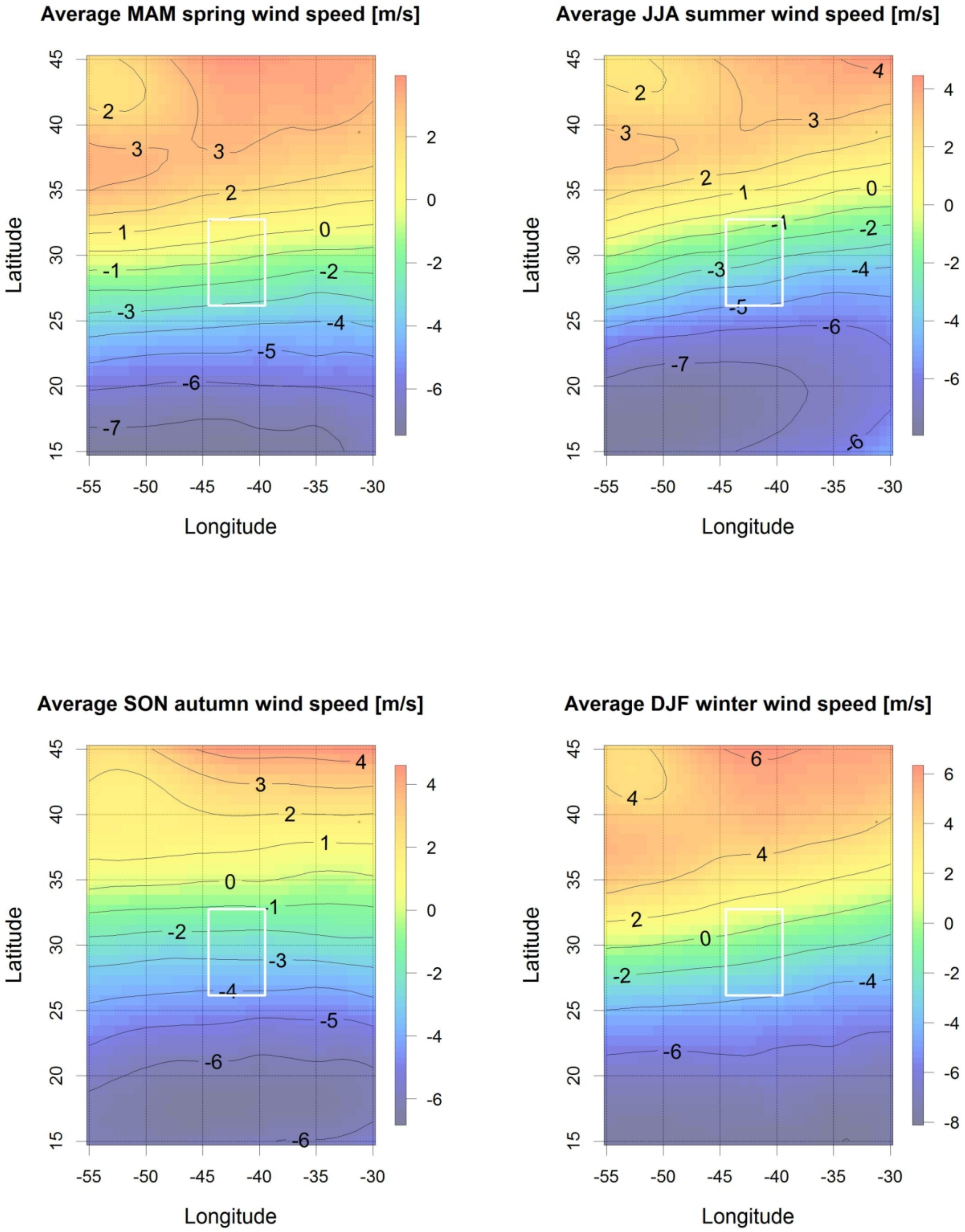

Fig. 2.2. Average zonal (east-west) component of the surface winds in the central North Atlantic by season. Data for 2010-2019 based on the NCEP/NCAR reanalysis. Positive numbers denote westerly winds. The Polish contract area is marked with a white rectangle (MAM, March-April-May; JJA, June-July-August; SON, September-October-November; DJF, December-January-February).

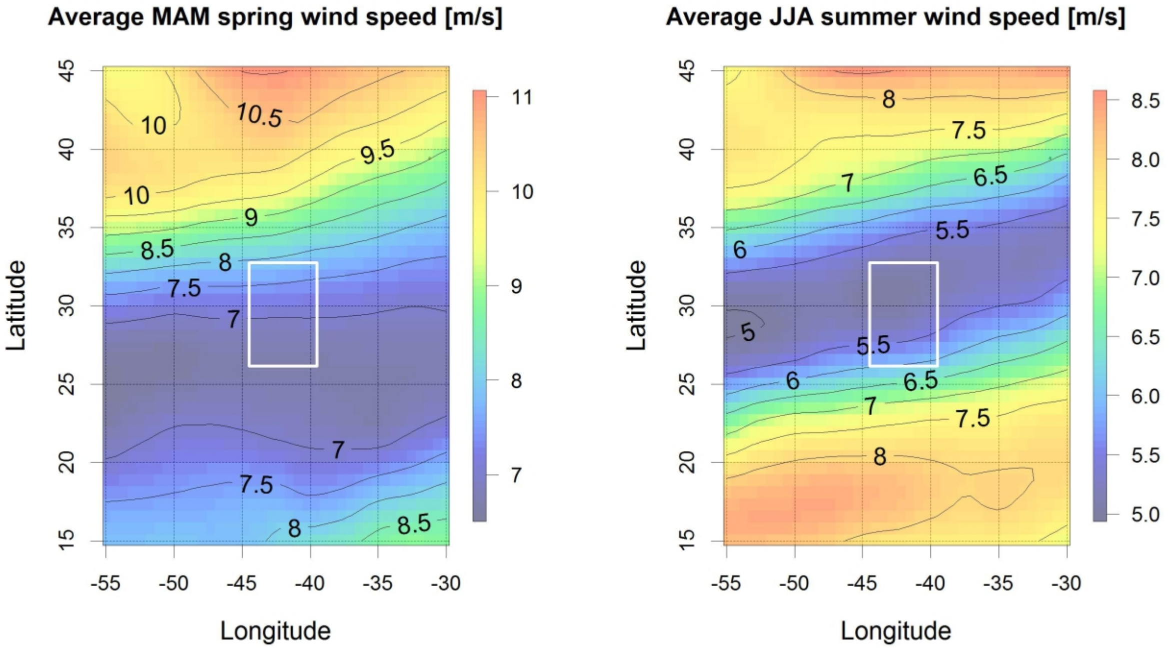

Average MAM spring wind speed [m/s]

Average JJA summer wind speed [m/s]

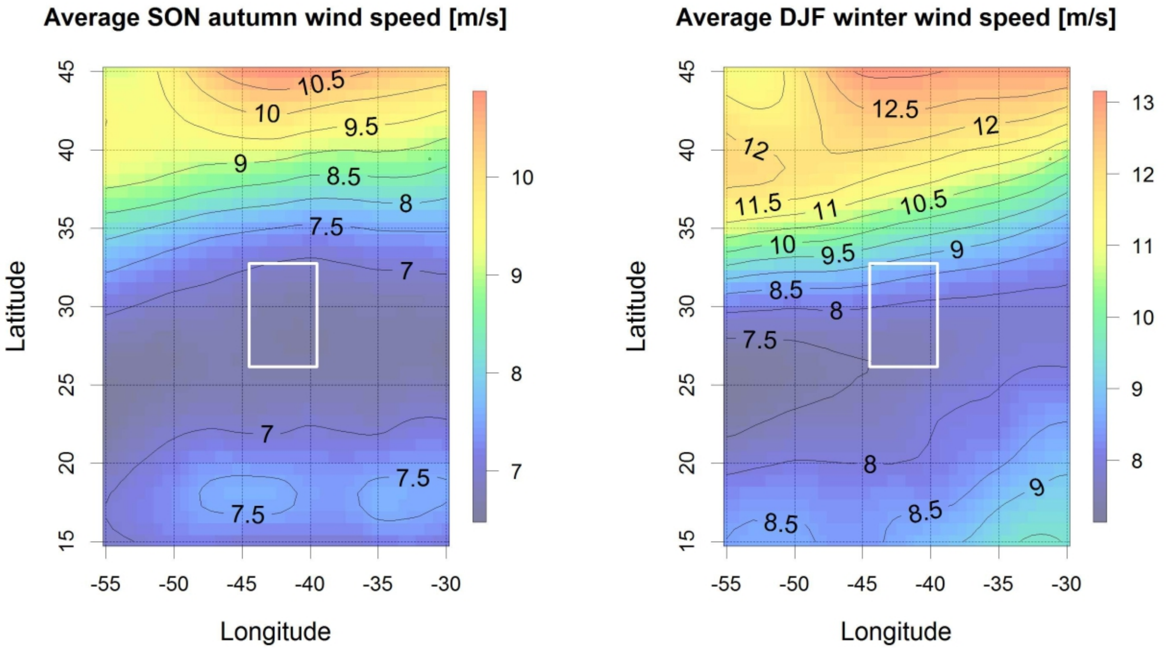

Average SON autumn wind speed [m/s]

Average DJF winter wind speed [m/s]

Fig. 2.3. Average surface (U10) wind speed in the central North Atlantic by season for 2010-2019, based on the NCEP/NCAR reanalysis. The Polish contract area is marked with a white rectangle. See Fig. 2.2. for explanation of season symbols

Fig. 2.2. shows the average zonal (east-west) wind component for 10 years (2010-2019) for each season, based on data from the NCEP/NCAR reanalysis (Kalnay et al., 1996). The data show the northern part of the contract area to be within the Westerlies zone during the winter and spring seasons (more precisely from December to June, not shown). The subtropical area of trade winds is generally a region of steady and predictable winds, but the Westerlies area is dominated by extratropical cyclonic (storms) and anticyclonic systems driven by atmospheric Rossby waves (Rhines, 2015). Fig. 2.3. shows the average wind speeds for each season in the region. The seasonal (and monthly, not shown) averages are between 6 and 8 m/s, except for the northernmost part where the average wind speed reaches 9 m/s in winter. North of the contract area, the average wind speed increases due to the region being situated in the Atlantic storm track. In a warming world, a slow northward shift of the Atlantic storm tracks is both observed (Bender et al., 2012) and projected (Yin, 2005), but also the trends are too inconspicuous to move the storm track away from the contract area in the near future.

2.1.2. Extreme weather events

The mean values of hydrographic parameters obscure extreme events such as winter storms in the northern part of the contract area as well as summer hurricanes. The maximal sustained 6-hour values of wind are shown in Fig. 2.4. The values of the maximal sustained wind in the license area are lowest (14-18 m/s) in summer (June-August) and highest (20-25 m/s) in winter (December-February). As the values are averages for 2.5° x 2.5° areas, local values are expected to be even higher. In particular, tropical cyclones (called hurricanes in the North Atlantic basin) are too small for their maximum wind speed to be fully registered with the spatial averaging used in the NCEP/NCAR reanalysis. However, it is evident from Fig. 2.4. that several hurricane tracks appear on the autumn (September-November) map, the closest track occurring just south of the contract area. That hurricane was the 2019 Lorenzo which reached its peak intensity of 140 kt (72 m/s) on September 29, 2019, just south of the contract area (Zelinsky, 2019), to become briefly a Category 5 hurricane on the Saffir-Simpson scale (AMS, 2020). It moved northward, still with a hurricane strength, along the westerly edge of the contract area. Even if there was only one hurricane moving over the contract area during the last 30 years (1990-2019), this shows that such a possibility exists and has to be taken into account.

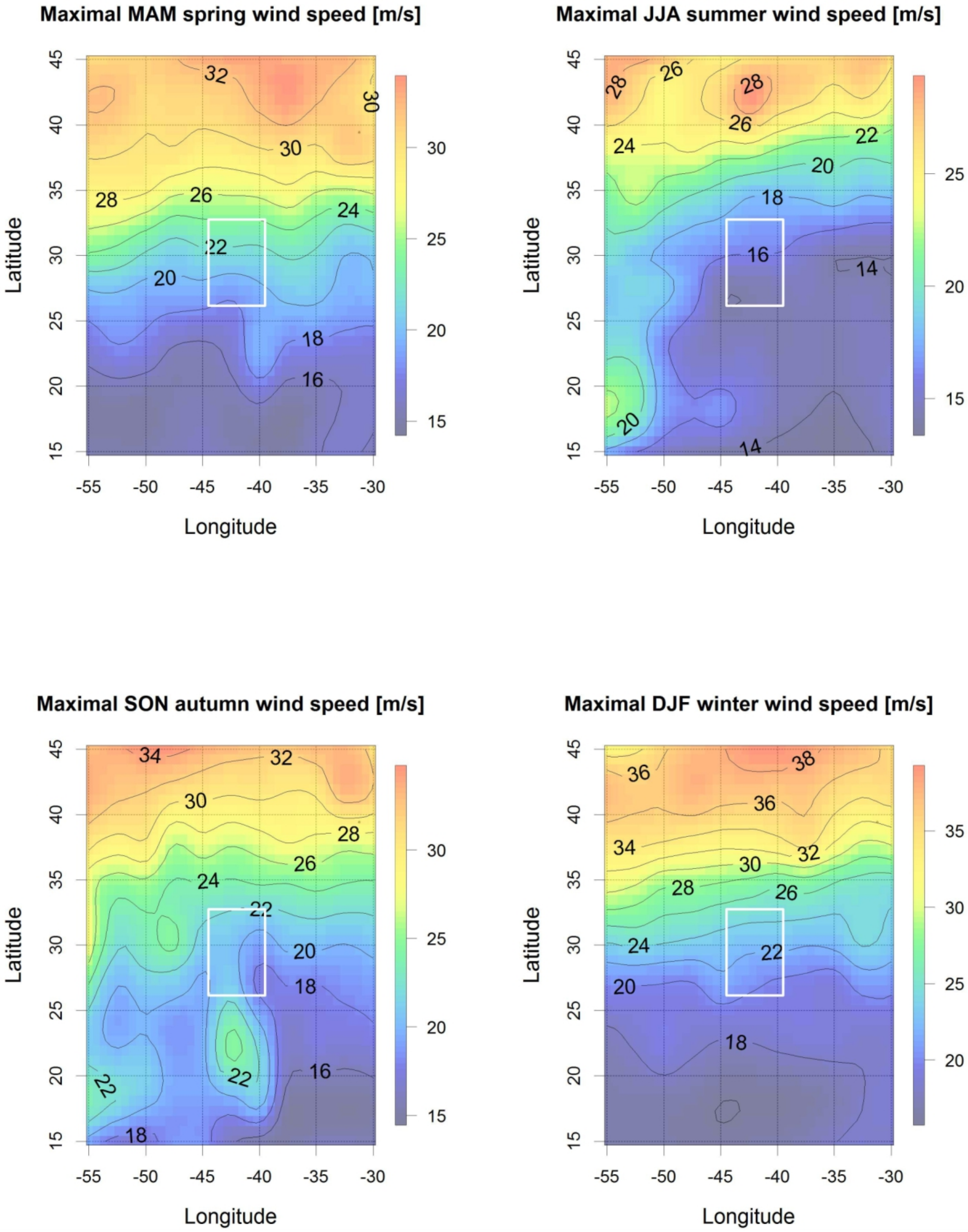

Maximal MAM spring wind speed [m/s]

Maximal JJA summer wind speed [m/s]

Maximal SON autumn wind speed [m/s]

Maximal DJF winter wind speed [m/s]

Fig. 2.4. Maximal 6-hour suistaned values of surface (U10) wind speed in the central North Atlantic by season for 1990-2019, based on the NCEP/NCAR reanalysis. The Polish contract is marked with a white rectangle. See Fig 2.2 for explanation of season symbols.

A review of the whole HURDAT (Landsea and Franklin, 2013) tropical cyclone climatology (1851-2015) shows a total of 26 tracks of named tropical storms and hurricanes crossing the contract area, i.e., 1.5 per decade, although this number needs to be treated as only approximate as the storm tracks in the pre-aircraft era (before 1945) are known only from reanalytical reconstructions based on few observational data. Fig.2.5. shows all the reconstructed tropical storm and hurricane tracks for 1851-2015. It is evident that hurricanes in the region of the contract area usually move from south to north. This is caused by the so-called beta effect, i.e., the force exerted on a tropical cyclone by the meridional gradient of the Coriolis force (Chan and Williams, 1987), thereby pushing the system northward, towards the pole. The U-shaped tracks visible in Fig. 2.5. are the result of the beta effect working together with the easterly circulation south of 30° N and the westerlies north of it. As the contract area is at (or very close to) the latitude of zero zonal circulation in late summer and early autumn, the only significant force working on the cyclone is the beta effect. As a result, the hurricanes threatening the contract area need to be generated south of it or within the area itself. It is well known that tropical cyclones develop and are sustained only over ocean waters of a sea surface temperature (SST) higher than 27°C (various authors refer to a range 25.5 to 27°C). However, the strongest (Category 4 and 5) hurricanes are sustained only above water with SST of 28°C or more (Elsner et al., 2013). Fig. 2.6. shows the September average SST in the central part of North Atlantic for three periods: 1981-2010, 2010-2019, and the year 2029. It can be seen that the 28°C isotherm has, with time, shifted towards the contract area, rendering it warmer than the threshold in 2019, which may explain why the hurricane Lorenzo visited the area at the end of September. With global warming, climate models (Harsma et al., 2013) predict such extreme meteorological events to be become increasingly frequent in the area.

2.1.3.Atmospheric pollution

The Polish contract area lies in the central part of the North Atlantic in a region far away from any continent. The nearest land are the Azores. The upwind position of the archipelago makes it unlikely that any pollution from the archipelago may reach the contract area in question, except for periods in autumn and winter when the westerlies (storms) pass over its northern part. With a typical trade-wind circulation, the closest land areas downwind are the Caribbean islands and South America. The same circulation may bring the Saharan dust plume to the contract area, especially in summer.

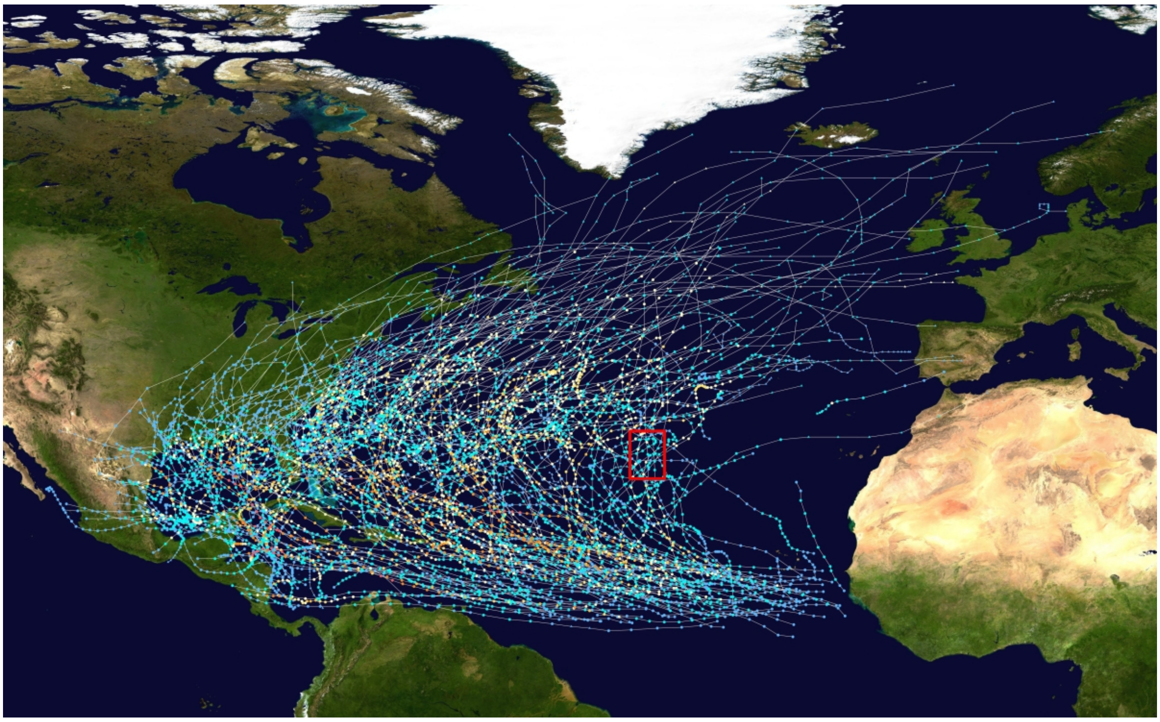

Fig. 2.5. Hurricane and tropical storm tracks, 1851-2015. Approximate location of the Polish contract area is marked with a red rectangle (source: Wikipedia).

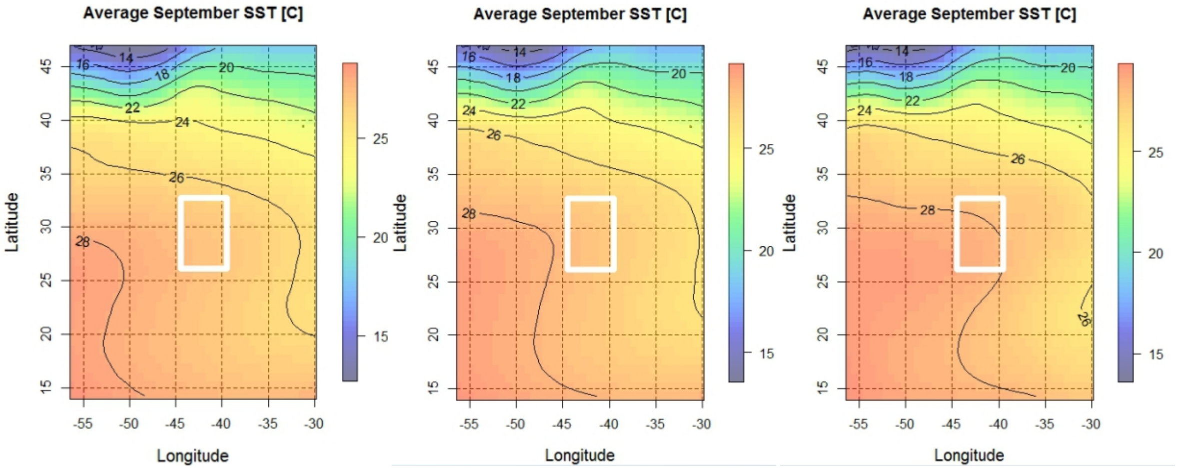

Fig. 2.6. Average September sea surface temperature (SST) in the central North Atlantic from the NCEP/NCAR reanalysis; left: 1081-2010; centre: 2010-2019; right: 2019; the Polish contract area is marked with a white rectangle.

References

American Meteorological Society, 2020. "Saffir–Simpson hurricane scale".

Glossary of Meteorology. [Available at https://glossary.ametsoc.org/wiki/Saffir-simpson_hurricane_scale].

American Meteorological Society, 2020. "Subtropics". Glossary of Meteorology. [Available athttps://glossary.ametsoc.org/wiki/Subtropics].

Bender, F.A.-M., Ramanathan V., Tselioudis, G., 2012. Changes in extratropical storm track cloudiness 1983–2008: observational support for a poleward shift. *Climate Dynamics*, 38, 2037-2053.

Chan, J.C.L., Williams, R.T., 1987. Analytical and numerical studies of the beta-effect in tropical cyclone motion. Part I: Zero mean flow. *Journal of Atmospheric Science*, 44, 1257-1265.

Elsner, J.B., Strazzo, S.E., Jagger, T.H., LaRow, T., Zhao, M., 2013. Sensitivity of limiting hurricane intensity to SST in the Atlantic from observations and GCMs. *Journal of Climate*, 26, 5949-5957.

Gläser, G., Wernli, H., , Kerkweg, A., Teubler, F., 2015. The transatlantic dust transport from North Africa to the Americas—Its characteristics and source regions. *Journal of Geophysical Research: Atmospheres*, 120, 11231-11252.

Haarsma, R.J., Hazeleger, W., Severijns, C., de Vries, H., Sterl, A., Bintanja, A., van Oldenborgh, G.J., van den Brink, H.W., 2013. More hurricanes to hit western Europe due to global warming. *Geophysical Research Letters*, 40, 1783-1788.

Holton, J., Hakim, G.J., 2012. The general circulation. In: Holton, J., Hakim, G.J., *An Introduction to Dynamic Meteorology*, fifth edition. Academic Press, San Diego, CA, 325-375.

Kalnay, E., Kanamitsu, M., Kistler, R., Collins, W., Deaven, D., Gandin, L., Iredell, M., Saha, S., White, G., Woollen, J., Zhu, Y., Chelliah, M., Ebisuzaki, W., Higgins, W., Janowiak, J., Mo, K.K. C., Ropelewski, C., Wang, J., Leetmaa, A., Reynolds, R., Jenne, R., Joseph, D., 1996. The NCEP/NCAR 40-year reanalysis project. *Bulletin of the American Meteorological Society*, 77 (3), 437-471; dx.doi.org/10.1175/1520-0477(1996)077<0437:TNYRP>2.0.CO.

Landsea, C.W., Franklin, J.L., 2013. Atlantic Hurricane Database Uncertainty and Presentation of a New Database Format. *Monthly Weather Review*, 141, 3576-3592.

Rhines, P.B., 2015. Rossby waves. In: North, G.R., Pyle, J., Zhang, F. (eds), *Encyclopaedia of Atmospheric Sciences*. Academic Press, San Diego, CA, vol. 2, 404-416.

Yin, J.H., 2005, A consistent poleward shift of the storm tracks in simulations of 21st century climate. *Geophysical Research Letters*, 32, L18701.

Zelinsky, D.A., 2019. Hurricane Lorenzo (AL 132019), National Hurricane Center Tropical Cyclone Report, https://www.nhc.noaa.gov/data/tcr/AL132019_Lorenzo.pdf

2.2. Hydrography (Waldemar Walczowski)

The Polish contract area is located in the subtropical zone of North Atlantic. The Mid-Atlantic Ridge (MAR) extends across the centre of the area, from the southwest to the northeast. In the region, the highest underwater elevations rise to a depth less than 800 m, the deepest parts are 4900 m deep (EMODnet, 2018). The MAR is crossed by the Atlantis and Hayes fracture zones.

2.2.1.Oceanic circulation

Due to the shape of the Atlantic Ocean, its meridional extension and open, broad connections with the Southern and the Arctic oceans, the circulation is dominated by the large-scale Atlantic Meridional Overturning Circulation (AMOC) (Kuhlbrodt et al., 2007). In the surface layer, the AMOC carries warm, salty water towards the northern and southern polar regions where it cools down, sinks to deep water column layers, and returns towards the equator as dense, cold deep waters. The surface currents (Fig. 2.7.), forced mainly by the wind and thermohaline effects, are more intense and concentrated than the intermediate and deep ones. The temporal, short-term variability of the AMOC is maintained by the Ekman transport; the thermohaline geostrophic component which reflects the east-west density contrasts across the ocean, dominates on interannual to decadal timescales (Buckley and Marshall, 2016).

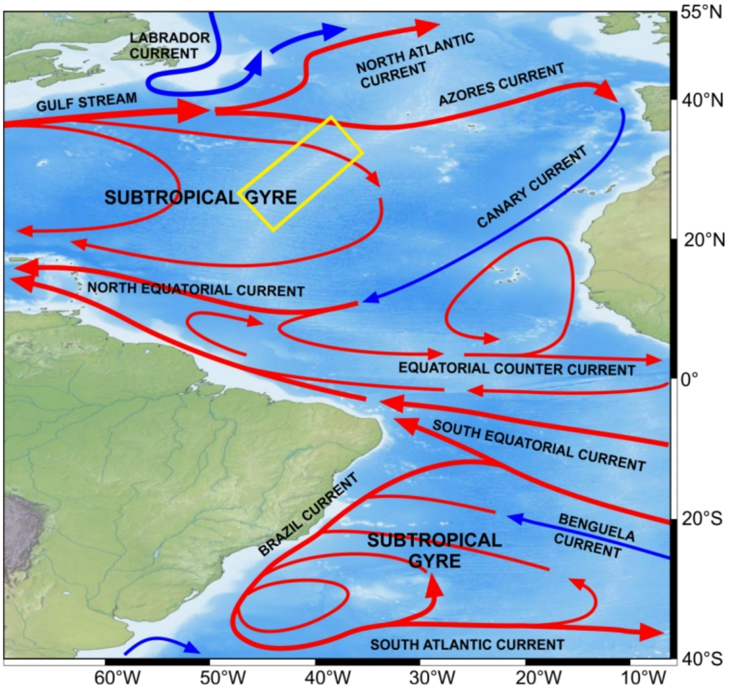

Fig. 2.7. The current pattern in the region.

In the northern hemisphere, the Coriolis force results in a clockwise circulation and concentration of the strongest currents at the western side of the subtropical Atlantic Ocean. The surface northward water transport is dominated by the Gulf Stream. North of the 40° N parallel, the Gulf Stream splits into the northward-flowing North Atlantic Current and eastward-propagating Azores Current (Tomczak and Godfrey, 2001). The Portugal and Canary currents carry the water southward along the southern Europe and the western coasts of Africa. The anticyclonic loop of the North Atlantic Gyre (NAG) is closed by the North Equatorial Current flowing westward between latitudes 10° N and 20° N. The maximum current velocities in the surface layer exceed 100 cm/s, the climatic, averaged transports being an order of magnitude slower. The region of the Polish contract area is situated in the centre of the NAG, so the surface currents sustained by inner, southward flowing branches are less intensive there. The intermediate water pattern is similar to the surface flows, but the velocities much lower, on the order of a few cm/s.

The deep circulation of the Atlantic Ocean is dominated by the Deep Western Boundary Current carrying cold, dense water southward from the Arctic. The presence of the MAR results in numerous local deep currents, steered by the seabed topography. They carry the water both along the MAR and across it, through underwater canyons and rift valleys. All these flows contribute significantly to the enhanced vertical mixing of the deep waters (Mauritzen et al., 2002). The turbulent, diapycnal mixing in rift valleys plays an especially important role (Thurnherr et al., 2002). Tidal processes enhanced by bottom topography also increase mixing. Horizontal and vertical flows associated with hydrothermal vent plumes are observed as well (Thurnherr et al., 2008).

2.2.2. *Water masses*

The distinct layers visible in the circulation pattern result in a general division of water masses (Figs 2.8., 2.9.) into the surface (0-500 m), intermediate (500-1500 m), and deep (1500-bottom) waters (Emery, 2001). Each region features more complex sub-divisions. In general, the surface waters are subject to seasonal variability in solar radiation and atmospheric forcing. Therefore, properties (temperature, salinity, density) of these waters undergo the highest seasonal variability. In addition, a distinct spatial variability is present as well. Argo data from the region over MAR in Polish contract area have revealed temperature and salinity ranges of 20.5-28.0°C and 36.4-37.8, respectively. The intermediate waters are less variable: the temperature and salinity ranges for the Western Atlantic Subarctic Intermediate Water (WASIW) are 3.0-9.0°C and 34.0-35.1, respectively, the respective ranges for the Eastern Atlantic Subarctic Intermediate Water (EASIW) being 3.0-9.0°C and 34.4-35.3.

Dominant is the regional variability, with no distinct seasonal variations. The most stable are the properties of the deep waters. The dominant abyssal water mass in the MAR region is the North Atlantic Deep Water (NADW) with mean temperature and salinity of 1.5-4.0°C and 34.-35.0, respectively. As NADW is formed at the surface from salty waters of the Atlantic origin, it is characterised by relatively high salinity and dissolved oxygen content. The Antarctic Bottom Water (AABW) (-0.9-1.7°C; 34.64-34.72) occurs in the abyssal zone, both on the eastern and western sides of the MAR.

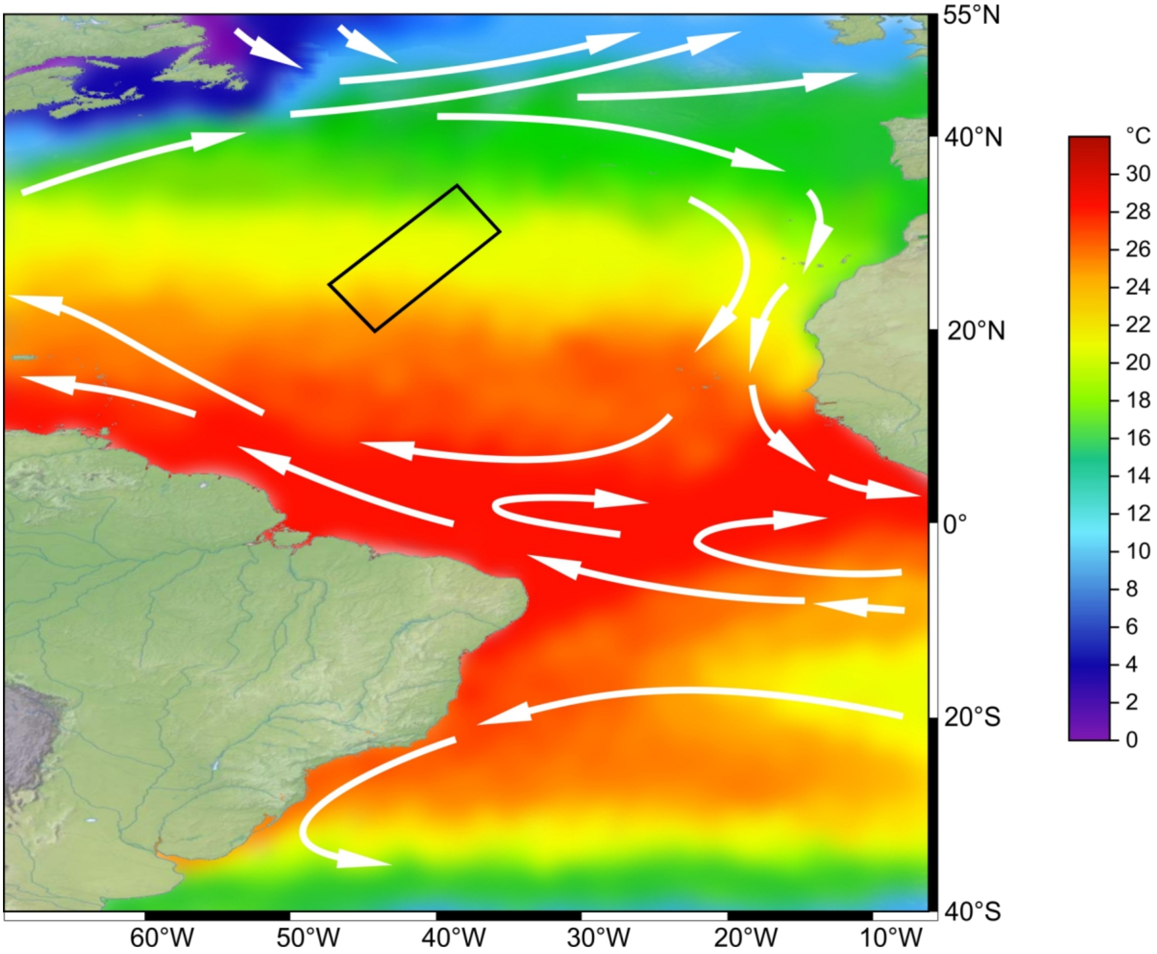

Fig. 2.8. Sea surface temperature in summer

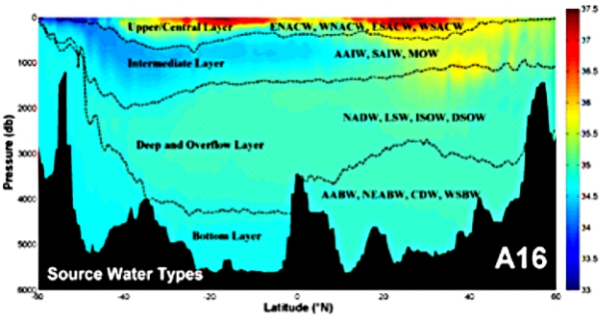

A

Figure 1: Salinity section from the A16 GO-SHIP cruises in 2013

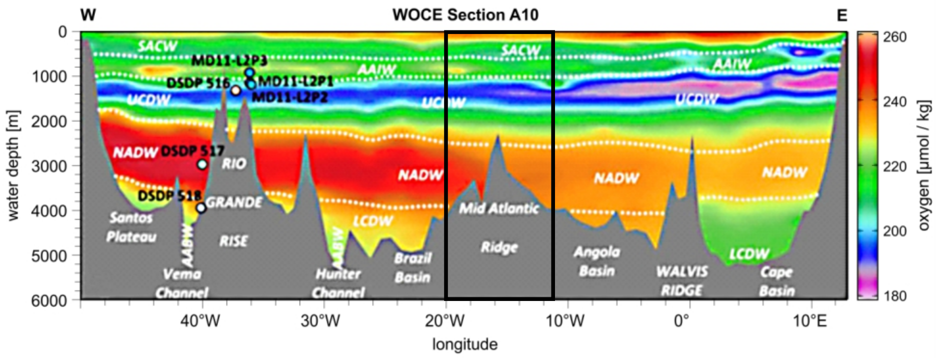

B

Fig. 2.9. Vertical distribution of water masses in the area:
A) N+ S section based on GLODAP v2 data Mian Liu, Toste Tanhua OS 2019
B) East – West cross section showing oxygen content, based on WOCE Section 5
https://www.nodc.noaa.gov/woce/woce_v3/wocedata_2/ewoce/gallery/whp/A5_OXYGEN.gif

References

Buckley M.W., Marshall, J., 2016. Observations, inferences, and mechanisms of the Atlantic Meridional Overturning Circulation: A review. *Reviews of Geophysics*, 54: 5-63.

Emery W.J., 2001. Water Types And Water Masses. In: Steele, J.H. (ed.), *Encyclopedia of Ocean Sciences*, Academic Press, 3179-3187.

EMODnet Bathymetry Consortium (2018): EMODnet Digital Bathymetry (DTM).
doi.org/10.12770/18ff0d48-b203-4a65-94a9-5fd8b0ec35f6

Kuhlbrodt T., Griese, A., Montoya, M., Levermann, A., Hofmann, M., Rahmstorf, S., 2007. On the driving processes of the Atlantic Meridional Overturning Circulation. *Reviews of Geophysics*, 45, 2004RG000166; doi.org/10.1029/2004RG000166

Liu, M., Tanhua, T., 2019. Distribution of Water Masses in the Atlantic Ocean based on 1 GLODAPv2. *Ocean Science Discussions*, doi.org/10.5194/os-2018-140

Mauritzen C., Polzin, K.L., McCartney, M.S., Millard, R.C., West-Mack, D.E., 2002. Evidence in hydrography and density fine structure for enhanced vertical mixing over the Mid-Atlantic Ridge in the western Atlantic. *Journal of Geophysical Research*, 107, C10, 3147, doi:10.1029/2001JC001114, 2002

Thurnherr A.M., Richards, K.J., German, C.R., Lane-Serff, G.F., Speer, K.G., 2002. Flow and Mixing in the Rift Valley of the Mid-Atlantic Ridge. *Journal of Physical Oceanography*, 32, 1763-1778.

Thurnherr A.M., Reverdin, G., Bouruet-Aubertot, P., St. Laurent, L.C., A. Vangriesheim, A., Ballu, V., 2008. Hydrography and flow in the Lucky Strike segment of the Mid-Atlantic Ridge. *Journal of Marine Research*, 66, 347-372.

Tomczak, M., Godfrey, J.S., 2001. *Regional Oceanography: an Introduction*. Pergamon Press.

2.3. **Optical properties of water** (Sławomir Sagan)

According to the classification of oceanic biogeochemical provinces (Longhurst, 2007), the contract area is located in the central part of the North Atlantic Subtropical Gyre (NASTG) province. The optical classification of waters assigns the area to so-called 'Case 1' waters, i.e. whose optical properties depend on the water chlorophyll content, with a small or insignificant influence of non-organic particles and chromophoric dissolved organic matter (CDOM) (Morel and Prieur, 1977). The concurrent processes of light scattering and absorption by water constituents and molecules of water result here in distinctive blue colour of water and its high transparency, with Secchi disc visibility reaching 50 m (Longhurst, 2007). Consequently, the euphotic zone, defined as a depth of 1% of surface solar radiation, reaches down to the 150-200 m depth. Due to the high water transparency, light is detectable down to the bottom of the mesopelagic zone (1000 m), and it colour is centred around the blue light of 485 nm wavelength (Li et al., 2014).

However, compared to the clearest world oceans, the NASTG is considerably less blue than other oligotrophic subtropical zones. The area is characterized by a CDOM content higher than the ocean average, with the light absorption coefficient a_{CDOM}(380 nm) of 0.015-0.025/m (Organelli and Claustre, 2018). This enhanced light absorption in the blue region of the light spectrum is attributed to an elevated local CDOM production by the picophytoplankton, believed to increase in importance under the ocean warming scenario (Organelli and Claustre, 2018). The other water constituent affecting optical properties, i.e., suspended particles, remains low. The light scattering coefficient, b_p(526 nm), a proxy for particle concentration, varies from 0.03 to 0.05/m, which is typical of oligotrophic oceanic waters (Dall'Olmo et al., 2012).

Primary production, chlorophyll contents, and optical properties of the surface water in the area are assessed based on a combination of satellite observations with *in situ* data, acquired mainly during several expeditions of the Atlantic Meridional Transect (AMT) programme (Longhurst, 2007; Tilstone et al., 2009; Brewin et al., 2017; Rees et al., 2017; Tilstone et al., 2017). Primary production varies with the seasonal cycles of chlorophyll contents and changes of the mixed-layer depth (Fig. 2.10.). The monthly averaged depth-integrated primary production varies from 0.15 to 0.65 gC/m^2 d, the chlorophyll concentration ranging within 0.05-0.25 mg/m. The euphotic zone thickness remains relatively stable and varies seasonally between 48 and 52 m. Primary producers in the area are dominated by the smallest phytoplankton size spectra, and the multiyear trend points to a relatively stable primary production (Gregg et al., 2003; Varela et al., 2005; Vicente et al., 2013).

Optical properties of the deep ocean waters depend mainly on the presence of sinking particles, the uniform spatial distribution of which constitutes the background level of the light scattering coefficient similar to that in the upper layer, i.e., around 0.05/m or – in terms of turbidity units – ~40 NTU (Murton et al., 1994). However, optical properties of the water 50-500 m above the bottom might be affected by the buoyant plumes from hydrothermal vents, which transport particulate material (Fig. 2.11.). Hydrothermal plumes can spread laterally over distances of a few to several hundreds kilometres (Resing et al., 2015). Contrasting with the transparent, virtually particle-free background water, the plumes showed turbidity values of 200 NTU, as the light attenuation coefficient in the vicinity of vents exceeding 100/m (Estapa et al., 2015); typical values recorded in coastal waters considered turbid are 5-20/m.

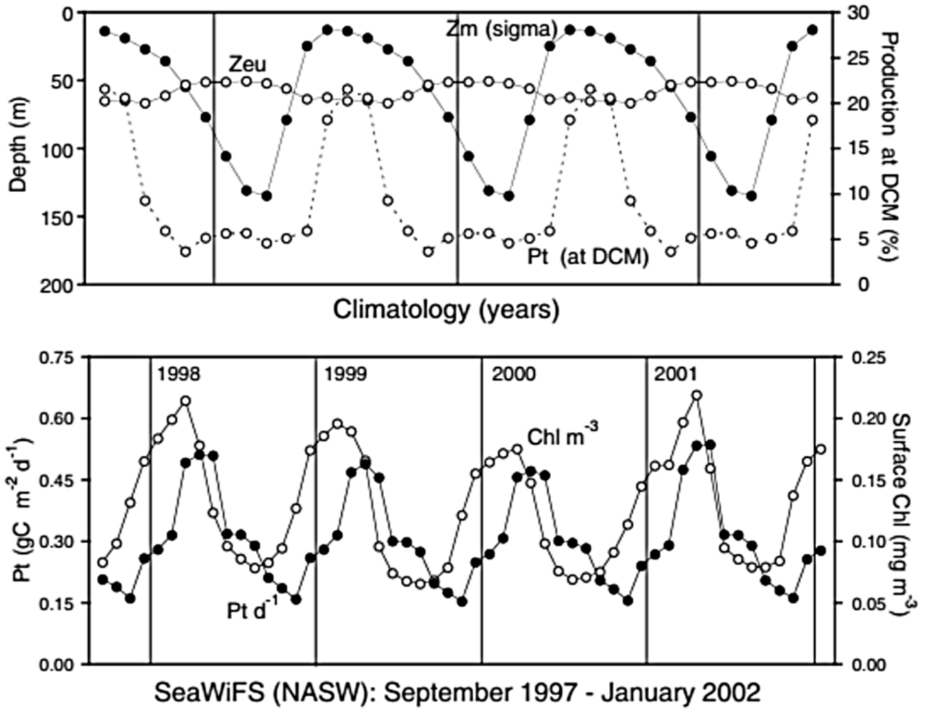

Fig. 2.10. Seasonal cycles of monthly surface chlorophyll (Chl) and depth-integrated autotrophic production (Pt) in the North Atlantic Subtropical Gyre (NASTG) province for 1997–2002 from SeaWiFS data together with characteristic seasonal cycles of mixed-layer depths (Zm), euphotic zone (Zeu) and Pt at the Deep Chlorophyll Maximum depth (Longhurst, 2007).

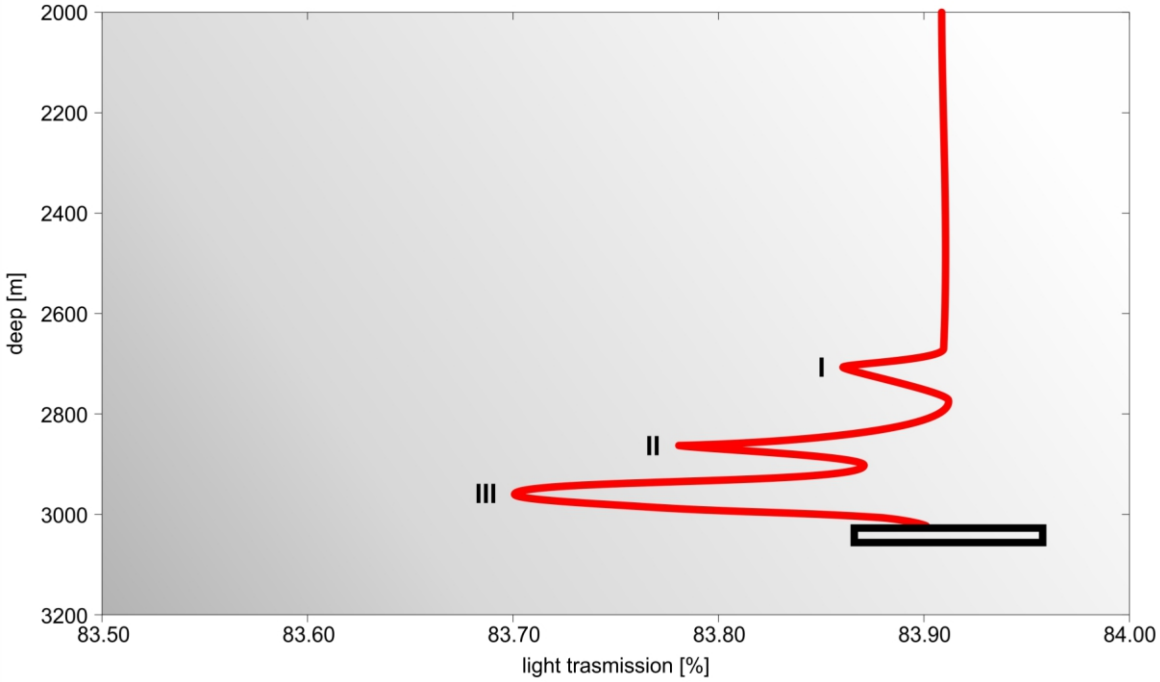

Fig. 2.11. Evidence of the lateral transport of a particle plume from a hydrothermal vent seen as a drop of the light transmission (Murton et al., 1994).

References

Dall'Olmo, G., Boss, E., Behrenfeld, M.J., Westberry, T.K., 2012. Particulate optical scattering coefficients along an Atlantic Meridional Transect. *Optics Express*, 20, 21532. doi.org/10.1364/OE.20.021532

Estapa, M.L., Breier, J.A., German, C.R., 2015. Particle dynamics in the rising plume at Piccard Hydrothermal Field, Mid-Cayman Rise. *Geochemistry, Geophysics, Geosystems*, 16, 2762-2774. doi.org/10.1002/2015GC005831

Gregg, W.W., Conkright, M.E., Ginoux, P., O'Reilly, J.E., Casey, N.W., 2003. Ocean primary production and climate: Global decadal changes. Geophysical Research Letters, 30; 1809, doi: 10.1029/2003GL016889

Li, L., Stramski, D., Reynolds, R.A., 2014. Characterization of the solar light field within the ocean mesopelagic zone based on radiative transfer simulations. *Deep-Sea Research Part I*: *Oceanographic Research Papers*, 87, 53-69. doi.org/10.1016/j.dsr.2014.02.005

Longhurst, A.R., 2007. *Ecological geography of the sea*, 2nd edition. Academic Press, Amsterdam.

Morel, A., Prieur, L., 1977. Analysis of variations in ocean color. *Limnology and Oceanography*, 22, 709-722. doi.org/10.4319/lo.1977.22.4.0709

Murton, B.J., Klinkhammer, G., Becker, K., Briais, A., Edge, D., Hayward, N., Millard, N., Mitchell, I., Rouse, I., Rudnicki, M., Sayanagi, K., Sloan, H., Parson, L., 1994. Direct evidence for the distribution and occurrence of hydrothermal activity between 27° N–30° N on the Mid-Atlantic Ridge. *Earth and Planetary Science Letters*, 125, 119-128. doi.org/10.1016/0012-821X(94)90210-0

Organelli, E., Claustre, H., 2019. Small Phytoplankton Shapes Colored Dissolved Organic Matter Dynamics in the North Atlantic Subtropical Gyre. *Geophysical Research Letters*, 46, 12,183-12,191. doi.org/10.1029/2019GL084699

Rees, A.P., Nightingale, P.D., Poulton, A.J., Smyth, T.J., Tarran, G.A., Tilstone, G.H., 2017. The Atlantic Meridional Transect programme (1995–2016). *Progress in Oceanography*, 158, 3-18. doi.org/10.1016/j.pocean.2017.05.004

Resing, J.A., Sedwick, P.N., German, C.R., Jenkins, W.J., Moffett, J.W., Sohst, B.M., Tagliabue, A., 2015. Basin-scale transport of hydrothermal dissolved metals across the South Pacific Ocean. *Nature,* 523, 200-203. doi.org/10.1038/nature14577

Tilstone, G., Smyth, T., Poulton, A., Hutson, R., 2009. Measured and remotely sensed estimates of primary production in the Atlantic Ocean from 1998 to 2005. *Deep Sea Research Part II: Topical Studies in Oceanography*, 56, 918-930. doi.org/10.1016/j.dsr2.2008.10.034

Tilstone, G.H., Lange, P.K., Misra, A., Brewin, R.J.W., Cain, T., 2017. Micro-phytoplankton photosynthesis, primary production and potential export production in the Atlantic Ocean. *Progress in Oceanography*, 158, 109-129. doi.org/10.1016/j.pocean.2017.01.006

Vicente, V.M., Tilstone, G.H., Sathyendranath, S., Miller, P.I., Groom, S.B., 2012. Contributions of phytoplankton and bacteria to the optical backscaterring coefficient over the Mid- Atlantic Ridge. *Marine Ecology Progress Series*, 445, 37-51.

Varela, M.M., Bode, A., Fernandez, E., Gonzalez, N., Kitidis, V., Varela, M., Woodward, E.M.S., 2005. Nitrogen uptake and dissolved organic nitrogen release in planktonic communities characterised by phytoplankton size-structure in the Central Atlantic Ocean. *Deep Sea Research Part 1*, 52, 1637-1661.

3. Seafloor morphology, geology, sediments and sedimentation processes

Paweł Sydor, Witold Szczuciński, Tomasz Żuk

3.1. Introduction

The mid-ocean ridges form a submarine mountain range (Fig. 3.1.) and are considered to be the largest geological feature on Earth. Their total length is approximately 65,000 km, while they are about 1000 km wide. Altogether they cover ca. 23% of Earth's surface (Earle, 2020). The mid-ocean ridges are located at divergent oceanic plate boundaries, where magmatic and volcanic processes associated with seafloor spreading generate new oceanic crust. The rate of seafloor spreading determines the morphology of the crest of a mid-ocean ridge and its width, with higher spreading rates producing more gentle and wider ridge (e.g., in the Pacific Ocean) and lower spreading rates resulting in a more pronounced, narrower ridge (e.g., in the Atlantic Ocean; Fig. 3.2.). The morphology of mid-ocean ridges is a result of interplay of volcanic, tectonic and sedimentary processes. In the central part, there is usually a well-visible rift valley (Fig. 3.1.). The ridge is dissected by multiple faults: small-scale faults forming local-scale complex topography (e.g., Fig. 3.3.) and large transform faults / fracture zones (Fig. 3.2.), perpendicular to the ridge axis. The accumulation of sediments (mainly pelagic carbonate ooze; Fig. 3.4.) renders – with time and distance from the ridge axis – the seafloor flatter (Figs. 3.1. and 3.3.) (e.g., Mitchell et al., 1998; Priede et al., 2013).

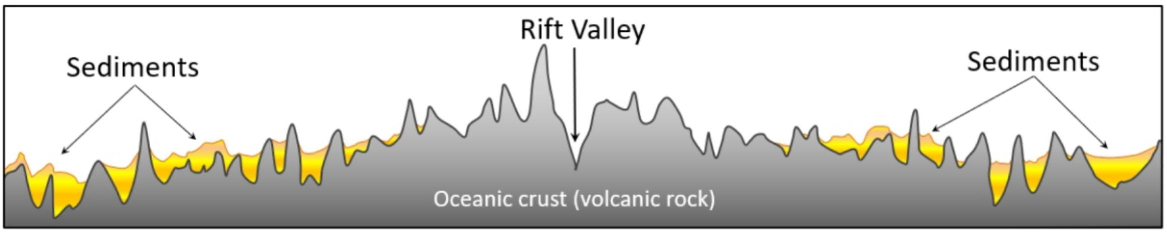

Fig. 3.1. A Cross-section across a typical mid-ocean ridge. Note generally decreasing elevation from the ridge crest outwards, rift valley in the axial part of the ridge, rugged topography and sediment distribution. Sediments cover is thin or absent near the ridge, but it gets generally thicker on either side, as the age of the oceanic crust increases with the distance from the ridge. The cross-section is approximately 50 km long, and has a 10x vertical exaggeration (from Earle, 2020).

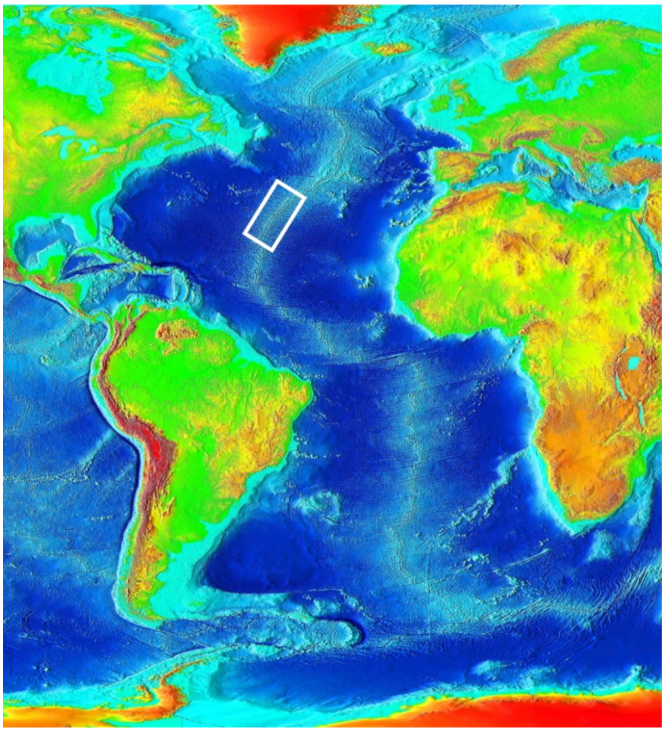

Fig. 3.2. The general view and bathymetry of the Mid-Atlantic Ridge (MAR) (source: http://www.ngdc.noaa.gov/mgg/image/2minrelief.html).

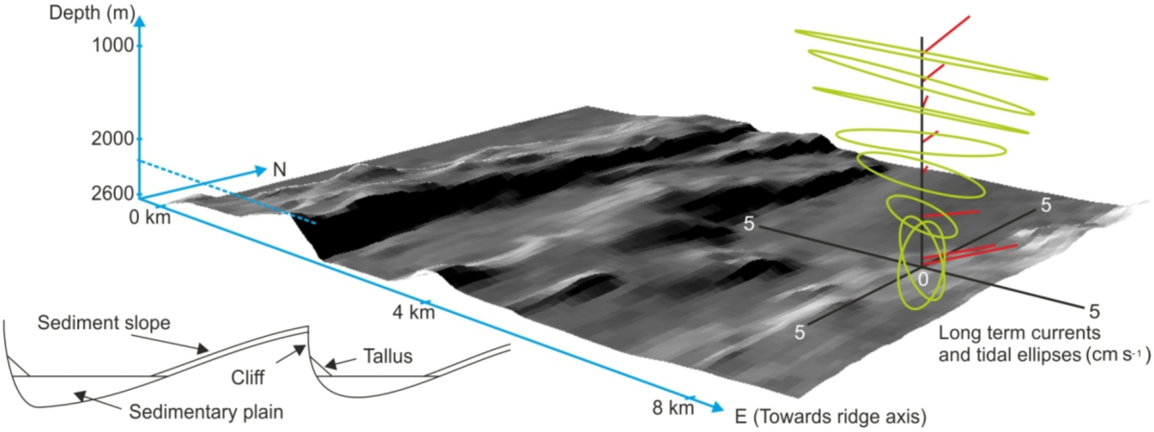

Fig. 3.3. Seafloor topography and water flow on the flanks of the MAR (around 52° N). (a) a 3D projection from swath bathymetry, vertical and horizontal scales are the same; (b) location of the mooring and flow at different heights above the sea floor. Red vectors - long term mean velocity; (c) a diagrammatic cross-section of a flank of the ridge showing the relationship between flat plains, gentle slopes and steep cliffs. The steep cliffs face towards the ridge axis. (Source: Priede et al. 2013). See Fig. 3.4. for typical surface deposits along the cross section.

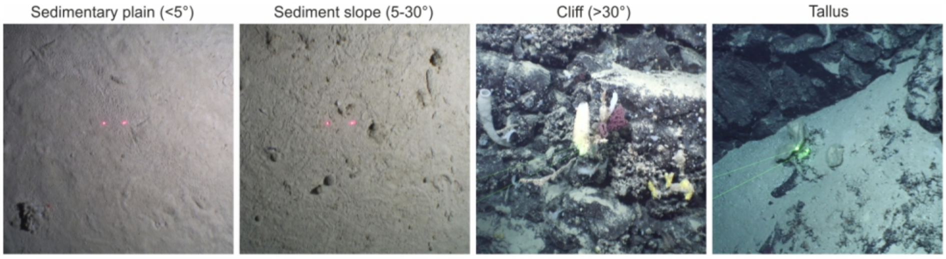

Fig. 3.4. Seafloor images of the Mid-Atlantic Ridge (MAR) (the area identical as that in Fig. 3.3.). Optical ROV images of the seafloor in flat (<5°), gentle-sloping (5–30°) and steep (>30°) terrains on the MAR. Red or green laser spots are 10 cm apart. (Source: Priede et al. 2013).

The first mid-ocean ridge discovered was the Mid-Atlantic Ridge (MAR) (Fig. 3.2.) which was documented already during the famous *Challenger* expedition in 1872-1876. Later, the MAR was the major case study for the development of the plate tectonic theory, while currently it is studied for various basic science goals as well as for practical reasons. The latter includes research on potential environmental impacts of seafloor massive sulphide (SMS) mining. The Polish exploration area is located within the MAR, in the central part of the Atlantic Ocean (Fig. 3.5.), and the objective of the present chapter is to summarise the state-of-the-art data on topography, geology, sedimentary processes and sediments in the MAR, with a particular reference to the Polish exploration contract area (ca. 26-32° N).

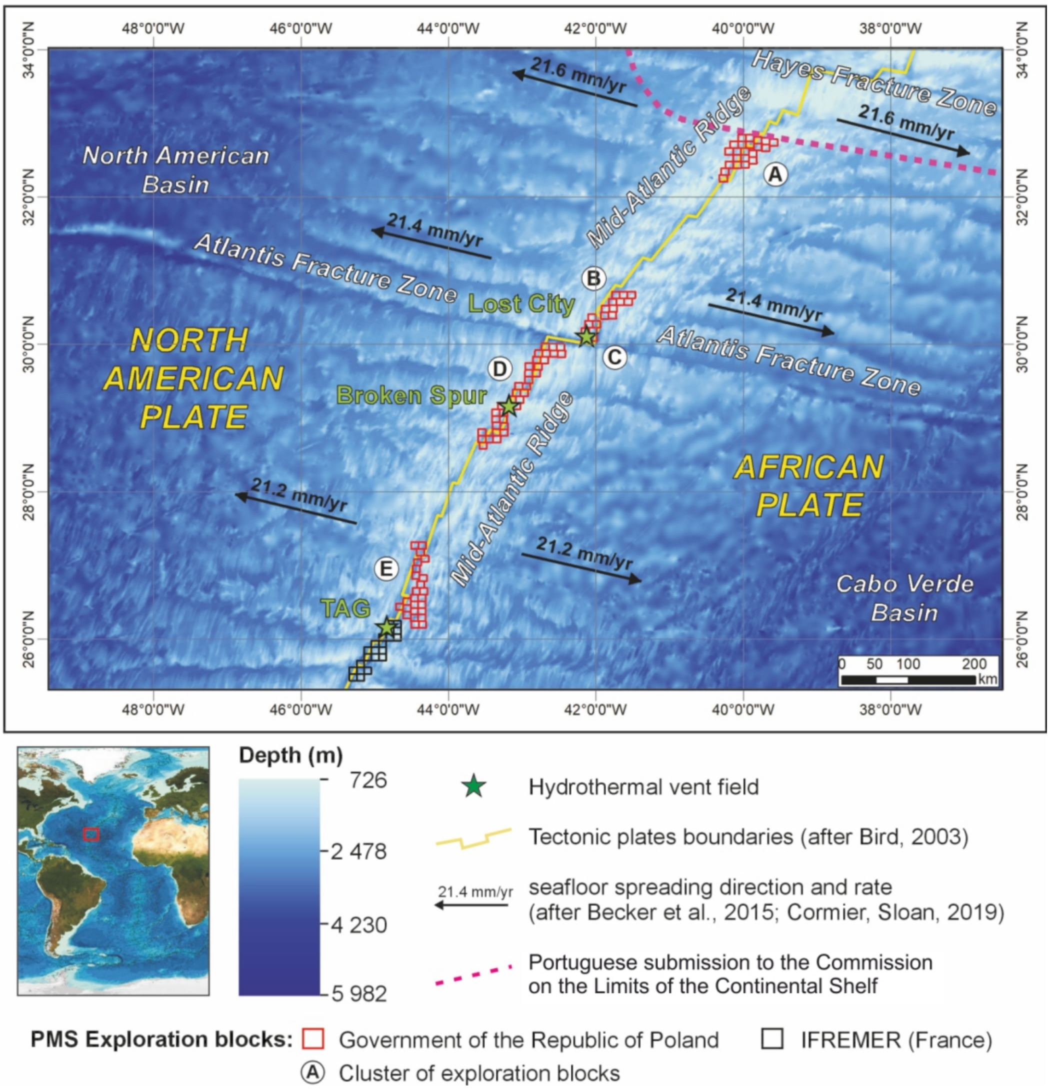

Fig. 3.5. Location of the Polish polymetallic sulphides (PMS) exploration areas [bathymetric data: GEBCO Compilation Group (2020); maritime boundaries: Flanders Marine Institute (2019)].

3.2. Location, morphology and bedrock geology

3.2. Location, morphology and bedrock geology

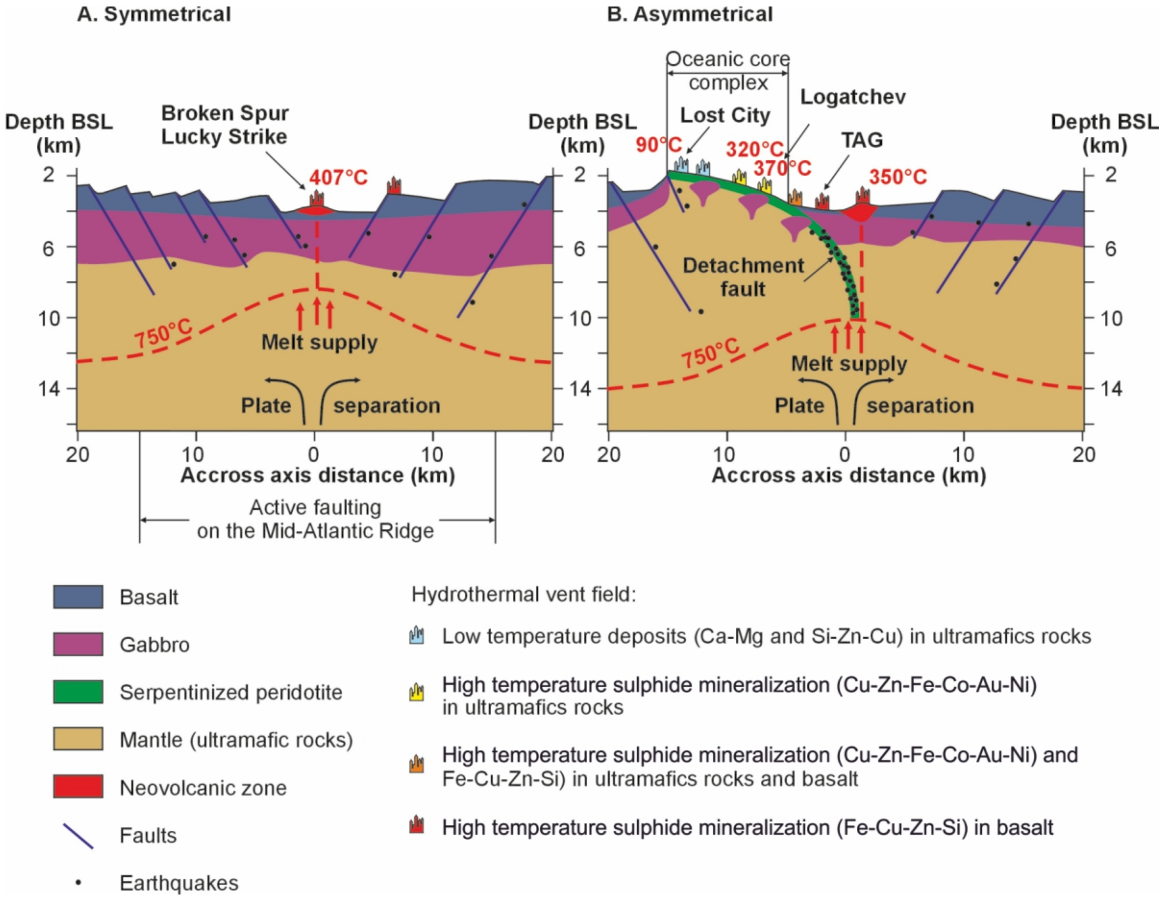

Fig. 3.6. Two types of slow-spreading ridges (McCaig et al., 2007; Escartin et al., 2008; Fouquet et al., 2010, modified). BSL, below the sea level. Locations are provided in Fig. 3.5.

The dominant feature of the seafloor morphology in the area is the MAR (Figs 3.2., 3.5., 3.6.). In this part of the Atlantic Ocean, the MAR trends SW-NE, its relative height being up to 3,000 m. From the west, it is flanked by the North American Basin, the Cabo Verde Basin flanking it from the east. The MAR is divided into segments located between transform faults/fracture zones. In the Polish exploration contract area and its immediate vicinity, there are two large fracture zones perpendicular to the ridge: the Atlantis Fracture Zone and the Hayes Fracture Zone (Fig. 3.5.). These fracture zones are narrow valleys with steep walls over 2,000 m high. The MAR axis features a rift valley, varying in width in the area between 6,000 m in the Atlantis Fracture Zone area to 13,000 m in the southern part of the area. The average relative depth is about 1,700 m. The greatest depth of the rift valley (ca. 4,500 m) is to located in the Atlantis Fracture Zone.

From the tectonic point of view, the area of interest stretches along the divergent boundary of the North American and the African lithospheric plates (Bird, 2003) (Figs. 3.2., 3.5.). The plots located between transform faults/fracture zones were formed by strike-slip faults cutting through the lithospheric plates and laterally displacing sections of the mid-ocean ridge, sometimes by several hundreds of kilometers. Similarly to faults along the mid-ocean ridge, transform fault zones also act as conduits for fluid migration reaching the Earth's mantle, which drives hydrothermal metamorphic processes of the ocean floor. In contrast to the mid-ocean ridge, however, the transform fracture zones usually are free of volcanism, for which reason the upper flanks of normal faults often expose mafic rocks of the lower lithospheric crust and ultramafic rocks of the upper mantle (Wilson, 1965; Batista et al., 2019). In the area of concern, the spreading rates are relatively low, between 21.2 mm/yr in the southern part of to 21.6 mm/yr in the northern part (Fig. 3.5.) (Becker et al., 2015; Cormier and Sloan, 2019). Based on the accretion mode, symmetry of spreading, and type of hosted rocks, two types of slow-spreading ridges have been distinguished: symmetrical accretion with basalts and asymmetrical accretion with gabbro-peridotites (Fig. 3.6.) (McCaig et al., 2007; Escartin et al., 2008; Fouquet et al., 2010). These two geological settings corresponding to two types of segments of the slow-spreading MAR: magmatic, dominated by volcanic processes, and tectonic, where faulting processes predominate (Cherkashov et al., 2016; German et al., 2016).

The oceanic lithosphere in the discussed MAR area is younger than 10 million years, and the age increases with distance from the ridge axis (Müller et al., 2016) (Fig. 3.7.). Thus, in the area of the Polish exploration blocks, the oceanic lithosphere is younger than 3.3 million years.

The seafloor is covered mainly by calcareous ooze (Dutkiewicz et al., 2015) (Fig. 3.8.), as described in more detail below.

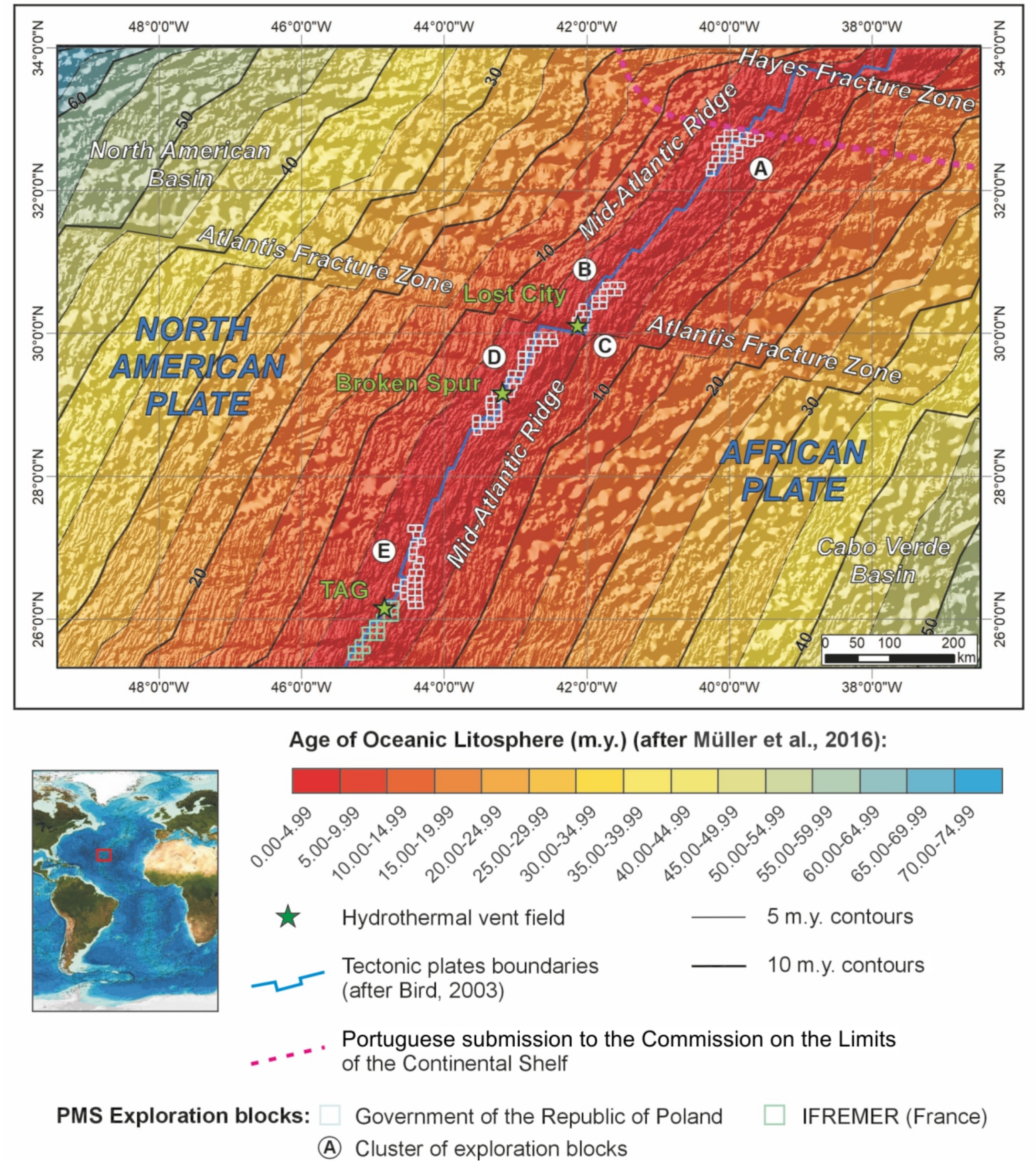

Fig. 3.7. Age of the oceanic lithosphere in the area of concern (after Müller et al., 2016).

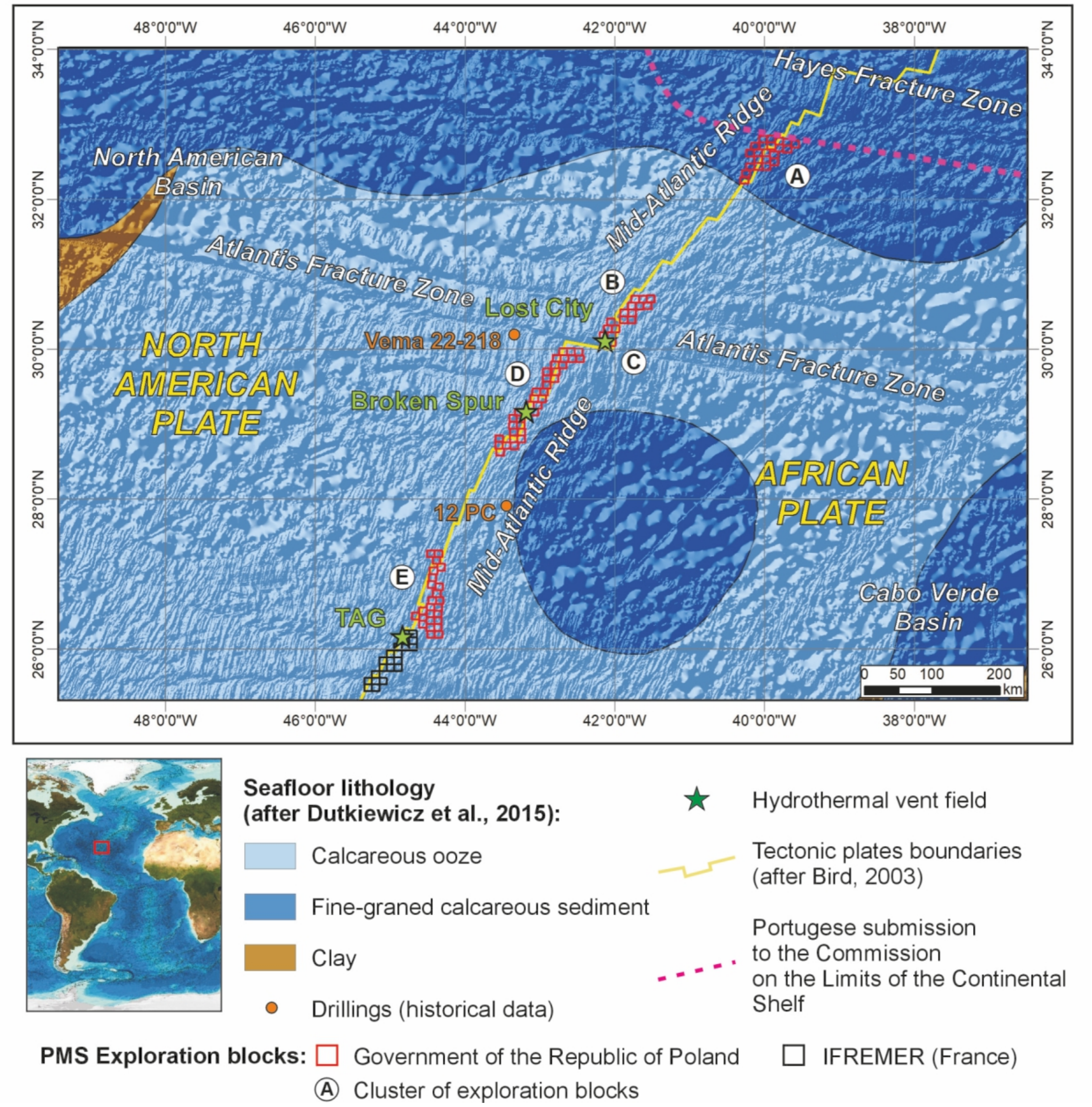

Fig. 3.8. Seafloor sediments in the area adjacent to the Polish PMS exploration blocks (after Dutkiewicz et al., 2015).

The two spectacular features of the area in question are hydrothermal vent fields: Broken Spur and Lost City (Fig. 3.5.). The Broken Spur Hydrothermal Vent Field was discovered in 1993 (Murton, 1993; Murton and Van Dover, 1993). It is located at 29°10’ N on the MAR (Fig. 3.5.). The field is associated with symmetrical seafloor spreading, and is characterized by high-temperature sulphide mineralization (Fig. 3.6.) (McCaig et al., 2007; Escartin et al., 2008; Fouquet et al., 2010). The field covers an area of 150 m from east to west and 100 m from north to south. Broken Spur features two morphological forms with black smoker vents and relicts of sulphide/anhydrite platforms and inactive mounds: the Eastern Valley and the Western Plateau (Fig. 3.9.) (Nesbitt, 1995).

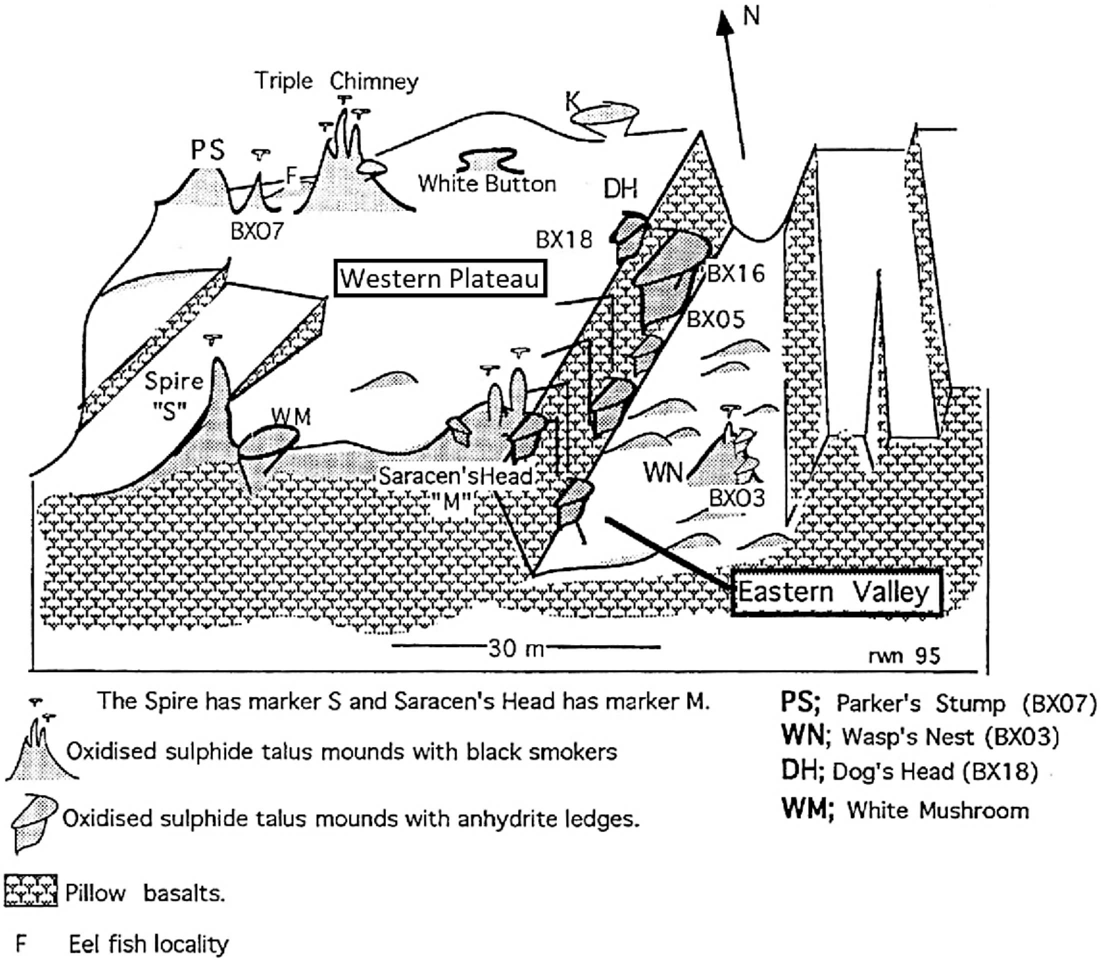

Fig. 3.9. Morphology of the seafloor around Broken Spur (Nesbitt, 1995). For the field location and additional data see Figs 3.5.-3.8.

The Lost City Hydrothermal Vent Field (Figs 3.5.-3.8., 3.10.) was discovered in 2000 (Kelley et al., 2001). The field is associated with asymmetrical seafloor spreading, and is characterized by accumulation of a low-temperature deposit (Fig. 3.6.) (McCaig et al., 2007; Escartin et al., 2008; Fouquet et al., 2010). It is located within the Atlantis Massif, a well-mapped and -studied oceanic core complex (OCC) at ca. 30° N, on the inside corner high between the Atlantis Transform Fault and the MAR (Blackman et al., 2002; Kelley et al., 2005; Karson et al., 2006; Blackman et al., 2008, 2009; Kelley and Shank, 2010) (Figs 3.5., 3.10.). The field hosts carbonate towers rising 60 m above the seafloor (Kelley et al., 2001, 2005; Proskurowski et al., 2008; Lang et al., 2010).

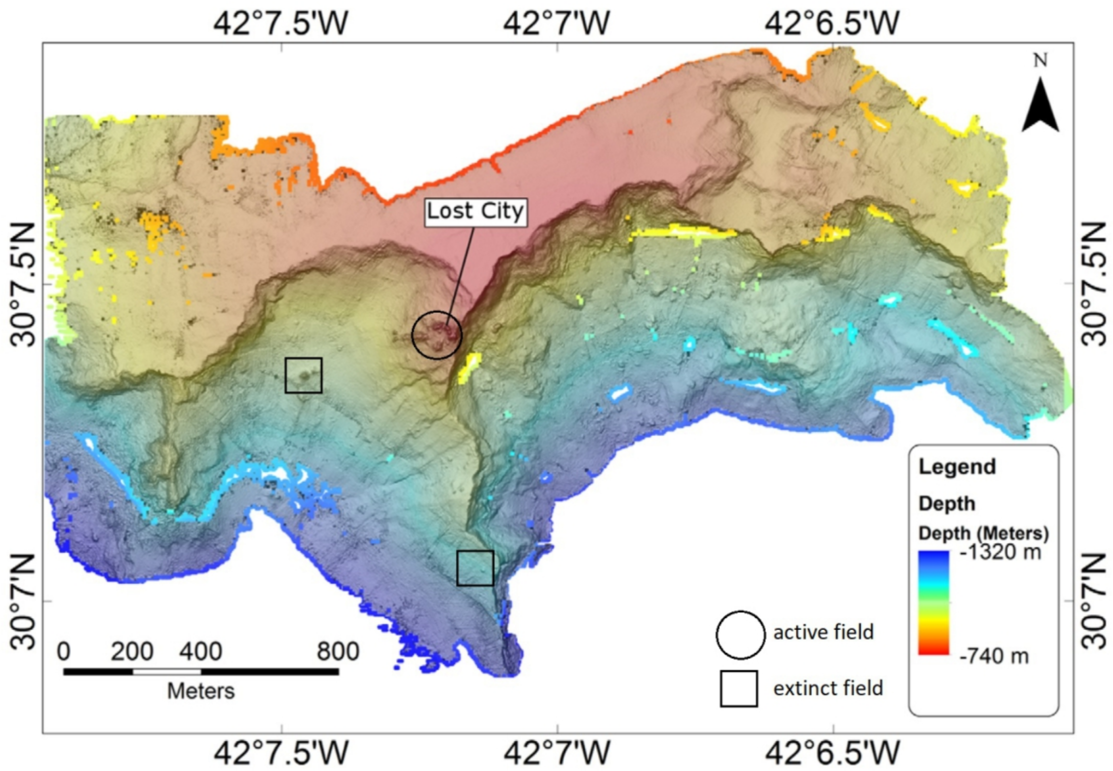

Fig. 3.10. Bathymetry of the Atlantis Massif summit with the Lost City Hydrothermal Vent Field (Denny et al., 2015).

The southern exposure of the Atlantis Massif rises 3,800 m from the base of the Atlantis Transform Fault, culminating in a cliff face about 200 m high (Fig. 3.10.).The cliff rises to a water depth of 740 m below the sea level. It is deeply embayed due to mass wasting and faulting, which exposes massive serpentinite with lesser gabbroic rocks. The wall terminates in a 50-100 m thick, variably deformed zone that defines the main Atlantis Massif Detachment Shear Zone at the summit of the massif. Over the summit of the Atlantic Massif, there lies unconformably a polymict breccia (rounded clasts of serpentinite, gabbro, talc-tremolite nodules, and subangular weathered basalt in a micritic carbonate matrix) and carbonate caprock (pelagic fossil-rich micritic carbonate and hydrothermal carbonate). These deposits are up to 2 m thick (Kelley et al., 2001; 2005; Früh-Green et al., 2003; Karson et al., 2006; Denny et al., 2015).

The main part of the field is at a water depth of about 740 m (Fig. 3.10.). The core of the field is dominated by the Poseidon complex comprised of four adjoining massive edifices. Discrete chimneys, and chimney arrays, extend from the Poseidon complex northward and to the east (Kelley et al., 2005, Denny et al., 2015). The main tower rises 60 m above the seafloor and tapers to a summit 15 m in diameter. The bulk of the main tower is composed of indurated carbonate heavily crosscut with more recent carbonate veins. The summit of the tower hosts two carbonate structures venting fluids at up to 88°C (Ludwig et al., 2006). Age-dating of 67 carbonate deposits within the central Lost City Hydrothermal Field yielded the ages ranging from modern to 120,000 years old (Ludwig et al., 2011). In addition, two relict hydrothermal fields were discovered within the area (Fig. 3.10).

3.3. Deep-sea sediments

The sediment distribution on the MAR was of interest already since the 1960s, as the sediment cover thickness was used as an indicator of the seafloor spreading rate and an argument on the nature of this process (continues vs. stepwise) (e.g., Ewing and Ewing, 1967). However, although generally the sediment thickness is expected to thicken systematically with distance from the spreading axis, as would be expected from the increasing seafloor age (Figs. 3.1., 3.7.), it is not always the case (see Fig. 3.3.). For instance, Mitchell et al. (1998) applied a deep-tow sediment profiler system in the ridge area around 29^{0} N, and found the sediments on the young (<2.5 million years) seafloor, at a distance up to about 40 km west and east from the spreading axis, respectively, to reveal no consistent thickening with distance from the axis. They have documented thicker deposits in depressions, with sediment thickness on the order of 10-15 m, in some cases >25 m. Many of the deposits appeared to drape the basement topography and occured also on promontories, so the sediment was probably mainly deposited from suspension rather than from turbidity currents or other gravity flows. Enhanced sedimentation rates in deeper areas could partly be due to redeposition, as the MAR is well-known as a seismically active area (e.g., Fig. 3.6.). Mitchell et al. (1998) estimated also the sediment accumulation rate over the MAR. They computed sediment accumulation rates by dividing the average thicknesses by the corresponding basement ages estimated from magnetic field reversals, and came with values on the order of 5 to 24 mm/kyr. This range is similar to the sediment accumulation rate estimates from elsewhere along the MAR, for instance along 37° N (Marks, 1981; Mitchell, 1995).

There are only several published observational data on the seafloor sediments within the Polish exploration blocks on the MAR. In general, since the area is shallower than the carbonate compensation depth (CCD; ca. 5,000 m below the sea surface), the seafloor surface sediments are composed mainly of calcareous ooze (Dutkiewicz et al., 2015) (Fig. 3.8.). In the area of interest, as few as four longer cores were obtained (the IODP site in Lost City, Vema 22-218, 12PC, and TAG; see Fig. 3.8. for locations).

In the IODP drilling within Lost City, the bottom of the calcareous ooze was reached at 2 m below the seafloor (Denny et al., 2015). The rock samples obtained from dredges and IODP drillings (https://maps.ngdc.noaa.gov/viewers/marine_geology) implied that the calcareous ooze was underlined by igneous rocks (porphyritic olivine basalt, feldspar rich basalt, glassy basalt) and serpentine with relics of pyroxene and olivine (Denny et al., 2015).

The thickest cover of at least 5.85 m (the bottom of the sedimentary cover was not reached during the coring) was found in the Atlantis Fracture Zone, 115 km west of the Lost City Hydrothermal Vent Field in core Vema 22-218 (https://maps.ngdc.noaa.gov/viewers/marine_geology) (Fig. 3.8.). The sediment in that core was grayish-orange to moderate yellowish-brown, and the vertical sedimentary profile was composed of intercalated layers of foraminiferal chalk, marl and ooze. The coarse fraction was made up of planktonic and benthic foraminifera as well as rare pteropods. Moreover, infrequent manganese micronodules and andesite-basaltic rock fragments were encountered.

Core No. 12PC, taken on the MAR in an area between the D and E exploration cluster blocks (https://maps.ngdc.noaa.gov/viewers/marine_geology) (Fig. 3.8.), showed 5.17 m of calcareous ooze. The bottom of the series was not reached. The coarse fraction was made up by foraminifera. The ooze was light-yellow-brown to very pale brown.

In the southern part of the studied area, in the axial part of MAR, is located Trans-Atlantic Geotraverse (TAG) Hydrothermal Field (Fig. 5) at about 26° N. Metz et al. (1988) have collected and investigated a 120 cm long core from metalliferous sediment, covering app. 14,000 years of hydrothermal depositional history in that area. During the periods of high hydrothermal activity, the sediments were composed almost entirely from hydrothermally derived elements (Fe, Cu, Zn, Mn, V, Pb, Cd, Hg) with less than 3% of carbonates. While, during periods of decreased hydrothermal activity the sediments were composed in over 60% of carbonates. The calculated sediment accumulation rates varied in that core from 1 to >30 g/cm2/kyr throughout the core.

3.4. Sediment sources and sedimentation processes

The scarcity of data on sediments and sedimentary processes within the area of concern does not allow for any comprehensive overview of the sedimentary regime over the MAR between 26 and 34° N. However, the available information on similar sediment accumulation rate in this part of the MAR (Mitchel et al., 1998) and in the sectors nearby (e.g., Marks, 1988) as well as similar general properties of the sediments along most of the northern MAR (Dutkiewicz et al., 2015; Khusid et al., 2018; Fig. 3.8.) suggest similarity of some major sediment sources and the sedimentation processes.

With regard to the MAR sediment sources, an interesting study based on mineralogical and geochemical properties of mid-oceanic ridge sediments (for section between 45 and 65^{0} N) was conducted by Grousset and Chesselet (1986). They focussed on the sediment mineral fraction (so the analysis excluded the dominant biogenic carbonates).

Using a number of tracers, they identified the North America mainland (Fig. 3.2.) as the main source of the sediment supplied by surface currents, turbidity currents and aeolian transport, Iceland being the second major source, with the material transported by turbidity currents and the geostrophic current flow. The MAR itself was found to supply only a minor amount of the sedimentary material. The MAR section of interest for this report is more southward. It is located further away from the North America mainland and Iceland, while the Azores are much closer, so the relative contribution of the particular sources may be different.

In terms of the acting processes, it seems that sedimentation from the pelagic the dominant mode of deposition (Mitchell et al., 1998). However, the existing data suggest also a likely sediment redistribution. The latter is facilitated by seismic activity mobilizing sediments on the slopes (e.g., Figs. 3.3.-3.4.), regular near-bottom currents (e.g., Priede et al., 2013; Fig. 3.3.), or benthic storms (Kerr, 1980). The mineral fraction of the MAR may be easily mobilised because of its very fine fraction, often in the fine silt mode (Alt et al., 2019). This sediment fraction is easier to resuspend than the smaller clay fraction, as cohesion forces are of less importance. The resuspension susceptibility of the sediment must be considered as an important environmental issue, particularly in the regions where seafloor massive sulphides (SMS; also referred to as polymetallic sulphides, PMS) are intended for mining (e.g., Dunn et al., 2018). It is exceptionally important in the case of sediments sourced from hydrothermal vents, which contain very high concentrations of potentially toxic metals and metalloids (e.g., Metz et al., 1988; Dias et al., 2008).

3.5. Conclusions

In terms of the sea-floor morphology and some of the geological problems, the Polish exploration contract area on the MAR is moderately known. However, the current knowledge of sediments and sedimentary processes is very limited. The sedimentary cover is from few to over 20 m thick, thicker in depressions, composed mainly of carbonate ooze, which in the neighbourhood of hydrothermal vents may be extremely enriched in metals and metalloids. Any future activity in the region will need to include sediment mapping, to consider analysis of modern sedimentation processes and sediment sources, and will have to assess a potential impact of metal-enriched sediment resuspension on the benthic ecosystems.

References

Alt, C.H.S., Kremenetskaia (Rogacheva), A., Gebruk, A.V., Gooday, A.J., Jones, D.O.B., 2019. Bathyal benthic megafauna from the Mid-Atlantic Ridge in the region of the Charlie-Gibbs fracture zone based on remotely operated vehicle observations. Deep-Sea Research Part I, 145, 1-12. https://doi.org/10.1016/j.dsr.2018.12.006

Batista, L., Gasperini, L., Burwicz, E.B., Neres, M., Nuzzo, M. 2019. Marine Transform Faults and Fracture Zones: A Joint Perspective Integrating Seismicity, Fluid Flow and Life. Frontiers in Earth Science, 7 (Article 39). 1-29. https://doi.org/10.3389/feart.2019.00039

Becker, T.W., Schaeffer, A.J., Lebedev, S., Conrad, C.P., 2015. Toward a generalized plate motion reference frame. Geophysical Research Letters, 42. 3188-3196. https://doi.org/10.1002/2015GL06369

Bird, P., 2003. An updated digital model of plate boundaries. Geochemistry, Geophysics, Geosystems, 4. 1027. https://doi.org/10.1029/2001GC000252

Blackman, D.K., Canales, J.P., Harding, A., 2009. Geophysical signatures of oceanic core complexes, Geophysical Journal International, 178, 593-613. doi:10.1111/j.1365-246X.2009.04184.x

Blackman, D.K., Karner, G.D., Searle, R.C., 2008. Three-dimensional structure of oceanic core complexes: Effects on gravity signature and ridge flank morphology, Mid-Atlantic Ridge, 30° N. Geochemistry, Geophysics, Geosystems, 9(6), Q06007. https://doi.org/doi:10.1029/2008GC001951

Blackman, D.K., Karson, J.A., Kelley, D.S., Cann, J.R., Früh-Green, G.L., Gee, J.S., Hurst, S.D., John, B.E., Morgan, J., Nooner, S.L., Kent Ross, D., Schroeder, T.J., Williams, E.A., 2002. Geology of the Atlantis Massif (Mid-Atlantic Ridge, 30° N): Implications for the evolution of an ultramafic oceanic core complex. Marine Geophysical Research, 23, 443-469. https://doi.org/10.1023/B:MARI.0000018232.14085.75

Cherkashov, G., Egorov, I., Kuznetsov, T., Mitina, E., Petukhov, S., Poroshina, I., Seleznev, A., 2016. Materials for ISA application for the exploration of the polymetallic massive sulfides (Report according to the agreement with Polish Geological Institute – National Research Institute). Federal State Budget Enterprise, "I.S. Gramberg All-Russia Research Institute for Geology and Mineral Resources of the Ocean" (FSBE "VNIIOkeangeologia")

Cormier, M.□H., Sloan, H., 2019. Distinctive seafloor fabric produced near western versus eastern ridge transform intersections of the northern Mid-Atlantic Ridge: Possible nfluence of ridge migration. Geochemistry, Geophysics, Geosystems, 20(4). 1734-1755. https://doi.org/10.1029/2018GC008101

Denny, A.R., Kelley, D.S., Früh-Green, G.L., 2015. Geologic evolution of the Lost City Hydrothermal Field. Geochemistry, Geophysics, Geosystems, 17, 375-394. https://doi.org/10.1002/2015GC005869

Dias, A.S., Millis, R.A., Taylor, R.N., Ferreira, P., Barriga, F.J.A.S., 2008. Geochemistry of a sediment push-core from the Lucky Strike hydrothermal field, Mid-Atlantic Ridge. *Chemical Geology*, 247, 339-351. https://doi.org/10.1016/j.chemgeo.2007.10.015

Dunn, D.C., Van Dover, S.L., Etter, R.J., Smith, C.R., Levin, L.A., Morato, T., Colaço, A., Dale, A.C., Gebruk, A.V., Gjerde, K.M., Halpin, P.N., Howell, K.L., Johnson, D., Perez, J.A.A., Ribeiro, M.C., Stuckas, H., Weaver, P., SEMPIA Workshop Participants, 2018. A strategy for the conservation of biodiversity on mid-ocean ridges from deep-sea mining. *Science Advances*, 4, eaar4313. doi: 10.1126/sciadv.aar4313

Dutkiewicz, A., Müller R.D., O'Callaghan, S., Jóson, H., 2015. Census of seafloor sediments in the world's ocean. *Geology*, 43, 795-798. https://doi.org/10.1130/G36883.1

Earle, S., 2020. *Physical Geology*, 2nd edition. Thompson Rivers University.

Escartín, J., Smith, D.K., Cann, J., Schouten, H., Langmuir, C.H., Escrig, S., 2008. Central role of detachment faults in accretion of slow-spreading oceanic lithosphere. *Nature*, 455(7214), 790-794.
https://doi.org/10.1038/nature07333

Ewing, J., Ewing, M., 1967. Sediment distribution on the Mid-Ocean Ridges with respect to Sspreading of the sea floor. Science, 156, 1590-1592. doi: 10.1126/science.156.3782.1590

Flanders Marine Institute, 2019. *Maritime Boundaries Geodatabase*, version 11. Available online at http://www.marineregions.org/. https://doi.org/10.14284/382

Fouquet, Y., Cambon, P., Etoubleau, J., Charlou, J.L., Ondreas, H., Barriga, F.J.A.S., Cherkashov, G., Semkova, T., Poroshina, I., Bohn, M., Donval, J.P., Henry, K., Murphy, P., Rouxel, O., 2010. Geodiversity of hydrothermal processes along the Mid-Atlantic Ridge and ultramafic hosted mineralization: a new type of oceanic Cu-Zn-Co-Au volcanogenic massive sulfide deposit. *Geophysical Monograph Series*, 188, 321-367.
https://doi.org/10.1029/2008GM000746

Früh-Green, G.L., Kelley, D.S., Bernasconi, S.M., Karson, J.A., Ludwig, K.A., Butterfield, D.A., Boschi, C., Proskurowski, G., 2003. 30,000 years of hydrothermal activity at the Lost City vent field. *Science*, 301, 495-498. https://doi.org/10.1126/science.1085582

GEBCO Compilation Group, 2020. GEBCO 2020 Grid. https://doi.org/10.5285/a29c5465-b138-234d-e053-6c86abc040b9

German, C., Petersen, S., Hannington, M.D., 2016. Hydrothermal exploration of midocean ridges: Where might the largest sulfide deposits occur? *Chemical Geology*, 420, 114-126. https://doi.org/10.1016/j.chemgeo.2015.11.006

Grousset, F.E., Chesselet, R., 1986. The Holocene sedimentary regime in the northern Mid-Atlantic Ridge region. *Earth and Planetary Science Letters*, 78, 271-287. https://doi.org/10.1016/0012-821X(86)90067-1
https://maps.ngdc.noaa.gov/viewers/marine_geology - drillings profiles and drillings location data (version 2.7.0, last updated 5/17/2019)

Karson, J.A., Früh-Green, G.L., Kelley, D.S., Williams, E.A., Yoerger, D.R., Jakuba, M., 2006. Detachment shear zone of the Atlantis Massif core complex, Mid-Atlantic Ridge, 30°N. *Geochemistry, Geophysics, Geosystems*, 7, Q06016. https://doi.org/10.1029/2005GC001109

Kelley, D.S., Karson, J.A., Blackamn, D.K., Früh-Green, G.L., Butterfield, D.A., Lilley, M.D., Olson, E.J., Schrenk, M.O., Roe, K.K., Lebon, G.T., Rivizzigno, P., the AT3-60 Shipboard Party, 2001. An off-axis hydrothermal vent field near the Mid-Atlantic Ridge at 30°N. *Nature*, 412, 145-149. https://doi.org/10.1038/35084000

Kelley, D.S., Karson, J.A., Früh-Green, G.L., Yoerger, D.R., Shank, T.M., Butterfield, D.A., Hayes, J.M., Schrenk, M.O., Olson, E.J., Proskurowski, G., Jakuba, M., Bradley, A., Larson, B., Ludwig, K., Glickson, D., Buckman, K., Bradley, A.S., Brazelton, W.J., Roe, K., Elend, M.J., Delacour, A., Bernasconi, S.M., Lilley, M.D., Baross, J.A., Summons, R.E., Sylva, S.P., 2005. A serpentinite-hosted ecosystem: The Lost City hydrothermal field. *Science*, 307, 1428-1434. https://doi.org/10.1126/science.1102556

Kelley, D.S., Shank, T.M., 2010. Hydrothermal systems: A decade of discovery in slow spreading environments. Diversity of Hydrothermal Systems on Slow Spreading Ocean Ridges, 188, 369–407. https://doi.org/10.1029/2010GM000945

Kerr, R.A., 1980. A New Kind of Storm Beneath the Sea. *Science*, 208, 484-486. doi: 10.1126/science.208.4443.484

Khusid, T.A., Os'kina, N.S., Lukashina, N.P., Gablina, I.F., Libina, N.V., Matul, G., 2018. Benthic and plankton foraminifers in hydrothermally active zones of the Mid-Atlantic Ridge (MAR). *Stratigraphy and Geological Correlation*, 26, 109-120. doi:10.1134/S0869593817060041

Lang, S.Q., Butterfield, D.A., Schulte, M., Kelley, D.S., Lilley, M.D., 2010. Elevated concentrations of formate, acetate and dissolved organic carbon found at the Lost City hydrothermal field. *Geochimica et Cosmochimica Acta*, 74(3), 941-952. https://doi.org/10.1016/j.gca.2009.10.045

Ludwig, K.A., Kelley, D.S., Butterfield, D.A., Nelson, B.K., Früh-Green, G.L., 2006. Formation and evolution of carbonate chimneys at the Lost City Hydrothermal Field. *Geochimica et Cosmochimica Acta*, 70, 3625-3645. https://doi.org/10.1016/j.gca.2006.04.016

Ludwig, K.A., Shen, C.C., Kelley, D.S., Cheng, H., Edwards, R.L., 2011. U-Th systematics and 230Th ages of carbonate chimneys at the Lost City Hydrothermal Field. *Geochimica et Cosmochimica Acta*, 75(7), 1869-1888. https://doi.org/10.1016/j.gca.2011.01.008

Marks, N.S., 1981. Sedimentation on new ocean crust: The Mid-Atlantic Ridge at 37° N. *Marine Geology*, 43, 65-82. https://doi.org/10.1016/0025-3227(81)90129-8

McCaig, A.M., Cliff, R.A., Escartín, J., Fallick, A.E., MacLeod, C.J., 2007. Oceanic detachment faults focus very large volumes of black smoker fluids. *Geology*, 35(10), 935-938. https://doi.org/10.1130/G23657A.1

Metz, S., Trefry, J.H., Nelsen, T.A., 1988. History and geochemistry of a metalliferous sediment core from the Mid-Atlantic Ridge at 26° N. *Geochimica et Cosmochimica Acta*, 52, 2369-2318.

Mitchell, N.C., 1995. Diffusion transport model for pelagic sediments on the Mid-Atlantic Ridge. *Journal of Geophysical Research,* 100, 19991-20009.

Mitchell, N.C., Allerton, S., Escartin, J., 1998. Sedimentation on young ocean floor at the Mid-Atlantic Ridge, 29° N. *Marine Geology, 148, 1-8.*

Murton, B.J., 1993. Geological and geochemical investigations between 27° N and 30° N of the Kane-Atlantis segment: the Mid-Atlantic Ridge. I*nstitute of Oceanographic Sciences Deacon Laboratory, Cruise Report* No. 236.

Murton, B.J., Van Dover, C.L., 1993. ALVIN dives on the Broken Spur Hydrothermal Vent Field at 29°10' N on the Mid-Atlantic Ridge. *BRIDGE Newsletter*, 5, 11-14.

Müller, R.D., Seton, M., Zahirovic, S., Williams, S.E., Matthews, K.J., Wright, N.M., Shephard, G.E., Maloney, K.T., Barnett-Moore, N., Hosseinpour, M., Bower, D.J., Cannon, J., 2016. Ocean basin evolution and global-scale plate reorganization events since Pangea breakup. *Annual Review of Earth and Planetary Sciences*, 44, 107-138. https://doi.org/10.1146/annurev-earth-060115-012211

Nesbitt, R.W., 1995. The geology of the Broken Spur Hydrothermal Vent Site; a new look at an old field. *BRIDGE Newsletter*, 8, 30-34.

Priede, I.G., Bergstad, O.A., Miller, P.I., Vecchione, M., Gebruk, A., Falkenhaug, T., Billett, D.S., Craig, J., Dale, A.C., Shields, M.A., Tilstone, G.H., Sutton, T.T., Gooday, A.J., Inall, M.E., Jones, D.O., Martinez-Vicente, V., Menezes, G.M., Niedzielski, T., Sigurðsson, Þ., Rothe, N., Rogacheva, A., Alt, C.H., Brand, T., Abell, R., Brierley, A.S., Cousins, N.J., Crockard, D., Hoelzel, A.R., Høines, Å., Letessier, T.B., Read, J.F., Shimmield, T., Cox, M.J., Galbraith, J.K., Gordon, J.D., Horton, T., Neat, F., Lorance, P., 2013. Does presence of a mid-ocean ridge enhance biomass and biodiversity? *PLoS ONE*, 8(5), e61550. doi: 10.1371/journal.pone.0061550

Proskurowski, G., Lilley, M.D., Seewald, J.S., Früh-Green, G.L., Olson, E.J., Lupton, J.E., Sylva, S.P., Kelley, D.S., 2008. Abiogenic hydrocarbon production at Lost City hydrothermal field. *Science*, 319, 604-607. https://doi.org/10.1126/science.1151194

Wilson, J.T., 1965. A New Class of Faults and Their Bearing on Continental Drift. *Nature*, 207, 343-347. https://doi.org/10.1038/207343a0

4. Pelagic environment and its biocoenosis

Katarzyna Błachowiak-Samołyk, Tomasz B. Linkowski, Lech Stempniewicz, Michał Tomczak, Jan Marcin Węsławski and Bartosz Kotrys

Deep-sea pelagic habitats include the dark ocean (>200 m depth) beneath the epipelagic (0–200 m depth) layer as well as the mesopelagic (200–1000 m) and bathypelagic (water column >1000 m) zones (Fig. 3.1; cf. Fig. 1.3.). Except for limited areas of hydrothermal vents and seeps, life patterns in deep-sea pelagic habitats along the Mid-Atlantic Ridge (MAR) depend on biological production exported from the sunlit epipelagic layers (Vecchione et al., 2010). In this section, we will describe individual components of the pelagic environment in the MAR region (Fig. 4.1.).

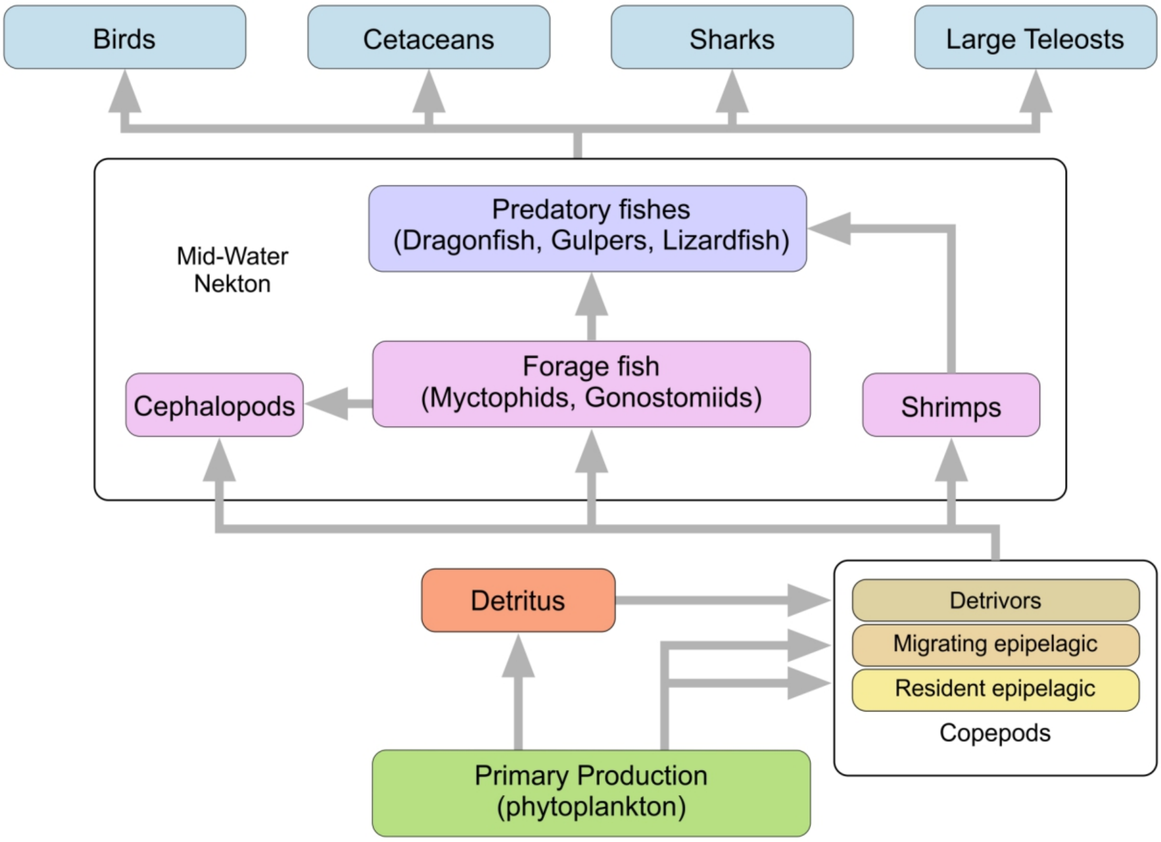

Fig. 4.1. A schematic diagram of the pelagic trophic web in the mid-Atlantic region (modified after Anderson et al., 2019)

References

Anderson, T.R., Martin, A.P., Lampitt, R.S., Trueman, C.N., Henson, S.A., Mayor, D.J., 2019. Quantifying carbon fluxes from primary production to mesopelagic fish using a simple food web model. ICES *Journal of Marine Science*, 76, 690-701. https://doi.org/10.1093/icesjms/fsx234

Vecchione, M., Bergstad, O.A., Byrkjedal, I., Falkenhaug, R., Gebruk, A.V., Godø, O.R., Gislason, A., Heino, M., Høines, A.S., Menezes, G., Piatkowski, U., Priede, I.G., Skov, H., Søiland, H., Sutton, T., de Lange Wenneck, T., 2010. Biodiversity Patterns and Processes on the Mid-Atlantic Ridge. In: McIntyre, A. (ed.), Life in the World's Oceans: *Diversity, Distribution, and Abundance.* Wiley Blackwell, Oxford, 103-121.

4.1. Microplankton

4.1.1. Diatoms (Michał Tomczak)

Diatoms are unicellular or chain-forming algae that incorporate silicon in the construction of their exoskeleton. Their size typically ranges from 1.5 to 500 µm and the number of diatom species is estimated for over 100,000 (Norton et al., 1996). Diatom growth depends on the availability of sunlight, carbon dioxide, and nutrients like nitrate, phosphorous, silica, and iron which are key in cell production. Because of massive presence and high diversity in the oceanic waters, diatoms are the most important component of phytoplankton and provide a significant amount of the world's oxygen supply (25%), and the main source of marine primary production (up to 40%), which makes them crucial for ocean biological carbon pump (Tréguer et al., 1995). The modern distribution of diatoms in the North Atlantic depends on nutrients availability, changes in surface water salinity, temperature, circulation pattern which results from ocean surface conditions and atmospheric forcing. These ecological parameters are important as having the potential to impact the marine food chain, as well as biogeochemical cycles, or climate system (Agusti et al., 2015; Allen et al., 2005; Sieracki et al., 1993).

The available literature shows that the research area (central Mid-Atlantic Ridge) is understudied in terms of diatom identification number of stations as well as taxonomic recognition of species. Available research results obtained from the research conducted in the Polish contract area, concentrate mainly on the zooplankton analysis, and to a small extent on radiolarian recognition (e.g. Vereshchaka and Vinogradov, 1999). Due to the fact that the Atlantic Ocean is free to mixing of surface waters, it can be assumed that the data in the axial part of the Ocean, far from the sources of sediments, will be quite homogeneous and may provide an indication to expected communities of diatoms within the research area. The research area is spread out in the subtropical zone, however, the complex system associated with the circulation of surface and deep-water currents, including upwelling zones, may cause great diversity within the diatom assemblages in research area, which is situated in the middle of a large gyre shaped by trade-winds, and Gulf stream. Regional research mainly provides the spatial distribution of nutrients and chlorophyll which reflects that Area, located in the central part of the Atlantic Ocean, is characterized by low chlorophyll concentrations (0.01 - 0.1 mg/m3), what results from depleted nutrients that prevent the growth of phytoplankton. Following the spring stratification, diatoms are the first phytoplankton to bloom. Due to the higher silica, nitrate, and phosphate availability, the northern Atlantic (and the Arctic) waters are characterized by a high abundance of diatoms (Hector et al., 2006; Barton et al., 2015; Okman et al., 2019). The highest values >100 x 106 cells/L are recorded along the shelf areas, while the highest values in the open Atlantic Ocean are south of Iceland (10 x 106), decreasing towards the central part of the North Atlantic to an average of >0.25 x 106 c/l and increase again around the equator to about 3-4 x 106 c/l. The central North Atlantic feature lower primary production in the photic zone and very low abundance in the water surface, and few diatoms in the surface sediments. Published data shows that diatom communities in the central North Atlantic have very low diversity and concentration in surface water, which varies between 1 - 0.05 x 106 c/l. The assemblages are dominated by cosmopolitan planktonic diatoms represented in 50 % by Chaetoceros (and Bacteriastrum) whereas central and pennate diatoms represent around 40 % and 10 % respectively. More than 75 species have been identified within the central North Atlantic, with a much higher diversity occurring closer to the Equator and towards the coasts (Maynard et al., 1976; Schrader et al., 1993).

Tab. 4.1.1. Common species in the diatom assemblages from central MAR (compilation)

Temperate water species	**Warm water species**
Chaetoceros contortus Schütt 1895,	*Chaetoceros danicus* Cleve 1889,
Chaetoceros rostratus Ralfs 1864,	*Coscinodiscus lineatus* Ehrenberg 1839,
Cerataulina pelagica (Cleve) Hendey 1937,	*Coscinodiscus nodulifer* A.W.F.Schmidt 1878,
Detonula pumila (Castracane) Gran 1900,	*Coscinodiscus tuberculatus* Greville 1861,
Coscinodiscus granii L.F.Gough 1905,	*Mastogloia rostrata* (Wallich) Hustedt 1933,
Leptocylindrus danicus Cleve 1889,	*Nitzschia marina* Grunow 1880,
Minutocellus polymorphus (Hargraves & Guillard) Hasle, Stosch, & Syvertsen 1983,	*Thalassionema nitzschioides* (Grunow) Mereschkowsky 1902
Pseudo-nitzschia multiseries (Hasle) Hasle 1995,	*Thalassiosira eccentrica* (Ehrenberg) Cleve 1904,
Rhizosolenia bergonii H.Peragallo 1892,	*Thalassiosira oestrupii* (Ostenfeld) Hasle, 1972.
Rhizosolenia styliformis T.Brightwell 1858,	
Thalassiosira decipiens (Grunow) Jørgensen1905,	
Thalassiothrix longissima Cleve & Grunow 1880.	

From the perspective of the planned research, it is necessary to take into account the seasonality, which shows a close relationship between the physical parameters and the diversity of diatom communities. Generally, weaker stratification, increased water mixing, turbulence, and reduced transparency, while maintaining access to light and nutrients, causes an increase in diatoms abundance in the central ocean areas of the subtropical zone. Possible exploitation of massive sulphides from the bottom of the ridge and delivering a suspension to the water column (so-called plume discharge), a material that exhibits toxic properties, but is rich in silica, may cause diatom blooms in surface waters (which are partially toxic themselves). The initiation of mining processes can cause an increase in productivity in the photic zone, leading to an increase in the amount of organic matter falling to the bottom (known as marine snow), which will lead to further changes in the food chain. As a result, the diatom communities may be similar to those in upwelling zones. A similar increase in the productivity of Atlantic surface waters occurs when the ocean surface is 'fertilised' by dust carried from the Sahara desert.

References

Agusti, S., González-Gordillo, J., Vaqué, D., 2015. Ubiquitous healthy diatoms in the deep sea confirm deep carbon injection by the biological pump. *Nat Commun 6*, 7608. https://doi.org/10.1038/ncomms8608

Allen, J., Brown, L., Sanders, R., 2005. Diatom carbon export enhanced by silicate upwelling in the northeast Atlantic. *Nature 437*, 728–732. https://doi.org/10.1038/nature03948

Barton, A.D., Lozier, M.S. and Williams, R.G., 2015. Physical controls of variability in North Atlantic phytoplankton communities. *Limnol. Oceanogr.*, 60: 181-197. https://doi.org/10.1002/lno.10011

Héctor F. Olguín, Demetrio Boltovskoy, Carina B. Lange, Frederico Brandini, K.J. Flynn, 2006. Distribution of spring phytoplankton (mainly diatoms) in the upper 50 m of the Southwestern Atlantic Ocean (30–61°S), *Journal of Plankton Research*, Volume 28, Issue 12, Pages 1107–1128, https://doi.org/10.1093/plankt/fbl045

Maynard, N.G., 1976. Relationship between Diatoms in Surface Sediments of the Atlantic Ocean and the Biological and Physical Oceanography of Overlying Waters Author(s): Source: *Paleobiology*, Vol. 2, No. 2, pp. 99-121

Norton, T.A., Melkonian, M., Andersen, R.A., 1996. Algal biodiversity. Phycologia 35, 308– 326.

Oksman, M., Juggins, S., Miettinen, A., Witkowski, A., Weckström, K., 2019. The biogeography and ecology of common diatom species in the northern North Atlantic, and their implications for paleoceanographic reconstructions. *Marine Micropaleontology*, Volume 148, Pages 1-28, ISSN 0377-8398, https://doi.org/10.1016/j.marmicro.2019.02.002

Schrader, H., Swanberg, I.L., Burckle, L.H. et al., 1993. Diatoms in recent Atlantic (20° S to 70° N latitude) sediments: abundance patterns and what they mean. *Hydrobiologia 269*, 129–135 (1993). https://doi.org/10.1007/BF00028012

Sieracki, M.E, Verity, P.G., Stoecker, D.K., 1993. Plankton community response to sequential silicate and nitrate depletion during the 1989 North Atlantic spring bloom. *Deep Sea Research Part II: Topical Studies in Oceanography*, Volume 40, Issues 1–2, Pages 213-225, ISSN 0967-0645, https://doi.org/10.1016/0967-0645(93)90014-E

Tréguer, P., Nelson, D.M., Vanbennekom, A.J., Demaster, D.J., Leynaert, A., Quéguiner, B., 1995. The silica balance in the world ocean: a reestimate. *Science 268,* 375–379.

Tréguer P, Bowler C, Moriceau B, Dutkiewicz S, Gehlen M, Aumont O, et al. 2018. Influence of diatom diversity on the ocean biological carbon pump. *Nat Geosci*;11:27–37.

Vereshchaka, A.L., Vinogradov, G.M., 1999. Visual observations of the vertical distribution of plankton throughout the water column above Broken Spur vent field, Mid-Atlantic Ridge, *Deep Sea Research Part I: Oceanographic Research Papers*, Volume 46, Issue 9, Pages 1615-1632, ISSN 0967-0637, https://doi.org/10.1016/S0967-0637(99)00018-7

4.1.2 Radiolaria (Bartosz Kotrys)

Siliceous microorganisms, including radiolarians (Radiolaria), are marine planktonic protozoans which range in size from 20 up to 300 µm and are widely distributed in the oceans. They occur throughout the water column, from near the surface to the deep ocean (Anderson, 1983). Their production in the northern hemisphere is highest in July-September and decreases in October-June (Voituriez and Herbland 1977). Under favourable conditions, radiolarian tests preserve very well in the sediment and are important component of the siliceous ooze (De Wever et al., 2001; Kotrys, 2012).

The spatial distribution of living radiolarians reflects primarily the temperature of the surface and subsurface water (Haq and Boersma, 1998), but the radiolarian habitat is also influenced by a combination of other environmental factors such as the nutrient availability, dissolved silica content, seasonal productivity regime and salinity (Bjørklund et al., 1998). Therefore, the highest radiolarian abundances are restricted to upwelling and silica sink zones, particularly in the Southern Ocean (de Master, 1981).

Dissolved silica in the water column and the fossilized silica content in the sediment decline sharply towards low latitudes of the central part of the Atlantic Ocean, for which reason the radiolarian zooplankton occurrence in the Polish contract area on the Mid-Atlantic Ridge (MAR) is very limited. However, the limitation may also result from the existing knowledge gap. In fact, the radiolarian zooplankton in the subtropical-tropical areas has been poorly studied compared to other World Ocean regions. Boltovskoy et al. (1996) conducted one of the very few studies addressing radiolarians of the water column in the vicinity of MAR (20°55.3' N; 19°44.5' W). Based on that study, its seems likely that some of the radiolarian species listed in Table 1 occur in the Polish contract area.

Vereshchaka and Vinogradov (1999) who performed visual censuses of the zooplankton over the Broken Spur hydrothermal field (in the Polish contract area) reported the two zooplankton biomass aggregations they observed along the vertical profiles over the vents to be dominated by gelatinous zooplankton and by radiolarians. For obvious reasons (no actual sampling), they could not provide any detailed taxonomic information but reported that radiolarian 'colonies' were 45 cm wide and 12 cm high. In their opinion, radiolarians contributed substantially to the planktonic biomass in the area.

As to the radiolarian remains in the surface sediment, the seafloor in the Polish contract area does not generally feature siliceous ooze, but Nigrini (1967) reported on radiolaria found in the sediment cores from a few areas in the vicinity (Table 4.2.).

Table 4.1.2. Radiolarian taxa present in the water column at 20°55.3' N; 19°44.5' W (Boltovskoy et al., 1996b) which may occur in the Polish contract area on the MAR.

Radiolarian taxa	
Arachnocoraiiium caivata a	*Hexacontium armatum/hostiie*
Arachnocoraiiium caivata e	*Lamprocycias hannai*
Tetrapiecta pinigera	*Actinomma leptodermum*
Botryocephaiina armata	*Hexaionche aristarchi*
Siphocampe arachnea	*Triceraspyris antarctica*
Artostrobus joergenseni	*Botryostrobus auritus/australis*
Artostrobus annulatus	*Trisulcus triacanthus*
Heiothoius histricosa	*Lophophaena buetschlii*
Actinomma sp. 1	*Pseudocubus obeliscus*

Table 4.1.3. Abundance of radiolarian remains in the Atlantic Ocean sediment sampled in the vicinity of the Polish contract area (Nigrini, 1967).

Coordinates	**Water depth (m)**	**Abundance and preservation state of radiolarian remains**
29°35' N, 42°33' W	2820	Moderately abundant, well-preserved
21°05' N, 58°50' W	5596	Very rare
34°54' N, 44°20' W	4281	Abundant, well-preserved
33°07' N., 52°14' W	5651	Very rare

References

Anderson, R.O., 1983. Radiolaria. *Springer*, New York.

Bjørklund, K.R., Cortese, G., Swanberg, N., Schrader, H.J., 1998. Radiolarian faunal provinces in surface sediments of the Greenland, Iceland and Norwegian (GIN) Seas. *Marine Micropaleontology*, 35, 105-140.

Boltovskoy, D., Uliana, E., Wefer, G. 1996. Seasonal Variation in the Flux of Microplankton and Radiolarian Assemblage Compositions in the Northeastern Tropical Atlantic at 2,195 m. *Limnology and Oceanography*, 41(4), 615-635.

de Master, D.J., 1981. The supply and accumulation of silica in the marine environment. *Geochimica et Cosmochimica Acta*, 45, 1715-1732.

De Wever, P., Dumitrica, P., Caulet, J.P., Nigrini, C., Caridroit, M., 2001. Radiolarians in the Sedimentary Record. *Gordon and Breach Science Publishers*.

Haq, B., U., Boersma, A., 1998. Introduction to Marine Micropaleontology. *Elsevier*.

Kotrys, B., 2012. Palaeotemperature reconstructions at the Polar Front in the Southern Ocean (Atlantic sector) based on middle–late Pleistocene radiolarian record from ODP Leg 177 Site 1091. *Ph.D. Thesis*, University of Szczecin.

Nigrini, C., 1967. Radiolaria in pelagic sediments from the Indian and Atlantic Oceans. *Bulletin of the Scripps Institution of Oceanography*, 11, 1-125.

Vereshchaka, A.L., Vinogradov, G.M., 1999. Visual observations of the vertical distribution of plankton throughout the water column above Broken Spur vent field, Mid-Atlantic Ridge. *Deep-Sea Research* Part I, 46, 1615-1632.

4.2. The Mid-Atlantic Ridge zooplankton (Katarzyna Błachowiak-Samołyk)

The zooplankton described here comprise animals ranging in size from 0.2 up to 20 mm. Generally, the zooplankton can be subdivided into two major groups: the holoplankton (e.g., copepods and krill) which spend their entire lives as plankton drifting with ocean currents, and thus provide major food sources for higher trophic levels and act as major contributors to the oceanic "biological pump"; and the meroplankton (e.g., larvae of barnacles, mussels, annelids and fish) which spend only part of their lives in the pelagial.

The zooplankton are difficult to sample adequately because individual organisms are tiny and often patchily distributed. Moreover, some zooplankton species that live mainly in the water between 500 and 1000 m deep perform massive diel vertical migrations (DVM), ascending the surface layers of the ocean at night, where they feed on plankton, and descend at dawn, to digest the food and to minimise the predation risk, at its highest in the upper water layers. Until recently, it had been thought that DVMs were triggered by a relative change in the visible light intensity. However, acoustic data, a measure of zooplankton abundance and movement in the North-Atlantic Ocean in the vertical range of 500–1600 m, provided evidence that DVMs also occur in the deep sea where no direct and background sunlight penetrates (van Haren and Compton, 2013). Acoustic Doppler current profilers were moored at a location similar to the MAR at eight different sub-tropical positions (from 33°N to the equator and from 22°W to 37°W), and the migrations precisely followed the rhythm of local sunrise and sunset between 500 and 650 m. They continued below 650 m where the deepest penetrable irradiance levels are $<10^{-7}$ times their near-surface values, but the plankton shortened their time at depth by up to about 63% at 1600 m. The trend was consistent both across the latitudes investigated and between different seasons. It was thus hypothesized that the solar diurnal and seasonal rhythms in the deep sea plankton migrations could be controlled by a mechanism other than light, e.g., a precise biochemical clock. In accordance with this hypothesis, the deepest plankton were consistently the first to migrate upwards (van Haren and Compton, 2013).

Deep-sea zooplankton communities are generally very diverse, but occur at low abundances. Thus, large sampling systems are needed to filter sufficient amounts of water (Vinogradov et al., 1996). In consequence, the zooplankton of the subtropical-tropical regions are generally very poorly studied. The first comprehensive assessment of the zooplankton community in the Atlantic Ocean at low latitudes (35°N-40°S, near the Polish contract area) covered a broad depth range (0–3,000 m) (de Puelles et al., 2019). The study demonstrated that the zooplankton abundance declined sharply with depth, comprising, on average, 82% of the depth-integrated abundance in the epipelagic layer. The mesopelagic zooplankton contributed 4 to 12% of the water column abundance, while the bathypelagic zooplankton accounted for <1% of the total abundance. Tropical-subtropical zooplankton abundances reported by de Puelles et al. (2019) were generally low, usually amounting to >200 ind./m3 in the epipelagic layer, around 100 ind./m3 in the mesopelagic layer, and <3 ind./m3 in the bathypelagic zone. These low values might be an artefact of the relatively large mesh size (>300 μm) of the plankton net used, and thus an underrepresentation of the numerically important tiny copepods. However, similar values were found in the upper 300 m when a smaller (150 μm) mesh size net was used along a latitudinal transect in the eastern Atlantic from 34°49.5′ N to 27°28.1′ S, but further east (Schnack-Schiel et al., 2010) than the stations sampled by de Puelles et al. (2019).

Zooplankton communities in subtropical-tropical regions are numerically dominated by small-sized copepods, particularly calanoids of the families Clausocalanidae and Paracalanidae and cyclopoids, often contributing jointly more than 50% to the total number of copepods (e.g., Schnack-Schiel et al., 2010). They are generally known to be well adapted to low phytoplankton concentrations in oligotrophic waters. De Puelles et al. (2019) identified seventeen different, dominant zooplankton groups, of which seven displayed contributions <1%. Overall, copepods were the dominant group in all the samples (80%), followed by chaetognaths (5%), ostracods (3%), and siphonophores (3%). Other groups such as appendicularians (2%), euphausiids (1%), and amphipods (1%) were rarely observed (de Puelles et al., 2019). The high dominance of copepods confirms their key role in the marine pelagic food web – in the transfer of primary production and microzooplankton biomass to higher trophic levels (Vinogradov et al., 1996). The study by de Puelles et al. (2019) clearly demonstrated that smaller copepods were usually abundant in the upper strata, while large copepods were mainly distributed in deeper waters.

Schnack-Schiel et al. (2010) identified a total of 149 calanoid copepod species in the upper 300 m of their area of study. They pointed to Clausocalanus as the most abundant genus, accounting for on average of about 45% of all calanoids. It was followed by Calocalanus (13%), Delibus (9%), Paracalanus (6%), and Pleuromamma (5%). The list of the most abundant cosmopolitan cyclopoid genera in the area was topped by *Oithona*, followed by *Oncaea*, both are widely distributed throughout the low latitudes, particularly in the upper 300 m.

The study of de Puelles et al. (2019), carried out in the epipelagic zone of subtropical-tropical Atlantic [35ºN-40ºS but further west from the area sampled by Schnack-Schiel et al. (2010)] showed, too, the zooplankton to be numerically dominated by small-sized cosmopolitan species such as *Clausocalanus furcatus*, *Nannocalanus minor* and *Oithona plumifera*. The upper mesopelagial (200-500 m) was inhabited mainly by three representatives of *Pleuromamma* (*P. abdominalis*, *P. gracilis* and *P. piseki*), while the lower part of the zone (500-1000 m) featured *Metridia brevicauda*, *Conaea* sp. and *Pleuromamma* *xiphias*. Dominants similar to those in the lower mesopelagial were characteristic of the bathypelagic zone (>1 000 m depth), with a substantial contribution of *Triconia conifera* (de Puelles et al., 2019). The mesopelagic zone dominants (*P. abdominalis*, *P. gracilis*, *P. piseki*, and *P. xiphias*), reported as the daytime inhabitants of the deeper layer, are known to be the strong vertical migrants (e.g., Gaard et al., 2008).

The high species diversity found by de Puelles et al. (2019) and Schnack-Schiel et al. (2010) is a common feature of the tropical and subtropical domains. The diversity peaks in mid-waters, and the species richness declines with depth, which demonstrates the global nature of such patterns, earlier reported in regional assessments of planktonic ostracods (e.g., Angel et al., 2007). The tropical zooplankton communities are characterized by a high species richness and small changes of biomass throughout the year (e.g., Longhurst, 1993; Bode et al., 2018, Schnack-Schiel et al., 2010, Vereshchaka et al., 2017).

The horizontal distribution of planktonic organisms in tropical latitudes is more or less unrestricted due to the absence of physical barriers, thus allowing the co-occurrence and wide latitudinal ranges of many oceanic species (e.g., Schnack-Schiel et al., 2010). In contrast, a strong vertical stratification, i.e., a pronounced thermocline and oxycline, effectively separates the mixed, well oxygenated, warm surface layer from cooler, less oxygenated waters below. Hence, zooplankton communities may show differences in their vertical distribution, consistent with species-specific ecophysiological preferences; however, depth and temperature are usually the most important factors structuring their populations throughout the water column (de Puelles et al., 2019). A strong vertical zonation of the zooplankton was reported by Vereshchaka and Vinogradov (1999) from visual censuses at the Broken Spur hydrothermal field (in the Polish contract zone on the MAR). They found the plankton biomass to form 2 major aggregations, one within the main pycnocline (~1000 m depth) and the other near the hydrothermal fluid plume, both aggregations being dominated by the gelatinous zooplankton (medusae, ctenophores, siphonophores) and radiolarians (see above), in addition to the abundant copepods.

Lost City, another hydrothermal field in the Polish contract area on the MAR was surveyed for the zooplankton (visual census from a submersible) by Vinogradov et al. (2003). In their study, a characteristic and common feature of the site, not encountered elsewhere, were accumulations of the macroplankton and nektobenthos (see below).

The study of zooplankton on hydrothermal vent system-supporting mid-oceanic ridges such as the MAR carries a benefit of contributing to the assessment of connectivity between different areas, particularly important for conservation and management purposes (see below). The connectivity is provided primarily by the transport of benthic organisms' larvae, i.e., the meroplankton (e.g., Comtet et al., 2000; Beaulieu et al., 2009). In this regard, mention has to be made of the sp. *Rimicaris* shrimp larvae observed by Vinogradov et al. (2003) over the Broken Spur hydrothermal field in the layers closest to the seafloor.

References

Angel, M.V., Błachowiak-Samołyk, K., Drapun, I., Castillo, R., 2007. Changes in the composition of planktonic ostracod populations across a range of latitudes in the North-east Atlantic. *Progress in Oceanography*, 73, 60-78.

Beaulieu, S.E., Mullineaux, L.S., Adams, D.K., Mills, S.W., 2009. Comparison of a sediment trap and plankton pump for timeseries sampling of larvae near deep-sea hydrothermal vents. *Limnology and Oceanography Methods*, 7, 235-248.

Bode, M., Hagen, W., Cornils, A., Kaiser, P., Auel, H., 2018. Copepod distribution and biodiversity patterns from the surface to the deep sea along a latitudinal transect in the eastern Atlantic Ocean (24°N to 21°S). *Progress in Oceanography*, 161, 66-77.

Comtet, T., Jolliver, D., Khripounoff, A., Segonzac, M., Dixon, D., 2000. Molecular and morphological identification of settlement-stage vent mussel larvae, *Bathymodiolus azoricus* (Bivalvia: Mytilidae), preserved in situ at active vent fields on the Mid-Atlantic Ridge. *Limnology and Oceanography*, 45, 1655-1661.

de Puelles, M.L.F., Gazá, M., Cabanellas-Reboredo, M.S, Santandreu, M.M., Irigoien, X., González-Gordillo, J.I., Duarte, C.M., Hernández-León, S. 2019. Zooplankton Abundance and Diversity in the Tropical and Subtropical Ocean. *Diversity*, 11, 203.

Gaard, E., Gislason, A., Falkenhaug, T., Søiland, H., Musaeva, E., Vereshchaka, A., Vinogradov, G., 2008. Horizontaland vertical copepod distribution and abundance on the Mid-Atlantic Ridge in June 2004. *Deep Sea Research Part II Topical Studies in Oceanography*, 55, 59-71.

Longhurst, A., 1993. Seasonal cooling and blooming in tropical oceans. *Deep-Sea Research Part I*, 40, 2145-2165.

Schnack-Schiel, S.B., Mizdalski, E., Cornils, A., 2010. Copepod abundance and species composition in the Eastern subtropical/tropical Atlantic. *Deep Sea Research Part II Topical Studies in Oceanography*, 57, 2064-2075.

van Haren, H., Compton, T.J., 2013. Diel Vertical Migration in Deep Sea Plankton Is Finely Tuned to Latitudinal and Seasonal Day Length. PLoS ONE 8(5): e64435. doi:10.1371/journal.pone.0064435

Vereshchak,a A., Abyzov,a G., Lunina, A., Musaeva, E. 2017. The deep-sea zooplankton of the North, Central and South Atlantic: Biomass, abundance, diversity. *Deep Sea Research Part II Topical Studies in Oceanography*, 137, 89-101.

Vereshchaka, A.L., Vinogradov, G.M., 1999. Visual observations of the vertical distribution of plankton throughout the water column above Broken Spur vent field, Mid-Atlantic Ridge. *Deep-Sea Research Part I*, 46, 1615-1632.

Vinogradov. G. M., Vereshchaka, A.L., 2006. Zooplankton Distribution above the Lost City (Atlantis Massif) and Broken Spur Hydrothermal Fields in the North Atlantic According to the Data of Visual Observations. *Oceanology*, 46, 217-227.

Vinogradov, G.M., Vereshchaka, A.L., Aleinik, D.L., 2003. Zooplankton Distribution over Hydrothermal Fields of the Mid-Atlantic Ridge. *Oceanology*, 43, 656-669.

Vinogradov, M.E., Vereshchaka, A.L., Shushkina, E.A. 1996. Vertical structure of the zooplankton community in the oligotrophic areas of the north Atlantic and influence on the hydrothermal vent. *Okeanologiya*, 36, 64-71.

4.3. Macroplankton and micronekton (Jan Marcin Węsławski)

These categories of pelagic organisms group water column inhabitants larger than 5 mm in size, both passive floaters (the majority of gelatinous plankton) and active swimmers (cephalopods, shrimps, krill and amphipods). They occur throughout the water column, the surface to the near-bottom water layer (benthopelagic crustaceans). Due to their size, the organisms dealt with here are of special importance for large predators, from fish to seabirds and sea mammals. A number of macroplankton and micronekton species tend to occur in aggregations; they form swarms and shoals, due to both physical forcing (aggregations on the density interface, internal waves or eddies) and biological (behavioural) reactions (mainly krill, shrimps, and cephalopods).

The pelagic area of concern (Central North Atlantic) belongs to the subtropical zone, one of the biodiversity-richest among open ocean regions (McRae et al., 2017), and is inhabited by a mixture of boreal and tropical faunal elements (Judkins and Haedrich, 2018).

The dominant non-fish pelagic organisms include 65 shrimp species (Cardoso et al., 2014), followed by 41 species of cephalopods (Vecchione et al., 2010). The benthopelagic carrion-feeding amphipods are represented by over 35 species (Horton et al., 2013); other pelagic Amphipoda are the Hyperiida represented by several mesopelagic species (Bellan- Santini and Thurston, 1996; Burukovsky and Falkenhaug, 2015), with a generally very wide distribution in the deep Atlantic.

The jellyfish, representing the gelatinous plankton and important for their role in the food web, are widespread over the central Atlantic, and count at least 51 species (scyphozoans, cnidarians, and appendicularians), most feeding on the microplankton and mesozooplankton (Steemann et al., 2008; Hosia et al., 2017).

As regards the macroplankton and non-fish micronekton at individual hydrothermal vent fields, from the standpoint of the Polish exploration at the MAR, important are data of Russian researchers, e.g., Vinogradov et al. (2003) who conducted visual censuses of organisms in the water column from a manned submersible (known also as a human-operated vehicle, HOM) MIR 1 at the Lost City vent field in the Polish contract area. In their study, a characteristic and common feature of the site, not encountered elsewhere, were accumulations of the euphausiids *Nematoscelis* aff. *tenellae* (preying on copepods) in the near-bottom layer as well as the presence of free-swimming amphipods *Paraphronima crassipes*, *Streetsia challengeri*, and *Primno* sp. In addition, there were abundant benthic amphipods *Bouvierella* aff. *curtirama* popping up into the water column. Further data on the large zooplankton of both Broken Spur and Lost City (supplied by visual censuses and net hauls) were discussed by Vinogradov and Vereshchaka (2006).

Table 4.3. shows the main macroplanktonic species recorded in the central part of MAR, usually the most common species are also most important for the food web structure and parasites transmission to the top predators. The conservation value of the listed species is difficult to assess, as this whole ecological group is data deficient and potentially widespread both over the Atlantic and the depth zones as well.

Table 4.3. Principal non-fish micronekton and macroplankton species in the area (compiled from the literature cited)

Species	Higher taxon	Depth strata (m)	Remarks
Aeginura grimaldii	Scyphozoa	500-800	Most common gelatinous zooplankter in the area
Lensia subtilis	Siphonophora	Pelagic, 100-1000 m	Common cosmopolitan species
Abyssorchomene abyssorum	Amphipoda	Near bottom waters	Most common necrophagic amphipod in the area
Paraphronima crassipes	Amphipoda	Near bottom waters	Lost City (Polish contract area)
Streetsia challengeri	Amphipoda	Near bottom waters	Lost City (Polish contract area)
Primno sp.	Amphipoda	Near bottom waters	Lost City (Polish contract area)
Phronima sedentaria	Hyperiida	Mesopelagic, 500-1000 m	Cosmopolitan common species
Meganyctiphanes norvegica	Euphausiacea	Pelagic, 100-1000 m	Common, northern element
Nematoscelis aff. *tenellae*	Euphausiacea	Near bottom waters	Lost City (Polish contract area)
Acanthephyra pelagica	Decapoda	Mesopelagic, bathy-pelagic – 500-3500	Most common pelagic shrimp in the area
Gonatus steenstrupi	Cephalopoda	100-1000 m	Most common squid in the northern sector of the area

References

Bellan-Santini, D., Thurston, M.H., 1996. Amphipoda of the hydrothermal vents along the mid-Atlantic Ridge. Journal of Natural History, 30 (5), 685-702. doi: 10.1080/00222939600770381

Burukovsky, R.N., Falkenhaug, T. 2015. Feeding of the pelagic shrimp Acanthephyra pelagica (Risso, 1816) (Crustacea: Decapoda: Oplophoridae) in the northern Mid-Atlantic Ridge area in 1984 and 2004. Arthropoda Selecta, 24(3), 303-316.

Cardoso, I.A., Falkenhaug, T., Fernandes, L.F.L., 2014. Comparison between the shrimp species richness (Caridea and Dendrobranchiata, Decapoda, Crustacea) of the south and North Mid-Atlantic Ridge. Brazilian Journal of Oceanography, 62, 47- 56.

Horton, T., Thurston, M.H., Duffy, G.A., 2013. Community composition of scavenging amphipods at bathyal depths on the Mid-Atlantic Ridge. *Deep-Sea Research*, 98, 352-359.

Hosia, A., Falkenhaug, T., Baxter, E.J., Pagès, F., 2017. Abundance, distribution and diversity of gelatinous predators along the northern Mid-Atlantic Ridge: A comparison of different sampling methodologies. *PLoS ONE* 12(11): 0187491. doi.org/10.1371/journal.pone.0187491

Judkins, D., Haedrich, R., 2018. The deep scattering layer micronektonic fish faunas of the Atlantic mesopelagic ecoregions with comparison of the corresponding decapod shrimp faunas., Deep Sea Research Part I Oceanographic Research Papers, 136, 1-30. doi: 10.1016/j.dsr.2018.04.008

Lindsay, D., Umetsu, M., Grossmann, M., Miyake, H., Yamamoto, H., 2015. The Gelatinous Macroplankton Community at the Hatoma Knoll Hydrothermal Vent. In: Ishibashi, J., Okino, K., Sunamura, M. (eds), *Subseafloor Biosphere Linked to Hydrothermal Systems*. Springer, Tokyo. doi.org/10.1007/978-4-431-54865-2_51

McRae, L., Deinet, S., Freeman, R., 2017. The Diversity-Weighted Living Planet Index: Controlling for Taxonomic Bias in a Global Biodiversity Indicator. *PLoS ONE*, 12(1): e0169156. doi.org/10.1371/journal.pone.0169156

Stemmann, L., Hosia, A., Youngbluth, M.J., Soiland, H., Picheral, M., Gorsky, G., 2008. Vertical distribution (0–1000 m) of macrozooplankton, estimated using the Underwater Video Profiler, in different hydrographic regimes along the northern portion of the Mid- AtlanticRidge. *Deep-Sea Research Part II Topical Studies in Oceanography*, 55 (1-2), 94-105. doi:10.1016/j.dsr2.2007.09.019

Vecchione, M., Bergstad, O.A., Byrkjedal, I., Falkenhaug, R., Gebruk, A.V., Godø, O.R., Gislason, A., Heino, M., Høines, A.S., Menezes, G., Piatkowski, U., Priede, I.G., Skov, H., Søiland, H., Sutton, T., de Lange Wenneck, T., 2010. Biodiversity Patterns and Processes on the Mid-Atlantic Ridge. In: McIntyre, A. (ed.), *Life in the World's Oceans: Diversity, Distribution, and Abundance*. Wiley Blackwell, Oxford, 103-121.

Vecchione, M., Young, R.E., Piatkowski, U., 2010. Cephalopods of the northern Mid-Atlantic Ridge. Marine Biology Research, 6, 1, 25-52. doi: 10.1080/17451000902810751

Vinogradov, G.M., Vereshchaka, A.L., 2006. Zooplankton Distribution above the Lost City (Atlantis Massif) and Broken Spur Hydrothermal Fields in the North Atlantic According to the Data of Visual Observations. *Oceanology*, 46, 217-227.

Vinogradov, G.M., Vereshchaka, A.L., Aleinik, D.L., 2003. Zooplankton Distribution over Hydrothermal Fields of the Mid-Atlantic Ridge. *Oceanology*, 43: 656-669.

4.4. Fishes (Tomasz B. Linkowski)

As there is no published information about any demersal fishing activities in the Polish contract area of the Mid-Atlantic Ridge, there are pretty good chances that bottom fishing is not commercially feasible there. Contrary to that, the epipelagic waters of the MAR area in question were under a very moderate pressure from the long-line tuna, billfish and shark fisheries, but free of any purse seine or bait boat fishing activities, according to data on the fishing effort allocated to five-degree statistical squares and published up to 2010 (ICCAT Stat. Bull. https://www.iccat.int/en/scrs.html).

The Polish contract area is located approximately within the two ICCAT statistical squares, i.e., 25°-35° N and 40°-45° W. On the basis of the reported commercial catches per those squares, the following large pelagic fish species are expected to be the most frequent visitors in the area: albacore (*Thunnus alalunga*), bigeye (*T. obesus*), northern bluefin tuna (*T. t. thynnus*), blue marlin (*Macaira nigricans*), sailfish (*Istiophorus albicans)*, white marlin (*Terapturus albidus*), swordfish (*Xiphias gladius*), blue shark (*Prionace glauca*), and shortfin mako (*Isurus oxyrinchus*). They are apex predators which feed on a variety of smaller fish, cephalopods, and crustaceans which are distributed in a wide depth range of epi- and mesopelagic zones. Therefore, some of them, e.g., billfish and swordfish, but also certain tuna species, perform diurnal feeding migrations while, e.g,. sailfish stay at shallower depths (Carey and Robinson, 1981; Dagorn et al., 2000; Lerner et al., 2013; Bubley et al., 2020). Food resources of the apex predators do not consist of mesopelagic species only, but also include epipelagic ones, e.g., flying fish and Atlantic saury (*Scomberesox saurus*) (Biton Porsmoguer et al., 2014). Although the major prey composition of the apex species mentioned differs from region to region, in the open oceanic waters the mesopelagic organisms constitute their important prey (Moteki et al., 2001; Satoh et al., 2004). Therefore, the vertically migrating mesopelagic fish, mainly numerous species of the family Myctophidae, but also species of the family Gonostomatidae which perform vertical migrations, play an important role in the vertical energy transfer process in the oceanic ecosystems. The most abundant *Cyclotone* spp. (Gonostomatidae) are too small as a prey for apex predators and do not perform vertical migrations (Badcock and Merrett, 1976), but certainly are utilized as prey by much smaller mesopelagic predators.

Thus, information on mesopelagic fishes within the study area is so important. As the relevant data for the Polish contract area on the MAR are missing, the most representative information on the mesopelagic fish abundance, species composition, and vertical distribution could be extracted from datasets collected within the same mesopelagic ecoregion, i.e., the

Northeastern Central Atlantic sub-ecoregion (Judkins and Haedrich, 2018), or from the geographically closest sampling sites. The primary factor determining the pelagic fish assemblage composition in the northern part of the MAR (from Iceland to the Azores) is the depth, while the geographic region is of secondary importance (Sutton et al., 2008).

In addition to the results from the southernmost part of the area studied by Sutton et al. (2008), the mesopelagic fish structure close to the border between the Mauretania-Cape Verde ecoregion and Northeastern Central Atlantic (Badcock and Merrett, 1976) and Northern Sargasso Sea and Southern Sargasso Sea subregions (Sutton et al., 2010), could provide proxy information on the mesopelagic fishes assemblage in the Polish contract area on the MAR.

For example, the 33 stratified samples collected with RMT 1+8 net between the surface and 2010 m depth showed the following peaks of mesopelagic fish abundance: one peak in the 405-600 m depth stratum during the day and two peaks within 100-200 m and 405-500 m during the night (Badcock and Merrett, 1976). The species composition was highly dominated by small Cyclothone species (Gonostomatidae), i.e., C. braueri (9-38 mm, occurring in the 400-600 m depth stratum during day and night), and C. microdon (11-59 mm, occurring in the 600-1250 m depth stratum during the day and 500-2000 m during the night). Vallencienellus tripunctulatus and Argyropelecus hemigymnus (Sternoptychidae) were the third and fourth most numerous species, while the two most abundant myctophids (Benthosema suborbitale and Hygophum hygomii) were far less numerous than the gonostomatid and sternoptychid species (Badcock and Merrett, 1976) mentioned above. The samples analyzed by Badcock and Merrett (1976) included 37 taxa of stomiatoid fishes (suborder Stomiatoidei), while the single family Myctophidae was represented by 31 species. In the Azorean Zone (0–750 m), 29 myctophid species contributed half (50.8%) of the total assemblage number and one-quarter of the biomass (26.9%) (Sutton et al., 2008) with the myctophid Lobianchia dofleini dominating (18.6%), and the gonostomatids C. microdon (14.2%) and C. braueri (8.1%) taking the second and third place in the overall number of the specimens collected, respectively. Samples collected in the Sargasso Sea (0-1000 depth stratum) differed from those reported in papers mentioned earlier in that four Cyclotone species were the most abundant ones (C. braueri, C. pallida, C. microdon and C. pseudopalida with 47.5, 19.9, 5.9 and 3.2%, respectively), while the first myctophid species was the fifth (Lepidophanes guentheri with 2.5%) (Sutton et al., 2010).

Cyclotone spp. and myctophid species were reported by Vereshchaka and Vinogradov (1999) from the area of the Broken Spur vent field in the Polish contract area on the MAR. The authors found the fish mentioned, with a biomass of 3 to 40 mg/m^3, to inhabit primarily the main pycnocline (~1000 m depth). Cyclotone spp. were also observed in the vicinity of the hydrothermal fluid discharge. Myctophids were present, too, within the main pycnocline, with vertical ranges overlapping those of *Cyclotone* spp.

References

Afonso, P., McGinty, N., Graca, G., Fontes, J., Inacio, M., Totland, A., Menezes, G., 2014. Vertical Migrations of a Deep-Sea Fish and Its Prey. *PLoS ONE*, 9(5): e97884. doi:10.1371/

Biton Porsmoguer, S., Banaru, D., Bearez, P., Dekeyser, I., Merchan Fornelino, M., Boudouresque, C.F., 2014. Unexpected Headless and Tailless Fish in the Stomach Content of Shortfin Mako *Isurus oxyrinchus. PLoS ONE*, 9(2): e88488. doi:10.1371/journal.pone.0088488

Bubley, W.J., Galuardi, B., Dukes, A.W., Jenkins. W.E., 2020. Incorporating depth into habitat use descriptions for sailfish *Istiophorus platypterus* and habitat overlap with other billfishes in the western North Atlantic. *Marine Ecology Progress Series*, 638, 137-148.

Carey, F.G., Robison, B.H., 1981. Daily patterns in the activities of Sword-fish, *Xiphias gladius,* observed by acoustic telemetry. *U.S. National Marine Fisheries Service Fishery Bulletin*, 79: 277-292.

Dagorn, L., Bach, P., Josse, E., 2000. Movement patterns of large bigeye tuna (*Thunnus obesus*) in the open ocean, determined using ultrasonic telemetry. *Marine Biology,* 136**,** 361-371. doi.org/10.1007/s002270050694

Judkins, D., Haedrich, R., 2018. The deep scattering layer micronektonic fish faunas of the Atlantic mesopelagic ecoregions with comparison of the corresponding decapod shrimp faunas. *Deep-Sea Research Part I*, 136, 1-30. doi: 10.1016/j.dsr.2018.04.008

Lerner, J.D., Kerstetter, D.W., Prince, E.D., Talaue-McManus, L., Orbesen E.S., Mariano, A., Snodgrass, D., Thomas, G.L., 2013. Swordfish Vertical Distribution and Habitat Use in Relation to Diel and Lunar Cycles in the Western North Atlantic. *Transactions of the American Fisheries Society*, 142, 95-104.

Moteki, M., Arai, M., Tsuchiya, K., Okamoto, H.,. 2001. Composition of piscine prey in the diet of large pelagic fish in the eastern tropical Pacific Ocean. *Fisheries Science*, 67, 1063-1074.

Satoh. K., Yokawa, K., Saito, H., Matsunaga, H., Okamoto, H., Uozumi, Y., 2004. Preliminary stomach contents analysis of pelagic fish collected by Shoyo-Maru 2002 research cruise in the Atlantic Ocean. *Collected Volume of Scientific Papers of ICCAT*, 56 (3), 1096-1114.

Sutton, T.T., Porteiro, F.M., Heino, M., Byrkjedal, I., Langhelle, G., Anderson, C.I.H., Horne, J., Søiland, H., Falkenhaug, T.,. Godø. O.R., Bergstad, O.A., 2008. Vertical structure, biomass and topographic association of deep-pelagic fishes in relation to a mid-ocean ridge system. *Deep-Sea Research II Topical Studies in Oceanography,* 55**,** 161-184.

Sutton, T.T., Wiebe, P.H., Madin, L., Bucklin, A., 2010. Diversity and community structure of pelagic fishes to 5000 m depth in the Sargasso Sea. *Deep Sea Research Part II Topical Studies in Oceanography, 57*(*24-26*), 2220-2233. doi:10.1016/j.dsr2.2010.09.024

Vereshchaka, A.L., Vinogradov, G.M., 1999. Visual observations of the vertical distribution of plankton throughout the water column above Broken Spur vent field, Mid-Atlantic Ridge. *Deep-Sea Research I*, 46, 1615-1632.

4.5. Marine birds, mammals and turtles (Lech Stempniewicz)

This section provides a list of species and basic information about the distribution, abundance, breeding and conservation status of pelagic seabirds, cetaceans and sea turtles observed in the Mid-Atlantic Ridge area; the list does not contain sea snakes, as these are not found here.

The attached tables (with information extracted from the references listed at the end of the section) cover 60 species of seabirds (including 19 breeding [Br]), 28 cetaceans and 5 sea turtles (including 4 breeding), for which the closest breeding sites are Cape Verde in the north and Saint Helena and Ascension islands in the south. The others live in the area all year round – they are non-breeding species or their breeding has not been confirmed here. This group also includes species that winter here and migrate through the area seasonally. However, in the tropics, with the exception of a few migratory species, seasonal changes in the abundance of birds, mammals and sea turtles are hardly noticeable.

The Mid-Atlantic Ridge area hosts several species of greatest concern, including two endemic (E) species (the Ascension frigatebird and the Atlantic humpback dolphin), two critically endangered (CR) species (the Atlantic humpback dolphin and the hawksbill sea turtle), as well as four vulnerable (VU) seabirds, one cetacean and three species of sea turtles (see Tables 4.4., 4.5., 4.6.).

Table 4.4. Seabirds found in the tropical/Mid-Atlantic region

Taxonomic position	English name	Latin name	Conservation status	Comments
Diomedeidae	Wandering albatross	*Diomedea exulans*	VU	A
	Black-browed albatross	*Thalassarche melanophris*	LC	A
	Yellow-nosed albatross	*Thalassarche chlororhynchos*	EN	A
	Sooty albatross	*Phoebetria fusca*	EN	A
Procellariidae	Antarctic giant petrel	*Macronectes giganteus*	LC	A
	Southern fulmar	*Fulmarus glacialoides*	LC	A
	Cape petrel	*Daption capense*	LC	A
	Fea's petrel	*Pterodroma feae*	NT	(Br) Cape Verde & Madeira

	Murphy's petrel	*Pterodroma ultima*	NT	A
	Soft-plumaged petrel	*Pterodroma mollis*	LC	A
	Broad-billed prion	*Pachyptila vittata*	LC	A
	Bulwer's petrel	*Bulweria bulwerii*	LC	(Br) Cape Verde & St Helena
	White-chinned petrel	*Procellaria aequinoctialis*	VU	A
	Cory's shearwater	*Calonectris borealis*	LC	A
	Scopoli's shearwater	*Calonectris diomedea*	LC	A
	Cape Verde shearwater	Calonectris edwardsii	NT	(Br) Cape Verde & Canary I.
	Great shearwater	Ardenna gravis	LC	
	Sooty shearwater	Ardenna griseus	NT	A
	Manx shearwater	Puffinus puffinus	LC	A
	Boyd's shearwater	*Puffinus boydi*	EN	(Br) Cape Verde
	Barolo shearwater	*Puffinus baroli*	Ex	A; (Br) north of Canary I.
Oceanitidae	Wilson's storm petrel	*Oceanites oceanicus*	LC	
	White-faced storm petrel	*Pelagodroma marina*	LC	(Br) Cape Verde
	White-bellied storm petrel	*Fregetta grallaria*	LC	A
	Black-bellied storm petrel	*Fregetta tropica*	LC	A
Hydrobatidae	European storm petrel	*Hydrobates pelagicus*	LC	
	Cape Verde storm petrel	*Oceanodroma jabejabe*	EN	(Br) Cape Verde

	Band-rumped storm petrel	*Oceanodroma castro*	LC	(Br) Cape Verde & Ascension I.
	Leach's storm petrel	*Oceanodroma leucorhoa*	LC	
Phaethontidae	Red-billed tropicbird	*Phaethon aethereus*	LC	(Br) Cape Verde, St Helena & Ascension I.
	White-tailed tropicbird	*Phaethon lepturus*	LC	(Br) Ascension I.
Sulidae	Northern gannet	Morus bassanus	LC	A
	Masked booby	*Sula dactylatra*	LC	(Br) Ascension I.
	Red-footed booby	*Sula sula*	LC	(Br) Ascension I.
	Brown booby	*Sula leucogaster*	LC	(Br) Cape Verde, St Helena & Ascension I.
Fregatidae	Magnificent frigatebird	*Fregata magnificens*	LC	(Br) Cape Verde
	Great frigatebird	*Fregata minor*	LC	
	Lesser frigatebird	*Fregata ariel*	LC	
	Ascension frigatebird	*Fregata aquila*	VU	(E), (Br) Ascension I.
Stercorariidae	Great skua	*Catharacta skua*	LC	
	Pomarine jaeger	*Stercorarius pomarinus*	LC	
	Parasitic jaeger	*Stercorarius parasiticus*	LC	
	Long-tailed jaeger	*Stercorarius longicaudus*	LC	A
	Brown skua	*Stercorarius antarctica*	LC	A
Laridae	Lesser black-backed gull	*Larus fuscus*	LC	

	Caspian gull	*Larus cachinnans*	LC	
	Yellow-legged gull	*Larus michahellis*	LC	
	Black-headed gull	*Chroicocephalus ridibundus*	LC	
	Slender-billed gull	*Chroicocephalus genei*	LC	A
	Sabine's gull	*Xema sabini*	LC	
	Black-legged kittiwake	*Rissa tridactyla*	VU	
	Roseate tern	*Sterna dougallii*	LC	
	Common tern	*Sterna hirundo*	LC	
	Arctic tern	*Sterna paradisaea*	LC	
	Brown noddy	*Anous stolidus*	LC	(Br) Ascension I.
	Black noddy	*Anous minutus*	LC	(Br) Ascension I.
	White tern	*Gygis alba*	LC	(Br) St Helena & Ascension I.
	Antarctic tern	*Sterna vittata*	LC	A
Alcidae	Common guillemot	*Uria aalge*	LC	

Table 4.5. Cetaceans reported from the tropical/Mid-Atlantic region

Taxonomic position	**English name**	**Latin name**	**Conservation status**	**Comments**
Mysticeti	Fin whale	*Balaenoptera physalus*	VU	
	Humpback whale	*Megaptera novaeangliae*	LC	
	Bryde's whale	*Balaenoptera brydei*	LC	
	Sei whale	*Balaenoptera borealis*	EN	
	Blue whale	*Balaenoptera musculus*	EN	
	Northern minke whale	*Balaenoptera acutorostrata acutorostrata*	LC	

Odontoceti				
Delphinidae	Short-beaked common dolphin	*Delphinus delphis*	LC	shelf areas
	Long-beaked common dolphin	*Delphinus capensis*	DD	
	Fraser's dolphin	*Lagenodelphis hosei*	LC	
	Atlantic humpback dolphin	*Sousa teuszi*	CR	(E) W Africa shelf
	Pantropical spotted dolphin	*Stenella attenuate*	LC	
	Atlantic spotted dolphin	*Stenella frontalis*	LC	
	Spinner dolphin	*Stenella longirostris*	LC	
	Clymene dolphin	*Stenella clymene*	LC	
	Striped dolphin	*Stenella coeruleoalba*	LC	
	Common bottlenose dolphin	*Tursiops truncates*	LC	
Orcininae	Pygmy killer whale	*Feresa attenuate*	LC	
	Short-finned pilot whale	*Globicephala macrorhynchus*	LC	
	Killer whale (orca)	*Orcinus orca*	DD	
	Melon-headed whale	*Peponocephala electra*	LC	
	False killer whale	*Pseudorca crassidens*	NT	
	Rough-toothed dolphin	*Steno bredanensis*	LC	
Physeteroidea	Dwarf sperm whale	*Kogia sima*	LC	
	Pygmy sperm whale	*Kogia breviceps*	LC	
	Sperm whale	*Physeter macrocephalus*	EN	dives to 2,250 m
Ziphioidea	Gervais' beaked whale	*Mesoplodon europaeus*	DD	
	Blainville's beaked whale	*Mesoplodon densirostris*	DD	
	Cuvier's beaked whale	*Ziphius cavirostris*	LC	

Table 4.6. Sea turtles known from the tropical/Mid-Atlantic region

Taxonomic position	**English name**	**Latin name**	**Conservation status**	**Comments**
Carettinae	Loggerhead sea turtle	*Caretta caretta*	VU	Br
	Olive ridley sea turtle	*Lepidochelys olivacea*	VU	
Cheloniinae	Green sea turtle	*Chelonia mydas*	EN	Br
	Hawksbill sea turtle	*Eretmochelys imbricata*	CR	Br
Dermochelyinae	Leatherback	*Dermochelys coriacea*	VU	Br

IUCN Red List of Threatened Species: CR, Critically endangered; EN, Endangered; VU, Vulnerable; LC, Least concern; (Br) Breeding; (A) Accidental – occurs rarely or accidentally; (E) Endemic

References

Ashmole, N.P., Ashmole, M.J., 2000. *St Helena and Ascension Island: a Natural History*. Oswestry, U.K. Anthony Nelson.

Birdlife international, 2000. *Threatened Birds of the World.* Lynx Edicions and BirdLife International. Barcelona and Cambridge, UK.

BirdLife International, 2012. *Calonectris edwardsii. IUCN Red List of Threatened Species*.

Bourne, W.R.P., 2008. The birds of the Cape Verde Islands. *Ibis*, 97(3), 508-556.
doi: 10.1111/j.1474-919X.1955.tb04981.x

Harrison, P. 1983. *Seabirds - An Identification Guide*. London & Sydney: Croom Helm.

Hazevoet, C.J., 1995. *The birds of the Cape Verde Islands*. Tring, UK: British Ornithologists' Union (Check-list 13).

IUCN, 2015. *The IUCN Red List of Threatened Species*. IUCN.

Klinowska, M., Cooke, J., 1991. *Dolphins, Porpoises, and Whales of the World: the IUCN Red Data Book.* Columbia University Press, NY: IUCN Publications.

McCulloch, N., 2004. *A guide to the birds of St Helena and Ascension Island.* Royal Society for the Protection of Birds.

Prater, T. 2012. Important Bird Area. St Helena. *British Birds*, 105 (11), 638-653.

Fishpool, L.D.C., Evans, M.I., 2001. *Important Bird Areas in Africa and Associated Islands: Priority sites for conservation.* Pisces Publications and BirdLife International (BirdLife Conservation Series No. 11). Newbury and Cambridge, UK.

Wilson, D.E., Reeder, D.A.M., 2005. Cetacea. In: *Mammal Species of the World. A Taxonomic and Geographic Reference* (3rd ed.). Johns Hopkins University Press.

5. Benthic organisms

Krzysztof Pabis, Piotr Jóźwiak and Teresa Radziejewska

5.1. Meiobenthos (Teresa Radziejewska)

With most research on the hydrothermal vent meiobenthos (benthic meiofauna) having been so far carried out in the Pacific ridge areas (Zeppilli et al., 2018), the Mid-Atlantic Ridge (MAR) meiobenthos appears greatly understudied. There have been few dedicated studies (Flint, 2007; Zekely et al., 2006; Cuvelier et al., 2014; Sarrazin et al., 2015; Tchesunov, 2015; Spedicato et al. 2020), and some additional data can be gleaned from more general overviews of the MAR benthic communities (Gebruk and Mironov, 2006).

The MAR meiobenthos has been so far sampled at various known active hydrothermal fields (Menez Gwen, Lucky Strike, Rainbow, Lost City, Broken Spur, TAG, Snake Pit, Logatchev), two of which (Lost City and Broken Spur) are situated within the Polish contract area.

The meiobenthos composition was reported from samples collected, as a rule, with push-corers from a remote-operated vehicle (ROV) (Flint, 2007) (see Section 10.3.) or a human-operated vehicle (HOV) (*MIR 1* in Tchesunov, 2015; *Nautile* in Spedicato et al., 2020); Zekely et al. (2006) collected their samples with a special device called 'Bushmaster Jr.' operated from an HOV (see Section 10.3.). The meiobenthos studied by Sarrazin et al. (2015) was collected with a suction sampler or the ROV's arm grab.

Generally, the number of samples analysed for the meiobenthos (i.e., the sampling effort) has been low; usually, the researchers had access to 2-12 cores/samples.

The composition of meiobenthic assemblages (Table 5.1.A) shows the presence of a total of 45 taxa. Numerous of them were identified to the species level, although many were reported at a much lower taxonomic resolution (genus, family or order).

All the meiofaunal studies on the MAR show the meiobenthos assemblages to consist of the Nematoda, Gastrotricha, Polychaeta, Halacaroidea, Ostracoda, Copepoda (Calanoida, Cyclopoida, Harpacticoida, Poecilostomatoida, Siphonostomatoida), Tantulocarida and Bivalvia (Table 5.1.A). The hydrothermal fields within the Polish contract area (Lost City and Broken Spur) have proven very impoverished in this respect, and also differing in terms of their taxonomic richness: while no non-nematode taxon has been reported from Lost City, Broken Spur turned out to support 5 meiofaunal taxa, all of them representing copepods. Noteworthy is the presence there of 3 species of the copepod siphonostomatoid family Dirivultidae, regarded as endemic to the hydrothermal vents worldwide (cf. Section 7.2.) and particularly well adapted to life in the vicinity of the hot venting fluid (Zeppilli et al., 2018).

As shown in Fig. 5.1., the similarity in faunistic composition between meiobenthic assemblages reported so far from different vent fields on the MAR is quite low, the assemblages for which data are known from Broken Spur and Lost City being, interestingly, more similar to one another (and to that at Rainbow) than to the remaining fields. It has to be remembered, however, that the similarity analysis shown in Fig. 5.1. has been carried out on a very limited amount of data.

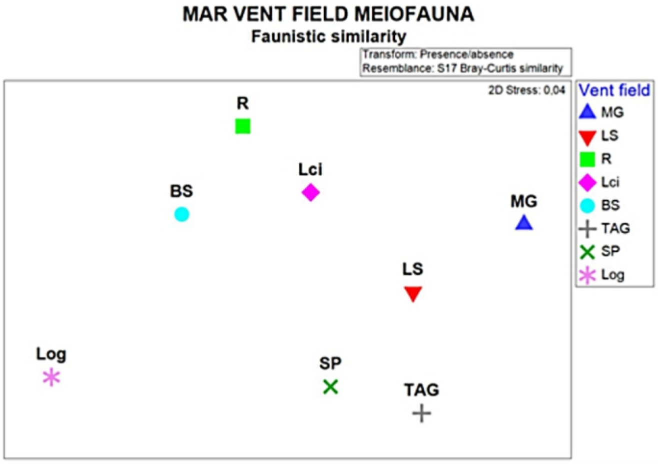

Fig. 5.1. MDS plot of similarity/dissimilarity between meiobenthos faunistic composition at different MAR vent fields (presence-absence transformation; Bray-Curtis similarity); Vent field name symbols: R, Rainbow; BS, Broken Spur; Lci, Lost City; MG, Menez Gwen; LS, Lucky Strike; SP, Snake Pit; TAG, Trans-Atlantic Geotraverse; Log, Logatchev

All the MAR studies report the meiobenthos assemblages to be dominated by nematodes, copepods (notably harpacticoids) being the second most abundant taxon; it was only at a non-vent site at the TAG field sampled by Flint (2007) that the proportion between the two higher taxa was reversed. On account of the nematode dominance, most of the meiofaunal studies on MAR have been, in fact, focussing on nematodes. This is evident from the list of meiofaunal taxa reported from the MAR hydrothermal vent fields provided by the relevant publications. In fact, the list of nematode taxa (mostly genera, but also species and families) is quite long (a total of 74), considering the low number of samples analysed so far (Table 5.1.B).

The hydrothermal fields within the Polish contract area (Lost City and Broken Spur) have been reported to differ in terms of their nematode taxonomic richness (Table 5.1.B). While 13 nematode taxa have been reported from Lost City, as few as 3 have been found at Broken Spur. Interestingly, the Lost City nematode assemblage features the genus Oncholaimus, reported as very abundant at most active vent sites (Tchesunov, 2015; Zeppilli et al., 2018), specialising in feeding on free-living chemoautotrophic microorganisms and harbouring an epibiotic microbial community dominated by the Gammaproteobacteria lineage, including vent symbionts (Zeppilli et al., 2018).

At hydrothermal vent sites worldwide, the meiobenthos has been found to be associated with various habitats, from inactive bare basalts (Gollner et al., 2010) and sediments (Vanreusel et al., 1997) to diffuse vent flow areas colonised by macrofaunal assemblages (Zekely et al., 2006; Sarrazin et al., 2015). When working in the Pacific (Fiji-Lau area), Vanreusel et al. (1997) found none of the nematode species found in the hydrothermal sediments to occur in the surrounding abyssal areas. No such comparisons have been conducted on MAR.

Meiofaunal (nematode) colonisation of artificially deployed, organic (wood and bone) and inorganic (slate), substrata at the MAR's Lucky Strike hydrothermal vent site was addressed by a French research group (Cuvelier et al., 2014; Zeppilli et al., 2015;). A fast colonisation as well as a clear preference with respect to the substratum type, depending on the distance from the vent, was reported, particularly evident during the first 9 months of the study. Such experiments are important as they provide data with which to assess the community's ability to recover from a disturbance, and confirm the utility of the meiobenthos in studies on post-disturbance recovery.

Table 5.1. Meiofaunal taxa reported from the hydrothermal vent fields in the Polish contract area (Lost City, Broken Spur) and elsewhere on MAR; A) non-nematode taxa; B) nematode taxa (data from Gebruk and Mironov, 2006; Flint, 2007; Tchesunov, 2015; Zeppilli et al., 2015; Sarrazin et al., 2015; Spedicato et al., 2020); +, taxon recorded; -, taxon not recorded

A

Taxon		**Lost City**	**Broken Spur**	**Other MAR fields**
Gastrotricha	Gastrotricha indet.	–	–	+
Polychaeta	Polychaeta indet.	–	–	+
Halacaroidea	*Agauopsis auzendei*	–	–	+
	Bathyalacarus sp.	–	–	+
	Halacarellus alvinus	–	–	+
	Halacarus prolongatus	–	–	+
	Copidognathus nautilei	–	–	+
	Copidognatus alvinus	–	–	+
Tantulocarida	Tantulocarida indet.	–	–	+
Copepoda Siphonostomatoida	*Aphotopontius atlanteus*	–	–	+
	A. temperatus	–	–	+
	A. forcipatus	–	–	+
	Rimipontius mediospinifer	–	+	+
	Stygiopontius rimivagus	–	–	+
	S. bulgisetiger	–	–	+
	S. cladarus	–	+	+
	S. latulus	–	–	+
	S. mirus	–	–	+

	S. pectinatus	–	+	+
	S. regius	–	–	+
	S. serratus	–	–	+
	S. teres	–	–	+
	Dirivultidae indet.	–	–	+
Copepoda Harpacticoida	*Bathylaophonte azorica*	–	–	+
	Microsetella norvegica	–	+	–
	Aegisthidae indet.	–	–	+
	Ectinosomatidae indet.	–	–	+
	Miraciidae indet.	–	–	+
	Pseudotachidiidae indet.	–	–	+
	Tegastidae indet.	–	–	+
	Tisbidae indet.	–	–	+
Copepoda Cyclopoida	*Heptnerina confusa*	–	–	+
	Oncaea sp.	–	+	–
	Cyclopinidae indet.	–	–	+
	Oithonidae indet.	–	–	+
	Lubbockiidae	–	–	+
Copepoda Spinocalanoida	Spinocalanoida indet.	–	–	+
Ostracoda	*Bathyconchoecia paulula*	–	–	+
	Bairdia sp.	–	–	+
	Bythocypris sp.	–	–	+
	Krithe sp.	–	–	+
	Propontocypris sp.	–	–	+
	Poseidonamicus sp.	–	–	+
	Ostracoda indet.	–	–	+
Bivalvia	Bivalvia indet.	–	–	+

B

Taxon	**Lost City**	**Broken Spur**	**Other MAR fields**
Acantholaimus	–	–	+
Acanthopharynx	–	–	+
Actinonema	+	–	–
Anoplostoma	–	–	+
Anticoma	–	–	+
Anticomidae indet	+	+	+
Amphimonhystrella	–	–	+
Aponema	–	–	+
Araeolaimus	–	–	+
Benthimermitidae indet.	–	–	+
Calomicrolaimus	–	–	+
Camacolaimus	–	–	+
Capsula	–	–	+
Cephalochaetosoma	–	–	+
Chromadorella	–	–	+
Chromadorina	–	–	+
Chromadorita	–	–	+
Cobbia	–	–	+
Cyatholaimus	–	–	+
Daptonema	+	–	+
Desmodora	+	–	+
Desmoscolex	–	–	+
Dinetia	–	–	+
Diplopeltidae indet.	–	–	+
Diplopeltoides	–	–	+
Dracogallus	–	–	+
Draconema	–	–	+
Eleutherolaimus	–	–	+

Enchelidiidae indet.	+	–	–
Enoplus	+	–	–
Enoplidae indet.	–	–	+
Epsilonema	–	–	+
Epsilonematidae indet.	–	–	+
Euchromadora	–	–	+
Eurystomina	–	–	+
Halalaimus	–	–	+
Halomonhystera	–	–	+
Halichoanalaimus	–	–	+
Leptolaimus	–	–	+
Leptloaimidae indet.	–	–	+
Megadesmolaimus	–	–	+
Metacomesoma	–	–	+
Metacylicolaimus	+	–	–
Metachromadora	–	–	+
Metadesmolaimus	–	–	+
Metalinhomoeus	–	–	+
Metepsilonema	–	–	+
Microlaimus	–	–	+
Molgolaimus	–	–	+
Monhysteridae indet.	–	–	+
Oncholaimus	+	–	+
Oncholaimidae indet.	–	–	+
Oxystomina	–	–	+
Palinchomeous	+	–	+
Paracanthonchus	–	–	+
Paracanthonchus olgae	+	+	+
Parapinnanema	–	–	+
Prochaetosoma ventriverruca	+	–	+

Prochromadora helenae	+	+	+
Prooncholaimus	–	–	+
Pselionema	–	–	+
Quadricoma	–	–	+
Retrotheristus	–	–	+
Rhabdocoma	–	–	+
Sabatieria	–	–	+
Sphaerolaimus	–	–	+
Synonchus	–	–	+
Syringolaimus	+	–	+
Terschellingia	–	–	+
Thalassolaimus	–	–	+
Thalassomonhystera	–	–	+
Theristus	–	–	+
Tricoma	–	–	+
Viscosia	–	–	+

References

Cuvelier, D., Beesau, J., Ivanenko, V.N., Zeppilli, D., Sarradin, P.M., Sarrazin, J., 2014. First insights into macro- and meiofaunal colonisation patterns on paired wood/slate substrata at Atlantic deep-sea hydrothermal vents. *Deep Sea Research Part I*, 87, 70-81.

Flint, H.C., 2007. *Diversity of meiofauna at deep-sea hydrothermal vents and cold seeps with particular reference to nematodes*. Ph.D. thesis, National Oceanography Centre, Southampton.

Gebruk, A.V., Mironov, A.N., 2006. Biogeografiya gidroterm Sredinno-Atlanticheskogo Khrebta. In: Vinogradov, M.E., Vereshchaka, A.L. (eds), *Ekosistemy atlanticheskikh gidroterm*. Nauka, Moskva, 119-162.

Gollner, S., Riemer, B., Martínez Arbizu, P., Le Bris, N., Bright, M. 2010. Diversity of meiofauna from the 9°50′N East Pacific Rise across a gradient of hydrothermal fluid emissions. *PLoS ONE,* 5:e12321.

Sarrazin, J., Legendre, P., De Busserolles, F., Fabri, M.C., Guilini, K., Ivanenko, V.N., Morineaux, M., Vanreusel, A., Sarradin, P.M., 2015. Biodiversity patterns, environmental drivers and indicator species on a high temperature hydrothermal edifice, Mid-Atlantic Ridge. *Deep Sea Research Part II*, 121, 177-192.

Spedicato, A., Sánchez, N., Pastor, L., Menot, L., Zeppilli, D., 2020. Meiofauna Community in Soft Sediments at TAG and Snake Pit Hydrothermal Vent Fields. *Frontiers in Marine Science*, 7, 200.

Tchesunov, A.V., 2015. Free-living nematode species (Nematoda) dwelling in hydrothermal sites of the North Mid-Atlantic Ridge. *Helgoland Marine Research*, 69, 343-384.

Vanreusel, A., Bossche, I. van den, Thiermann, F., 1997. Free-living marine nematodes from hydrothermal sediments: similarities with communities from diverse reduced habitats. *Marine Ecology Progress Series*, 157, 207-219.

Zekely, J., Van Dover, C. L., Nemeschkal, H. L., Bright, M., 2006. Hydrothermal vent meiobenthos associated with mytilid mussel aggregations from the Mid-Atlantic Ridge and the East Pacific Rise. *Deep Sea Research Part I*, 53, 1363-1378.

Zeppilli, D., Vanreusel, A., Pradillon, F., Fuchs, S., Mandon, P., James, T., Sarrazin, J., 2015. Rapid colonisation by nematodes on organic and inorganic substrata deployed at the deep-sea Lucky Strike hydrothermal vent field (Mid-Atlantic Ridge). *Marine Biodiversity*, 45, 489-504.

Zeppilli, D., Leduc, D., Fontanier, C., Fontaneto, D., Fuchs, S., Gooday, A.J., Goineau, A., Ingels, J., Ivanenko, V.N., Kristensen, R.M., Cardoso Neves, R., Sanchez, N., Sandulli, R., Sarrazin, J., Sørensen, M.V., Tasiemski, A., Vanreusel, A., Autret, M., Bourdonnay, L., Claireaux, M., Coquillé, V., De Wever, L., Rachel, D., Marchant, J., Toomey, L., Fernandes, D., 2018. Characteristics of meiofauna in extreme marine ecosystems: a review. *Marine Biodiversity*, 48, 35-71.

5.2. Macrobenthos (Krzysztof Pabis and Piotr Jóźwiak)

Macrofaunal benthic communities of the Mid-Atlantic Ridge (MAR) have been studied less extensively than the assemblages of megafaunal invertebrates (cf. Section 5.3.). More comprehensive data sets concern the larger epibenthic macrofauna, such as echinoderms and all the other organisms visible in seafloor imagery, including the temporary macrofauna, e.g., the *Rimicaris* shrimps. Therefore, data on macrofaunal distribution patterns have been, at least in part, acquired as a “side effect” of studies focussing on the megafaunal communities, for which reason identification has been often limited to higher taxonomic units (genera or families). The information provided in publications makes it occasionally difficult to conclude whether the analysis concern the macro- or the megafaunal organisms (e.g., Desbruyères et al., 2000; Kelley et al., 2005; Alt et al., 2013; Bell et al., 2016; Alt et al., 2019).

Knowledge on the most important and diverse macrofaunal taxa, such as polychaetes, peracarid crustaceans, bivalves and gastropods is very scant, and there have been only a few quantitative assessments of the standing stock and diversity. The limitation is due to constraints associated with the so-called physical sampling that requires the use of dredges, epibenthic sledge or various grabs and corers, as well as to the need of taxonomic expertise. A particularly wide knowledge gap concerns the fauna associated with soft sediments (Bergstad et al., 2008; Gebruk et al., 2010; Shields and Blanco-Perez, 2013; Priede et al., 2013), although this habitat is a very important component of the MAR region (Niedzielski et al., 2013).

There are almost no data on the biology and habitat requirements of most of the macrofaunal taxa. Some case studies revealed certain very interesting interspecific associations, such as those between polynoid polychaetes and holothurians or bivalves (Shields et al,. 2012; Bebianno et al., 2018), demonstrating a unique nature of biological interactions, particularly in the vent systems. Other authors elucidated differences in the composition, abundance, and diversity of macrofaunal assemblages, shaped by key environmental factors (temperature, total dissolved iron, sulphide and copper, pH), but on a very small scale (less than 1m^2) (Sarrazin et al., 2015). Studies of the reproductive behaviour, physiology, and development have also been infrequent, a particular attention being paid to the vent fauna (e.g., Blake and Van Dover, 2005; Riou et al., 2010; Marticorena et al., 2020).

The available species lists are often scattered among various publications, including short taxonomic notes, and there is a limited information on distribution patterns and factors controlling the diversity, species composition, and abundance of the communities (e.g,, Bellan-Santini and Thurston, 1996; Gebruk et al., 2010; Goroslavskaya and Galkin. 2011; Dilman, 2013; Shields and Blanco-Perez, 2013; Kongsrud et al., 2013).

The scale of the undescribed biodiversity is most probably huge. The study of polychaete fauna collected with a megacorer (Shields and Blanco-Perez, 2013) resulted in finding 133 species in just 11 samples (only 0.54m^2 of the total surface sampled). The mean abundance reached 1285 ± 464 ind./m^2, while the mean biomass was 19.60 ± 713.27 mg/m^2. The fauna was dominated by spionids (mainly *Aurospio dibranchiata* and *Prionospio* sp.), syllids, and cirratulids. The communities were substantially (in 70%) dominated by surface deposit feeders. Most of the species collected were singletons, therefore a high level of rarity can be assumed, although the final conclusion is difficult without any higher sampling effort. Many of the species collected are also new to science, although most of them are still awaiting the formal description. Similar results were reported for scavenging amphipods, with about 50% of the species not being previously known (Horton et al., 2013).

It is also impossible to properly assess the level of endemism in the most important invertebrate groups (cf. Section 7.2.), although the few available taxonomic studies showed the presence of new species on the MAR, including in vent habitats (e.g., Tyler et al., 1995, Sigvaldadottir and Desbruyères, 2003; Myers and Cunha, 2004; Cunha and Wilson, 2006; Larsen et al., 2006; Bellan-Santini, 2007; Corbera et al., 2008; Budaeva, 2012), and there is a great need for an increased taxonomic effort in the whole region. Many new species can be expected among small peracarids with limited dispersal potential, such as tanaidaceans and isopods, which are a very important component of the deep-sea communities worldwide (e.g., Błażewicz-Paszkowycz et al., 2015; Pabis et al., 2015; Riehl et al., 2018). Molecular studies focussed on the analysis of species composition and diversity are almost absent, whereas such studies might be crucial for an appropriate future assessment of impacts produced by mining activities (Klunder et al., 2020).

Analyses of spatial distribution of some taxa showed a certain division between the north-east and south-east sites in the case of polychaetes (Shields and Blanco-Perez, 2013), whereas scavenging amphipods were shown to be more widely distributed, most probably as a result of their higher mobility and feeding mode (Horton et al., 2013). Generally, the abundance and biomass of the macrofauna seems to be at a level similar to that in other deep-sea sites (Priede et al., 2013), although some scavengers such as amphipods may form temporary aggregations of even 40,000 individuals, food availability allowing (Horton et al., 2013). Jones et al. (2013) showed also that enteropneusts can be important bioturbators at bathyal depth of MAR.

As summarised by Kelley et al. (2005) for MAR vent sites, the number of species per site may vary between 30 and 50, while for eight major MAR vent fields about 100 species were recorded at each location. The fauna of the hydrothermal vent fields located in the Polish contract area has been studied intermittently only, and the available data likely provide a highly incomplete picture of its diversity, abundance, and biomass. The data on the Lost City macrofauna are very scant. Nevertheless, the available reports show the presence of at least 65 species (collected with a suction sampler), including gastropods, amphipods (e.g., *Bouvierella curtirama, Primno evansis*), polychetes, euphausiids, and ostracods. The level of endemism has been estimated at about 58% (Kelley et al. 2005, 2007), although recent molecular studies demonstrated that problem of endemism, cryptic diversity and connectivity along the MAR is very complex (cf. Section 7.2.) and requires further studies (Teixeira et al., 2013; Yahagi et al., 2019), which are important for appropriate conservation strategies and/or management plans associated with any type of human activities that may influence seabed communities (Hilario et al., 2015). Information on the Broken Spur vent field macrobenthos is also fairly scant; that fauna includes, for example, the bivalve *Bathymodiolus puteoserpentis*, the ampharetid polychaete *Amathys lutzi*. and the ophiuroid *Ophioctenella acies* (Rybakova and Galkin, 2014) as well as temporarily macrofaunal shrimps or polychaetes that can attain much larger sizes during their development and be classified as the megafauna (Desbruyères, 2000). A multivariate analysis of the faunistic similarity between the macrobenthos of individual vent fields (Fig. 5.2.), based on data reported by Gebruk and Mironov (2006) showed, firstly, a low overall similarity (except for the Logatchev and Snake Pit faunas); secondly, a low similarity between the faunas at Lost City and Broken Spur; and, thirdly, a low similarity between the fauna at Lost City and at other fields.

The available data studies demonstrate the MAR macrofauna to be a diverse and abundant component of a very complex system that needs further, much more comprehensive research based on a higher sampling effort, accompanied by the analysis of various physico-chemical factors. At the moment, we have probably managed to get a glimpse on a tip of an iceberg.

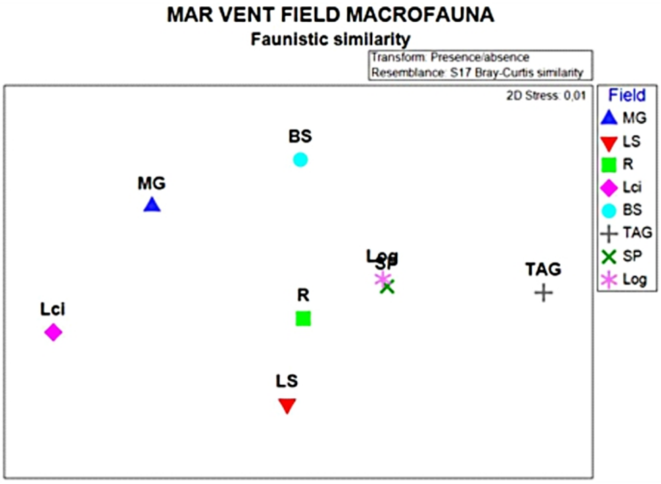

Fig. 5.2. MDS plot of similarity/dissimilarity between macrobenthos faunistic composition at different MAR vent fields (presence-absence transformation; Bray-Curtis similarity); Vent field name symbols: R, Rainbow; BS, Broken Spur; Lci, Lost City; MG, Menez Gwen; LS, Lucky Strike; SP, Snake Pit; TAG, Trans-Atlantic Geotraverse; Log, Logatchev

References

Alt, C.H.S., Rogacheva, A., Boorman, B., Hughes, J.A., Billett, D.S.M., Gooday, A.J., Jones, D.O.B. 2013. Trawled megafaunal invertebrate assemblages from bathyal depth of the Mid-Atlantic Ridge (48°-54° N). *Deep-Sea Research Part II Topical Studies in Oceanography*, 98, 326-340.

Alt, C.H.S., Kremenetskaia (Rogacheva), A., Gebruk, A.V., Gooday, A.J., Jones, D.O.B., 2019. Bathyal benthic megafauna from the Mid-Atlantic Ridge in the region of the Charlie-Gibbs fracture zone based on remotely operated vehicle observations. Deep-Sea Research Part I, 145, 1-12.

Bebianno, M.J., Cardoso, C., Gomes ,T., Blasco, J., Santos, R.S., Colaço A., 2018. Metal interactions between the polychaete Branchipolynoe seepensis and the mussel Bathymodiolus azoricus from Mid-Atlantic-Ridge hydrothermal vent fields. *Marine Environmental Research*, 135, 70-81.

Bell, J.B., Alt, C.H.S., Jones, D.O.B., 2016. Benthic megafauna on steep slopes at the Northern Mid-Atlantic Ridge. *Marine Ecology*, 37, 1290-1302.

Bellan-Santini, D., 2007. New amphipods of hydrothermal vent environments on the Mid-Atlantic Ridge, Azores Triple junction zone. *Journal of Natural History*, 41, 567-596.

Bellan-Santini, D., Thurston, M.H., 1996. Amphipoda of the hydrothermal vents along the mid-Atlantic Ridge. *Journal of Natural History*, 30, 685-702.

Bergstad, O.A., Falkenhaug, T., Astthorsson, O.S., Byrkjedal, I., Gebruk, A.V., Piatkowski, U., Priede, I.G., Santos, R.S., Vecchione, M., Lorance, P., Gordon, J.D.M., 2008. Towards improved understanding of the diversity and abundance patterns of the mid-ocean ridge macro- and megafauna. *Deep-Sea Research Part II Topical Studies in Oceanography*, 55, 1-5.

Blake, E.A., Van Dover, C.L., 2005. The reproductive biology of *Amathys lutzi*, an ampharetid polychaete from hydrothermal vents on the Mid-Atlantic Ridge. *Invertebrate Biology*, 124, 254-264.

Błażewicz-Paszkowycz, M., Pabis, K., Jóźwiak, P., 2015. Tanaidacean fauna of the Kuril-Kamchatka Trench and adjacent abyssal plain – abundance, diversity and rare species. *Deep-Sea Research Part II Topical Studies in Oceanography,* 111, 325-332.

Budaeva, N., 2012. Leptoecia midatlantica, a new species of the deep-sea quill-worms (Polychaeta: Onuphidae: Hyalinoeciinae) from the Mid-Atlantic Ridge. *Zootaxa*, 3176, 45-60.

Corbera, J., Segonzac, M., Cunha, M.R., 2008. A new deep-sea genus of Nannastacidae (Crustacea, Cumacea) from the Lucky Strike hydrothermal vent field (Azores Triple Junction, Mid-Atlantic Ridge). *Marine Biology Research*, 4, 180-192.

Cunha, M.R., Wilson, G.D.F., 2006. The North Atlantic genus *Heteromesus* (Crustacea: Isopoda: Asellota: Ischnomesidae). *Zootaxa*, 1192, 3-76.

Desbruyères, D., Almeida, A., Biscoito, M., Comtet, T., Khripounoff, A., Le Bris, N., Sarradin, P.M. Segonzac, M., 2000. A review of the distribution of hydrothermal vent communities along the northern Mid-Atlantic Ridge: dispersal vs. environmental controls. *Hydrobiologia*, 440, 201–216.

Dilman, A.B., 2013. Asteroid fauna of the northern Mid-Atlantic Ridge: additional records, *Marine Biology Research*, 9, 563-586.

Gebruk, A.V., Mironov, A.N., 2006. Biogeografiya gidroterm Sredinno-Atlanticheskogo Khrebta. In: Vinogradov, M.E., Vereshchaka, A.L. (eds), *Ekosistemy atlanticheskikh gidroterm*. Nauka, Moskva, 119-162.

Gebruk, A.V., Budaeva, N.E., King, N.J., 2010. Bathyal benthic fauna of the Mid-Atlantic Ridge between the Azores and the Reykjanes Ridge. *Journal of the Marine Biological Association of the United Kingdom*, 90, 1-14.

Goroslavskaya, E.I., Galkin, S.V., 2011. Benthic fauna associated with mussel beds and shrimp swarms at hydrothermal fields on the Mid-Atlantic Ridge. *Oceanology*, 51, 69-79.

Hilário, A., Metaxas, A., Gaudron, S.M., Howell, K.L., Mercier, A., Mestre, N.C., Ross, R.E., Thurnherr, A.M., Young, C., 2015. Estimating dispersal distance in the deep sea: challenges and applications to marine reserves. *Frontiers in Marinne Science*, 2, 6.

Horton, T., Thurston, M.H., Duffy, G.A., 2013. Community composition of scavenging amphipods at bathyal depths on the Mid-Atlantic Ridge. *Deep Sea Research Part II Topical Studies in Oceanography*, 98, 352-359.

Jones, D.O.B., Alt, C.H.S., Priede, I.G., Reid, W.D.K., Wigham, B.D., Billett, D.S.M., Gebruk, A.V., Rogacheva, A., Gooday, A.J., 2013. Deep-sea surface-dwelling enteropneusts from the Mid-Atlantic Ridge: Their ecology, distribution and mode of life. *Deep Sea Research Part II Topical Studies in Oceanography*, 98, 374-387.

Kelley, D.S., Früh-Green, G.L., Karson, J.A., Ludwig, K.A. 2007. The Lost City hydrothermal field revisited. *Oceanography*, 20, 90-99.

Kelley, D.S., Karson, J.A., Früh-Green, G.L., Yoerger, D.R., Shank, T.M., Butterfield, D.A., Hayes, J.M., Schrenk, M.O., Olson, E.J., Proskurowski, G., Jakuba, M., Bradley, A., Larson B., Ludwig, K., Glickson, D., Buckman, K., Bradley, A.S., Brazelton, W.J., Roe K., Elend, M.J., Delacour, A., Bernasconi, S.M., Lilley, M.D., Baross, J.A., Summons, R.E., Sylva, S.P. 2005. A Serpentinite-Hosted Ecosystem: The Lost City Hydrothermal Field. *Science*, 307, 1428-1433.

Klunder, L., Stigter, H., Lavaleye, M.S.S., van Bleijswijk, J.D.L., van der Veer, H.W., Reichart, G.J., Duineveld, G.C.A., 2020. A Molecular Approach to Explore the Background Benthic Fauna Around a Hydrothermal Vent and Their Larvae: Implications for Future Mining of Deep-Sea SMS Deposits. Frontiers in Marine Science, 7, 134.

Kongsrud, J.A., Budaeva, N., Barnich, R., Oug, E., Bakken, T., 2013. Benthic polychaetes from the northern Mid-Atlantic Ridge between the Azores and the Reykjanes Ridge. Marine Biology Research, 9, 516–546.

Larsen, K., Błażewicz-Paszkowycz, M., Cunha, M.R., 2006. Tanaidacean (Crustacea: Peracarida) fauna from chemically reduced habitats – the Lucky Strike hydrothermal vent system, mid-Atlantic ridge. Zootaxa, 1187, 1-36.

Marticorena, J., Matabos, M., Sarrazin. J., Ramirez-Llodra, E., 2020. Contrasting reproductive biology of two hydrothermal gastropods from the Mid-Atlantic Ridge: implications for resilience of vent communities. Marine Biology, 167, 1-19.

Myers, A.A., Cunha, M.R., 2004. New and little known corophiidean amphipods from the 'Lucky Strike' hydrothermal vent, Mid-Atlantic Ridge. Journal of the Marine Biological Association of the United Kingdom, 84, 1019-1025.

Niedzielski, T., Høines, A., Shields, M.A., Linley, T.D., Priede, I.G., 2013. A multi-scale investigation into seafloor topography of the northern Mid-Atlantic Ridge based on geographic information system analysis. Deep Sea Research Part II Topical Studies in Oceanography, 98, 231-243.

Pabis, K., Błażewicz-Paszkowycz, M., Jóźwiak, P., Barnes, D.K.A., 2015. Tanaidacea of the Amundsen and Scotia Seas: an unexplored diversity. Antarctic Science, 27, 19-30.

Riehl, T., Lins Pereira, L., Brandt, A., 2018. The effects of depth, distance, and the Mid-Atlantic Ridge on genetic differentiation of abyssal and hadal isopods (Macrostylidae). Deep Sea Research Part II Topical Studies in Oceanography, 148, 74-90.

Riou, V., Duperron, S., Dehairs, H.F., Bouillon, S., Martin, I., Colaço, A., Santos, R.S., 2010. Variation in physiological indicators in Bathymodiolus azoricus (Bivalvia: Mytilidae) at the Menez Gwen Mid-Atlantic Ridge deep-sea hydrothermal vent site within a year. Marine Environmental Research, 70, 264-271.

Rybakova, E., Galkin, S., 2014. Hydrothermal assemblages associated with different foundation species on the East Pacific Rise and Mid-Atlantic Ridge, with a special focus on mytilids. Marine Ecology, 36, 45-61.

Sarrazin, J., Legendre, P., De Busserolles, F., Fabri M.C., Guilini, K., Ivanenko, V.N., Morineaux, M., Vanreusel, A., Sarradin, P.M., 2015. Biodiversity patterns, environmental drivers and indicator species on a high-temperature hydrothermal edifice, Mid-Atlantic Ridge. Deep-Sea Research Part II Topical Studies in Oceanography, 121, 177-192.

Shields, M.A., Blanco-Perez, R., 2013. Polychaete abundance, biomass and diversity patterns at the Mid-Atlantic Ridge, North Atlantic Ocean. Deep Sea Research Part II Topical Studies in Oceanography, 98, 315-325.

Shields, M.A., Glover, A.G., Wiklund, H., 2013. Polynoid polychaetes of the Mid-Atlantic Ridge and a new holothurian association. Marine Biology Research, 9, 547-553.

Sigvaldadottir, E., Desbruyères, D., 2003. Two new species of spionidae (Annelida : Polychaeta) from Mid-Atlantic Ridge hydrothermal vents. *Cahiers de Biologie Marine*, 44, 219-225.

Teixeira, S., Olu, K., Decker, C., Cunha, R.L., Fuchs, S., Hourdez, S., Serrão, E.A., Arnaud-Haond, S., 2013. High connectivity across the fragmented chemosynthetic ecosystems of the deep Atlantic Equatorial Belt: efficient dispersal mechanisms or questionable endemism? *Molecular Ecology*, 22, 4663-4680.

Tyler, P.A., Paterson, G.J.L., Sibuet, M., Guille, A.F., 1995. A New Genus of Ophiuroid (Echinodermata: Ophiuroidea) from Hydrothermal Mounds Along The Mid-Atlantic Ridge. *Journal of the Marine Biological Association of the United Kingdom*, 75, 977-986.

Yahagi, T., Fukumori, H., Warén, A., Kano, Y., 2019. Population connectivity of hydrothermal-vent limpets along the northern Mid-Atlantic Ridge (Gastropoda: Neritimorpha: Phenacolepadidae). *Journal of Marine Biological Association of the United Kingdom*, 99, 179-185.

5.3. Megabenthos (Krzysztof Pabis)

The general knowledge about benthic megafaunal communities of the Mid-Atlantic Ridge (MAR) is still insufficient, although – considering the substantial undersampling of the deep-sea benthic communities worldwide (Menegotto and Rangel, 2018) and large gaps in knowledge on benthic deep-sea faunas, even at the basic level of species richness (Costello and Chaudhary, 2017) – the area is relatively well-studied (Perez et al., 2012; Priede et al., 2013; Thaler and Amon, 2020 and references therein).

The MAR has been studied in the framework of several international projects, for example the Mid-Atlantic Ridge Ecosystem Project (MAR-ECO) which resulted in papers about the distribution patterns and taxonomy of selected benthic megafaunal invertebrates, such as sponges (Hestetun et al., 2015; Cárdenas and Rapp, 2015), corals (Buhl-Mortensen et al., 2008; Molodtsova et al., 2008; Morris et al,. 2012; Braga-Henriques et al., 2013) or echinoderms (Martynov and Litvinova, 2008; Gebruk, 2008; Dilman, 2008, 2013; Rogacheva et al., 2013a). The communities are dominated by surface deposit feeders and suspension feeders (Alt et al., 2019).

Differences in the distribution of megafauna on a smaller, local scale might be associated with microhabitat variation (e.g., the type of substratum, the presence of hard bottom) and food availability (the quantity and quality of organic matter, effects of currents), which may result in temporary aggregations of motile species (Morris et al., 2012; Alt et al., 2019). On the other hand, considerable spatial variability is encountered even in communities of sessile organisms, despite the absence of differences in the substratum type (Bell et al., 2016). Some of the studies revealed also a depth-related zonation (Gebruk and Krylova, 2013; Molodtsova et al., 2017). The role of sessile megafaunal communities must also be viewed through their importance as ecosystems engineers that may shape the overall biodiversity by increasing the habitat complexity and providing microhabitats for other invertebrates. Generally, recovery of such sessile communities after disturbances is known to take a long time, resulting in a substantial impoverishment of the associated fauna of smaller organisms (Buhl-Mortensen et al., 2008; Alt et al., 2019).

Research on the megafaunal biomass demonstrated that the observed values were similar to those reported from other deep-sea locations (Priede et al., 2013).

The high habitat heterogeneity, especially along steep slopes, results in mosaic patches of different taxa, although it is worth mentioning that distribution patterns may change horizontally along the MAR (Gebruk et al., 2010; Alt et al., 2013; Rogacheva et al., 2013b; Bell et al., 2016; Alt et al., 2019; Afonso et al., 2020).

The hydrothermal vents are particularly important components of the MAR ecosystem, with the Lost City hydrothermal field (in the Polish contract area) as a unique and the most striking example. Discovered only 20 years ago, the field is not only a unique habitat, but also a biodiversity hotspot with a high number of endemic taxa. A multivariate analysis of faunistic similarity between megafaunal assemblages at the eight MAR hydrothermal vent fields (Fig. 5.3.), based on data provided by Gebruk and Mironov (2006), produced a very interesting pattern, with the Lost City megafauna being the least similar to the assemblages recorded at the remaining fields. Those assemblages, in turn, are separated into a northern (Rainbow, Lucky Strike, Menez Gwen) and southern (Broken Spur, TAG, Logatchev, and Snake Pit) component. Future research should show whether this pattern is a persistent one.

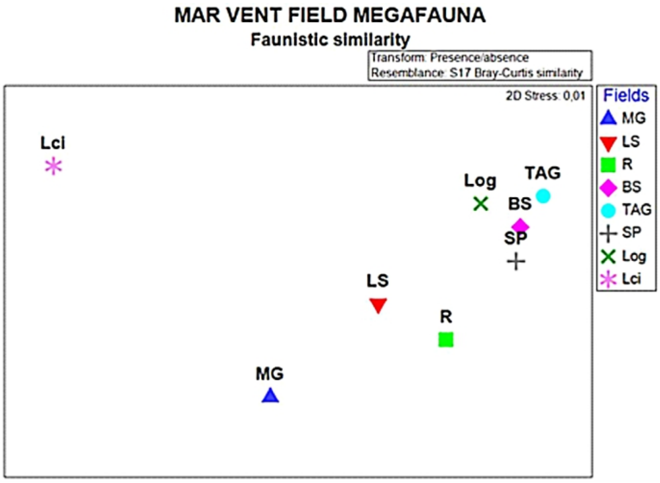

Fig. 5.2. MDS plot of similarity/dissimilarity between megabenthoc faunistic composition at different MAR vent fields (presence-absence transformation; Bray-Curtis similarity); Vent field name symbols: R, Rainbow; BS, Broken Spur; Lci, Lost City; MG, Menez Gwen; LS, Lucky Strike; SP, Snake Pit; TAG, Trans-Atlantic Geotraverse; Log, Logatchev.

Generally, the megafauna in vent habitats is dominated by motile invertebrates, including large crabs of the family Geryonidae. Non-venting habitats located close to active areas are inhabited by corals (e.g., *Lophelia* sp., *Desmophyllum* sp.), but also by motile invertebrates, including echinoderms and crabs of the family Galatheidae. Despite the relatively low biomass, the Lost City ecosystem likely supports the highest diversity among all the MAR hydrothermal vent fields surveyed (Kelley et al., 2005, 2007; Johnson, 2019). The megafauna at Broken Spur, another hydrothermal field in the Polish contract area, is dominated by shrimps (e.g., *Rimicaris exoculata*, particularly on chimneys walls), crabs (*Segonzacia mesatlantica*), polychaetes (e.g., *Chaetopterus*) and actiniarians (Desbruyères et al., 2000). Some studies suggest that, even in the areas away from the hydrothermal vent ecosystems, the contribution of endemic species may reach several per cent in some groups (e.g., Molodtsova et al., 2008; Tabachnick and Collins 2008; Braga-Henriques et al., 2015) (cf. Section 7.2.).

It has to be borne in mind that the general knowledge on the megafaunal communities on the MAR, and the Polish contract area in particular, is based on only a relatively low number of published reports. Therefore, any generalisations and more comprehensive conclusions regarding the distribution patterns and factors influencing the megabenthic communities are very tentative and need verification by further studies based on a higher sampling effort. Moreover, methodological constraints of megafaunal studies (e.g., commonly conducted observations from ROVs) produce low-resolution taxonomic assessments leading to underestimation of the diversity (e.g., Alt et al., 2019). However, the technical advances in imaging technology (e.g., Dumke et al., 2018) and annotation software (Gomes-Pereira et al., 2016) have allowed a progress to be made in this respect. Also, methods are at present in use with which to estimate the megafaunal biomass from underwater imagery (Benoist et al., 2019). Nevertheless, it is still very difficult to identify factors shaping spatial patterns of the megabenthos and to predict possible responses of the communities to anthropogenic impacts (Dunn et al., 2018).

References

Afonso, P., Fontes, J., Giacomello, E., Magalhães, M.C., Martins, H.R., Morato, T., Neves, V., Prieto, R., Santos, R.S., Silva, M., Vandeperre, F. 2020. The Azores: a mid-Atlantic hotspot for marine megafauna research and conservation. *Frontiers in Marine Science*, 6, 826. https://doi.org/10.3389/fmars.2019.00826

Alt, C.H.S., Rogacheva, A., Boorman, B., Hughes, J.A., Billett, D.S.M., Gooday, A.J., Jones, D.O.B., 2013.Trawled megafaunal invertebrate assemblages from bathyal depth of the Mid-Atlantic Ridge (48°–54°N). *Deep-Sea Research Part II Topical Studies in Oceanography*, 98, 326-340.

Alt, C.H.S., Kremenetskaia (Rogacheva), A., Gebruk, A.V., Gooday, A.J., Jones, D.O.B., 2019. Bathyal benthic megafauna from the Mid-Atlantic Ridge in the region of the Charlie-Gibbs fracture zone based on remotely operated vehicle observations. Deep-Sea Research Part I, 145, 1-12.

Bell, J.B., Alt, C.H.S., Jones, D.O.B., 2016. Benthic megafauna on steep slopes at the Northern Mid-Atlantic Ridge. *Marine Ecology*, 37, 1290-1302.

Benoist, N.M.A., Bett, B.J., Morris, K.J., Ruhl, H.A., 2019. A generalised volumetric method to estimate the biomass of photographically surveyed benthic megafauna. *Progress in Oceanography*, 178, Article 102188.

Buhl-Mortensen, P., Buhl-Mortensen, L., Gebruk, A.V., Krylova, E.M. 2008. Occurrence of deep-water corals on the Mid-Atlantic Ridge based on MAR-ECO data. *Deep Sea Research Part II Topical Studies in Oceanography*, 55, 142-152.

Costello, M J., Chaudary, C. 2017. Marine biodiversity, biogeography, deep-sea gradients, and conservation. *Current Biology*, 27, 511-527.

Braga-Henriques, A., Porteiro, F.M., Ribeiro, P.A., de Mato,s V., Sampaio, I., Ocaña, O., Santos, R.S. 2013. Diversity, distribution and spatial structure of the cold-water coral fauna of the Azores (NE Atlantic). *Biogeosciences*, 10, 4009-4036.

Cardenas, P., Rapp, T., 2015. Demosponges from the Northern Mid-Atlantic Ridge shed more light on the diversity and biogeography of North Atlantic deep-sea sponges. *Journal of the Marine Biological Association of the United Kingdom*, 95, 1475-1516.

Desbruyères, D., Almeida, A., Biscoito, M., Comtet, T., Khripounoff, A., Le Bris, N., Sarradin, P.M., Segonzac, M., 2000. A review of the distribution of hydrothermal vent communities along the northern Mid-Atlantic Ridge: dispersal vs. environmental controls. *Hydrobiologia*, 440, 201-216.

Dilman, A. 2008. Asteroid fauna of the northern Mid-Atlantic Ridge with description of a new species *Hymenasterides mironovi* sp. nov. *Marine Biology Research*, 4, 131-151.

Dilman, A. 2013. Asteroid fauna of the northern Mid-Atlantic Ridge: Additional records. *Marine Biology Research*, 9, 563-586.

Dumke, I., Purser, A., Marcon, Y., Nornes, S.M., Johnsen, G., Ludvigsen, M., Søreide, F., 2018. Underwater hyperspectral imaging as an in situ taxonomic tool for deep-sea megafauna. *Scientific Reports*, 8, 12860.

Dunn, D.C., Van Dover, C.L., Etter, R.J., Smith, C.R., Levin, L.A., Morato, T., Colaço, A., Dale, A.C., Gebruk, A.V., Gjerde, K.M., Halpin, P.N., Howell, K.L., Johnson, D., Perez, J.A.A. Ribeiro, M.C., Stuckas, H., Weaver, P., SEMPIA Workshop Participants, 2018. A strategy for the conservation of biodiversity on mid-ocean ridges from deep-sea mining. *Science Advances*. 4: eaar4313

Gebruk, A. 2008. Holothurians (Holothuroidea, Echinodermata) of the northern Mid-Atlantic Ridge collected by the G.O. Sars MAR-ECO expedition with descriptions of four new species. *Marine Biology Research*, 4(1), 48-60.

Gebruk, A.V., Budaeva, N.E., King, N.J., 2010. Bathyal benthic fauna of the Mid-Atlantic Ridge between the Azores and the Reykjanes Ridge. *Journal of the Marine Biological Association of the UK*, 90, 1-14.

Gebruk, A.V., Krylova, E.M., 2013. Megafauna of the Charlie–Gibbs Fracture Zone (northern Mid-Atlantic Ridge) based on video observations. *Journal of the Marine Biological Association of the United Kingdom*, 93, 1143-1150.

Gebruk, A.V., Mironov, A.N., 2006. Biogeografiya gidroterm Sredinno-Atlanticheskogo Khrebta. In: Vinogradov, M.E., Vereshchaka, A.L. (eds), *Ekosistemy atlanticheskikh gidroterm*. Nauka, Moskva, 119-162

Gomes-Pereira, J.N., Auger, V., Beisiegel, K., Benjamin, R., Bergmann, M., Bowden, D., Buhl-Mortensen, P., De Leo, F.C., Dionísio, G., Durden, J.M., Edwards, L., Friedman, A., Greinert, J., Jacobsen-Stout, N., Lerner, S., Leslie, M., Nattkemper, T.W., Sameoto, J.A., Schoening, T., Schouten, R., Seager, J., Singh, H., Soubigou, O., Tojeira, I., van den Beld, I., Dias, F., Tempera, F., Santos, R.S., 2016. Current and future trends in marine image annotation software. *Progress in Oceanography*, 149, 106-120.

Hestetun, J., Fourt, M., Vacelet, J., Boury-Esnault, N., Rapp, H., 2015. Cladorhizidae (Porifera, Demospongiae, Poecilosclerida) of the deep Atlantic collected during IFREMER cruises, with a biogeographic overview of the Atlantic species. *Journal of the Marine Biological Association of the United Kingdom*, 95, 1311-1342.

Johnson, D.E., 2019. Protecting the Lost City hydrothermal vent system: All is not lost, or is it? *Marine Policy*, 103, 103593.

Kelle,y D.S., Früh-Green, G.L., Karson J.A., Ludwig K.A., 2007. The Lost City hydrothermal field revisited. *Oceanography,* 20, 90-99.

Kelley, D.S., , Karson, J.A., Früh-Green, G.L., Yoerger, D.R., Shank, T.M., Butterfield, D.A., Hayes, J.M., Schrenk, M.O., Olson, E.J., Proskurowski, G., Jakuba, M., Bradley, A., Larson, B., Ludwig, K., Glickson, D., Buckman, K., Bradley, A.S., Brazelton, W.J., Roe, K., Elend, M.J., Delacour, A., Bernasconi, S.M., Lilley, M.D., Baross, J.A., Summons, R.E., Sylva S.P., 2005. A Serpentinite-Hosted Ecosystem: The Lost City Hydrothermal Field. *Science*, 307, 1428-1433.

Martynov, A.V., Litvinova, N.M., 2008. Deep-water Ophiuroidea of the northern Atlantic with descriptions of three new species and taxonomic remarks on certain genera and species. *Marine Biology Research*, 4, 76-111

Menegotto, A., Rangel, T.F., 2018. Mapping knowledge gaps in marine diversity reveals a latitudinal gradient of missing species richness. *Nature Communications,* 9, 4713.

Molodtsova, T., Sanamyan, N.P., Keller ,N.B., 2008. Anthozoa from the northern Mid-Atlantic Ridge and Charlie-Gibbs Fracture Zone. *Marine Biology Research*, 4, 112-130.

Molodtsova, T.N., Galkin, S.V., Kobyliansky, S.G., Simakova, U.V., Vedenin, A.A., Dobretsova, I.G., Gebruk, A.V., 2017. First data on benthic and fish communities from the Mid-Atlantic Ridge, 16°40′– 17°14′ N. *Deep Sea Research Part II Topical Studies in Oceanography*, 137, 69-77.

Morris, K.J., Tyler, P.A., Murton, B., Rogers, A.D., 2012. Lower bathyal and abyssal distribution of coral in the axial volcanic ridge of the Mid-Atlantic Ridge at 45°N. *Deep-Sea Research Part I*, 62, 32-39.

Perez, J.A.A., dos Santos Alves, E., Clark, M.R., Bergstad, O.A., Gebruk, A., Azevedo Cardoso, I., Rogacheva, A., 2012. Patterns of life on the southern Mid-Atlantic Ridge: Compiling what is known and addressing future research. *Oceanography*, 25(4), 16-31.

Priede, I.G., Bergstad, O.A., Miller, P.I., Vecchione, M., Gebruk A., ;Falkenhaug T., Billett T., Craig D.S.M., Dale J., Shields A.C., Tilstone M.A., Sutton G.H., Gooday T.T., Inall A.J., Jones M.E., Martinez-Vicente D.O.B., Menezes V., , Niedzielski G.M., Sigurðsson T., , Rothe, N., Rogacheva, A., Alt, C. H. S., Brand, T., Abell, R., Brierley, A.S., , Nicola C., Crockard, D., Hoelzel, A. R., ; Høines, Å., Letessier, T.B., Read, J.F., Shimmield, T., Cox, M.J., Galbraith, J.K., Gordon, J. D. M., Horton, T., Neat, F., Lorance, P. 2013. Does Presence of a Mid-Ocean Ridge Enhance Biomass and Biodiversity? *PLoS ONE*, 8: e61550.

Rogacheva, A., Gebruk A., Alt, C.H.S., 2013a. Holothuroidea of the Charlie Gibbs Fracture Zone area, northern Mid-Atlantic Ridge. *Marine Biology Research*, 9, 587-623.

Rogacheva, A., Boormana, B., Hughes, A.J., Billett, D.S.M., Gooday, A.J., Jones, D.O.B., 2013b. Trawled megafaunal invertebrate assemblages from bathyal depth of the Mid-Atlantic Ridge (48°–54°N). *Deep Sea Research Part II Topical Studies in Oceanography*, 98, 326-340.

Tabachnick, K., Collins, A.G., 2008. Glass sponges (Porifera, Hexactinellida) of the northern Mid-Atlantic Ridge. *Marine Biology Research*, 4, 25-47.

Thaler, A.D., Amon, D. 2020. 262 Voyages Beneath the Sea: a globalassessment of macro- and megafaunalbiodiversity and research effort atdeep-sea hydrothermal vents. *PeerJ* 7:e7397

5.4. Nektobenthos (Piotr Jóźwiak)

Since there are methodological difficulties in examining the MAR area, and because the majority of the studies were based on video recordings, data on the nektobenthos are scarce and often limited to higher taxa (e.g., Biscoito et al., 2006; Felley et al., 2007).

The nektobenthos on the MAR is represented mainly by the typical North Atlantic lower-bathyal species known from the ocean margins, and the endemicity of the MAR species is most probably not high, e.g., non-existent in both fishes and cephalopods (Priede et al., 2013) (cf. Section 7.2.). A comparison of the MAR fish fauna with that of the North Atlantic margins showed stronger similarities between the MAR and the eastern, rather than the western, Atlantic. Moreover, based on their fish data, Priede et al. (2013) pointed out that the biodiversity on the MAR is higher than that in the adjacent abyssal plain.

Shallower areas of the MAR are characterized by a more diverse fauna as well as a higher abundance and biomass than deeper bottom areas (Felley et al., 2007). Similar findings were reported by by Bergstad et al. (2008) for demersal fishes, and by Vecchione et al. (2010) for cephalopods. The non-vent nektobenthos is often widely distributed and shows no clear habitat preferences (Horton et al., 2013).

The non-vent nektobenthic fish fauna of the MAR area is represented by, e.g., the Macrouridae (including Coryphaenoides brevibarbis and C. armatus), Halosauridae (e.g., Halosauropsis macrochir and Aldrovandia sp.), Bathysauridae (e.g., Bathysaurus ferox), Notacanthidae (e.g., Polyacanthonotus challengeri) and Moridae (e.g., Antimora rostrata), all recorded from the Charlie-Gibbs Fracture Zone (CGFZ) (Felley et al., 2008; Linley et al., 2013). Cousins et al. (2013), who used a baited-camera lander, list 19 species, with the dominant C. armatus and A. rostrata. Barathronus multidens (Aphyonidae), Ipnops murray (Ipnopidae) and Holtbyrnia anomala (Platytroctidae) were collected between

16°40' and 17°14'N (Molodtsova et al., 2017). A transect from Iceland to the Azores (36 stations) brought records of Eurypharynx pelecanoides, Bathylagus euryops, Sigmops bathyphilum, Scopeloberyx robustus, Serrivomer beanii, and Borostomias antarcticus (Sutton et al., 2008).

The nektobenthic invertebrates on the MAR feature primarily two groups: decapod crustaceans and cephalopods. The decapod fauna in non-vent MAR habitats includes penaeid shrimps (Penaeidea) and the squat lobster (Munidopsis sp.) reported from the Charlie-Gibbs Fracture Zone (Felley et al., 2008). Horton et al. (2013) listed 39 species of necrophagous amphipods from samples taken north and south of the Charlie-Gibbs Fracture Zone and east and west from the ridge. A total of 31 species on their list represent the superfamily Lysianassoidea, with the most abundant Abyssorchomene abyssorum. Vecchione et al. (2010) provided a list of 34 cephalopod species found on the MAR, collected with a bottom trawl north of the Azores and in areas just north and south of the Charlie Gibbs Fracture Zone. Because of the sampling gear used, those species might be considered as belonging to the nektobenthos, but the authors quoted considered some of them as pelagic forms that contaminated the sample during gear deployment. Fifteen of those 34 species were collected only with the benthic trawl. Among them, 14 species are considered to represent the true bottom fauna, with Mastigoteuthis agassizii, Gonatus steenstrupi and Stauroteuthis syrtensis as the dominant species.

The nektobenthic fish fauna of the vent habitats has been seldom studied. There are, however, some data from the Broken Spur hydrothermal field in the Polish contract area where two vent-associated fish species: Haptenchelys texis (Synaphobranchidae) and Pachycara thermophilum (Zoarcidae) have been recorded (Parin, 1995). Some data from other fields do exist as well. For example, Desbruyères et al. (2006) listed four species (Gaidropsaurus sp., Ilyophis saldanhai, Pachycara saldanhai and P. termophilum) as typical of MAR vent fields. P. thermophilum (Zoarcidae) was common at the Logatchev field as well (Gebruk et al., 2000). Biscoito et al. (2006) listed 19 species of demersal fishes from the Saldanha vent field.

The MAR decapod vent fauna is represented by, e.g., shrimps of the genus Nematocarcinus found at the Saldanha vent field (Biscoito et al., 2016) or Mirocaris fortunata and Rimicaris exoculata, both recorded also at Broken Spur (Desbruyères et al., 2000, 2001) and often referred to as the megafauna (cf. Section 5.3.). Single records of cephalopods Cirroteuthis sp. and Grimpoteuthis sp. were provided by Biscoito et al. (2006) from the Saldanha vent field.

References

Biscoito, M. Almeida, A.J., Segonzac, M. 2006. Preliminary biological characterization of the Saldanha hydrothermal field at the Mid-Atlantic Ridge (36 34' N, 32 26' W, 2200 m). *Cahiers de Biologie Marine*, 47, 421-427.

Cousins, N.J., Linley, T.D., Jamieson, A.J., Bagley, P.M., Blades, H., Box, T., Chambers, R., Ford, A., Shields, M.A., Priede, I.G., 2013. Bathyal demersal fishes of Charlie-Gibbs Fracture Zone region (49–54°N) of the Mid-Atlantic Ridge: II. Baited camera lander observations. *Deep Sea Research Part II*, 98, 397-406.

Desbruyères, D., Almeida, A., Biscoito, M., Comtet, T., Khripounoff, A., Le Bris, N., Sarradin, P.M., Segonzac, M., 2000. A review of the distribution of hydrothermal vent communities along the northern Mid-Atlantic Ridge: dispersal vs. environmental controls. *Hydrobiologia*, 440: 201-216.
doi.org/10.1023/A:1004175211848

Desbruyères, D., Biscoito, M., Caprais, J.-C., Colaço, A., Comtet, T., Crassous, P., Fouquet, Y., Khripounoff, A., Le Bris, N., Olu, K., Riso, R., Sarradin, P.-M., Segonzac, M., Vangriesheim, A., 2001. Variations in deep-sea hydrothermal vent communities on the Mid-Atlantic Ridge near the Azores plateau. *Deep-Sea Research*, 48(5), 1325-1346.

Desbruyères, D., Segonzac, M., Bright, M. 2006. *Handbook of deep-sea hydrothermal vent fauna*. Denisia: 18, Linz-Dornach.

Felley, J.D., Vecchione, M., Wilson, R.R. 2008. Small-scale distribution of deep-sea demersal nekton and other megafauna in the Charlie-Gibbs Fracture Zone of the Mid-Atlantic Ridge. *Deep-Sea Research. Part II Topical Studies in Oceanography*, 55 (1-2): 153–160. https://doi.org/10.1016/j.dsr2.2007.09.021

Gebruk, A.V., Chevaldonné, P., Shank, T., Lutz, R.A., Vrijenhoek, R.C., 2000. Deep-sea hydrothermal vent communities of the Logatchev area (14°45′ N, Mid-Atlantic Ridge): diverse biotypes and high biomass. *Journal of the Marine Biological Association of the United Kingdom*, 80, 383-393.

Horton, T., Thurston, M.H., Duffy, G.A., 2013. Community composition of scavenging amphipods at bathyal depths on the Mid-Atlantic Ridge. *Deep-Sea Research Part II Topical Studies in Oceanography,* 98, 352-359.

Linley, T.D., Alt, C.H.S., Jones, D.O.B., Priede, I.G., 2013. Bathyal demersal fishes of the Charlie-Gibbs Fracture Zone region (491–541N) of the Mid-Atlantic Ridge: III. Results from remotely operated vehicle (ROV) video transects. *Deep Sea Research Part II Topical Studies in Oceanography, 98,* 407-411.

Molodtsova, T.N., Galkin, S.V., Kobyliansky, S.G., Simakova, U.V., Vedenin, A.A., Dobretsova, I.G., Gebruk, A.V., 2017. First data on benthic and fish communities from the Mid-Atlantic Ridge, 16°40'–17°14' N. *Deep Sea Research Part II Topical Studies in Oceanography*, 137, 69-77. doi:10.1016/j.dsr2.2016.10

Parin, N.V., 1995. Deep-sea fishes, *Haptenchelys texis* (Synaphobranchidae) and *Pachycara thermophilum* (Zoarcidae) from the Broken Spur hydrothermal vent field (Mid-Atlantic Ridge). Journal of Ichthyology 35, 328-332.

Priede, I.G., Bergstad, O.A., Miller, P.I., Vecchione, M., Gebruk, A., Falkenhaug, T., Billet,, D.S.M., Craig, J., Dale, A.C., Shields, M.A., Tilstone, G.H., Sutton, T.T., Gooday, A.J., Inall, M.E., Jones, D.O.B., Martinez-Vicente, V., Menezes, G, M., Niedzielski, T., Sigurðsson, Þ., Rothe, N., Rogacheva, A., Alt, C.H.S., Brand, T., Abell, T., Brierley, A.S., Cousins, N.J., Crockard, D., Hoelzel, A.R., Høines, A., Letessier, T.B., Read, J.F., Shimmield, T., Cox, M.J., Galbraith, J.K., Gordon, J.D.M., Horton, T., Neat, F., Porance, P., 2013. Does Presence of a Mid-Ocean Ridge Enhance Biomass and Biodiversity? *PLoS ONE,* 8(5): e61550. https://doi.org/10.1371/journal.pone.0061550

Sutton, T., Porteiro, F., Heino, M., Byrkjedal, I., Langhelle, G., Anderson, C., Horne, J., Søiland, H., Falkenhaug, T., Godø, O., 2008. Vertical structure, biomass and topographic association of deep-pelagic fishes in relation to a mid-ocean ridge system. Deep *Sea Research. Part II Topical Studies in Oceanography,* 55,161-184.

Vecchione, M., Young, R.E., Piatkowski, U., 2010. Cephalopods of the northern Mid-Atlantic Ridge. *Marine Biology Research*, 6 (1), 25-52.

6. Seabed communities

Maria Włodarska-Kowalczuk, Teresa Radziejewska and Katarzyna Jankowska

6.1. Functioning: energy source and trophic pathways (Maria Włodarska-Kowalczuk)

Benthic systems on the Mid-Atlantic Ridge (MAR) are fuelled by two main energy sources (Fig. 6.1.): *in-situ* chemosynthetic production and/or photosynthetic production that is transported from the distant euphotic zone. Microbial chemolithoautotrophs (converting chemical energy and inorganic carbon to biomass) exploit energy sources provided by the hydrothermal vent fluids.

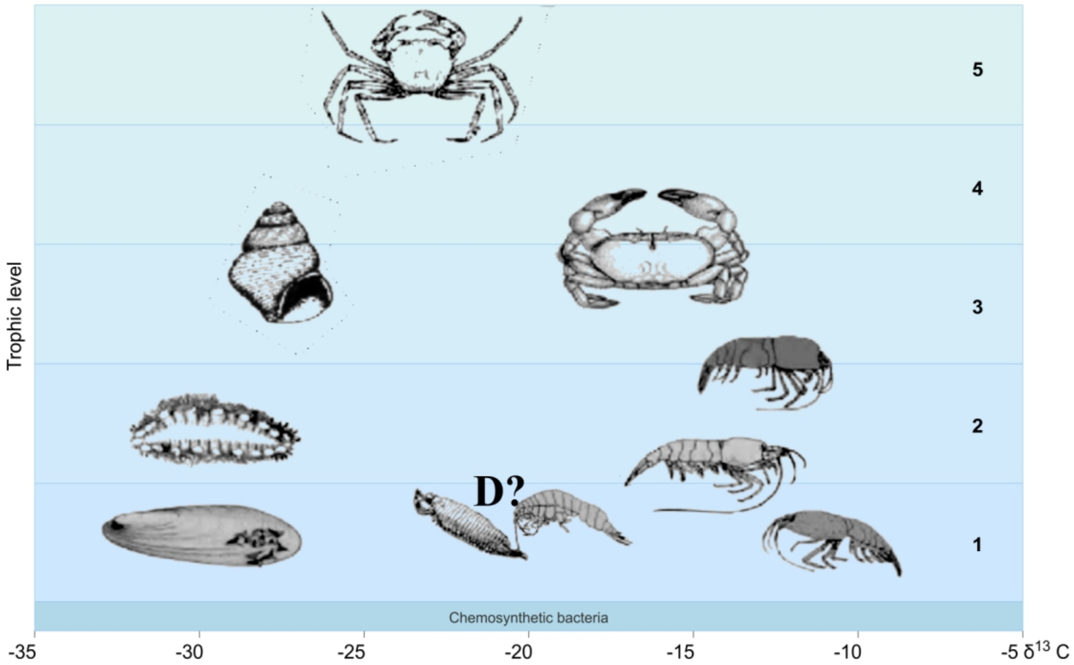

Fig. 6.1. Two main trophic pathways in benthic hydrothermal vent food webs at Mid-Atlantic Ridge (from Colaço et al., 2002). "D?" refers to uncertain trophic position (primary consumers or detritivores).

The off-axis Lost City Hydrothermal Field (LCHF) is a unique system where serpentinization of ultramafic rocks (peridotites) produce warm (40-70°C), alkaline (pH 9 and above) fluids rich in Ca, H_2 and CH_4 but poor in sulphides (Kelley et al., 2005; Von Damm, 2001). Thermodynamic modelling pointed to metabolic reactions involving H_2 and CH_4 (particularly hydrogen oxidation, methanotrophy, sulphate reduction, and methanogenesis) as the predominant energy sources in ultramafic-hosted hydrothermal systems, and indicated that they can supply about twice as much chemical energy and potentially support a much higher biomass than analogous systems hosted in basaltic rocks (McCollom, 2007). The Lost City hydrothermal field appeared to be 'an energy bonanza in comparison with the majority of deep-sea habitats' (Lang and Brazelton, 2020). Indeed, isotope analyses of organic carbon in active carbonate chimneys at Lost City evidenced microbial utilization of H_2 (in the form of sulphate reduction) and mantle inorganic carbon (Lang et al., 2012). The benthic macrofaunal invertebrates dwelling at Lost City that most likely graze on microbial biofilms (Boetius, 2005) are diverse but not abundant (Kelley et al., 2005). However, high numbers of mussels, clams and gastropods recorded in 100-kyr old Lost City-like carbonates (Ghost City, 36°N) suggest that serpentinization-based hydrothermal systems are able to sustain high standing stocks of marine invertebrates (Lartaud et al., 2011). DeChaine et al. (2006) showed that few *Bathymodiolus* mussels present at Lost City harbour endosymbionts closely phylogenetically related to those in mussels collected at basalt-based hydrothermal vents. Understanding the Lost City ecosystem functioning is of crucial importance as it can provide important insights into the origin of life on Earth and other planetary bodies in the solar system (Lang and Brazelton, 2020).

At in-axis basalt-hosted hydrothermal fields, seawater-basalt interactions produce fluids that are hot (~350°C), acid (pH 3-5) and enriched in H_2S, H_2, CH_4, Mn and other metals (Van Dover, 2000). Energy sources for primary production are oxidative reactions (predominantly sulphide oxidation) at lower temperatures (below ~38°C) and reductive reactions within the walls of vent chimneys (McCollom and Shock, 1997). Extreme environmental conditions constrain the invertebrate species pools and favour simple food webs with short food chains (Colaço et al., 2002). The basic trophic structure is similar across different fields on the MAR (including Broken Spur located in the Polish contract area), with chemosynthetic producers at the base of the food web and two main types of primary consumers: endosymbiont-hosting (e.g., *Bathymodiolus* mussels) or feeding on free-living bacteria (e.g., *Rimicaris* shrimps). Predators depend on one (the crab *Sergonzacia* preferring shrimps, the gastropod *Phymporhychus* feeding almost exclusively on mussels) or both groups of primary consumers. Deep-sea bathyal species making incursions into the vent fields act as top predators (Colaço et al., 2002). These pathways of energy flow have been observed in a number of studies performed at different sites (including Broken Spur) and employing *in-situ* and experimental observations as well as analyses of chemical biomarkers (stable isotopes and fatty acid profiles) (e.g., Gebruk et al., 2000; Vereshchaka et al., 2000; Colaço et al., 2007). Portail et al. (2018) compared 13 faunal assemblages in the Azores triple junction and demonstrated that benthic consumers were highly flexible (in terms of their dependence on the composition of producers and metabolic diversity), which secured the efficient functioning and stability of trophic systems across different MAR hydrothermal vent localities.

Organic matter produced at hydrothermal fields can be advected at least 2 km away from the site of active venting (Roth and Dymond, 1989) and, to some extent, support benthic communities therein (Erickson et al., 2009). However, functioning of non-vent deep-sea communities depends essentially on the organic matter transported from the sea surface where light penetration allows photosynthetic production. Reid et al. (2012) indicated two main trophic pathways linking pelagic producers and benthic consumers in non-hydrothermal MAR benthic habitats: (1) invertebrate consumers (detritus and suspension feeders) dependent on the downward flux of phytodetritus to the seafloor; (2) mobile predator and scavenging fishes and crustaceans exploiting aggregations of meso- and bathypelagic biomass associated with topographic features of the ridge (Sutton et al., 2008).

References

Boetius, A., 2005. Lost City life. *Science*, 307(5714), 1420-1422.

Colaço, A., Dehairs, F., Desbruyères, D. 2002. Nutritional relations of deep-sea hydrothermal fields at the Mid-Atlantic Ridge: a stable isotope approach, *Deep Sea Research Part I Oceanographic Research Papers*, 49(2), 395-412.

Colaço, A., Desbruyères, D., Guezennec, J., 2007. Polar lipid fatty acids as indicators of trophic associations in a deep-sea vent system community. *Marine Ecology*, 28(1), 15-24.

DeChaine, E. G., Bates, A.E., Shank, T.M., Cavanaugh, C.M., 2006. Off-axis symbiosis found: characterization and biogeography of bacterial symbionts of Bathymodiolus mussels from Lost City hydrothermal vents. *Environmental Microbiology*, 8(11), 1902-1912.

Erickson, K., Macko,S., Van Dover, C., 2009. Evidence for a chemoautotrophically based food web at inactive hydrothermal vents (Manus Basin). *Deep Sea Research Part II Topical Studies in Oceanography,* 56(19-20), 1577-1585.

Gebruk, A., Southward, E., Kennedy, H., Southward, A., 2000. Food sources, behaviour, and distribution of hydrothermal vent shrimps at the Mid-Atlantic Ridge. *Journal of the Marine Biological Association of the United Kingdom*, 80(3), 485-499.

Kelley, D.S., Karson, J.A, Früh-Green, G.L., Yoerger, D.R., Shank, T.M., Butterfield, D.A,. Hayes, J.M., Schrenk, M.O., Olson, E.J., Proskurowski, G., 2005. A serpentinite-hosted ecosystem: the Lost City hydrothermal field. *Science*, 307(5714), 1428-1434.

Lang, S.Q., Brazelton, W.J., 2020. Habitability of the marine serpentinite subsurface: a case study of the Lost City hydrothermal field. *Philosophical Transactions of the Royal Society A*, 378(2165), 20180429.

Lang, S.Q., Früh-Green, G.L. Bernasconi, S.M., Lilley, M.D., Proskurowski, G., Méhay, S., Butterfield, D.A., 2012. Microbial utilization of abiogenic carbon and hydrogen in a serpentinite-hosted system. *Geochimica et Cosmochimica Acta*, 92, 82-99.

Lartaud, F., Little, C. T., De Rafelis, M., Bayon, G., Dyment, J., Ildefonse, B., Gressier, V., Fouquet, Y., Gaill, F., Le Bris, N., 2011. Fossil evidence for serpentinization fluids fueling chemosynthetic assemblages. *Proceedings of the National Academy of Sciences*, 108(19), 7698-7703.

McCollom, T.M., 2007. Geochemical constraints on sources of metabolic energy for chemolithoautotrophy in ultramafic-hosted deep-sea hydrothermal systems. *Astrobiology*, 7(6), 933-950.

McCollom, T.M., Shock, E.L., 1997. Geochemical constraints on chemolithoautotrophic metabolism by microorganisms in seafloor hydrothermal systems. *Geochimica et cosmochimica acta*, 61(20), 4375-4391.

Portail, M., Brandily, C., Cathalot, C., Colaço, A., Gélinas, Y., Husson, B., Sarradin, P.-M., Sarrazin, J., 2018. Food-web complexity across hydrothermal vents on the Azores triple junction. *Deep Sea Research Part I: Oceanographic Research Papers*, 131, 101-120.

Reid, W.D., Wigham, B.D., McGill, R.A., Polunin, N.V., 2012. Elucidating trophic pathways in benthic deep-sea assemblages of the Mid-Atlantic Ridge north and south of the Charlie-Gibbs Fracture Zone. *Marine Ecology Progress Series*, 463, 89-103.

Roth, S.E., Dymond, J., 1989. Transport and settling of organic material in a deep-sea hydrothermal plume: evidence from particle flux measurements. *Deep Sea Research Part A. Oceanographic Research Papers*, 36(8), 1237-1254.

Sutton, T., Porteiro, F., Heino, M., Byrkjedal, I., Langhelle, G., Anderson, C., Horne, J., Søiland, H., Falkenhaug, T., Godø, O., 2008. Vertical structure, biomass and topographic association of deep-pelagic fishes in relation to a mid-ocean ridge system, *Deep Sea Research Part II Topical Studies in Oceanography*, 55(1-2), 161-184.

Van Dover, C., 2000. *The ecology of deep-sea hydrothermal vents*, Princeton University Press.

Vereshchaka, A., Vinogradov, G., Lein, A.Y., Dalton, S., Dehairs, F., 2000. Carbon and nitrogen isotopic composition of the fauna from the Broken Spur hydrothermal vent field. *Marine Biology*, 136(1), 11-17.

Von Damm, K.L., 2001. Lost City found, *Nature*, 412(6843), 127-128.

6.2. Benthic abundance and biomass (Teresa Radziejewska)

Since their discovery in the late 1970s, hydrothermal vent ecosystems have often been referred to, both in scientific publications and in popular-science literature, as “oases of life” on the generally depauperate deep-sea floor (e.g., Carney, 1994; wwf.panda.org/our_work/our_focus/oceans_practice/deep_sea/vents_seeps/). In fact, the richness of life associated with the newly discovered hydrothermal vent fields was the most striking feature recorded and reported by the researchers who discovered the vents on the East Pacific Rise (Oceanus, 2018; www.whoi.edu/oceanus/feature/the-discovery-of-hydrothermal-vents/). The oasis analogy is justified also with respect to hydrothermal fields explored on the Mid-Atlantic Ridge (MAR), primarily in view of the mass occurrence of megafaunal organisms, visible in numerous images collected during exploration of different fields and sites within them (Galkin, 2006 and references therein; Van Dover, 2014).

A summary of benthic abundance and standing stock data collected from the MAR up to 2005 (Galkin, 2006) focuses primarily on the dominant and foundation species [Rybakova (Goroslavskaya) and Galkin, 2015]. These include bresilioid (Bresilioidea) shrimps found in all the MAR fields explored. They are most prominently represented by the landscape-forming species *Rimicaris exoculata* (family Alvinocarididae) with abundances of up to 2500-3000 ind./m^2 and biomass of up to 1-1.5 kg/m^2; such abundances have been reported from, *inter alia*, the Broken Spur field in the Polish contract area. The *Rimicaris* occur frequently in associations with other shrimps (*Chorocaris chacei*, up to 50 ind./m^2 in the TAG field; Gebruk et al., 1997), *Segonzacia mesatlantica* crabs, and ectinosomatid harpacticoids; Segonzac (1992) estimated the biomass of those associations at up to 1.2 kg/m^2.

Another group of foundation and dominant species is formed by bivalves of the families Mytilidae (genus *Bathymodiolus*) and Vesicomyidae (genus *Calyptogena*) (Galkin, 2006). In terms of abundance and biomass, the two *Bathymodiolus* species: *B. azoricus* and *B. puteoserpentis* known from the MAR, are very unevenly distributed among individual fields. While *B. azoricus* is more abundant at shallower fields (Rainbow, Lucky Strike, Menez Gwen, with abundances of up to 10^3 ind./m^2), *B. puteoserpentis* forms very dense and extensive beds in other (Logatchev, Snake Pit and Broken Spur), with more than 70 kg/m^2 biomass at the Logatchev field, but is much less abundant and occur in local patches only at Broken Spur. The vesicomyid bivalves are primarily represented by *Calyptogena* aff. *kaikoi*, found in aggregations of a spatial extension, e.g., at the Logatchev field, of up to 100 m^2 (Galkin, 2006).

Important, in terms of abundance, are gastropods: for instance, limpets *Peltospira smaragdina* were reported with abundances of up to several hundred individuals per m^2, while gastropods of the genus *Phymorchynchus* (e.g., *Ph. moskalevi*), found, for instance, in the inactive part of the TAG field, occurred at abundances of up to 3-10 ind./m^2 (Galkin, 2006).

As stated by Van Dover (2014), the hydrothermal vent ecosystems are dominated by the so-called holobiont taxa, i.e., organisms that host symbiotic chemoautotrophic microorganisms. They often occur as the foundation species forming complex 3-dimensional habitats (Gerdes et al., 2019), for example those created by the mytilid and vesicomyid bivalves mentioned above as well as the chaetopterid polychaetes (genus *Chaetopterus*) occurring in masses away from active smokers. Those aggregations serve as a substratum for the growth of epizoic microorganisms, refugia for juvenile invertebrates, and a habitat for associated organisms, including the meiobenthos (nematodes, harpacticoids, halacarids) – occasionally, e.g., in Broken Spur, found in abundance, primary consumers (e.g., limpets such as *Peltospira smaragdina* and *Lepetodrilus atlanticus* grazing on microbial biofilms) as well as secondary and tertiary consumers such as scavenging and predatory crustaceans and fishes. The *Bathymodiolus* bed-associated macrofaunal abundance at Logatchev has been reported by Van Dover and Doerries (2005) as ranging (by sample volume, collected with 'benthic pots') within 209-2390 ind./dm^3.

Holobiont taxa typically dominate the biomass of habitable diffuse flow regions (in the vicinity of active smokers) and show abrupt transitions from one dominant species to another, reflecting different interspecific tolerances for thermal and chemical conditions and to biotic interactions (facilitation, competition, predation) (Van Dover, 2014). The total biomass values, indicated above (aggregations of *Rimicaris exoculata* or *Bathymodiolus puteoserpentis*) are typically very high at vents. Beyond the periphery of a vent field, the faunal abundance and biomass values are usually much lower, the megafauna being represented by solitary large anemones (e.g., *Maractis rimicarivora*, which occurs also on hard substrata in the vicinity of venting; Fabri et al., 2011) and gorgonian corals (Van Dover, 2014).

Observations on the macrofauna at Lost City (Shank, 2005 at: oceanexplorer.noaa.gov/explorations/05lostcity/background/macrofauna/macrofauna.html) showed a high biodiversity ("over 70 potential species"). The biomass (wet weight) was apparently lower compared to a typical hydrothermal vent on the MAR. The major contributors to the biomass at Lost City are the larger more mobile megafauna, including the (grouper-like) wreckfish, cut-throat eels, and large red geryonid crabs, all readily visible around the spires. Shank (op. cit.) reported also on a sharp difference between the fauna of vent and non-vent habitats at Lost City, whereby typical vent areas are sparsely populated, whereas non-venting habitats less than a few metres away (e.g., on the sides of inactive solidified carbonate structures, sedimented areas, and breccia cap rock just to the north of the field) are dominated by hard corals *(Lophelia pertusa* and *Desmophyllum)*, octocorals (gorgonians), galatheid crabs, turrid gastropods, foraminifera, pteropods, urchins, asteroids, ophiuroids, and typical deep-sea barnacles.

The soft sediment-covered areas away from active venting have been reported as supporting fairly abundant (considering the low general abundances of deep-sea infauna; cf. Radziejewska, 2014) meiobenthos (e.g., 11-35 and 72-86 inds/10 cm^2 at TAG and Snake Pit, respectively). Faunal density responses appear to be a function of stress level. For example, at Middle Valley (2410 m, the Juan de Fuca hydrothermal vent field in the Pacific), extremely hot sediments (e.g., 94°C at 5 cm into the sediment column) support very few macrofauna, whereas moderately warm sediments inhabited by vesicomyid bivalves may support elevated macrofaunal densities (16,500 ind./ m^2) relative to those in microbial mats (6,840 ind./m^2), hot sediment (1,690 ind./m^2), and control (not heated) sediments (2,218 ind./m^2) (Bernardino et al., 2012). However, no comparative data are available from the MAR as yet.

References

Bernardino, A.F., Levin, L.A., Thurber, A.R., Smith, C.R., 2012. Comparative Composition, Diversity and Trophic Ecology of Sediment Macrofauna at Vents, Seeps and Organic Falls. *PLoS ONE*, 7, e33515.

Carney, R.S., 1994. Consideration of the oasis analogy for chemosynthetic communities at Gulf of Mexico hydrocarbon vents. *Geo-Marine Letters*, 14, 149-159.

Fabri, M.-C., Bargain, A., Briand, P., Gebruk, A., Fouquet, Y., Morineaux, M., Desbruyères, D., 2011. The hydrothermal vent community of a new deep-sea field, Ashadze-1, 12°58′ N on the Mid-Atlantic Ridge. *Journal of the Marine Biological Association of the United Kingdom*, 91, 1-13.

Galkin, S.V., 2006. Prostranstvennaya struktura gidrotermalnykh soobshchestv Sredinno-Atlanticheskogo Khrebta. In: Vinogradov, M.E., Vereshchaka, A.L. (eds), *Ekosistemy Atlanticheskikh Gidroterm*. Nauka, Moskva, 163-202.

Gebruk, A.V., Galkin, S.V., Vereshchaka A.L., Moskalev, L.I., Southward, A.J., 1997. Ecology and biogeography of the hydrothermal vent fauna of the Mid-Atlantic Ridge. *Advances in Marine Biology*, 32, 93-144.

Gerdes, K., Martínez Arbizu, P., Schwarz-Schampera, U., Schentner, M., Kihara, T.C., 2019. Detailed Mapping of Hydrothermal Vent Fauna: A 3D Reconstruction Approach Based on Video Imagery. *Frontiers in Marine Science*, 6, Article 96.

Radziejewska, T., 2014. *Meiobenthos in the Sub-equatorial Pacific Abyss. A Proxy in Anthropogenic Impact Evaluation.* Springer, Heidelberg.

Rybakova (Goroslavskaya), E., Galkin, S., 2015. Hydrothermal assemblages associated with different foundation species on the East Pacific Rise and Mid-Atlantic Ridge, with a special focus on mytilids *Marine Ecology* 36 (Suppl. 1), 45–61

Segonzac, M., 1992. Les peuplements associés a l'hydrothérmalisme océanique du Snake Pit (dorsal Médio-Atlantique; 23° N, 3480 m): Composition et microdistribution de la megafaune. *Comptes rendues de l'Academie des Sciences*, 314, 593-600.

Van Dover, C.L., 2014. Impacts of anthropogenic disturbances at deep-sea hydrothermal vent ecosystems: A review. *Marine Environmental Research*, 102, 59-72.

Van Dover, C.L., Doerries, M.B., 2005. Community structure in mussel beds at Logatchev hydrothermal vents and a comparison of macrofaunal species richness on slow- and fast-spreading mid-ocean ridges. *Marine Ecology*, 26, 110-120.

6.3. Microbial communities: Lost City (Katarzyna Jankowska)

The Lost City hydrothermal field on the Mid-Atlantic Ridge supports dense microbial life on the lofty calcium carbonate chimney structures (McGonigle et al., 2020). The dense microbial biofilms of Lost City chimneys are fuelled by the carbon and energy released by serpentinization of the underlying ultramafic rock – 2010, 2011;(Schrenk et al., 2004; Brazelton et al., 2006, Lang et al., 2018).

Prior to the discovery of chemoautotrophic ecosystems in seafloor hydrothermal systems in the 1970-80s, it had been accepted that all ecosystems ultimately depend on energy from the sunlight. The discovery implied a possibility for life to exist outside Earth to include potential habitats that are magmatically active even if they lack abundant sunlight (Lang and Brazelton, 2020).

In addition, the high concentrations of H_2 and appropriate catalysts in a hydrothermal system can lead to the abiotic synthesis of organic molecules which provide a source of food for life and could have also played a major role in early biochemical evolution (Mccollom and Seewald, 2007; Martin et al., 2008). Serpentinites were probably more abundant and active on the early Earth than they are now –(Sleep et al., 2004), and serpentinization has probably occurred to some degree on all rocky planetary bodies in the solar system –(Sleep et al., 2004). These systems are thought to be present on icy worlds, such as Jupiter's moon Europa and Saturn's moon Enceladus '(Kargel et al., 2000; Oze et al., 2015; 'Glein et al., 2015; Waite et al., 2016, 2017). Therefore, a better understanding of the biological opportunities and challenges in serpentinizing systems provides important insights into the potential for the origin and persistence of life on Earth and elsewhere in the solar system (Lang and Brazelton, 2020).

Research of the microbial biofilm communities that live in the chimneys of the Lost

City hydrothermal field can help to decide whether serpentinization and its associated geochemical reactions are sufficient to support the origin and evolution of life independently of other geological processes, or if the products of serpentinization must be mixed with other materials to meet all of the requirements for continuous habitability (Stüeken et al., 2013).

H_2 is highly abundant (up to 14 µM) in the Lost City chimneys, which contributes to high concentrations of methane (CH_4) and formate (Kelley et al., 2005; Proskurowski et al., 2006; Lang et al., 2010; Proskurowski et al., 2013). Consequently, the Lost City biofilm communities are dominated by organisms likely to consume H_2, CH_4 and formate (Brazelton et al., 2006, 2011; Lang et al., 2018).

However, the Lost City chimneys are mixing zones where anoxic, high pH subsurface fluids mix with oxic seawater. The remarkable density of microbes in the chimneys [up to 10^9 cells per gram (Schrenk et al., 2004)] is a product of the many physical and chemical gradients formed within the porous matrix of the chimneys when these two very different kinds of water are mixed together. Wherever and whenever these gradients can be established, the potential for biochemical and microbial activity is high (Summit and Baross, 2011; McCollom and Seewald, 2007).

Interestingly, as shown by the Integrated Ocean Drilling Project (IODP) 304 and 305 (Lang and Barelton, 2020), data from the first microbiological investigation of rock cores collected of the Atlantis Massif, a large seafloor mountain located near the Lost City chimneys, have revealed a much lower biological content compared with the Lost City chimneys. Microbial cells are nearly undetectable by microscopy in many serpentinite core samples and are typically present at densities approximately 100 cells/cm^3 –(Früh-Green et al., 2018). Similarly, low cell densities (below the detection limit of less than 10^3 cells/cm^3) were also found in gabbroic core samples drilled on an earlier expedition (Mason et al., 2010). These low microbial densities suggest that the habitability of the serpentinite subsurface is limited by physical and/or geochemical conditions. However, it remains possible that the active microbial populations in serpentinite subsurface habitats are present in sparse but dense patches, most likely concentrated along pathways of the fluid flow through the basement rocks (Lang and Brazelton, 2020).

During the last expedition in 2018 (https://lostcity.biology.utah.edu) (the public data available under BCO-DMO Project No. 658604), an attempt has been made to investigate in a comprehensive way the relationship between factors relevant understanding and predicting the habitability of serpentinite-hosted environments. The research has been structured by the requirements for habitability as summarized by Cockell et al. '(2016) such as a solvent, physico-chemical conditions, energy, major elements needed for life (C, H, N, O, P, S), and additional required elements, such as trace metals (Lang and Brazelton, 2020). Lang and Brazelton (2020) concluded, *inter alia*, that the evolution and maintenance of a robust biological ecosystem requires continuous habitability over geological time scales '(Cockell et al., 2016). The absence of certain elemental requirements (e.g., a solvent, energy, appropriate physico-chemical conditions, major and minor elements for life) will preclude life from being able to maintain its complex state. But simply meeting the criteria may also be insufficient to achieve habitability. Rather, amounts of resources also matter for each parameter individually and in combination (Hoehler, 2007). In serpentinizing systems, life may not be limited by a single limiting factor, but instead by combinations of factors that cannot be overcome simultaneously. These observations complement well the studies on microbial biofilm communities that live in the chimneys of the Lost City hydrothermal field presented by McGonigle et al. (2020).

Previous studies (Schrenk et al., 2004) indicated that in interiors of chimneys where the temperatures of venting fluids can reach 95°C, and the pH of the fluids can be as high as 11 –(Butter et al., 2001), are dominated by a single archaeal phylotype, the Lost City Methanosarcinales (Schrenk et al., 2004; Kelley et al., 2005;– Brazelton et al., 2006, 2010, 2011; Lang et al., 2018). In contrast, the chimney exteriors host a more complex microbial community, including organisms involved in the oxidation of sulphur and methane (e.g., *Methylomonas*, *Thiomicrospira*). It was noted that these organisms likely thrive in the mixing zones, where they can take advantage of the cooling effect of the seawater and more efficient electron acceptors (e.g., oxygen), but still access the products of serpentinization supplied by venting fluids.

Previous studies (Lang et al., 2012, 2018) showed, too, that much of the microbial biomass at Lost City is derived from carbon that originated deep in the Earth's subsurface. In most ecosystems, inorganic carbon (CO_2) serves as the starting carbon source for primary production. However, the Lost City fluids contain extremely low concentrations of dissolved inorganic carbon (DIC) due to its reduction to hydrocarbons and its rapid precipitation as calcium carbonate at a pH above □9 (Kelley et al., 2005; Proskurowski et al., 2013). The organic acid formate has been proposed to be an alternative primary carbon source; it is present in high concentrations (36 to 158 μM) in Lost City fluids and is expected to form abiotically in serpentinizing fluids (Lang et al., 2010; –McDermott et al., 2015; Lang et al., 2018). Formate is unable to enter carbon fixation pathways directly and needs to be converted to CO_2 for autotrophic metabolism (Yishai et al., 2016).The enzyme formate dehydrogenase catalyzes the reversible oxidation of formate to CO_2.

The Methanosarcinales phylotype has previously been shown to dominate the anoxic, interior zones of Lost City chimneys (Schrenk et al., 2004; –Brazelton et al., 2010, 2011), yet it appears to be unable to use one of the most abundant carbon sources, formate. Although novel, previously undiscovered formate metabolism genes may exist, no archaeal formate dehydrogenase gene sequences (fdhA, fdhB) or fdhC sequences affiliated with methanogens were detected in the metagenome (McGonigle et al., 2020). These studies also identify the genomic potential of the Chloroflexi and Sulfurovum populations to utilize formate, which maybe required to make mantle-derived carbon available to the rest of the chimney ecosystem, although the Chloroflexi is seven times less abundant than the Methanosarcinales in the chimney sample. However, it was noted that the potential explanation is that Chloroflexi species are highly active and able to rapidly cycle carbon while maintaining a low abundance in the biofilm community. Alternatively, the Chloroflexi population may be more abundant in subsurface habitats underlying the chimneys, where formate is expected to be generated(Lang et al., 2018).

In conclusion, it should be noted how valuable the Lost City hydrothermal field on the Mid-Atlantic Ridge is. Getting to know this environment will help to understand even better how multiple extreme limitations of life interact to restrict, or perhaps even promote, habitability in unusual and complex environments.

References

Brazelton, W.J., Ludwig, K.A., Sogin, M.L., Andreishcheva, E.N., Kelley, D.S., Shen, C., Edwards, R.L., Baross, J.A., 2010. Archaea and bacteria with surprising microdiversity show shifts in dominance over 1000-year time scales in hydrothermal chimneys. *Proceedings of the National Academy of Sciences*, 107(4), 1612-1617. https://doi.org/10.1073/pnas.0905369107

Brazelton, W.J., Mehta, M.P., Kelley, D.S., Baross, J.A., 2011. Physiological Differentiation within a Single-Species Biofilm Fueled by Serpentinization. *MBio*, 2(4), e00127-11. https://doi.org/10.1128/mBio.00127-11

Brazelton, W.J., Schrenk, M.O., Kelley, D.S., Baross, J.A. (2006). Methane- and Sulfur-Metabolizing Microbial Communities Dominate the Lost City Hydrothermal Field Ecosystem. *Applied and Environment Microbiology*, 72, 6257–6270. https://doi.org/10.1128/AEM.00574-06

Butter, D.A., Lilley, M.D., Kelley, D.S., Karson, J.A., Blackman, D.K., Früh, G.L., Olson, E.J., Schrenk, M.O., Roe, K.K., Lebon, G.T., Rivizzigno, P., Party, A.-S., 2001. An off-axis hydrothermal vent feld near the Mid-Atlantic Ridge at 30° N. *Nature*, 412, 145-149.

Cockell, C.S., Bush, T., Bryce, C., Direito, S., Fox-Powell, M., Harrison, J.P., Lammer, H., Landenmark, H., Martin-Torres, J., Nicholson, N., Noack, L., O'Malley-James, J., Payler, S.J., Rushby, A., Samuels, T., Schwendner, P., Wadsworth, J., Zorzano, M.P., 2016. Habitability: A Review. *Astrobiology*, 16(1), 1-29. https://doi.org/10.1089/ast.2015.1295

Früh-Green, G.L., Orcutt, B.N., Rouméjon, S., Lilley, M.D., Morono, Y., Cotterill, C., Green, S., Escartin, J., John, B.E., Mccaig, A.M., Ménez, B., Schwarzenbach, E.M., Morgan, J., Morgan, S., Lang, S.Q., Schrenk, M.O., Brazelton, W.J., Akizawa, N., Boschi, C., Hesse, K., 2018. Magmatism, serpentinization and life: Insights through drilling the Atlantis Massif (IODP Expedition 357). *Lithos*, 323, 137-155. https://doi.org/10.1016/j.lithos.2018.09.012

Glein, C.R., Baross, J.A., Waite, J.H., 2015. The pH of Enceladus' ocean. *Geochimica et Cosmochimica Acta*, 162, 202-219. https://doi.org/10.1016/j.gca.2015.04.017

Hoehler, T.M., 2007. An energy balance concept for habitability. *Astrobiology*, 7(6), 824-838. https://doi.org/10.1089/ast.2006.0095

Kargel, J.S., Kaye, J.Z., Head, J.W., Marion, G.M., Sassen, R., Crowley, J.K., Grant, S.A., Hogenboom, D.L., 2000. Europa's Crust and Ocean: Origin, Composition, and the Prospects for Life. *Icarus*, 265, 226-265. https://doi.org/10.1006/icar.2000.6471

Kelley, D.S., Karson, J.A., Früh, G.L., Yoerger, D.R., Shank, T.M., Butterfield, D.A., Hayes, J.M., Schrenk, M.O., Olson, E.J., Proskurowski, G., Jakuba, M., Bradley, A., Larson, B., Ludwig, K., Glickson, D., Buckman, K., Bradley, A.S., Brazelton, W.J., Roe, K., Sylva S.P., 2005. A Serpentinite-Hosted Ecosystem: The Lost City Hydrothermal Field. *Science*, 307, 1428-1433. https://doi.org/10.1126/science.1102556

Lang, S.Q., Brazelton, W.J., 2020. Habitability of the marine serpentinite subsurface: a case study of the Lost City hydrothermal field. *Philosophical Transactions of the Royal Society A*, 378, 20180429. http://dx.doi.org/10.1098/rsta.2018.0429

Lang, S.Q., Butterfield, D.A., Schulte, M., Kelley, D.S., Lilley, M.D., 2010. Elevated concentrations of formate, acetate and dissolved organic carbon found at the Lost City hydrothermal field. *Geochimica et Cosmochimica Acta*, 74(3), 941-952. https://doi.org/10.1016/j.gca.2009.10.045

Lang, S.Q., Früh, G.L., Bernasconi, S. M., Lilley, M. D., Proskurowski, G., Me, S., 2012. Microbial utilization of abiogenic carbon and hydrogen in a serpentinite-hosted system. *Geochimica et Cosmochimica Acta*, 92, 82-99. https://doi.org/10.1016/j.gca.2012.06.006

Lang, S.Q., Früh-Green, G.L., Bernasconi, S.M., Brazelton, W.J., Schrenk, M.O., Mcgonigle, J.M., 2018. Deeply-sourced formate fuels sulfate reducers but not methanogens at Lost City hydrothermal field. *Nature Scientific Reports*, 8, 755. https://doi.org/10.1038/s41598-017-19002-5

Martin, W., Baross, J., Kelley, D., Russell, M.J., 2008. Hydrothermal vents and the origin of life. *Nature Reviews Microbiology*, 6, 805-814. https://doi.org/10.1038/nrmicro1991

Mason, O.U., Nakagawa, T., Rosner, M., van Nostrand, J.D., Zhou, J., Maruyama, A., Fisk, M. R., Giovannoni, S.J., 2010. First Investigation of the Microbiology of the Deepest Layer of Ocean Crust. *PLoS ONE*, 5(11), e15399. https://doi.org/10.1371/journal.pone.0015399

McCollom, T.M., Seewald, J.S., 2007. Abiotic Synthesis of Organic Compounds in Deep-Sea Hydrothermal Environments. *Chemical Reviews*, 107, 382-401.

McDermott, J.M., Seewald, J.S., German, C.R., Sylva, S.P., 2015. Pathways for abiotic organic synthesis at submarine hydrothermal fields. *Proceedings of the National Academy of Sciences*, 112(25), 7668-7672. https://doi.org/10.1073/pnas.1506295112

McGonigle, J. M., Lang, S. Q., Brazelton, W. J., 2020. Genomic Evidence for Formate Metabolism by Chloroflexi as the Key to Unlocking Deep Carbon in Lost City Microbial Ecosystems. *Applied and Environmental Microbiology*, 86(8), e02583-19. https://doi.org/10.1128/AEM.02583-19

Oze, C., Mousis, O., Waite, J.H., 2015. Serpentinization and the Formation of H_2 and CH_4 on Celestial Bodies (Planets, Moons, Comets) 1. *Astrobiology*, 15(7), 587-600. https://doi.org/10.1089/ast.2014.1188

Proskurowski, G., Lilley, M.D., Kelley, D.S., Olson, E.J., 2006. Low temperature volatile production at the Lost City Hydrothermal Field, evidence from a hydrogen stable isotope geothermometer. *Chemical Geology*, 229, 331343. https://doi.org/10.1016/j.chemgeo.2005.11.005

Proskurowski, G., Lilley, M.D., Seewald, J.S., Früh-Green, G.L., Olson, E.J., Lupton, J.E., Sylva, S.P., Kelley, D.S., 2013. Abiogenic Hydrocarbon Production at Lost City Hydrothermal Field. *Science*, 319(5863), 604-608.
Schrenk, M.O., Kelley, D.S., Bolton, S.A., Baross, J.A., 2004. Low archaeal diversity linked to subseafloor geochemical processes at the Lost City Hydrothermal Field, Mid-Atlantic Ridge. *Environmental Microbiology*, 6(10), 1086-1095. https://doi.org/10.1111/j.1462-2920.2004.00650.x

Sleep, N.H., Meibom, A., Fridriksson, T., Coleman, R.G., Bird, D.K., 2004. H_2-rich fluids from serpentinization: Geochemical and biotic implications. *Proceedings of the National Academy of Sciences*, 101(35), 12818-12823. www.pnas.org/cgi/doi/10.1073/pnas.0405289101

Stüeken, E.E., Anderson, R.E., Bowman, J.S., Brazelton, W.J., Colangelo-Lillis, J., Goldman, A.D., Som, S.M., Baross, J.A., 2013. Did life originate from a global chemical reactor? *Geobiology*, 11(2), 101-126. https://doi.org/10.1111/gbi.12025

Summit, M., Baross, J.A., 2001. A novel microbial habitat in the mid-ocean ridge subseafloor. *Proceedings of the National Academy of Sciences*, 98(5), 2158-2163.

Vance, S.D., Hand, K.P., Pappalardo, R.T., 2016. Geophysical controls of chemical disequilibria in Europa. *Geophysical Research Letters*, 43, 4871-4879. https://doi.org/10.1002/2016GL068547.

Waite, J.H., Glein, C.R., Perryman, R.S., Teolis, B.D., Magee, B.A., Miller, G., Grimes, J., Perry, M.E., Miller, K.E., Bouquet, A., Lunine, J.I., Brockwell, T., Bolton, S.J., 2017. Cassini finds molecular hydrogen in the Enceladus plume: Evidence for hydrothermal processes. *Science*, 159, 155-159.

Yishai, O., Lindner, S.N., Gonzalez, J., Cruz, D., Tenenboim, H., Bar-Even, A., 2016. The formate bio-economy. *Current Opinion in Chemical Biology*, 35, 1-9. https://doi.org/10.1016/j.cbpa.2016.07.005

7. Deep-sea environmental protection and conservation issues as applied to the MAR ecosystem

Teresa Radziejewska, Magdalena Błażewicz, Maria Włodarska-Kowalczuk and Elżbieta Maszloch

7.1. Ecosystem resilience and connectivity (Teresa Radziejewska)

A system's resilience is a trait encompassing three major components: **resistance** (sometimes referred to as "sensitivity"), **recovery**, and **reversibility** (Goode et al., 2020).

Resistance is defined (Lotze et al., 2011) as the ability of a system to remain unchanged despite disturbances. It can be assessed at a population and community level. During a PMS mining operation, there will be no question of organisms occurring at the mining site to resist being removed. However, at a distance from the mining site, under potential exposure to tailing discharge and other disturbance, resistance may be exhibited by populations and communities capable of withstanding such disturbance, by analogy to seamount populations and communities showing resistance to disturbance imposed by seabed trawling (Goode et al., 2020). However, resistance of populations at disturbed sites may in fact result from another process, whereby such sites are open for colonisation by opportunistic species (Goode et al., 2020). Therefore, the extent of post-disturbance resistance can only be assessed based on knowledge of the pre-disturbance status of the system, with its natural variability (see below).

Recovery is defined (Goode et al. 2020) as an ability of a system to exhibit improvement (in, e.g., abundance, diversity, productivity) following disturbance, ideally towards pre-disturbance levels (Lotze et al., 2011). If happening, recovery may be complete (a full return to the initial, pre-disturbance state) or partial (the post-disturbance state shows alteration and/or reduction of specific characteristics, relative to the pre-disturbance state). Whether or not recovery after a PMS mining operation will occur is open to debate. Observations at active vent sites showed the communities there, when disturbed and depleted, to be able to recover, the recovery taking, however, up to decades at fast-spreading ridges (Gollner et al., 2017). When initially PMS mining was envisaged as occurring at active vents (Clark and Smith, 2013), this propensity to recovery was viewed as an asset. However, as stated by Gollner et al. (2017), reversibility of mining impacts at active vents will depend on the frequency and scale of operations. Large-scale mining may considerably reduce populations and could hinder recolonisation by disrupting connectivity of source populations (Van Dover, 2014). The loss of foundation species may make it difficult for the associated fauna to settle, and the system may move to an alternative state dominated by bacterial mats instead of rich faunal communities.

The loss of topographic features such as black smokers may change settlement behaviour, and thus the diversity of fauna (Mullineaux and Butman, 1992). In addition, modification of vent fluid regimes as a result of black smoker removal could cause local habitat loss or change community composition at both active vents and sites not directly affected by mining.

Nowadays, however, the prevailing opinion holds that PMS will be mined at inactive vents the communities of which are much less known (Gollner et al., 2017; Van Dover, 2019). It is unclear whether assemblages at inactive vents are similar to those at active ones, are similar to the fauna inhabiting hard substrata on non-mineral-rich grounds, or are unique (Van Dover, 2011). It has to be borne in mind that removal of the PMS substratum at inactive vents cannot be reversed due to the lack of active hydrothermal venting. The limited knowledge on species diversity, functional groups, species distribution, connectivity, and settlement behaviour makes it impossible to estimate reversibility potential at inactive vents and in areas peripheral to vents, following mining disturbances. Primary considerations include habitat alterations; it is not known to what extent, if at all, species will be able to settle and grow in modified environments.

Recovery, whether at a mining site or at a distance from it, will depend on recolonisation potential of neighbouring communities, that is the availability of recruits (including the donor population size) and the suitability of the post-disturbance substrate for settlement and growth. Experiments with artificial substrates placed in the vicinity of active venting sites showed colonisation to occur within months (meiofauna: Cuvelier et al., 2014; Zeppilli et al., 2015) to years (megafauna, e.g., gorgonian corals; Lacharité and Metaxas, 2013; Girard et al., 2016). As pointed out above, no estimation of recovery potential of inactive site communities is available (Van Dover et al., 2020).

Reversibility is associated, on one hand, with the severity of disturbance, and with a system's ability to recover on the other (Lotze et al., 2011). A more severe disturbance will extend the time for the system to recover, provided some degree of recovery is possible. However, as pointed out by Lotze et al. (2011), it is difficult to distinguish reversible changes from alternative stable states a system may enter, or from phase shifts induced by various drivers, including climate change (Levin et al., 2020). With reference to PMS mining, whether the disturbance will produce reversible or irreversible damage will depend on a number of factors, including the disturbance severity and site. The system's ability to recover (and hence reversibility of changes and overall resilience) may also depend on connectivity between the communities affected by disturbance, whereby a population at a defaunated site can be re-established by recolonisation.

Connectivity is a term reflecting ecological connections between populations living distances apart, such as those at hydrothermal vents that are patchy and transient, and is effected primarily via larval dispersal mechanisms (Vrijenhoek, 2010; Baldrighi et al., 2018). As experimentally demonstrated by Yearsley et al. (2020), the spatial scale of dispersal varies along the ridge axis, with median dispersal distances for planktonic larval durations (PLD) of 75 days ranging from 67 km to 304 km, which leads to considerable opportunities for connectivity through mid-water dispersal. A stable pattern of five regions of biophysical connectivity was obtained for PLDs of 100 days or more. Connectivity barriers between these regions can persist even when planktonic larval duration is longer than 200 days. For a 50-day PLD, one connectivity barrier coincides with the region of the genetic hybrid zone for northern and southern vent mussel species at the Broken Spur vent field (in the Polish contract area). However, estimates of connectivity between populations of invertebrates are complicated, as dispersal and recruitment can be influenced by, e.g., hydrodynamic mechanisms (including currents acting as vectors or barriers to dispersal), larval survival, pelagic larval duration, presence of suitable habitats for settlement, and presence of predators (Goode et al., 2010).

The degree of connectivity between populations is usually estimated using genetic markers (Vrijenhoek, 2010). Connectivity estimation at an assemblage or community level may be attempted, as an approximation, by conducting a non-metric multidimensional similarity/dissimilarity analysis (e.g., a non-metric MDS). Such analyses for meiobenthic, microbenthic and megafaunal assemblages reported from the MAR vent fields sampled so far (see Section 5.1. for sources of information) (Figs 5.1., 5.2., 5.3., respectively) showed a fairly low between-field similarity, and thus limited connectivity, although - in the case of the meiobenthos – the two most closely located fields (Broken Spur and Lost City) were those in the Polish contract area. Interestingly, the vent field geographically closest to the Polish contract area (TAG) supported quite a dissimilar meiobenthic assemblage. In contrast, the Lost City macro- and megafaunal assemblages turned out to be most dissimilar from others. However, the patterns revealed by the MDS plots in Figs 5.1., 5.2., and 5.3. are by no means conclusive, as the available data base is scant and the benthic assemblages under-sampled. Nevertheless, it may be expected that anthropogenic intervention due to PMS mining at MAR (in individual contract areas and beyond them) will definitely put the ecosystem resilience, with all its attributes, to the test.

References

Baldrighi, E., Zeppilli, D., Crespin, R., Chauvaud, P., Pradillon, F., Sarrazin, J., 2018. Colonization of synthetic spontes at the deep-sea Lucky Strike hydrothermal vent field (Mid-Atlantic Ridge): a first insight. *Marine Biodiversity*, 48, 89-103.

Clark, M., Smith, S., 2013. Environmental Management Considerations. In: Baker, E., Beaudoin, Y. (Eds.), *Deep Sea Minerals: Sea-Floor Massive Sulphides, a physical, biological, environmental, and technical review*. Vol. 1A, Secretariat of the Pacific Community, 27-42.

Cuvelier, D., Beesau, J., Ivanenko, V.N., Zeppilli, D., Sarradin, P.M., Sarrazin, J., 2014. First insights into macro- and meiofaunal colonisation patterns on paired wood/slate substrata at Atlantic deep-sea hydrothermal vents. *Deep Sea Research Part I*, 87, 70–81.

Girard, F., Lacharité, M., Metaxas, A., 2016. Colonization of benthic invertebrates in a submarine canyon in the NW Atlantic. *Marine Ecology Progress Series*, 544, 53-64.

Gollner, S., Kaiser, S., Menzel, L., Jones, D.O.B., Brown, A., Mestre, N.C., Oevelen, D. Van, Menot, L., Colaco, A., Canals, M., Cuvelier, D., Durden, J.M., Gebruk, A., Egho, G.A., Haeckel, M., Marcon, Y., Mevenkamp, L., Morato, T., Pham, C.K., Purser, A., Sanchez-Vidal, A., Vanreusel, A., Vink, A., Martinez, P., van Oevelen, D., Menot, L., Colaço, A., Canals, M., Cuvelier, D., Durden, J.M., Gebruk, A., Egho, G. A., Haeckel, M., Marcon, Y., Mevenkamp, L., Morato, T., Pham, C.K., Purser, A., 2017. Resilience of benthic deep-sea fauna to mining activities. *Marine Environmental Research*, 129, 76-101.

Lacharité, M., Metaxas, A., 2013. Early life history of deep-water gorgonian corals may limit their abundance. *PLoS ONE* 8, e65394.

Levin, L.A., Wei, C.-L., Dunn, D.C., Amon, D.J., Ashford, O.S., Cheung, W.W.L., Colaço, A., Dominguez-Carrió, C., Escobar, E.G., Harden-Davies, H.R., Drazen, J.C., Ismail, K., Jones, D.O.B., Johnson, D.E., Le, J.T., Lejzerowicz, F., Mitarai, S., Morato, T., Mulsow, S., Snelgrove, P.V.R., Sweetman, A.K., Yasuhara, M., 2020. Climate change considerations are fundamental to management of deep-sea resource extraction. *Global Change Biology*, 26, 4664-4678.

Lotze, H.K., Coll, M., Magera, A.M., Ward-Paige, C., Airoldi, L., 2011. Recovery of marine animal populations and ecosystems. *Trends in Ecology and Evolution*, 26, 505-605.

Mullineaux, L.S., Butman, C.A., 1990. Recruitment of encrusting benthic invertebrates in boundary-layer flows: A deep-water experiment on Cross Seamount. *Limnology and Oceanography*, 35, 409-423.

Van Dover, C.L., 2011. Mining seafloor massive sulphides and biodiversity: what is at risk? *Journal of Marine Science*, 68(2), 341-348.

Van Dover, C.L., 2014. Impacts of anthropogenic disturbances at deep-sea hydrothermal vent ecosystems: A review. *Marine Environmental Research*, 102, 59-72.

Van Dover, C.L., 2019. Inactive Sulfide Ecocystems in the Deep Sea: a Review. *Frontiers in Marine Science*, 6, Article 461.

Van Dover, C.L., Colaço, A., Collins, P.C., Croot, P., Metaxas, A., Murton, B.J., Swaddling, A., Boschen-Rose, R.E., Carlsson, J., Cuyvers, L., Fukushima, T., Gartman, A., Kennedy, R., Krieten, C., Mestre, N.C., Molodtsova, T., Myhrvold, A., Pelleter, E., Popoola, S.O., Qiant, P.-Y., Sarrazin, J., Sharma, R., Suh, Y.J., Sylvan, J.B., Tao, C., Tomczak, M., Vermil, J., 2020.

Research is needed to inform environmental management of hydrothermally inactive and extinct polymetallic sulfide (PMS) deposits. *Marine Policy*, in press, 104183.

Vrijenhoek, R.C., 2010. Genetic diversity and connectivity of deep-sea hydrothermal vent metapopulations. *Molecular Ecology*, 19, 4391–4411.

Zeppilli, D., Vanreusel, A., Pradillon, F., Fuchs, S., Mandon, P., James, T., Sarrazin, J., 2015. Rapid colonisation by nematodes on organic and inorganic substrata deployed at the deep-sea Lucky Strike hydrothermal vent field (Mid-Atlantic Ridge). *Marine Biodiversity*, 45, 489–504.

Yearsley, J.M., Salmanidou, D.M., Carlsson, J., Burns, D., Van Dover, C.L., 2020. Biophysical models of persistent connectivity and barriers on the northern Mid-Atlantic. *Deep-Sea Research Part II,*
doi: https://doi.org/10.1016/j.dsr2.2020.104819

7.2. Endemism on the Mid-Atlantic Ridge (MAR) (Magdalena Błażewicz)

Endemism is understood as a restricted geographical distribution of a species to a well-defined area. The fauna associated exclusively with hydrothermal vents and absent outside the vent fields is classified as "vent-obligate". The vent-obligate fauna components, however, are often widely distributed, although their geographical ranges are usually disjunct –(Mironov et al., 2002; Gollner et al., 2015; Baco et al., 2016). The vent-obligate fauna is accompanied by "peripheral" or "penetrating" fauna, represented by taxa non-obligatorily associated with vent fields. In contrast to the vent-obligatory fauna, it is often recorded outside hydrothermal fields –(Desbruyères et al., 2002; Galkin and Sagalevich, 2016).

7.2.1. Fauna of Atlantic and Pacific hydrothermal sites

In the Pacific and the Atlantic, the vent-obligate fauna is represented by distinct sets of taxa; this is illustrated in Fig. 7.1. showing a clear separation between clusters of the Pacific and Atlantic vent faunas. Of the 56 vent-obligate families, 28 (50%) are present exclusively in the Pacific, 12 (21.4%) exclusively in the Atlantic, and 16 (28.6%) are common for both oceans. A relatively similar distinctness of the Pacific from the Atlantic fauna is observed on the genus level. Sixty of the 98 (61.2%) vent-obligate genera occur only in the Pacific, 26 (26.5%) in the Atlantic, and only 12 (12.2%) inhabit both oceans, including *Phymorhynchus* (Conidae), *Laeviphitus* (Elachisinidae), *Pseudorimula* (Lepetodrilidae), *Shinkailepas* (Phenacolepadidae), *Xylodiscula* (Xylodisculidae), *Bathymodiolus* (Mytilidae), *Copidognathus* (Halacaridea), *Alvinocaris* and *Chorocaris* (Alvinocarididae).

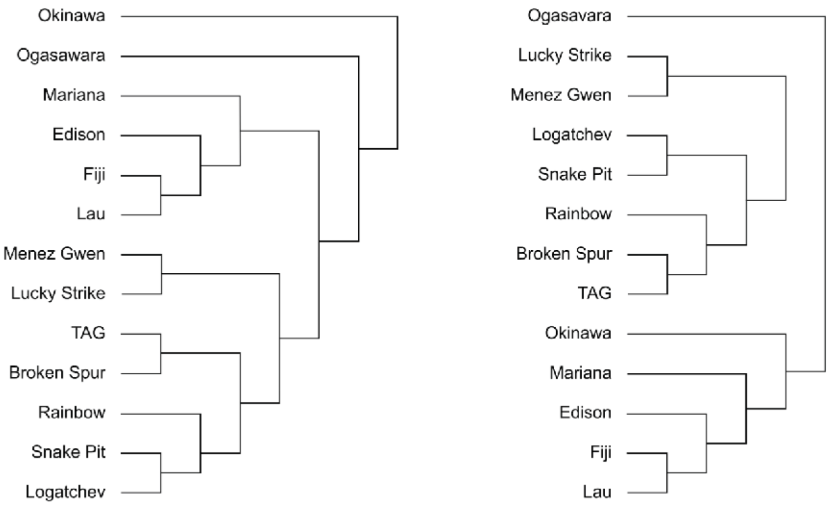

Fig. 7.1. Dendrograms of the Bray-Curtis similarity (presence-absence transformation, group average sorting) for vent-obligatory fauna of Pacific and Atlantic sites based on genera and family level listed by Mironov et al. (2002); family level (left) and genus level (right).

7.2.2. Vent-obligate and peripheral hydrothermal vent fauna of the Mid-Atlantic Ridge (MAR)

The undersampling of the vent-peripheral fauna on the Mid-Atlantic Ridge (MAR) hampers its reliable comparison against the vent-obligatory fauna, although distinct differences do exist (vent-obligatey taxa are not found away from the vent field). On the other hand, earlier observations suggest that the MAR peripheral fauna is not markedly different from the fauna inhabiting other deep-sea habitats (Larsen et al., 2006). Those observation, however, are based on taxonomic surveys, while with an appropriately selected molecular approach, some subtle differences may be observed in the peripheral vent fauna along the MAR (Silva, 2016).

7.2.3. Endemicity of the MAR vent-obligate fauna

The vent-obligate fauna on the MAR shows a moderate degree of endemicity only. Most members of the fauna are widely distributed along the MAR on account of their good swimming ability, the presence of planktonic larvae or due to passive migration aided by larger, actively migrating vent species (Jollivet, 1996;Teixeira et al., 2011; Hilário et al., 2015).

At the present state of knowledge, only five families are considered unique for individual vent fields: the sea anemones Actinostolidae (found at TAG), the gastropods Neolepetopsidae (Lucky Strike), the monoplacophorans Neopilinidae (Menez Gwen), and two amphipod families – the Amphilochidae (Lucky Strike) and the Stegocephalidae (Snake Pit).

Sixty-one species present in seven location of the MAR: Menez Gwen, Lucky Strike, Rainbow, Broken Spur, TAG, Snake Pit and Logatchev (Mironov et al., 2002) are considered vent-obligate fauna and half of them (30 species or 49%) are endemic (Fig. 7.2.; Table 7.2.). Furthermore, nine species (14.7%) were found at two sites, nine others (14.7%) at three sites, whereas six species (9.8%) were recorded at four stations and five species (8.2%) at three sites.

Generally, a high level of endemism is observed in crustacean amphipods and alvinocarids shrimps, with four species (80%) recorded in only one site.

The benthopelagic *Rimicaris exoculata* (Alvinocaridae), present in swarms at MAR hydrothermal vents and the benthic bivalves *Bathymodiolus azoricus* and *B. puteoserpentis* (Mytilidae) are not endemic for any single vent field on the MAR, but because they have not been recorded in non-Atlantic vent fields, they are recognized as the iconic megafauna of the MAR hydrothermal vents. Where their ranges overlap, like in the Broken Spur vent field (in the Polish contract area), they were observed to hybridise (O'Mullan et al., 2001).

Incidentally, a new shrimp species, *Keldyshicaris vavilovi* was discovered in 2001 in the Broken Spur vent field (Lunina and Vereshchaka, 2010). Since it has not been so far reported from any other location, it has to be regarded as strictly endemic.

Endemic taxa are also known within the macro- and meiofauna. For example, in the latter, the siphonostomatoid copepod family Dirivultidae is known exclusively from vent habitats (e.g., Gollner et al., 2010). Four known vent species of the Halacaridea (Acarina) and nine of the 13 (69.2%) species of Dirivultidae (Copoepoda) are known from only one location.

Table 7.1. Vent-obligate fauna recorded in seven locations of MAR (n, number of species)

MAR vent field	species n	endemic species (30) n	 %
Snake Pit	34	12	19.7
Lucky Strike	30	9	17.7
Logatchev	22	4	6.5
Menez Gwen	15	2	3.2
Rainbow	13	1	1.6
Broken Spur	12	1	1.6
TAG	12	1	1.6

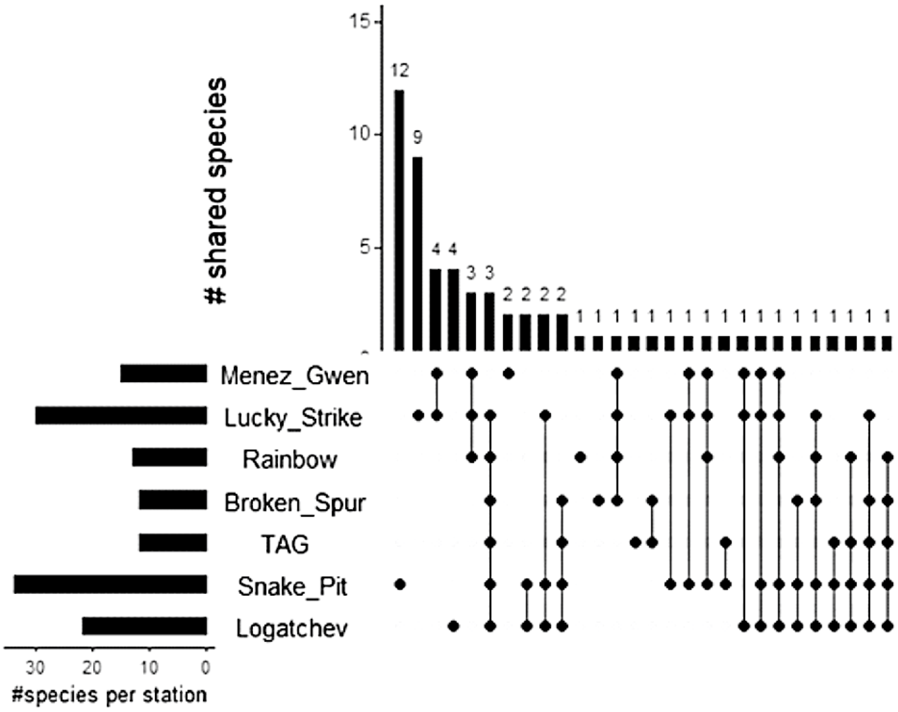

Fig. 7.2. Upset matrix design bi-plots representing obligatory vent species recorded on MAR (upper plot) across seven vent sites. Points connected by a line indicate the shared species between the different sites, for which the total number of species is reported on top of the bar. Single dots represent unique species per site.

References

Baco, A.R., Etter, R.J,. Ribeiro, P.A., von der Heyden, S., Beerli, P., Kinlan, B.P., 2016. A synthesis of genetic connectivity in deep-sea fauna and implications for marine reserve design. *Molecular Ecology*, 25, 3276-3298. doi.org/10.1111/mec.13689

Desbruyères, D., Almeida, A., Biscoito, M., Comte, T., Khripounoff, A., Le Bris, N., Sarradin, P.-M., Segonzac, M., 2000. A review of the distribution of hydrothermal vent communities along the northern Mid-Atlantic Ridge: dispersal vs. environmental controls. *Hydrobiologia*, 440, 201-216. doi.org/10.1023/A

Galkin, S.V., Sagalevich, A.M., 2016. Extreme biomimetics. In: Ehrlich, H. (ed.), *Extreme Biomimetics*. Springer, 97-118. doi.org/10.1007/978-3-319-45340-8

Gollner, S., Govenar, B., Fisher, C.R., Bright, M., 2015. Size matters at deep-sea hydrothermal vents: Different diversity and habitat fidelity patterns of meio- and macrofauna. *Marine Ecology Progress Series,* 520, 57-66. doi.org/10.3354/meps11078

Hilário, A., Metaxas, A., Gaudron, S.M., Howell, K.L., Mercier, A., Mestre, N.C., Ross, R.E., Thurnherr, A.M., Young, C., 2015. Estimating dispersal distance in the deep sea: challenges and applications to marine reserves. *Frontiers in Marine Science*, 2: 6. doi.org/10.3389/fmars.2015.00006

Jollivet, D., 1996. Specific and genetic diversity at deep-sea hydrothermal vents: An overview. *Biodiversity and Conservation*, 5, 1619-1653. doi.org/10.1007/BF00052119

Larsen, K., Błażewicz-Paszkowycz, M., Cunha, M.R., 2006. Tanaidacean (Crustacea: Peracarida) fauna from chemically reduced habitats - The Lucky Strike hydrothermal vent system, Mid-Atlantic Ridge. *Zootaxa*, 1187(1187), 1-36.

Lunina, A.A., Vereshchaka, A.L., 2010. A new vent shrimp (Crustacea: Decapoda: Alvinocarididae) from the Mid-Atlantic Ridge. In: De Grave, S., Fransen, C.H.J.M. (eds.), Contributions to shrimp taxonomy. *Zootaxa,* 2372: 69-74.

Mironov, A.N., Gebruk, A.V., Moskalev, L.I., 2002. Geografia gidrotermalnykh soobshchestv i obligatnykh gidrotermalnykh taksonov. In: Gebruk, A.V. (ed.), *Biology of hydrothermal systems*. KMK Press, Moscow, 410-455.

O'Mullan, G.D., Maas, P.A., Lutz, R.A., Vrijenhoek, R.C. (2001). A hybrid zone between hydrothermal vent mussels (Bivalvia: Mytilidae) from the Mid-Atlantic Ridge. *Molecular Ecology*, 10, 2819-2831.

Silva, M.A.A., 2016. Assessing potential impacts of deep-sea mining on dispersal and population connectivity of the vent mussel *Bathymodiolus azoricus*. Ph.D. thesis, Universidade dos Açores.

Teixeira, S., Cambon-Bonavita, M.A., Serrão, E.A., Desbruyéres, D., Arnaud-Haond, S., 2011. Recent population expansion and connectivity in the hydrothermal shrimp *Rimicaris exoculata* along the Mid-Atlantic Ridge. *Journal of Biogeography*, 38, 564-574. doi.org/10.1111/j.1365-2699.2010.02408.x

Table 7.2. Taxa characteristic of MAR vent fields studied

Broken Spur	**Lucky Strike**	**Snake Pit**	**Logatchev**	**Menez Gwen**	**Rainbow**	**TAG**
Alvinocaris markensis	*Alvania stenolopha*	*Alvinocaris markensis*	*Alvinocaris* aff *muricula*	*Alvania stenolopha*	*Alvinocaris sp. 2*	*Alvinocaris markensis*
Amathys lutzi	*Alvinocaris aff stactophila*	*Amathys lutzi*	*Alvinocaris markensis*	*Anisopes heteroscela*	*Amathys lutzi*	*Archinome aff rosacea*
Bathymodiolus puteoseprentis	*Alvinocaris markensis*	*Andaniotes ingens*	*Alvinocaris sp. 1*	*Aphotopontius atlanteus*	*Bathymodiolus azoricus*	*Bathymodiolus puteoseprentis*
Chorocaris chacei	*Amathys lutzi*	*Aphotopontius forcipatus*	*Amathys lutzi*	*Bathymodiolus azoricus*	*Chorocaris chacei*	*Chorocaris chacei*
Mirocaris fortunata	*Anisopes heteroscela*	*Archinome aff rosacea*	*Anisopes heteroscela*	*Halacarellus prolongus*	*Laeviphitus desbruyeresi*	*Maractis rimicarivora*
Mirocaris keldyshi	*Aphotopontius atlanteus*	*Bathymodiolus puteoseprentis*	*Archinome aff rosacea*	*Laeviphitus desbruyeresi*	*Leptodrilus atlanticus*	*Mirocaris keldyshi*
Ophictenella acies	*Aphotopontius temperatus*	*Candelabrum srepentari*	*Bathymodiolus puteoseprentis*	*Leptodrilus atlanticus*	*Mirocaris fortunata*	*Ophictenella acies*
Rimicaris exoculata	*Bathymodiolus azoricus*	*Chorocaris chacei*	*Calyptogena aff. kaikoi*	*Luckia striki*	*Ophictenella acies*	*Phymorhynchus moscalevi*
Rimipontius mediospinifer	*Bouvierella curtirama*	*Halacarellus auzendei*	*Candelabrum srepentari*	*Lurifax vitreus*	*Phymorhynchus moscalevi*	*Rimicaris exoculata*
Sengonzacia mesatlantica	*Chorocaris chacei*	*Leptodrilus atlanticus*	*Chorocaris chacei*	*Mirocaris fortunata*	*Rimicaris exoculata*	*Sengonzacia mesatlantica*
Stygiopontilus cladarus	*Dendronotus comteti*	*Lirapex sp.A*	*Copidognathus nautilei*	*Peltospira smaragdina*	*Sengonzacia mesatlantica*	*Stygiopontilus pectinatus*
Stygiopontilus pectinatus	*Gigantopsis alvina*	*Mirocaris keldyshi*	*Mirocaris keldyshi*	*Protolira valvatoides*	*Shinkailepas briandi*	*Stygiopontius pectinatus*

Broken Spur	Lucky Strike	Snake Pit	Logatchev	Menez Gwen	Rainbow	TAG
	Halacarellus alvinus	*Ophictenella acies*	*Ophictenella acies*	*Rocopella segonzaci*	*Xylodiscula analoga*	
	Laeviphitus desbruyeresi	*Peltospira smaragdina*	*Peltospira smaragdina*	*Shinkailepas briandi*		
	Leptodrilus atlanticus	*Phymorhynchus carinatus*	*Phymorhynchus carinatus*	*Xylodiscula analoga*		
	Lirapex costellata	*Phymorhynchus moscalevi*	*Phymorhynchus moscalevi*			
	Luckia striki	*Phymorhynchus ovatus*	*Phymorhynchus ovatus*			
	Lurifax vitreus	*Protolira valvatoides*	*Pseudorimula midatlantica*			
	Mirocaris fortunata	*Pseudorimula midatlantica*	*Rimicaris exoculata*			
	Ophictenella acies	*Rimicaris exoculata*	*Rimipontius mediospinifer*			
	Paralepetopsis ferrugivora	*Rimipontius mediospinifer*	*Sengonzacia mesatlantica*			
	Peltospira smaragdina	*Sengonzacia mesatlantica*	*Shinkailepas briandi*			
	Phymorhynchus ovatus	*Shinkailepas briandi*				
	Protolira valvatoides	*Steleuthera ecoprophycea*				

Broken Spur	**Lucky Strike**	**Snake Pit**	**Logatchev**	**Menez Gwen**	**Rainbow**	**TAG**
	Pseudorimula midatlantica	*Stygiopontius bulbisetiger*				
	Rimicaris exoculata	*Stygiopontius cladarus*				
	Shinkailepas briandi	*Stygiopontius latulus*				
	Stygopontilus rimivagus	*Stygiopontius mirus*				
	Sutilizona pterodon	*Stygiopontius pectinatus*				
	Xylodiscula analoga	*Stygiopontius regius*				
		Stygiopontius serratus				
		Stygiopontius teres *Sutilizona pterodon*				

7.3. Natural variability (Maria Włodarska-Kowalczuk and Teresa Radziejewska)

The greatest challenge in any environmental assessment is to disentangle effects of anthropogenic pressures from those resulting from natural variability (e.g., Osenberg et al., 1994). This challenge becomes more acute in areas which are greatly under-sampled, particularly along the temporal axis. This is the case of the Mid-Atlantic Ridge (MAR).

Natural variability in deep-sea communities is shaped by a number of abiotic and biotic factors operating at various spatial and temporal scales (Glover et al., 2010). The natural processes at hydrothermal vents can lead to disturbances operating with different frequencies, spatial range and severity ranging from rather negligible effects of regular tidal fluctuations in fluid flows to unpredictable and catastrophic regimes resulting from tectonic activity and volcanic eruptions and leading to local extinctions (Van Dover, 2014). The range of biotic factors bringing about natural variability in communities includes the growth rates of organisms, their life cycle (reproduction, maturation), and dispersal capabilities. Typically, these are biological traits that underpin temporal persistence of the communities in the face of natural disturbance (Van Dover, 2014). The structure of the natural processes that shape the chemoautotrophic production (the basis of the vent ecosystems functioning) spanning a range of increasing spatial and temporal scales has been summarized by Le Bris et al. (2019) (Fig. 7.3.).

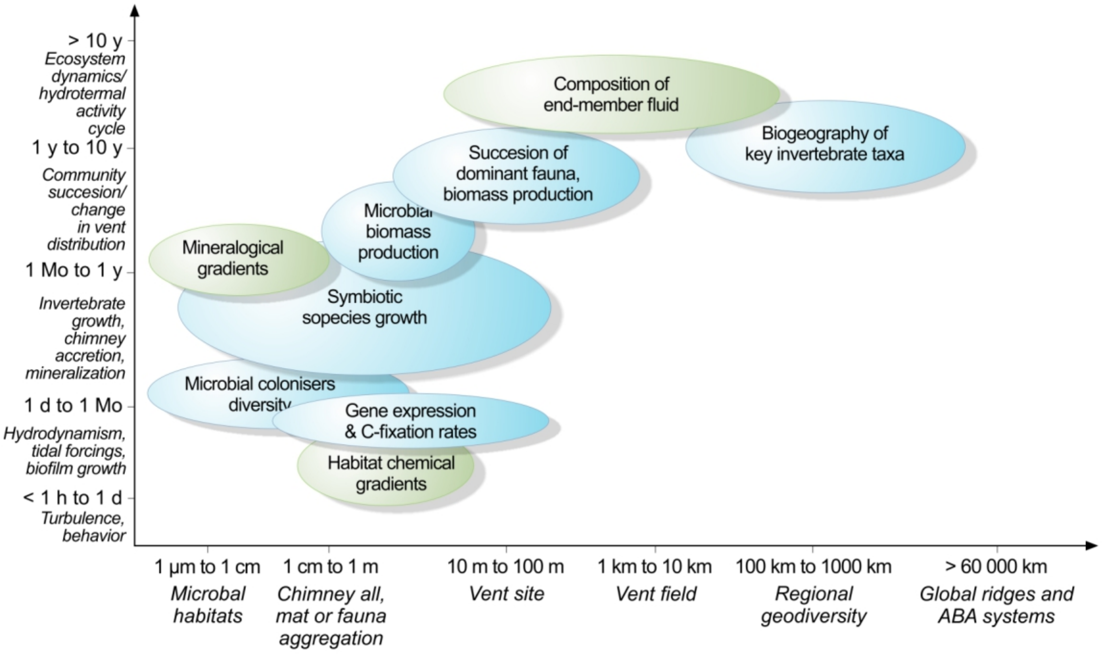

Fig. 7.3. Key natural processes shaping the variability in chemoauthotrophic productivity in deep-sea hydrothermal vent systems at different temporal and spatial scales (modified from Le Bris et al., 2019).

The large-scale spatial variability in biological communities of the MAR has been treated fairly extensively, based on the available data: for example, Galkin (2006) described differences and similarities in benthic communities between several active hydrothermal vents (including Broken Spur in the Polish contract area) and reported on some differences in the set of dominants and associated species. The natural variability on the scale of a single vent field was tackled by several studies. For example, spatial variability in vent communities of the Menez Gwen and Lucky Strike fields was treated by Desbruyères et al. (2001). They ascribed the variations observed in the structure and composition of the communities along the depth gradient to changes in vent fluid toxicity (metallic and sulphide content) and suspended mineral particles. Van Dover (2014) treats this spatial variability as zonation, with the holobiont (symbiont-supporting) taxa dominant in the habitable diffuse flow regions and abrupt transitions observed with a distance from the vent. While the total biomass of benthic organisms is very high at vents, at a hydrothermal periphery the biomass and abundances are greatly reduced. Nevertheless, information on patterns of natural spatial variability in many other MAR fields, including those in the Polish contract area, except for the information provided by Galkin (2006) is missing.

Knowledge of the temporal dimension in natural variability of deep-sea systems, particularly those of MAR, is rather fragmentary. Few studies that included repeated visits and/or observations at vent sites differed in temporal range and resolution and focused mostly on invertebrates visible on underwater images (large epifauna). For example at Lucky Strike vent field, day-to-day variations in *Bathymodiolus azoricus* mussel assemblages were monitored for a period of 48 days (Sarrazin et al., 2014), while another study focused on crustacean behaviour monitored for a week each month over a total period of 9 months (Matabos et al., 2015). A long term monitoring station was established at Lucky Strike vent field in 2010 (EMSO-Azores multidisciplinary seafloor observatory, http://www.emso-fr.org/EMSO-Azores). Glover et al. (2010) reviewed the current literature on temporal trends in different habitats and regions in the deep-sea and stated that slow-spreading venting sites (as MAR) and associated biological systems are relatively stable on decadal to century timescales. Establishing a long-term monitoring programme in the Polish contract area is needed to provide essential ecological baseline information necessary to recognise and predict ecosystem responses to anthropogenic impacts in the area.

References

Galkin, S.V., 2006. Prostranstvennaya struktura gidrotermalnykh soobshchestv Sredinno-Atlanticheskogo Khrebta. In: Vinogradov, M.E., Vereshchaka, A.L. (eds), *Ekosistemy Atlanticheskikh Gidroterm*. Nauka, Moskva, 163-202.

Desbruyères, D., Biscoito, M., Caprais, J.-C., Colaço, A., Comtet, T, . Crassous, P., Fouquet, Y., Khripounoff, A., Le Bris, N., Olu, K., 2001. Variations in deep-sea hydrothermal vent communities on the Mid-Atlantic Ridge near the Azores plateau. *Deep Sea Research Part I: Oceanographic Research Papers*, 48,1325-1346.

Desbruyères, D., Biscoito, M., Caprais, J.-C., Colaço, A., Comtet, T, . Crassous, P., Fouquet, Y., Khripounoff, A., Le Bris, N., Olu, K., 2001. Variations in deep-sea hydrothermal vent communities on the Mid-Atlantic Ridge near the Azores plateau. Deep Sea Research Part I: Oceanographic Research Papers, 48,1325-1346.

Glover, A.G., Gooday,A.J., Bailey,D.M., Billett, D.S.M., Chevaldonne, P., Colaço, A., Copley, J., Cuvelier, D., Desbruyères, D., Kalogeropoulou, V., Klages, M., Lampadariou,N., Lejeusne, D., Mestre, N.C., Paterson, G.L.J., Perez, T., Ruhl, H., Sarrazin, J., Soltwedel, T., Soto, E.H., Thatje, S., Tselepides, A., Van Gaever, S., Vanreusel, A., 2010. Temporal chnage in deep-sea benthic ecosystmes: a review of the evidence from recent time-searies studies. Advances in Marine Biology, 58,1-95.

Le Bris, N., Yücel, M.A. Das, Sievert, S.M., LokaBharathi, P,. Girguis, P.R., 2019. Hydrothermal energy transfer and organic carbon production at the deep seafloor. Frontiers in Marine Science, 5:531.

Matabos, M., Cuvelier, D., Brouard, J., Shillito, B., Ravaux, J., Zbinden, M., Barthelemy, D., Sarradin, P.-M., Sarrazin, J., 2015. Behavioural study of two hydrothermal crustacean decapods: Mirocaris fortunata and Segonzacia mesatlantica, from the Lucky Strike vent field (Mid-Atlantic Ridge). Deep Sea Research Part II Topical Studies in Oceanography, 121,146-158.

Osenberg, C.W., Schmitt, R.J., Holbrook, S.J., Abu-Saba, K.E., Flegal, A R., 1994. Detection of environmental impacts: natural variability, effect size, and power analysis. Ecological Applications, 4:16-30.

Sarrazin, J., Cuvelier, D., Peton, L., Legendre, P., Sarradin, P.-M., 2014. High-resolution dynamics of a deep-sea hydrothermal mussel assemblage monitored by the EMSO-Açores MoMAR observatory. Deep Sea Research Part I Oceanographic Research Papers, 90, 62-75.

Van Dover, C.L., 2014. Impacts of anthropogenic disturbances at deep-sea hydrothermal vent ecosystems: a review. Marine Environmental Research, 102, 59-72.

7.4. Hydrothermal vent fields in the Polish exploration contract area on the Mid-Atlantic Ridge as viewed from the protection and conservation standpoint (Teresa Radziejewska)

In a recent assessment, commenced during the ISA-sponsored "Workshop on the Regional Environmental Management Plan for the Area of the Northern Mid-Atlantic Ridge" in Evora, Portugal (https://www.isa.org.jm/files/files/documents/Evora%20Workshop_3.pdf; "the Evora workshop"), of the environmental characteristics of the 11 hydrothermal fields known from the northern part of the Mid-Atlantic Ridge (MAR) subjected to ISA contracts for exploration (Gollner et al., submitted; cf. the Evora Workshop Report, website as above), the fields were categorised, based on the geological and biological attributes, in terms of their meeting the criteria which are thought to be important for environmental management, protection, and conservation. These criteria were: Uniqueness and Rarity; Functional Significance; Fragility; Life-History Traits of Component Species that Make Recovery Difficult; Structural Complexity; Biological Diversity; Biological Productivity; Naturalness; and Ecosystem Services. Each field was assigned a score with respect to each criterion (High, Medium, Low), the scores reflecting the extent to which the field met that particular criterion. As repeatedly indicated in the present report, the Polish exploration contract area on the MAR encompasses two known hydrothermal vent fields: Lost City and Broken Spur.

The Lost City field (cf. Sections 3.2., 6.3.), covering 10,000 km^2, located at a depth range of 720-850 m, is characterised by a relatively low-temperature (90°C) high-pH (9-11), hydrogen- and methane rich vent fluid devoid of dissolved metals, and carbonate mineralogy (aragonite to calcite). The field has been intensively studied for its venting characteristics, geological set-up and microbiology (cf. Sections 3.2., 6.3.), and less so in terms of the faunal communities it supports (but cf. Sections 5., 6., 7.2.). Lost City was found to meet the criterion of Uniqueness and Rarity (score: High) in being distinct as an unusual serpentinite system, hosting unique microbial communities that may represent a "rare analogue for early Earth ecosystems" (e.g., Brazelton et al., 2010). The field scored High on the criterion Functional Significance, as it is exceptionally important for the survival of sulphur-cycling and methane-oxidising microorganisms adapted to high pH and methane-rich conditions; the vent-endemic taxa, including *Bathymodiolus azoricus*, are extremely rare, but the primary production of the field may be crucial for their reproduction. Lost City scored High on the criterion Fragility, as it is thought that it may be susceptible to degradation by human activities (considering its uniqueness and the hosted microorganisms regarded as a rare biosphere). The Lost City scoring on the criterion Life-History Traits of Component Species that Make Recovery Difficult was also High, in view of the poor knowledge on recruitment dynamics and the fact that the field hosts species without larval dispersal (e.g., morphologically distinct nematodes; cf. Section 5.1.). The Lost City scoring on the criterion Structural Complexity was High on account of within- and between-structure differences in mineralogy, carbonate age, fluid flux, chemistry, and associated microbiota and the presence of the engineer species, the vent-endemic *Bathymodiolus azoricus*. The Lost City scored High on the criterion Biological Diversity, primarily on account of the high diversity of microorganisms (cf. Section 6.3.), and the diversity of invertebrates inhabiting the flanges and spires (cf. Section 5.). In terms of the criterion Biological Productivity, the field scored High because of the abundant chemical energy for the synthesis of organic compounds. The scoring for the criterion Naturalness was High, as Lost City is considered to be, at present, relatively undisturbed. Finally, the Lost City scoring on the criterion Ecosystem Services was also High, as the field was considered to offer – like all active vent fields – provisioning, regulating, and supporting services, the latter including, *inter alia*, inspiration for art, and serving as a centre for knowledge generation.

The Broken Spur field, with its ~5000 m^2 seafloor massive sulphide area, lies at a depth range of 3970-3110 m and is a “typical” hydrothermal vent field in a basaltic hosting rock. It features seven known tall active high-temperature (360-364°C) black smokers as well as diffuse-vent platforms and inactive weathered sulphide mounds. The venting fluid is enriched in lithium, and poor in dissolved manganese and strontium; the field contains appreciable (compared to other MAR fields) amounts of gold and silver. In terms of the criterion Uniqueness and Rarity, Broken Spur was found to score High due to its hosting vent-endemic taxa (cf. Section 7.2.), including the shrimps *Rimicaris ecoxulata*, *Alvinocaris markensis*, *Mirocaris fortunata*, *Keldyshicaris vavilovi*, mussels *Bathymodiolus azoricus*, *B. puteoserpentis* and their hybrid (O'Mullan et al., 2001; Breusing et al., 2016), crabs *Segonzacia mesatlantica*, galatheid squat lobsters *Munidopsis* sp., gastropods *Phymorhynchus moskalevi*, and ophiuroids *Ophioctenella acies* (cf. Section 7.2.). The field scored High on the criterion Functional Significance as it is a discrete feeding area essential for the survival, reproduction and recovery of vent-endemic species listed above as well as two species of deep-sea fish *Haptenchelys texis* (Synaphobranchidae) and *Pachycara thermophilum* (Zoarcidae) (Parin, 1995) (cf. Section 5.4.); it is a zone of hybridisation between the two *Bathymodiolus* mussel species (see above) and the source of copepodid stages of the vent-endemic dirivultid copepods (cf. Section 7.2.). The field scored High on the criterion Fragility, the arguments being that it is a fragile, geographically isolated and discrete ecosystem, hosting populations of species documented as adversely affected by, e.g., illumination. The Broken Spur scoring on the criterion Life-History Traits of Component Species that Make Recovery Difficult was High, although the recovery dynamics of vent communities are unknown and many best-known species (e.g. *Bathymodiolus* mussels) have larval dispersal, but this trait is absent in many others. The field scored High on the criterion Structural Complexity, as it features several types of hydrothermal structures with different morphologies, chemical, and thermal conditions as well as the *Bathymodiolus* mussels as engineer species. The Broken Spur scoring on the criterion Biological Diversity was High on account of the field hosting vent-endemic invertebrate species and two rare species of deep-sea fishes (see above). Broken Spur scored High on the criterion Biological Productivity: its hydrothermal venting supports high *in situ* primary production which in turn supports biomass-rich communities. Broken Spur is relatively undisturbed at present, so it scored High on the criterion Naturalness. Finally, Broken Spur scored High on the criterion Ecosystem Services, as it has been, and continues to be, an important research site yielding new biological discoveries, for instance hybrid mussels and new species (e.g., the shrimp *Keldyshicaris vavilovi*; Lunina and Vereshchaka, 2010).

To sum up, both hydrothermal vent fields within the Polish exploration contract area on the MAR have been found to meet all the criteria of vulnerability and the need of protection.

References

Breusing, C., Biastoch, A., Drews, A., Metaxas, A., Jollivet, D., Vrijenhoek, R.C., Bayer, T., Melzner, F., Sayavedra, L., Petersen, J.M., Dubilier, N., Schilhabel, M.B., Rosenstiel, P, Reusch, T.B.H., 2016. Biophysical and population Genetic Models Predict the Presence of "Phantom" Stepping Stones Connecting Mid-Atlantic Ridge Vent Ecosystems. *Current Biology*, 26, 2257-2267.

Gollner, S., Colaço, A., Gebruk, A., Halpin, P.H., Higgs, N., Menini, E., Mestre, N.C., Quian, P-Q., Sarrazin, J., Szafranski, K., Van Dover, C.L., submitted. Application of scientific criteria for identifying hydrothermal ecosystems in need of protection. *Marine Policy* (Annex II, Evora Workshop Report;
https://www.isa.org.jm/files/files/documents/Evora%20Workshop_3.pdf

Lunina, A.A., Vereshchaka, A.L., 2010. A new vent shrimp (Crustacea: Decapoda: Alvinocarididae) from the Mid-Atlantic Ridge. In: De Grave, S., C.H.J.M. Fransen (eds.), Contributions to shrimp taxonomy. *Zootaxa*, 2372, 69-74.

O'Mullan, G.D., Maas, P.A., Lutz, R.A., Vrijenhoek, R.C., 2001. A hybrid zone between hydrothermal vent mussels (Bivalvia: Mytilidae) from the Mid-Atlantic Ridge. *Molecular Ecology*, 10, 2819-2831.

Parin, N.V., 1995. Deep-sea fishes, *Haptenchelys texis* (Synaphobranchidae) and *Pachycara thermophilum* (Zoarcidae) from the Broken Spur hydrothermal vent field (Mid-Atlantic Ridge). *Journal of Ichthyology*, 35, 328-332.

7.5. Protection of geological formations (Elżbieta Maszloch)

Hydrothermal vents are home to many remarkable organisms not found anywhere else in the world. Hence, discussion on the protection of these areas as valuable habitats has been carried out for years by many organizations. Extraction of massive sulphides from hydrothermal fields will physically destroy the chimneys, their fauna, and leave a flatter topography covered by compressed sediment. It is difficult to predict to what extent it will be possible for the habitats to recover and be re-colonized (Miller et al., 2018).

In order to reduce the negative human impacts on the deep sea, particularly valuable sites are defined as Marine Protected Areas (MPAs), marine reserves and no-take zones. Most of these areas are concentrated in exclusive economic zones (EEZs) or on respective extended continental shelves. An example is establishment, in 2016, of the Azores Hydrothermal Vent MPA in the area under Portugal's national jurisdiction in the Atlantic Ocean (Ramirez-Llodra et al., 2011). The OSPAR Commission also recognized hydrothermal vents as valuable sites in need of protection, and placed them on the List of Threatened and/or Declining Species and Habitats (OSPAR, 2008). Hydrothermal vents are also included within the category "reef" and are protected as one of the habitats within the EU Natura 2000 Network (European Commission DG Environment, 2007).

In areas beyond national jurisdiction, the major role in the protection of the marine environment is to be played by the International Seabed Authority (ISA). Within its remit, ISA is committed to ensuring the effective protection of the marine environment against harmful effects associated with mining activities on the international seabed, as stipulated by Article 145 of UNCLOS. As an endeavour to fulfil this commitment, Regional Environmental Management Plans (REMPs) are being developed, and Areas of Particular Environmental Interest (APEIs) have been designated in the Pacific's Clarion-Clipperton nodule field (Wedding et al., 2013). APEIs are to be excluded from future exploitation of mineral resources. On account of the uniqueness of active hydrothermal systems on the Mid-Atlantic Ridge, their legal protection has been deemed desirable (Freestone et al., 2016; Johnson, 2019). However, a REMP for the Mid-Atlantic Ridge is currently in a preparatory phase (International Seabed Authority, 2019).

The Polish contract area on the Mid-Atlantic Ridge encompasses two known (Beaulieu et al., 2013) hydrothermal fields: Broken Spur and Lost City. The latter is particularly important from the standpoint of protection of geological formations. Lost City is a hydrothermal field characterized by the occurrence of unique carbonate structures (Fig. 7.4.). Its discovery in 2000 caused a sensation, and since then it has been intensively researched (Kelley et al., 2001, 2005; Seyfried et al., 2015; Lang and Brazelton, 2020). The chimneys are 30 to 60 m tall and are composed of variable mixtures of calcite ($CaCO_3$), aragonite ($CaCO_3$), and brucite ($Mg(OH)_2$) (Dubinina et al., 2007; Kelley et al., 2001). They are located at a water depth of 750 to 900 m (Kelley et al., 2001, 2005). The fluid composition in Lost City hydrothermal field is derived from the reaction between seawater and uplifted mantle peridotite. This reaction produces a low temperature fluid (<40° to 116°C) with a high pH ranging from 9 to 11 (Kelley et al., 2001, 2005; Lang and Brazelton, 2020). Lost City does not have any mineral resources of interest, so it probably will never be mined. However, adjacent vents may be mined. Plumes of sediment in the water column and possible chemical contamination due to, e.g., equipment failure may have an unpredictable effect on the functioning of hydrothermal vent communities (Johnson, 2019).

Scientists, non-governmental organizations, and the international public opinion are concerned by the perceived threats to the ecosystems of hydrothermal vents. For instance, concern about the contracts for exploration signed by the ISA in the Mid-Atlantic Ridge has been expressed by Greenpeace (Casson et al., 2019). They fear the destruction of the unique and still poorly understood ecosystems existing around hydrothermal vents. Of a particular concern for Greenpeace and other organisation is Lost City, recognised as an Ecologically and Biologically Significant Area (EBSA) under the Convention on Biological Diversity (CBD) and still covered by the exploration contract signed between the ISA and Poland (Casson et al., 2019). Due to its outstanding universal value, Lost City has been also recognised by the UNESCO as a potential World Heritage Site in the high seas (Freestone et al., 2016). On account of the unusual nature of the structures such as hydrothermal chimneys, every effort should be made to preserve these valuable natural geological formations.

References

Beaulieu, S. E., Baker, E. T., German, C. R., Maffei, A., 2013. An authoritative global database for active submarine hydrothermal vent fields. *Geochemistry, Geophysics, Geosystems*, 14, 4892-4905. doi:10.1002/2013GC004998

Casson, L., Losada, S., Tsenikli, S., Santillo, D., Currie, D., Sharma, G., McCallum, W., 2019. *In Deep Water: The emerging threat of deep sea mining.* Greenpeace International. https://issuu.com/greenpeaceinternational/docs/in-deep-water-2019

Dubinina, E.O., Chernyshev, I.V., Bortnikov, N.S., Lein, A.Y., Sagalevich, A.M., Gol'tsman, Y.V., Bairova, E.D., Mokhov, A.V., 2007. Isotopic–Geochemical Characteristics of the Lost City Hydrothermal Field. *Geochemistry International*, 45(11), 1131-1143, doi.org/10.1134/S0016702907110067

European Commission DG Environment, 2007. *Natura 2000. Interpretation Manual of European Union Habitats* – EUR, 27.

Freestone, D., Laffoley D., Douvere F., Badman, T., 2016. *World heritage in the high seas: an idea whose time has come*. IUCN. https://unesdoc.unesco.org/ark:/48223/pf0000245467

International Seabed Authority, 2019. *Report of the Workshop on the Regional Environmental Management Plan for the Area of the Northern Mid-Atlantic Ridge*, 25-29 November 2019, Évora, Portugal. https://www.isa.org.jm/files/2020-01/Evora%20Workshop.pdf

Johnson, D.E., 2019. Protecting the Lost City hydrothermal vent system: All is not lost, or is it? *Marine Policy*, 107, 103593. doi.org/10.1016/j.marpol.2019.103593

Kelley, D.S., Karson, J.A., Blackamn, D.K., Früh-Green, G.L., Butterfield, D.A., Lilley, M.D., Olson, E.J., Schrenk, M.O., Roe, K.K., Lebon, G.T., Rivizzigno, P., the AT3-60 Shipboard Party, 2001. An off-axis hydrothermal vent field near the Mid-Atlantic Ridge at 30° N. *Nature*, 412, 145-149. doi.org/10.1038/35084000

Kelley, D.S., Karson, J.A., Früh-Green, G.L., Yoerger, D.R., Shank, T.M., Butterfield, D.A., Hayes, J.M., Schrenk, M.O., Olson, E.J., Proskurowski, G., Jakuba, M., Bradley, A., Larson, B., Ludwig, K., Glickson, D., Buckman, K., Bradley, A.S., Brazelton, W.J., Roe, K., Elend, M.J., Delacour, A., Bernasconi, S.M., Lilley, M.D., Baross, J.A., Summons, R.E., Sylva, S.P., 2005. A serpentinite-hosted ecosystem: The Lost City hydrothermal field. *Science*, 307, 1428-1434. doi.org/10.1126/science.1102556

Lang, S.Q., Brazelton, W.J., 2020. Habitability of the marine serpentinite subsurface: a case study of the Lost City hydrothermal field. *Philosophical Transcations of the Royal Society, A*, 378, 20180429. doi.org/10.1098/rsta.2018.0429

Miller, K.A., Thompson, K.F., Johnston, P., Santillo, D., 2018. An Overview of Seabed Mining Including the Current State of Development, Environmental Impacts, and Knowledge Gaps. *Frontiers in Marine Science*, 4, Article 418. doi.org/10.3389/fmars.2017.00418

OSPAR Commission, OSPAR. 2008. *List of Threatened and/or Declining Species and Habitats*, Reference Number: 2008-6. https://www.ospar.org/work-areas/bdc/species-habitats/list-of-threatened-declining-species-habitats, accessed 20/10/2020

Ramirez-Llodra, E., Tyler, P.A., Baker, M.C., Bergstad, O.A., Clark, M.R., Escobar, E., Menot, L., Rowden, A.A., Smith, C.R., Van Dover, C.L., 2011. Man and the Last Great Wilderness: Human Impact on the Deep Sea. *PLoS ONE*, 6(8): e22588. doi.org/10.1371/journal.pone.0022588

Seyfried, W.E, Pester, N.J., Tutolo, B.M., Ding, K., 2015. The Lost City hydrothermal system: constraints imposed by vent fluid chemistry and reaction path models on subseafloor heat and mass transfer processes. *Geochimica et Cosmochimica Acta*, 163, 59-79. doi.org/10.1016/j.gca.2015.04.040

Wedding, L.M., Friedlander, A.M., Kittinger, J.N., Watling, L., Gaines, S.D., Bennett, M., Hardy, S.M., Smith, C.R., 2013. From principles to practice: a spatial approach to systematic conservation planning in the deep sea. *Proceedings of the Royal Society B*, 280, 20131684.

Fig. 7.4. Carbonate structures on the east side of Lost City (Image: Kelley, D. S. and Elend, M., UW, URI, ROV *Hercules*; NOAA Ocean Exploration).

8. The legal and regulatory framework for protection and conservation of the deep-sea floor, with a particular reference to mid-ocean ridges: A summary

Teresa Radziejewska, Agata Kozłowska-Roman and Agata Szyduk

Activities aimed at protection and conservation of the deep-sea floor are at present based governed by legal instruments which form a multi-tier system (cf. Jaeckel et al., 2020). On the **most general level**, the relevant issues are treated by the United Nations Convention on the Law of the Sea of 1982 (UNCLOS, www.un.org/depts/los/convention_agreements/texts/unclos/UNCLOS-TOC.htm), and in particular by Part XI of the Convention and the Agreement on the Implementation of Part XI of 16 November 1994 (the date when UNCLOS entered into force; Van Dover et al., 2011) (www.un.org/Depts/los/convention_agreements/texts/unclos/closindxAgree.htm).

Auxiliary and complementary to UNCLOS are resolutions and documents issued by the UN General Assembly. Of a particular importance here is the 2015 Agenda for Sustainable Development 2030 which lists 17 Sustainable Development Goals (SDGs). In the context of deep-sea environment protection, particularly relevant is SDG 14 ("Conserve and sustainably use the oceans, seas and marine resources for sustainable development").

Protection and conservation of marine environment, its biodiversity in particular, are dealt with in a number of other international instruments, auxiliary to the UNCLOS, including the Stockholm Declaration (https://legal.un.org/avl/ha/dunche/dunche.html) signed following the 1972 United Nations Conference on the Human Environment (the so-called Stockholm Conference; www.un.org/ga/search/view_doc.asp?symbol=A/CONF.48/14/REV.1) which provided the basis for sustainable development as a core principle for the management of human impact on the environment. Subsequent declarations and instruments, including the Rio Declaration on Environment and Development of 1992 (https://www.un.org/en/development/desa/population/migration/generalassembly/docs/globalcompact/A_CONF.151_26_Vol.I_Declaration.pdf) and the Convention on Biological Diversity (CBD) of 1993 (www.cbd.int) have upheld the principle and developed it further. Although recognising that ecosystems, species and genes must be used for the benefit of mankind, this use should not result in a long-term decline in biodiversity and environmental damage, the hence the CBD's objective is conservation of all biodiversity. The CBD supports the Precautionary Principle (McIntyre and Mosedale, 1997) according to which the burden of proof should be shifted to those who intend to undertake or continue an activity that poses a threat of serious or irreversible damage. According to the CBD, the ecosystem approach (e.g., Rice et al., 2005) should be a strategy of preference for integrated and adaptive management to promote conservation and sustainable use of the environment. Moreover, the CBD promotes the use of area-based management tools (envisaged also for mid-oceanic ridge areas to be explored and developed; Van Dover et al., 2011). Consequently, the CBD lists 7 scientific criteria with which to identify, on a global scale, the so-called Ecologically and Biologically Significant Areas (EBSAs). Other international initiatives associated with the area-based management tools includes a call for the establishment of representative networks of marine protected areas (MPAs) consistent with international law and based on scientific information. The list of relevant resolution of the UN General Assembly (UNGA) includes UNGA 61/105 (2006) and UNGA 64/72 (2009) aimed at establishing the so-called Vulnerable Marine Ecosystems (VMEs) (a concept also applied to the mid-oceanic ridges, notably the Mid-Atlantic Ridge; Van Dover et al., 2012; Dunn et al., 2018).

Of relevance are the current negotiations within the framework of the Intergovernmental Conference on an International Legally Binding Instrument under the UN Convention on the Law of the Sea (UNCLOS) on the Conservation and Sustainable Use of Marine Biological Diversity of Areas Beyond National Jurisdiction (BBNJ) (www.un.org/bbnj/).

The UNCLOS, UNGA resolutions, and the CBD sparked several regional arrangements aimed at implementation of measures for the protection of the marine environment in areas beyond national jurisdiction. Most relevant here is the OSPAR Convention for the Protection of the Marine Environment of the North east Atlantic (www.ospar.org/convention) as well as Regional Fisheries Management Organizations (RFMOs). The latter are obliged to conserve all species associated with and dependent upon the fisheries they seek to regulate (Bell et al., 2019) and acting according to, *inter alia*, the FAO Code of Conduct for Responsible Fisheries (http://www.fao.org/fishery/code/en) and the UN Fish Stocks Agreement (http://www.fao.org/iuu-fishing/international-framework/un-fish-stocks-agreement/en/); some RFMOs have already enacted fisheries closures in areas beyond national jurisdiction (VMEs).

According to UNCLOS, marine seafloor areas beyond the areas of national jurisdictions (termed “the Area”) are regarded as “the common heritage of mankind”; their resources and overall management, including protection and conservation, form the remit of the International Seabed Authority (ISA) as the institution through which States Parties to UNCLOS are to organize and control prospecting, exploration and exploitation of mineral resources in the Area. Such activities may not be carried out without a contract with the ISA in accordance with its rules, regulations and procedures. UNCLOS Article 145 obliges ISA to provide an efficient protection of the marine environment from any harm which may be caused by activities in the Area. In particular, ISA is obliged to take necessary measures with respect to activities in the Area “to ensure effective protection for the marine environment from harmful effects which may arise from such activities. To this end the Authority shall adopt appropriate rules, regulations and procedures for inter alia: (a) the prevention, reduction and control of pollution and other hazards to the marine environment, including the coastline, and of interference with the ecological balance of the marine environment, particular attention being paid to the need for protection from harmful effects of such activities as drilling, dredging, excavation, disposal of waste, construction and operation or maintenance of installations, pipelines and other devices related to such activities; (b) the protection and conservation of the natural resources of the Area and the prevention of damage to the flora and fauna of the marine environment” (UNCLOS, Article 145).

Consequently, the **second level** of the legal system are the regulations issued by the ISA and its organ the Legal and Technical Commission (LTC). Of relevance here are the ISA Regulations on prospecting and exploration for polymetallic sulphides in the Area (adopted 7 May 2010) (www.isa.org.jm). These regulations contain requirements related to environmental protection, including obligations of contractors to collect and report environmental baseline data, carry out environmental monitoring programmes supervised by the ISA (cf. Section 9.2.), and to establish environmental baselines against which impacts from anticipated mining activities can be assessed. The LTC issues recommendations to guide contractors in performing these obligations (the most recent is ISBA/25/LTC/6/Rev.1/Corr.1 of 11 June 2020) and regularly reviews reports and data submitted by the contractors, with the assistance of scientists and other stakeholders. At present, the ISA is in the process of working out regulations on exploitation activities (the so-called Mining Code) such that they would not cause excessive harm to the marine environment (Levin et al., 2016), which is a formidable task given that commercial deep-sea mineral mining has not begun yet.

Based on UNCLOS Part XI and the 1994 Agreement, the ISA has developed detailed rules, regulations and recommendations for the contractors regarding the latter's obligation to carry out the assessment of potential environmental impacts (on the water column and the seafloor, including biodiversity) of exploration for marine minerals in the Area; those regulations (the most recent are contained in ISBA/26/LTC/CRP.12 of 4 March 2020) describe in detail the type of activities which require preparation of the formal Environmental Impact Assessment (EIA; see Section 9.1.) as well as its format and content, and provide recommendations on baseline research, monitoring, and reporting.

In parallel to the work on the Mining Code, the ISA and its stakeholders are involved in developing, for each resource type, a Regional Environmental Management Plan (REMP) to be used by the ISA and its contractors as a tool with which to resolve the sustainable use of the mineral resources with the need to protect and conserve the marine environment, and as way to attain the SDG 14. The first REMP, approved by the ISA Council in 2012 (ISBA/18/C/22), concerned the Clarion-Clipperton Fracture Zone nodule field and established nine Areas of Particular Environmental Interest (APEI) to be excluded from future exploitation (Wedding et al., 2013). At present, work is in progress on developing REMPS for mid-oceanic ridges, including the Mid-Atlantic Ridge (MAR) (e.g., www.isa.org.jm/files/files/documents/paris_meeting_report_for_webposting.pdf).

On the **third level** of the legal system discussed are national regulations governing activities of contractors based in (and/or endorsed by) individual countries. As yet, there are no Polish regulations directly applicable to exploration and exploitation of deep-sea resources which would govern exploration of the Polish contract area on the MAR. Exploration activities to be carried out there are being prepared based on the Programme for

Geological Exploration of the Oceans (PROGEO) adopted in 2017 by the Council of Ministers of the Republic of Poland (Anonymous, 2017).

In addition to the three-level system outlined above, codes of conduct related to environmental protection in the deep sea have been prepared by some of the principal stakeholder groups' (scientists and the mining industry) organisations. The most relevant of these include InterRidge and the International Marine Minerals Society (IMMS). InterRidge is a non-profit international scientific organisation with a mission to drive oceanic ridge research forward in a way that is cost-effective, cooperative and responsible. The InterRidge Statement of Commitment to Responsible Research Practices (http://www.interridge. org/IRStatement) at deep-sea hydrothermal vents affirms the commitment of the InterRidge community to responsible research (Glowka, 2003). The IMMS is a professional non-profit organisation the members of which are interested in marine minerals as resources with which to meet world demand for strategic minerals. The IMMS has drafted a Code for Environmental Management of Marine Mining (http://www.immsoc.org/IMMS_code.htm) which outlines environmental principles for the marine mining industry and operating guidelines that can be used as a basis for environmental management plans (Jones and Morgan, 2003; Verlaan, 2010). More general issues associated with corporate responsibility in the protection of the natural environment have been recently dealt with by Morgera (2020) and may be applicable to entities (contractors) carrying exploration of the deep seafloor, including on mid-oceanic ridges.

References

Anonymous, 2017. Program Rozpoznania Geologicznego Oceanów. *Monitor Polski*, 2, 77.

Bell, J.B., Guijarro-Garcia, E., Kenny, A., 2019. Demersal Fishing in Areas Beyond National Jurisdiction: A Comparative Analysis of Regional Fisheries Management Organisations. *Frontiers in Marine Science*, doi.org/10.3389/fmars.2019.00596

Dunn, D.C., Van Dover, C.L., Etter, R.J., Smith, C.R., Levin, L.A., Morato, T., Colaço, A., Dale, A.C., Gebruk, A.V., Gjerde, K.M., Halpin, P.N., Howell, K.L., Johnson, D., Perez, J.A.A., Ribeiro, M.C., Stuckas, H., Weaver, P., 2018. A strategy for the conservation of biodiversity on mid-ocean ridges from deep-sea mining. *Science Advances*, 4(7), eaar4313.

Glowka, L., 2003. Putting marine scientific research on a sustainable footing at hydrothermal vents. *Marine Policy*, 27, 303-312.

Jaeckel, A., Gjerde, K., Currie, D., 2020. The legal framework for resource management in the deep sea. In: Baker, M., Ramirez-Llodra, E., Tyler, P. (eds), *Natural Capital and Exploitation of the Deep Ocean*. Oxford University Press, 53-69.

Jones, A.T., Morgan, C.L., 2003. Code of practice for ocean mining: An international effort to develop a code for environmental management of marine mining. *Marine Geosciences and Geotechnology*, 21, 105-114.

Levin, L.A., Mengerink, K., Gjerde, K.M., Rowden, A.A., Van Dover, C.L., Clark, M.R., Ramirez-Llodra, A., Currie, B., Smith, C.R., Satoi, K.N., Galloi, N., Sweetman, A.K., Lily, H., Armstrong, C.W., Brider, J., 2016. Defining "serious harm" to the marine environment in the context of deep-seabed mining. *Marine Policy*, 74, 245-259.

McIntyre, O., Mosedale, T., 1997. The Precautionary Principle as a Norm of Customary International Law. *Journal of Environmental Law*, 9, 221-241.

Morgera, E., 2020. *Corporate Environmental Accountability in international Law*. 2nd Edition. Oxford University Press.

Rice, J., Trujillo, V., Jennings, S., Hylland, K., Hagstrom, O., Astudillo, A., Jensen, J.N., 2005. *Guidance on the Application of the Ecosystem Approach to Management of Human Activities in the European Marine Environment*, ICES Cooperative Research Report, No. 273, ICES, Copenhagen.

Van Dover, C.L., Smith, C.R., Ardron, J., Arnaud, S., Beaudoin, Y., Bezaury, J., Boland, G., Billett, D., Carr, M., Cherkashov, G., Cook, A., DeLeo, F., Dunn, D., Fisher, C.R., Godet, L., Gjerde, K., Halpin, P., Levin, L., Lodge, M., Menot, L., Miller, K., Milton, D., Naudts, L., Nugent, C., Pendleton, L., Plouviez, S., Rowden, A., Santos, R., Shank, T., Smith, S., Tao, C., Tawake, A., Thurnherr, A., Treude, T., 2011. *Environmental Management of deep-sea chemosynthetic ecosystems: justification of and considerations for a spatially-based approach*. ISA Technical Study, No. 9. International Seabed Authority, Kingston, Jamaica.

Van Dover, C.L., Smith, C.R., Ardron, J., Dunn, D., Gjerde, K., Levin, L., Smith, S., 2012. Designating networks of chemosynthetic ecosystem reserves in the deep sea. *Marine Policy*, 36, 378-381.

Verlaan, P., 2010. *The International Marine Mineral Society's Code for Environmental Management of Marine Mining.* Offshore Technology Conference. doi: 10.4043/20914-MS.

Wedding, L.M., Friedlander, A.M., Kittinger, J.N., Watling, L., Gaines, S.D., Bennett, M., Hardy, S.M., Smith, C.R., 2013. From principles to practice: a spatial approach to systematic conservation planning in the deep sea. *Proceedings of the Royal Society B*, 280: 20131684.

9. Ecosystem valuation and monitoring

Jan Marcin Węsławski, Teresa Radziejewska and Michał Tomczak

9.1. Valued ecosystem components – risk assessment (Jan Marcin Węsławski, Michał Tomczak)

Environmental Impact Assessment (EIA) is by definition an unbiased expert judgement, presenting possible impacts of the planned activity on the natural world. In such an assessment, environmental experts stand behind the Nature to sound a warning against possible consequences of human intervention. Impacts may affect the structure (presence/absence of species, existence of habitats) and the function (energy flow, food web alteration, seasonality disruption, life cycles) of an ecosystem (cf. According to the definitions of the 2010 Millenium Assessment (https://www.millenniumassessment.org), the system of goods and services provided by each ecosystem is a subject of valuation (cf. Armstrong et al., 2012; Thurber et al., 2014; Folkersen et al., 2018), and EIA shall indicate possible alterations there. Another approach is to define the Valued Ecosystem Components (VEC) and focus on the likely impacts they may be exposed to. Table 9.1. presents an approach integrating both aspects. The three main types of valuation are: 1) socioeconomic valuation, with reference to the market value of ecosystem goods and services; 2) biological valuation, presenting the intrisinc value of a natural ecosystem, without reference to its human use; and 3) socio-cultural valuation that considers the non-market value of a spiritual, educational and emotional character. An important part of the EIA is the initial risk assessment, as some VECs might be very resilient, other – extremely vulnerable; some are able to regenerate or restore, while others are almost unrepairable.

The United Nations Conventions on the Law of the Sea (UNCLOS, 1982) provide guidelines to use and conserve marine resources and to ensure preservation and protection of the marine ecosystems. There is a general understanding and commitment in the environmental discussion that all decisions related to activities in the areas beyond national jurisdictions must include reliable scientific assessment of the marine ecosystem to predict, assess and minimize its potentially harmful effects (UNCLOS, Part XI Article 145). Therefore, the International Seabed Authority (ISA), in order to identify and mitigate the interference of exploration for marine minerals and potential mining on the fragile deep-sea environment, requires submission of the Environmental Impact Assessment (EIA), known also as the Environmental Impact Statement. The main purpose is to assess the influence of sediment plume discharge from sea-bottom activities to the water column and surface sediments, particularly in relation to food chains and changes in the geochemistry of substrate.

Among a variety of technologies used in the exploration of deep-sea minerals, some solutions provide information without the potentially harmful impact on the marine environment and thus do not require an EIA (e.g. MBES surveying, CTD profiling). On the other hand, activities aiming at the sediment depth penetration related to the collection of mineral samples, sediments or rocks, or test mining required an EIA at the exploration stage.

The work plan for the proposed activities can only be approved when following rules, regulations, and procedures set by the ISA (Fig. 9.1). Research and reporting must comply with the “template” developed by the ISA to ensure uniform and consistent high environmental standards. The exploration of the area should be initiated by collecting various information about the current status of the environment (baseline studies), that involve both, the analysis of available information (also paleo-archives), and in-situ studies in the area carried out from the ship and continued with collected material in land-based laboratories.

The requested information concentrates on physical and chemical parameters, as well as biological communities assigned to the water column and sediments which are necessary to address impacts on marine biodiversity. Activities that require EIA during exploration of marine minerals, recommendation on baseline studies, monitoring, and reporting provided and requested by the ISA are summarized as guidance (ISBA/25/LTC/6/Rev.1, 2019).

The defined purpose of marine environment studies and compilation of environmental data is overlaid by potential technological processes involved in deep-sea mining. This allows estimating the potential impact on all components of the ecosystem, including benefits and disadvantages for humankind. Based on a complete overview, the contractor is obliged to develop strategies to prevent, reduce, and compensate for the severity and environmental risks related to the activity. This long and complicated process generates high scientific uncertainty, nevertheless, the effectiveness of these precautions should be measurable. Description of management and mitigation plans, as well as monitoring and reporting activities within EIA, must be summarized by the contractor as an Environmental Management Plan (Fig. 9.1). These steps, which are necessary to provide adequate protection to the marine environment, should involve independent experts and public participation as a part of good practice in the EIA process.

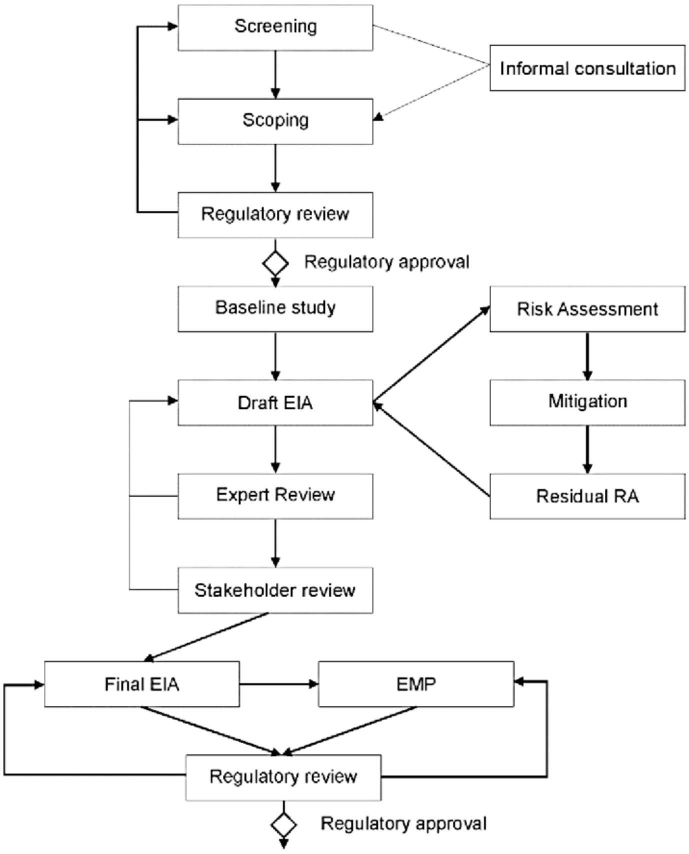

Fig. 9.1. Stages of EIA development. Source: Durden et al., 2018.

Table 9.1. Valued Ecosystem Components (VEC) and ecosystem goods and services associated with the MAR ecosystem

Assessment component	Term	Type of value	Monitoring method	Resilience
VEC 1	Benthic sea scape	Biological and socio-cultural	Remote video recording	extremaly low
VEC 2	Rare and charismatic species	Biological and socio-cultural	Ship-based observations	medium, species-dependent
VEC 3	Potentially commercial species	Socio-economic	Regular sampling and remote hydroacoustic survey	medium, depending on species
VEC 4	Pelagic-benthic coupling (connectivity)	Socio-economic, biological and socio-cultural	Regular sampling	probably high, considering the multitude of its components

The Environmental Impact Assessment (EIA) is a process (Collins et al., 2013; Durden et al., 2018; Clark, 2019) aimed at (i) describing the environment before an activity the impacts of which are to be assessed is commenced; (ii) assessing the effects of that activity (impacts); (iii) indicating follow-up activities and mitigation measures (Clark, 2019). As shown by Clark (2019), the process consists of three basic components, each being a responsibility of a different actor/group of actors. The first component is the overall environmental strategy framework, developed by the regulator (International Seabed Authority, ISA), and including a relevant regional environmental management plan (REMP) (cf. Section 8.). The second component is embedded in the first, and is the remit of a contractor who is required to develop its internal environmental management plans and environmental management system, conduct an EIA and risk assessment (cf. Section 9.1), and carry out the follow-up activities (monitoring and mitigation; cf. Cuvelier et al., 2018). Finally, the third component involves an external assessment (Lalier and Maes, 2016; Durden et al., 2018), to be conducted by state sponsors, stakeholders, and financing institutions.

It is thus evident that the fundamental part of the EIA process is the responsibility of the contractor, required – starting from the exploration phase – to provide a baseline assessment of the environment and to provide an evaluation of possible impacts arising from exploration activities. In fulfilling the obligations associated with the EIA process, the contractor is bound by the regulations, recommendations and guidelines issued by the International Seabed Authority (ISA). These regulations, binding for the contractor, are contained in three documents: ISBA/16/A/12/Rev.1, ISBA/26/LTC/CRP.12, and ISBA/25/LTC/6/Rev.1. The contractor is also mandated to conduct environmental monitoring, both as a way to collect baseline data and as an underpinning of the sound EIA.

References

Agreement relating to the Implementation of Part XI of the United Nations Convention on the Law of the Sea of 10 December 1982, New York; 28 July 1994. In force 28 July 1996. 1836 UNTS 3/ A/RES/48/263, annex.

Armstrong, C.W., Foley, N.S., Tinch, R., van den Hove, S., 2012. Services from the deep: Steps towards valuation of deep sea. *Ecosystem Services*, 2, 2-13.

Boschen, R.E., Rowden, A.A., Clark, M.R., Gardner, J.P.A. 2013. Mining of deep-sea seafloor massive sulfides: A review of the deposits, their benthic communities, impacts from mining, regulatory frameworks and management strategies. *Ocean & Coastal Managemen*t, Volume 84, 2013, Pages 54-67, ISSN 0964-5691, https://doi.org/10.1016/j.ocecoaman.2013.07.005

Clark, M., 2019. The Development of Environmental Impact Assessments for Deep-Sea Mining. In: Sharma, R. (ed.), *Environmental Issues of Deep-Sea Mining*. Springer, 447-470.

Collins, P.C., Croot, P., Carlsson, J., Colaço, A., Grehan, A., Hyeong, K., Kennedy, R., Mohn, C., Smith, S., Yamamoto, H., Rowden, A.A., 2013. A primer for the environmental impact assessment of mining at seafloor massive sulfide deposits. *Marine Policy*, 42, 198-209.

Cuvelier, D., Gollner, S., Jones, D.O.B., Kaiser, S., Arbizu, P.M., Menzel, L., Mestre, N.C., Morato, T., Pham, C., Pradillon, F., Purser, A., Raschka, U., Sarrazin, J., Simon-Lledó, E., Stewart, I.M., Stuckas, H., Sweetman, A.K., Colaço, A ., 2018. Potential Mitigation and Restoration Actions in Ecosystems Impacted by Seabed Mining. *Frontiers in Marine Science*, 5:467. doi: 10.3389/fmars.2018.00467

Durden, J.M., Lallier, L.E., Murphy, K., Jaeckel, A., Gjerde, K., Jones, D.O.B., 2018. Environmental Impact Assessment process for deep-sea mining in 'the Area'. *Marine Policy*, 87, 194-202.

Folkersen, M.V., Fleming, C.M., Hasan, S., 2018. The economic value of the deep sea: A systematic review and meta-analysis. *Marine Policy*, 94, 71-80.

ISBA/16/A/12/Rev.1 Decision of the Assembly of the International Seabed Authority relating to the regulations on prospecting and exploration for polymetallic sulphides in the Area. Kingston, 26 April-7 May 2010.

ISBA/26/LTC/CRP.12. Standard for ISA environmental impact assessment process. Kingston, 4 March 2020.

ISBA/25/LTC/6/Rev.1. Recommendations for the guidance of contractors for the assessment of the possible environmental impacts arising from exploration for marine minerals in the Area. Kingston, 30 March 2020

Jaeckel, A., 2016. Deep seabed mining and adaptive management: The procedural challenges for the International Seabed Authority. *Mar. Policy 70*, 205–211. https://doi.org/10.1016/j.marpol.2016.03.008

Jones, D.O.B., Durden, J.M., Murphy, K., Gjerde, K.M., Gebicka, A., Colaco, A., Morato, T., Cuvelier, D., Billet, D.S.M., 2019. Existing environmental management approaches relevant to deep-sea mining. *Marine Policy*, 103, 172-181.

Kaikkonen, L., Venesjärvi, R., Nygård, H., Kuikka, S., 2018. Assessing the impacts of seabed mineral extraction in the deep sea and coastal marine environments: Current methods and recommendations for environmental risk assessment. *Marine Pollution Bulletin*, Volume 135, Pages 1183-1197, ISSN 0025-326.
https://doi.org/10.1016/j.marpolbul.2018.08.055

Lallier, L.E., Maes, F., 2016. Environmental impact assessment procedure for deep seabed mining in the area: Independent expert review and public participation. *Marine Policy*, 70, 212–219.

Recommendations for the guidance of contractors for the assessment of the possible environmental impacts arising from exploration for marine minerals in the Area, ISBA/19/LTC/8, March 2013, replaced by ISBA/25/C/19, March 2019.

Recommendations for the guidance of contractors for the assessment of the possible environmental impacts arising from exploration for marine minerals in the Area, ISBA/25/LTC/6/Rev.1, March 2020.

Thurber, A.R., Sweetman, A.K., Narayanaswamy, B.E., Jones, D.O.B., Ingels, J., Hansman, R.L., 2014. Ecosystem function and services provided by the deep sea. *Biogeosciences*, 11, 3941–3963, 2014.

United Nations Convention on the Law of the Sea, Montego Bay; 10 December 1982. In force 16 November 1994, 1833 UNTS 3.

9.2. Monitoring: Benthos (Teresa Radziejewska)

In the classical sense, monitoring is “a programme of recurring, systematic studies that reveal the state of the environment. The specific aspects of the environment to be studied are determined by environmental objectives and environmental legislation” (https: //ec.europa.eu/jrc/en/research-topic/environmental-monitoring). The goals of those observations of and studies on the object(s) being monitored are three-fold: (i) to follow changes in the object(s) monitored to provide information on their current status; (ii) given certain environmental objectives being set, to assess the progress made to achieve those objectives; and (iii) to help to detect new environmental issues. As it is evident from the above, the stress is on recurrence (in temporal and spatial scale) and systematicity (in terms of methods applied) of monitoring activities.

The monitoring of deep-sea areas, including those earmarked for exploration and future resource development (i.e., deep-sea mining), as carried out to date has not met any of those criteria. Instead, monitoring activities undertaken (and reported) by contractors so far involve collection of baseline data, extremely needed, but obtained in a rather haphazard manner in terms of temporal and spatial resolution. This is, however, understandable in view of the vastness of the area(s) to be surveyed as well as the financial and temporal constraints. Nevertheless, monitoring – whether at the exploration or exploitation stage – is a prerequisite of acquiring a reliable data sets on which to base reliable environmental impact assessments (Jones et al., 2019), including cumulative impacts (Le Bris and Levin, 2020), and to disentangle natural variability from changes introduced by anthropogenic intervention.

This conviction is reflected in the International Seabed Authority (ISA) document ISBA/16/A/12/rev. 1 (“Contractors, sponsoring States and other interested States or entities shall cooperate with the Authority in the establishment and implementation of programmes for monitoring and evaluating the impacts of deep seabed mining on the marine environment.”) as well as in the most recent ISA documents ISBA/26/LTC/CRP.12 and ISBA/25/LTC/6/Rev.1.

Since key impacts from the development of deep seafloor resources (including polymetallic sulphides) are expected to be incurred by the benthic communities (e.g., Van Dover, 2014; Gollner et al., 2017; Danovaro et al., 2020), which is also reflected in the ISA document ISBA/25/LTC/6/Rev.1 (“On the basis of current proposed methodologies, the main impacts are expected to occur at the sea floor”), it is obvious that those communities should be monitored in the first place. This is reflected in recommendations for contractors regarding the assessment of environmental impacts of exploration (ISBA/25/LTC/6/Rev.1) which list the following information specific to polymetallic sulphide exploration required from contractors:

“(a) Any modification of fluid discharge in hydrothermal settings and associated fauna (using photo documentation, temperature measurements and other metrics, as appropriate) …;

(b) For active sulphide deposits, temperature-fauna relationships … (e.g. 5 to 10 discrete, video-documented temperature measures within each subhabitat);

(c) The distribution, abundance, species structure and diversity of the dominant taxa in each subhabitat (active, inactive vent areas, non-vent habitats) …. This includes the assessment of specialist localized chemosynthetic communities relative to potential mining locations; (d) Meiofaunal and microbial community structure and biomass associated with the polymetallic sulphide deposits ... A statistically defensible number of samples should be taken from polymetallic sulphides, where possible. Species that live on the rock or in crevices and pits in the deposit should be identified, where possible; (e) Biological samples from active hydrothermal vent systems should only be collected using precision sampling by remotely operated vehicle/submersible technology according to subhabitat”.

In addition, according to the documents mentioned, the contractors will be required to establish an environmental baseline against which the natural variability, including that imposed by climate change (cf. Le Bris and Levin, 2020), and impacts produced by mining will be assessed. The contractors will be also obliged to monitor and evaluate mining impacts on the marine environment by surveying the distribution and composition of faunal communities. The contractors will have to classify hydrothermal vent areas according to whether they are active vent sites or inactive/extinct sites (cf. Van Dover, 2019). From the biological standpoint, the baseline assessment should determine whether the proposed mining site supports active hydrothermal vents, inactive vents that may restart owing to mining activity, or extinct vents that will remain hydrothermally inactive even when disturbed by test-mining.

Monitoring of the benthos in the exploration/exploitation area should identify communities and their ecosystem functions, including their natural spatial and temporal variability (cf. Section 7.3.), so as to evaluate potential effects of the activities on the benthic fauna. The benthic communities should be characterised in all the subhabitats that may be impacted; such surveys are also important for establishing preservation and impact reference zones necessary for environmental management of the seafloor areas by the ISA (Jones et al., 2019).

The sampling design applied in monitoring surveys should be well thought-out and robust, including stratified random sampling approaches, if variation of ecological conditions or habitats is known or expected. With respect to the macro- and meiobenthos, analyses should be appropriate and detailed enough to be able to establish a species accumulation curve (from which to estimate the number of samples required to result in an adequate assessment of taxonomic richness) (ISBA/25/LTC/6/Rev.1).

The benthic categories the contractors will be required to monitor include the megafauna, macrofauna, meiobenthos, microeukaryotes (Foraminifera) as well as microorganisms (bacteria, archaea, fungi, viruses, microeukaryotes). In addition, environmental DNA (eDNA) will need to be analysed. Whenever possible, colour photographic documentation of organisms should be prepared (ISBA/25/LTC/6/Rev.1).

Prior to test mining or testing of mining components, spatial variation in the composition of the biological community and levels of connectivity must be evaluated, as it is important – for the future impact assessments – to know the degree of isolation of populations occupying the mineral deposits that are to be removed and to infer whether a given population serves as a critical brood stock for other populations (cf. Gollner et al., 2017). Sampling should occur at three mineral deposit sites as well as at background communities in the contract area. In some cases (particularly with respect to the megafauna), video documentation and photographic transects may be the only way to develop a species-abundance matrix (ISBA/25/LTC/6/Rev.1).

For monitoring of the benthos, it is also important to have knowledge on bioturbation (i.e., the mixing of sediment by benthic organisms) as a way to monitor the rates of sedimentary processes as well as to model and evaluate effects of mining activities on such processes. Bioturbation rates and depth will have to be measured (preferably by establishing excess Pb^{210} profiles in sediment cores), taking into account the variability in the sediment (ISBA/25/LTC/6/Rev.1).

References

Danovaro, R., Fanelli, E., Aguzzi, J., Billet, D., Carugati, L., Corinaldesi, C., Dell'Anno, A., Gjerde, K., Jamieson, A.J., Kark, S., McClain, C., Levin, L., Levin, N., Ramirez-Llodra, E., Ruhl, H., Smith, C.R., Snelgrove, P.V.R., Thomsen, L., Van Dover, C.L., Yasuhara, M., 2020. Ecological variables for developing a global deep-ocean monitoring and conservation strategy. *Nature Ecology & Evolution*, 4, 181-192.

Gollner, S., Kaiser, S., Menzel, L., Jones, D.O.B., Brown, A., Mestre, N., van Oevelen, D., Menot, L., Colaço, A., Canals, M., Cuvelier, D., Durden, J.N., Gebruk, A., Egho, G.A., Haeckel, M., Marcon, Y., Mevenkamp, L., Morato, T., Pham, C.K., Purser, A., Sanchez-Vidal, A., Vanreusel, A., Vink, A., Martinez Arbizu, P., 2017. Resilience of benthic deep-sea fauna to mining activities. *Marine Environmental Research*, 129, 76-101.

ISBA/16/A/12/Rev.1 Decision of the Assembly of the International Seabed Authority relating to the regulations on prospecting and exploration for polymetallic sulphides in the Area. Kingston, 26 April-7 May 2010.

ISBA/26/LTC/CRP.12. Standard for ISA environmental impact assessment process. Kingston, 4 March 2020.

ISBA/25/LTC/6/Rev.1. Recommendations for the guidance of contractors for the assessment of the possible environmental impacts arising from exploration for marine minerals in the Area. Kingston, 30 March 2020

Jones, D.O.B., Durden, J.M., Murphy, K., Gjerde, K.M., Gebicka, A., Colaço, A., Morato, T., Cuvelier, D., Billett, D.S.M., 2019. Existing environmental management approaches relevant to deep-sea mining. *Marine Policy*, 103, 172-181.

Le Bris, N., Levin, L.A., 2020. Climate change cumulative impacts on deep-sea ecosystems. In: Baker, M., Ramirez-Llodra, E., Tyler, P. (eds), *Natural Capital and Exploitation of the Deep Ocean*. Oxford University Press, 161-182.

Van Dover, C.L., 2014. Impacts of anthropogenic disturbances at deep-sea hydrothermal vent ecosystems: A review. *Marine Environmental Research*, 102, 59-72.

Van Dover, C.L., 2019. Inactive Sulfide Ecosystems in the Deep Sea: A Review. *Frontiers in Marine Science*, 6: 461.

10. Deep sea research methods to be used during the exploration of the Mid-Atlantic Ridge polymetallic sulphide areas

Teresa Radziejewska, Jan Marcin Węsławski, Sławomir Sagan, Michał Tomczak and Łukasz Smajdor

10.1. Water column ecosystem, imagery (Jan Marcin Węsławski)

Deep sea research and monitoring belong to the most expensive and technically challenging marine operations. The modern approach focuses on applying non-invasive and non-destructive methods, so all types of imagery and recording are in use, from microscopic *in situ* photography of the water column to detect marine snow and the microplankton, to acoustics, both passive (listening to sounds of marine organisms) and active (recognition of objects and structures in the water column and on the seabed). Some destructive sampling is unavoidable (plankton, fish, small nekton), the appropriate gear being listed in Table 10.1.

The seabirds and marine mammal censuses involve both direct sightings and counting from the ship (the Tasker method) and passive acoustic buoys recording vocalization of marine mammals.

Although the imagery is a key technique for the benthic biota – from small scale photoframes (cm^2) to larger seascape views (m^2) (see Section 10.3.), it has also been used to survey pelagic communities. For example, Vereshchaka and Vinogradov (1999) as well as Vinogradov et al. (2003), while working from a manned submersible (= human operated vehicle, HOV) combined direct observations, underwater photography, and plankton net hauls to sample zooplankton in a number of hydrothermal fields on the MAR (including Broken Spur and Lost City in the Polish contract area).

Description of various gear used in deep-sea exploration, in various compartments of the oceanic realm, can be found in a monograph edited by Clark et al. (2016) and in references therein (indicated also in Table 10.1.). In addition, a good review of the state-of-the-art equipment for deep sea pelagic sampling is provided by the web page describing the gear prepared for a new UK research vessel RV Sir Richard Attenborough (https://www.bas.ac.uk/polar-operations/sites-and-facilities/facility/rrs-sir-david-attenborough/science-facilities/net-trawl-sledge-systems/).

Table 10.1. Types of gear recommended for the deep sea exploration (see Section 10.4. for geological survey equipment)

Observed element	Main tools	Remarks	Reference
CTD profiles	CTD system with rosette water cast	Variety of standard gear	White et al. (2016)
Optical parameters in the epipelagial and at depth	Optical sensors	Mounted on ROV, AUV and landers	Cave and German (1998)
Plankton	Plankton nets, including multinet; direct visual observations from HOV and ROV		Christiansen (2016)
Mesopelagic fish and small nekton	RMT trawl; multinet	Shrimp pelagic trawl can also be used; Multinet designs include MOCNESS and Kiel	Clark et al. (2016); Christiansen (2016)
Sedimentation	Sediment traps deployed for various periods of time	Standard gear	White et al. (2016)

Observed element	Main tools	Remarks	Reference
Carnivorous and carrion feeding mobile fauna	Baited traps	Variety of non- standarised traps, size-dependant	Jamieson (2016)
Encrusting and sessile fauna	Photo documentation by ROV operator arms	Restricted destructive sampling	Carroll et al. (2018); Bowden and Jones (2016)
Soft-sediment fauna	Push-corer; multiple corer (multi-corer, MUC); mega-corer; box-corer	Push-corers are operated from ROV or HOV; box corers of different design, e.g., USNEL MkII box corer	Barnett et al. (1984) Bell et al. (2016) Narayanaswamy et al. (2016)
Geochemical processes	Lander with chemical probes	*Ad hoc* constructions and configuration	Jamieson (2016)

References

Barnett, P.R.O., Watson, J., Conelly, D., 1984. A multiple corer for taking virtually undisturbed samples from shelf, bathyal and abyssal sediments; *Oceanologica Acta*, 7, 399-408.

Carroll, A., Althaus F, Beaman R, Friedman A, Ierodiaconou D, Ingleton T, Jordan A, Linklater M, Monk J, Post A, Przeslawski R, Smith J, Stowar M, Tran M, Tyndall A. 2018. Marine sampling field manual for towed underwater camera systems. In: Przeslawski, R., Foster, S. (eds), *Field Manuals for Marine Sampling to Monitor Australian Waters*. National Environmental Science Programme (NESP), 131-152.

Christiansen, B., 2016. Deep-Sea Zooplankton Sampling. In: Clark, M., Consalvey, M., Rowden, A.A. (eds), 2016. *Biological Sampling in the Deep Sea*, Wiley Blackwell, Chichester, 103-125.

Clark, M., Bagley, N., Harley, B., 2016. Trawls. In: Clark, M., Consalvey, M., Rowden, A.A. (eds), 2016. *Biological Sampling in the Deep Sea*. Wiley Blackwell, Chichester, 126-158.

Clark, M., Consalvey, M., Rowden, A.A. (eds), 2016. *Biological Sampling in the Deep Sea*. Wiley Blackwell, Chichester.

Bowden, D., Jones, D., 2016. Towed Cameras. In: Clark, M., Consalvey, M., Rowden, A.A. (eds), 2016. *Biological Sampling in the Deep Sea*. Wiley Blackwell, Chichester, 260-284.

Jamieson, A. (2016). Landers: Baited Cameras and Traps. In: Clark, M., Consalvey, M., Rowden, A.A. (eds), 2016. *Biological Sampling in the Deep Sea*. Wiley Blackwell, Chichester, 228-259.

Narayanaswamy, B., Bett, B., Lamont, P., Rowden, A., Bell, E., Menot, L., 2016. Corers and Grabs. In: Clark, M., Consalvey, M., Rowden, A.A. (eds), 2016. *Biological Sampling in the Deep Sea*. Wiley Blackwell, Chichester, 207-259.

Vereshchaka, A.L., Vinogradov, G.M., 1999. Visual observations of the vertical distribution of plankton throughout the water column above Broken Spur vent field, Mid-Atlantic Ridge. *Deep-Sea Research Part I*, 46, 1615-1632.

Vinogradov, G.M., Vereshchaka, A.L., Aleinik, D.L., 2003. Zooplankton Distribution over Hydrothermal Fields of the Mid-Atlantic Ridge. *Oceanology*, 43, 696-709.

White, M., Mohn, C., Kiriakoulakis, K., 2016. Environmental Sampling. In: Clark, M., Consalvey, M., Rowden, A.A. (eds), 2016. *Biological Sampling in the Deep Sea*. Wiley Blackwell, Chichester, 57-79.

10.2. Optical properties (Sławomir Sagan)

The state of the epipelagial of the geographically remote areas can be successfully monitored remotely down to hundreds of meters with a swath of sensors designed for observations of various phenomena and processes. Features such as productivity, chlorophyll and particle content as well as dissolved organic matter can be assessedd with already fully developed and robust algorithms where the water constituencies are parameterised by a validated and calibrated combination of water-leaving radiances of carefully chosen light wavelengths in the visible part of the spectrum (Blondeau-Patissier et al., 2014; Vandermeulen et al., 2020). Other remote sensing methods allow to observe surface currents, waves, wind speed, water mass movements as well as the deep seafloor topography (Sandwell et al., 2014) .

In a deep sea, the near-bottom water optical properties are predominantly determined by the particles. As particles reduce the water transparency, making it turbid, the phenomena is commonly observed with turbidity meters, which basically measure the intensity of light scattered at 90 deg, calibrated in Nephelometric Turbidity Unit (NTU) or Formazin Nephelometric Units (FTU) (Thurnherr et al., 2008).

Possible sources of particles flow are the abyssal currents (Lahaye et al., 2019), sedimentation processes or the open-ocean convection which may produce a resuspension particle flow of thickness of meters above the seafloor (Madron et al., 2017), in the areas affected. In the contract area of MAR, the flow of particles may be released from hydrothermal vents. Hydrothermal vents produce buoyant plumes spreading with the currents, which can be detected at a distance by observing hydro-physical properties of the water. While monitoring the hydrothermal flow, the deployment of optical sensors together with acoustic and the CTD is of advantage, as the particulate enrichment may extend much further, on the order of several kilometers, than temperature anomalies. Presence of turbidity anomalies were documented on long distances from the vent at maximum level of 0.10 ΔNTU (Cave and German, 1998; Tao et al., 2017). Additionally, enhanced light scattering by particles might be easily connected with acoustically detected bottom features (Cave and German, 1998). In most of the observations, the plume core have been retaining its initial depth (Figure 10.1).

Monitoring of the deep-sea bottom requires demanding and robust techniques and platforms, such as remotely operated vehicles (ROVs), autonomous underwater vehicles (AUVs) or bottom landers with optical or acoustic telemetry. It has to be noted that permanent or long-term installations, either floating or located on the seafloor, might be subject to macrofouling, despite the apparent absence of the living material at large depths (Blanco et al., 2013).

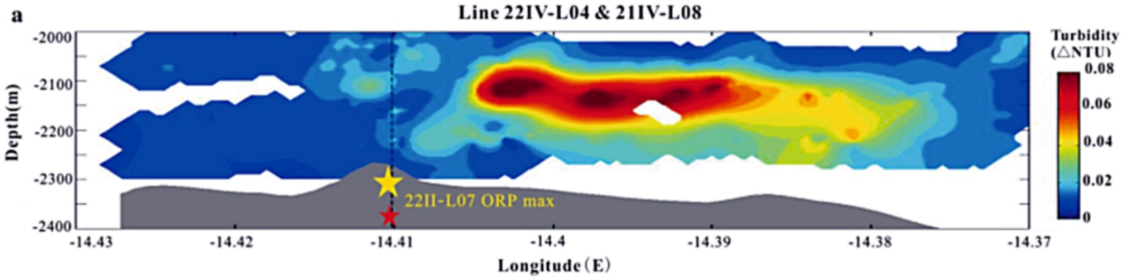

Fig. 10.1. Transects of turbidity from survey lines spanning 2009 to 2011. 21IV-L04/21IV-L08. Red stars show the vent location, (Tao et al., 2017).

References

Blanco, R., Shields, M.A., Jamieson, A.J., 2013. Macrofouling of deep-sea instrumentation after three years at 3690 m depth in the Charlie Gibbs fracture zone, mid-Atlantic ridge, with emphasis on hydroids (Cnidaria: Hydrozoa). *Deep Sea Research Part II Topical Studies in Oceanography*, 98, 370-373. doi.org/10.1016/j.dsr2.2013.01.019.

Blondeau-Patissier, D., Gower, J.F.R., Dekker, A.G., Phinn, S.R., Brando, V.E., 2014. A review of ocean color remote sensing methods and statistical techniques for the detection, mapping and analysis of phytoplankton blooms in coastal and open oceans. *Progress in Oceanography*, 123, 123-144. doi.org/10.1016/j.pocean.2013.12.008.

Cave, R.R., German, C.R., 1998. Hydrothermal plume detection in the deep ocean-A combination of technologies. *Underwater Technology*, 23, 71–75. doi.org/10.3723/175605498783258921.

Lahaye, N., Gula, J., Thurnherr, A.M., Reverdin, G., Bouruet-Aubertot, P., Roullet, G., 2019. Deep currents in the rift valley of the north mid-atlantic ridge. *Frontiers in Marine Science*, 6. doi.org/10.3389/fmars.2019.00597.

Madron, X.D.D., Ramondenc, S., Berline, L., Houpert, L., Bosse, A., Martini, S., Guidi, L., Conan, P., Curtil, C., Delsaut, N., Kunesch, S., Ghiglione, J., Marsaleix, P., Pujo-Pay, M., Séverin, T., Testor, P., Tamburini, C., 2017. Deep sediment resuspension and thick nepheloid layer generation by open-ocean convection. *Journal of Geophysical Research Oceans*, 122, 2291-2318. doi.org/10.1002/2016JC012062.

Sandwell, D.T., Müller, R.D., Smith, W.H.F., Garcia, E., Francis, R., 2014. New global marine gravity model from CryoSat-2 and Jason-1 reveals buried tectonic structure. *Science*, 346, 65-67. doi.org/10.1126/science.1258213.

Tao, C., Chen, S., Baker, E.T., Li, H., Liang, J., Liao, S., Chen, Y.J., Deng, X., Zhang, G., Gu, C., Wu, J., 2017. Hydrothermal plume mapping as a prospecting tool for seafloor sulfide deposits: a case study at the Zouyu-1 and Zouyu-2 hydrothermal fields in the southern Mid-Atlantic Ridge. *Marine Geophysical Research*, 38, 3-16. doi.org/10.1007/s11001-016-9275-2.

Thurnherr, A.M., Reverdin, G., Bouruet-Aubertot, P., St. Laurent, L.C., Vangriesheim, A., Ballu, V., 2008. Hydrography and flow in the Lucky Strike segment of the Mid-Atlantic Ridge. Journal of Marine Research 66, 347–372. https://doi.org/10.1357/002224008786176034.

Vandermeulen, R.A., Mannino, A., Craig, S.E., Werdell, P.J., 2020. 150 shades of green: Using the full spectrum of remote sensing reflectance to elucidate color shifts in the ocean. *Remote Sensing of Environment*, 247, 111900. doi.org/10.1016/j.rse.2020.111900.

10.3. Benthos (Teresa Radziejewska)

10.3.1. Sampling

The choice of methods, including sampling gear, to be used for benthic community surveys during the exploration of the Polish contract area on the Mid-Atlantic Ridge (MAR) should primarily follow recommendations of the regulatory body [International Seabed Authority's Legal and Technical Commission (LTC)]; these are contained in the document ISBA/25/LTC/6/Rev.1 (ISBA, 2020). In addition, standard practices of deep-sea biological surveys should be adhered to; these have been summarised, for different compartments of the deep-sea realm, in a collection of papers contained in a volume edited by Clark et al. (2016).

The methods and gear will differ depending on the habitat to be surveyed (rocks, soft sediments) and on the actual benthos category to be studied (mega-, macro-, meio- and microbenthos).

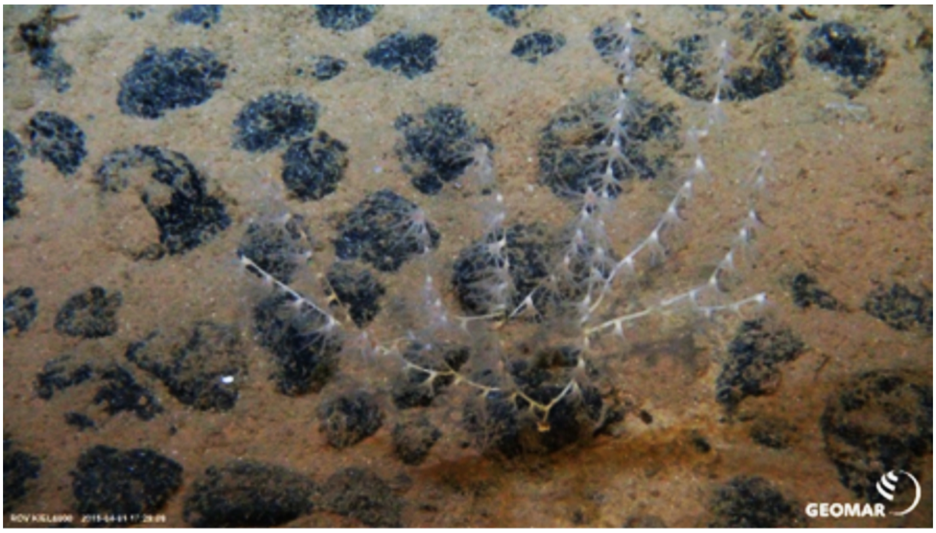

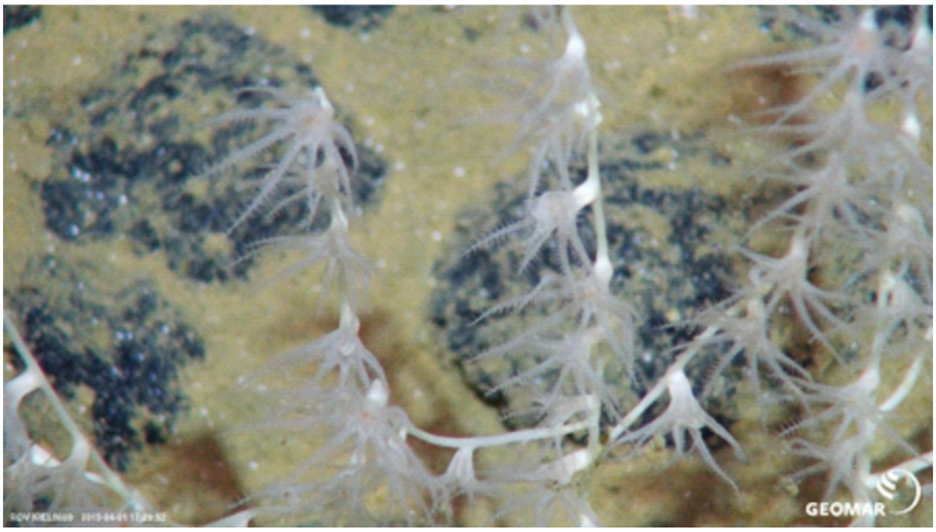

Fig. 10.2. Illustration of the level of morphological detail achievable with recent ROV-borne photo imagery; a hydroid attached to a polymetallic nodule in the Clarion-Clipperton Zone (Pacific); Cruise SO 239, RV Sonne (Photo credit: GEOMAR, Kiel).

Data on the abundance, biomass, species structure and diversity of the **megafauna** are preferably collected with underwater video and photography (with a scale visible, e.g., lasers a set distance apart), taken with towed cameras (Bowden and Jones, 2016), preferably operated by a remotely operated vehicle (ROV) (Kelley et al., 2016). Recently, substantial technological advances have been made with respect to the image resolution, particularly when the images (still and video) are recorded from ROVs with real-time shipboard control, which makes it possible to zoom in on the required details, even those of individual organisms (cf. photos in Fig. 10.2.). Advances have also been made in the annotation software (Gomes-Pereira, 2016), whereby organisms observed and photographed can be identified in real time, with the assistance of and reference to both taxonomic expertise and on-line image repositories. Landers with time-lapse cameras (Jamieson, 2016), deployed for periods of up to several months, have been used to document temporal changes in seafloor communities. However, they have been relatively more popular in abyssal plains than at hydrothermal fields.

It is important that photographs have sufficient resolution to identify organisms larger than 2 cm in the smallest dimension. The seafloor area photographed should be at least 2 m. It is also important that the images are georeferenced. Species identification should be confirmed by collecting specimens at the site, e.g., by using slurp guns (suction samplers) operated from an ROV (Copley et al., 2016). Dredges, epibenthic sleds and bottom trawls are not recommended for use in polymetallic sulphide (PMS) areas (ISBA, 2020).

The deep-sea **macrobenthos** (defined as proto- and metazoans retained on the 300 μm sieve mesh size) is usually sampled, from the soft-sediment seafloor, with a box corer,

such as the USNEL MkII box-corer (Narayanaswamy et al., 2016). Other corers can be deployed, such as a Bowers and Connelly dampened megacorer (Gage and Bett, 2005) used by

Bell et al. (2016) to sample the macrofauna from edifices on sedimented hydrothermal vent sites at the Bransfield Strait (Antarctica). Alternatively, push-corers of an appropriate diameter, operated by an ROV (Kelley et al., 2016) should be retrieved from soft-sediment areas. Sampling the macrofauna (and also the meiobenthos) associated with megafaunal assemblages on PMS hard (rock) surfaces is challenging, and has rarely been accomplished, although highly desirable (S. Gollner, pers. comm.), also in view of LTC recommendations for obtaining data from different sub-habitats (ISBA, 2020). For such purposes, Gollner et al. (2006) used a quantitative 'pot' sampler (Van Dover, 2002; Fig. 10.3.) and a 'Bushmaster Jr.' device (Govenar et al., 2005) operated from a human-operated vehicle (HOV). The Bushmaster Jr. is lined with a 63 μm Nitex mesh and can sample areas up to 60 cm in diameter (0.28 m^2).

The abundance, biomass and taxonomic structure of the protozoan (foraminiferal) and metazoan **meiofauna** (organisms retained on the 32 μm sieve mesh size) should be determined from quantitative samples. These are usually collected with a multiple corer (multi-corer, MUC) such as an SMBA MUC (Barnett et al., 1984; Narayanaswamy et al., 2016). Recent meiofauna studies on MAR (Spedicato et al., 2020), however, involved push-corers (5.5 cm diameter) operated from an ROV (Fig. 10.4), and these seem to be a sampling gear of choice, also on account of providing sediment samples for the study of microbiota (see below). After retrieval, the cores, regardless of their type, should be sliced into 1-cm thick layers down to 5 cm (ISBA, 2020). As pointed out above, of interest in the PMS setting would be to collect meiofauna associated with the megafauna assemblages on hard substrates. For such purposes, the sampling gear – mentioned above – applied by Gollner et al. (2006), but requiring the use of an HOV rather than an ROV, can be applicable.

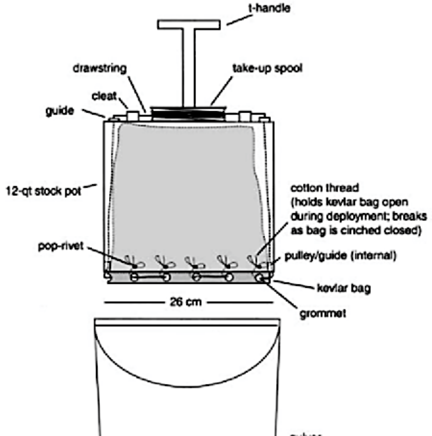

Fig. 10.3. A quantitative mussel 'pot' sampler for sampling macro- and meiofauna from hard substrates and mussel beds at hydrothermal vents (using HOV). With the bottom of the bag held open by cotton threads and flush with the metal rim of the stock pot (11.35 l), the sampler is manipulated down over a clump of mussels. Once the bottom of the pot rests against basalt, the t0handle is rotated, causing the drawtring to be taken up onto the spool and cinching up the bag beneath the mussel clump. Once the sample is collected, the pot fits a plastic bucked attached to the work basket of the submersible (source: Van Dover, 2002).

Fig. 10.4. Push-core sampling (from ROV Jason 2) of sulphide sediment at TAG hydrothermal field on MAR (source: Flint, 2007)

The **microbial** community, important for studying the ecosystem functioning, should be sampled – from soft sediments – using any corer (a MUC, a push-corer on an ROV). Usually, cores obtained with a MUC or a push-corer are subsampled (e.g., with a small-diameter plastic syringe) and sliced to obtain data from vertical intervals 1-cm thick (ISBA, 2020).

10.3.2. Fixation and preservation of benthos samples

As stated by LTC recommendations (ISBA, 2020), "standard practices for the fixation and preservation of organisms should be followed, while noting that formaldehyde/formalin fixation is not appropriate for all taxa". Depending on a taxon and study objective, multiple preservation methods may be necessary, including freezing or preservation in molecular grade ethanol for molecular studies; preservation in ethanol or formaldehyde for morphological taxonomic studies; or the immediate freezing of whole animals and/or selected tissues for stable isotope, trace metal and biochemical analyses (Schiaparelli et al., 2016). In the latter context, Rhiel et al. (2014) described methods of tissue sample collection for DNA studies on deep-sea crustaceans they had successfully applied in their studies.

References

Barnett, P.R.O., Watson, J., Conelly, D., 1984. A multiple corer for taking virtually undisturbed samples from shelf, bathyal and abyssal sediments. *Oceanologica Acta*, 7, 399-408.

Bell, J.B., Woulds, C., Brown, L.E., Sweeting, C.J., Reid, W.D.K., Little, C.T.S., Glover, A.G., 2016. Macrofaunal Ecology of Sedimented Hydrothermal Vents in the Bransfield Strait, Antarctica. *Frontiers in Marine Science*, doi.org/10.3389/fmars.2016.00032

Bowden, D., Jones, D., 2016. Towed Cameras. In: Clark, M.R., Consalvey, M., Rowden, A.A. (eds), *Biological sampling in the Deep Sea*. Wiley Blackwell, Chichester, 260-284.

Clark, M.R., Consalvey, M., Rowden, A.A., 2016. *Biological sampling in the Deep Sea*. Wiley Blackwell, Chichester.

Copley, J.T., Marsh, L., Glover, A.G., Hühnerbach, V., Nye, V.E., Reid, W.D.K., Sweeting, C.J., Wigham, B.D., Wiklund, H., 2016. Ecology and biogeography of megafauna and macrofauna at the first knosn deep-sea hydrothermal vents on the ultraslow-spreading Southwest Indian Ridge. *Scientific Reports*, 6, 39158.

Flint, H.C., 2007. *Diversity of meiofauna at deep-sea hydrothermal vents and cold seeps with particular reference to nematodes*. Ph.D. Thesis, National Oceanography Centre, Southampton, U.K.

Gage, J. D., Bett, B. J., 2005. Deep-sea benthic sampling. In: Holmes, N.A., McIntyre, A.D. (eds), *Methods for the Study of the Marine Benthos*, 3rd edition, Blackwell Scientific Publications, Oxford,
doi: 10.1002/9781118542392

Gollner, S., Zekely, J., Van Dover, C.L., Govenar, B., Le Bris, N., Nemeschka, H.L., Bright, M., 2006. Benthic copepod communities associated with tubeworm and mussel aggregations on the East Pacific Rise. *Cahiers de Biologie Marine*, 47, 397-402.

Gomes-Pereira, J.N., Auger, V., Beisiegel, K., Benjamin, R., Bergmann, M., Bowden, D., Buhl-Mortensen, P., De Leo, F.C., Dionísio, G., Durden, J.M., Edwards, L., Friedman, A., Greinert, J., Jacobsen-Stout, N., Lerner, S., Leslie, M., Nattkemper, T.W., Sameoto, J.A., Schoening, T., Schouten, R., Seager, J., Singh, H., Soubigou, O., Tojeira, I., van den Beld, I., Dias, F., Tempera, F., Santos, R.S., 2016. Current and future trends in marine image annotation software. *Progress in Oceanography*, 149, 106-120.

Govenar, B., Le Bris, N., Gollner, S., Glanville, J., Aperghis, A., Hourdez, S., Fisher, C.R., 2005. Epifaunal community structure associated with *Riftia pachyptila* aggregations in chemically different hydrothermal vent habitats. *Marine Ecology Progress Series*, 305, 67-77.

ISBA, 2020. Recommendations for the guidance of contractors for the assessment of the possible environmental impacts arising from exploration for marine minerals in the Area Issued by the Legal and Technical Commission. ISBA/25/LTC/6/Rev.1

Jamieson, A., 2016. Landers: Baited Cameras and Traps. In: Clark, M., Consalvey, M., Rowden, A.A. (eds), *Biological Sampling in the Deep Sea*. Wiley Blackwell, Chichester, 228-159.

Kelley, C., Kerby, T., Sarradin, P.-M., Sarrazin, J., Lindsay, D.J., 2016. Submersibles and Remotely Operated Vehicles. In: Clark, M.R., Consalvey, M., Rowden, A.A. (eds), *Biological sampling in the Deep Sea*. Wiley Blackwell, Chichester, 285-305.

Narayanaswamy, B.E., Bett, B.J., Lamont, P.A., Rowden, A.A., Bell, E.M., Menot, L., 2016. Corers and Grabs. In: Clark, M.R., Consalvey, M., Rowden, A.A. (eds), *Biological sampling in the Deep Sea.* Wiley Blackwell, Chichester, 207-227.

Rhiel, T., Brenke, N., Brix, S., Driskell, A., Kaiser, S., Brandt, A., 2014. Field and laboratory methods for DNA studies on deep-sea isopod crustaceans. Polish Polar Research, 35, 203-224. doi: 10.2478/popore-2014-0018

Schiaparelli, S., Schnabel, K., Richer de Forges, B., Chan, T.-Y., 2016. Sorting, Recording, Preservation and Storage of Biological Samples. In: Clark, M., Consalvey, M., Rowden, A.A. (eds), *Biological Sampling in the Deep Sea*. Wiley Blackwell, Chichester, 338-367.

Spedicato, A., Sánchez, N., Pastor, L., Menot, L., Zeppilli, D., 2020.. Meiofauna Community in Soft Sediments at TAG and Snake Pit Hydrothermal Vent Fields. *Frontiers in Marine Science*, 7, 200. doi.org/10.3389/fmars.2020.00200

Van Dover, C.L., 2002. Community structure of mussel beds at deep-sea hydrothermal vents. *Marine Ecology Progress Series*, 230, 137-158.

10.4. **Geological structures** (Łukasz Smajdor, Michał Tomczak)

Conventional marine-geological surveys involve ground-truthing methods which provide geological samples as well as physical evidence of seabed structure, usually at a local scale. Seafloor sediments can be sampled with a number of tools and the samples collected are used for geophysical and geochemical parameters useful in deciphering the driving forces undelying sediment formation and post-depositional processes affecting sediment properties. The spatial resolution of such samples is usually fairly low, and sampling operations are complex, costly, and time-consuming. Therefore, these methods are appropriate for identification or characterisation of small-scale structures.

However, regional assessments need a more general picture of the sediment structure. Decreasing the sampling density can deliver information about larger area, but the final results are based on interpolation between the sampling points, which carries some level of uncertainty. Such sampling approach is frequently applied following a regional reconnaissance achieved by a continued acquisition of geophysical data, i.e., the bathymetric survey achieved with a Multibeam Echo Sounder System (MBES) (e.g., Machida et al., 2019). In some cases, the actual sediment samples and their properties may provide information necessary for the proper calibration of certain geophysical methods.

The most important geophysical methods used for structural geology interpretation are those related to the acoustic wave propagation (MBES, SBP, seismic) and density measurements (gravimeter). The level of detail obtained with these methods is directly related to the survey design.

The surveys are carried out on different spatial scales: regional, semi-detailed, and detailed. The methods and the equipment used will depend on the level of detail required, which in turn will be achieved depending on the distance to the seafloor (altitude) the survey operation is being carried out.

Regional surveys provide information on large areas (on the order of $10^2 – 10^3$ km) and involve the use of equipment necessary for ship-borne bathymetry (MBES), bottom (ship-borne side-scan sonar, SSS), sub-bottom profiling (SBP), and ship-borne side-scan sonar (SSS) as well as the equipment with which to carry out seismic wave (reflection from boundaries having different acoustic impedance, appropriate for detecting large structures) and ship-borne gravity surveys (to detect density anomalies of underlying rocks) (Table 10.2.) (JAMSTEC, 2018).

Semi-detailed surveys provide high-resolution (both lateral and vertical) information on small areas (on the order of several km^2) and involve the use of AUV/ROV-borne MBES and AUV-borne SBP as well as the equipment with which to carry out autonomous cabled seismic (ACS) reflection (high lateral and vertical resolution) and AUV-borne gravity surveys (Table 10.2.).

Detailed surveys supply very high-resolution information on small spatial scale areas (a metre-scale resolution). The methods used include Vertical Cable Seismic (VCS) reflection, with hydrophone arrays; Zero-Offset (ZVCS), similar to Zero-Offset VSP used in oil and gas exploration (Asakawa et al., 2016, 2019), ROV-borne gravity surveys, Synthethic Aperture Sonar (SAS) surveys (Hansen, 2013; Kowalczyk and Lum, 2017), and AUV-borne interferometric bathymetry surveys (resolution of 2-10 cm) (Kowalczyk and Lum., 2017).

The surveys described above are complemented with point-source information on the sediment/deposit structure (including mineral composition), obtained from actual deposit samples collected with dredges (triangular or rectangular, with bottom-setting or target-setting design); solid deposit grabs (frequently equipped with cameras to document the process of sampling); box corers and multiple corers (multi-corers) for sampling soft sediment, providing cores of undisturbed sediment; gravity corers to obtain cores of up to 12 m in length, and providing data and insights on time-course of sediment accumulation on very long temporal scales.

The methods and equipment listed above are deployed from a variety of platforms (cf. Table 10.2): research vessels, remotely operated vehicles (ROV), autonomously underwater vehicles (AUV), and drilling rigs, of which the first three constitute standard equipment used during exploration on mid-ocean ridges, including the Mid-Atlantic Ridge (MAR).

Table 10.2. Methods and equipment used for seafloor mapping and exploration

Survey scale	**Exploration technique**	**Survey component**	**Platform**
Regional	Acoustic	MBES Bathymetry Sub-bottom profiler Seismic reflection survey Side Scan Sonar	Ship
	Gravity	Gravity survey	
Semi-detailed	Acoustic	AUV-based survey (MBES, SSS etc.) Seismic reflection by ACS	*Deep-tow, AUV*
	Gravity	AUV-borne gravity survey	
Detailed	Acoustic	Seismic reflection by VCS SAS/SSS Interferometric Bathymetry Sub-bottom profiler	*ROV and, AUV*
	Gravity	ROV based gravity survey	
	Geological survey (sediment sampling)	Dredge, Grab, Box-corer, Multi-corer, Gravity-corer ROV/ ROV Crawler Drilling rig	*Ship-borne, seafloor-based operations, ROV*

References

Asakawa, E., Lee, S., Sumi, T., Endo, M., 2019. Integrated geophysical approach for the seafloor massive sulfide (SMS) exploration. https://www.essoar.org/pdfjs/10.1002/essoar.10500412.1

Asakawa, E., Murakami, F., Tsukahara, H., Saito, S., Lee, S., Tara, K., 2016. New marine seismic survey techniques for seafloor massive sulphide (SMS) exploration. In: Proceedings of IEEE 2016 Techno-Ocean 2016, Kobe, Japan, Curran Ass., 134139.

Hansen, R. E., 2013. Synthetic Aperture Sonar Technology Review. Marine Technology Society Journal, 47, 117-127.

JAMSTEC, 2018. Cross-Ministerial Strategic Innovation promotion Program. Next-generation technology for ocean resources exploration (Zipangu in the Ocean Program. Japan Agency for Marine-Earth Science and Technology Project Team for Development of New-generation Research Protocol for Submarine Resources, Yokosuka.

Kowalczyk, P., Lum, B., 2017. Sea Floor Mining Exploration Technology and Methods. In: Tshirhart, B., Thomas, M.D. (eds), *Proceedings of Exploration 17: Sixth Decennial International Conference on Mineral Exploration*, Toronto, Canada, 305–318.

Machida, S., Sato, T., Yasukawa, K., Nakamura, K., Iijima, K., Nozaki, T., Kato, Y., 2019. Visualisation method for the broad distribution of seafloor ferromanganese deposits. *Marine Georesources and Geotechnology*, doi: 10.1080/1064119X.2019.1696432.